A MODEL OF DELTA FREQUENCY NEURONAL NETWORK ACTIVITY AND THETA-GAMMA INTERACTIONS IN RAT SENSORIMOTOR CORTEX *IN VITRO*

Swetha Sri Kalyanapu

Doctor of Philosophy

Aston University

June 2017

©Swetha S Kalyanapu

Swetha Kalyanapu asserts her moral right to be identified as the author of this thesis

Aston University

A MODEL OF DELTA FREQUENCY NEURONAL NETWORK ACTIVITY AND THETA-GAMMA INTERACTIONS IN RAT SENSORIMOTOR CORTEX *IN VITRO*

Swetha Sri Kalyanapu

Doctor of Philosophy, 2017

In recent decades, advances in electrophysiological techniques have enabled understanding of neuronal network activity, with *in vitro* brain slices providing insights into the mechanisms underlying oscillations at various frequency ranges. Understanding the electrical and neuro-pharmacological properties of brain networks using selective receptor modulators in native tissue allows to compare such properties with those in disease models (e.g. epilepsy and Parkinson's). *In vivo* and *in vitro* studies have implicated M1 in execution of voluntary movements and, from both local network *in vitro* and whole brain *in vivo* perspectives. M1 has been shown to generate oscillatory activity at various frequencies, including beta frequency and nested theta and gamma oscillations similar to those of rat hippocampus. *In vivo* studies also confirmed slow wave oscillations in somatosensory cortex including delta and theta band activity. However, despite these findings, non-thalamic mechanisms underlying cortical delta oscillations remain almost unexplored. Therefore, we determined to explore these oscillations *in vitro* in M1 and S1.

Using a modified sagittal plane slice preparation with aCSF containing neuroprotectants, we have greatly improved brain slice viability, enabling the generation and study of dual rhythms (theta and gamma oscillations) in deep layers (LV) of the *in vitro* sensorimotor slice (M1 and S1) in the presence of KA and CCh. We found that theta-gamma activity in M1 is led by S1 and that the amplitude of gamma oscillations was (phase-amplitude) coupled to theta phase in both regions. Oscillations were dependent on $GABA_AR$, AMPAR and NMDAR and were augmented by DAR activation. Experiments using cut/reduced slices showed both M1 and S1 could be intrinsic generators of oscillatory activity.

Delta oscillations were induced in M1 and S1 by maintaining a neuromodulatory state mimicking deep sleep, characterised by low dopaminergic and low cholinergic tone, achieved using DAR blockade and low CCh. Delta activity depends on $GABA_AR$, $GABA_BR$ and AMPAR but not NMDAR, and once induced was not reversible. Unlike theta-gamma activity, delta was led by M1, and activity took >20mins to develop in S1 after establishement of peak power in M1. Unlike M1, S1 alone was unable to support delta activity.

Dopamine modulates network activity in M1 and it is known that fast-spiking interneurons are the pacemakers of network rhythmogenesis. Recent studies reported that dopamine (DA) controled I_{tonic} in medium spiny, ventrobasal thalamus and nucleus accumbens neurons by modulation of GABARs or cation channels. In the current study, voltage-clamp whole cell recordings were performed in fast spiking interneurons (FS cells) in Layer V of M1. These recordings revealed tonic and phasic $GABA_AR$ inhibition and when DA was bath applied, a slow inward current (I_{DA}) was induced. I_{DA} was mediated by non-specific cationic TRPC channels following D2R-like receptor activation.

Overall, my studies show the strong interdependence of theta-gamma rhythmogenesis between M1 and S1, dominanace of M1 at delta frequency and the crucial role of dopamine in controlling FS cell activity. Further exploration of these rhythms in models of pathological conditions such as Parkinson`s disease and Epilepsy may provide insights into network changes underlying these disease conditions.

Keywords: oscillations, delta, theta and gamma, PAC, dopamine, interneurons.

Dedication

This thesis is dedicated to my beloved father, Mohan Rao and my loving husband, Uday Kiran.

My father has always been my strength and confidence since my childhood. Everything my mum and dad taught me is invaluable and made me a person who I am today. This would have been a most special and a proud moment if he had been with us. How I miss him but I do feel proud to be a daughter of someone who is still remembered by thousands of people for his kindness, love, care not least his great sense of humour even after 9 years of passing. Your memories stay with us for ever dad! Thank you for looking after me as a princess and giving us the best of everything.

Equally my husband has been an immense support and has been by my side ever since we were married. He dedicated his time and effort to enable me to do masters as well as PhD. I remember days when he used to work 20 hours a day with couple of hours sleep to pay my tuition fee. You walked on a thorny path whilst letting me walk on flowers for which am forever indebted. Surely, I would not have done this without your constant encouragement, motivation, care and support both spiritually and financially. `Thanks` will be too little to acknowledge what you have done.

Acknowledgements

First and foremost, I thank The Lord, Almighty for all His provisions! I would like to express my deepest gratitude to Prof Gavin Woodhall, who has been an amazing supervisor. I am thankful for his pastoral care, support, understanding, patience, kindness, enthusiasm in research and not least his sense of humour. Gav, I can have you as my boss for lifetime. A big thank you goes to my associate supervisor, Prof Ian Stanford for his passion for science, motivation and insightful feedback. Stan, I should admit, after struggling for weeks it was that one day when you taught me was when I first got the hang of patching for which I am grateful. I extend my thanks to Dr Stuart Greenhill for his constant encouragement during writing up time and for his always willing to help nature.

My appreciation extends to lab mates Tamara, Jane, Nick, Darshna, Ben, Serena, Mazhar, Emma and Sukhe. Thanks for helping me to learn stuff like dissection, analysis, making figures and making my PhD journey so enjoyable. Thanks for all the wonderful memories we made together at lab conferences as well as lab-out meals, parties, birthdays, cake, tea and curry times we shared. I would like to thank the bio-medical facility staff; Wayne, Jeffery, Matt and Kat for their prompt arrangement of animals for us. I would also like to thank Gill and Caroline for all the admin support by providing numerous letters when needed.

My sincere thanks goes to everyone at Slade Assembly as well as all the brothers and sisters for their prayerful support. A special thanks to Mrs Lee (our mum in Britain) who has been an immense blessing, Nigel for being a spiritual and financial support and Sarah for putting up with many unkept promises.

I am thankful to all my family members and friends both in India and in the UK for their constant support, encouragement and understanding. Special thanks to Savvy for your great help and Radhika for your ongoing care. Appreciate support from Dheeraj, Pavan, and Pradeep.

I am deeply grateful to mother-in-law, father-in-law and brother-in-law (Vijay) for their great support. I express my gratitude to my sweet sister, (Shilpa Satish) for helping me with formatting, my lovely brother (Bharath Lavanya) for your constant encouragement and grandparents for their countless sacrifices. Special thanks to grandad (MHR) for being passionate about education and providing us a car so that we can get to the best school. It was inspiring when he said that I should focus on my PhD and not worry about his passing. Other grandad (VRK) has been our great pillar of support in raising us. Words cannot express how grateful I am to my ever-cheerful mother for all the moral and intellectual education received from her for which am forever indebted. Thanks mum and mum-in-law for lending your ears whenever I needed. Again, thanks to my dear husband for all his dedication in helping me to finish my thesis. I am greatly blessed with a wonderful family and they are all part of my success.

Table of Contents

Table of figures

Table of tables

Abbreviations

μM	Micromolar
μs	Microsecond
μV	Microvolt
2-APB	2-Aminoethoxydiphenylborane
2-APV	D-(-)-2-Amino-5-phosphonopentanoic acid
5HT	Serotonin
AA	Ascorbic acid
AC	Adenyl cyclase
Ach	Acetylcholine
aCSF	Artificial cerebrospinal fluid
AD	Alzheimer disease
AHP	Afterhyperpolarisation
AMPAR	α-amino-3-hydroxy-5-methyl-4-isoxazolepropionic acid receptor
AMPH	Amphetamine sulphate
AP	Action potential
AT	Atropine
BG	Basal ganglia
BS	Brainstem nuclei
BZD	Benzodiazepine
CA1	Cornu ammonis-1 of hippocampus
Ca^{2+}	Calcium ion
CA3	Cornu ammonis-3 of hippocampus
cAMP	Cyclic adenosine monophosphate
CB	Calbindin
CBNX	Carbenexolone
CCh	Carbachol
CFC	Cross-frequency coupling
CGP 55845	[(2S)-3-[[(1S)-1-(3,4-Dichlorophenyl)ethyl]amino]-2-hydroxypropyl] (phenylmethyl) phosphinic acid hydrochloride
CHPG	2-Chloro-5-hydroxyphenylglycine
ChR2	Channel rhodopsin 2
CL	Centrolateral nucleus of thalamus
Cl^-	Chloride ion

CNQX	6-Cyano-7-nitroquinoxaline-2,3-dione
CNS	Central nervous system
CPCCOEt	7-(Hydroxyimino)cyclopropa[b]chromen-1a-carboxylate ethyl ester
CPPG	(RS)-α-Cyclopropyl-4-phosphonophenylglycine
CR	Calretinin
Cre	Causes recombination
D1R	D1-like dopamine receptor
D2R	D2-like dopamine receptor
DA	Dopamine
D-AP5	D-(-)-2-Amino-5-phosphonopentanoic acid
DHPG	(S)-3,5-Dihydroxyphenylglycine
EEG	Electroencephalography
EPSC	Excitatory postsynaptic current
EPSP	Excitatory postsynaptic potential
fMRI	Functional magnetic resonance imaging
FS	Fast-spiking
GABAR	γ-aminobutyric acid receptor
GAD 67	Glutamic acid decarboxylase 67 kDa
GBZ	Gabazine
GIRK	G protein-coupled inwardly-rectifying potassium channel
GPCR	G-protein-coupled receptor
GYKI 53655	1-(4-Aminophenyl)-3-methylcarbamyl-4-methyl-3,4-dihydro-7,8-methylenedioxy-5H-2,3-benzodiazepine hydrochloride
HA	Histamine
HCN	Hyperpolarisation-activated cyclic nucleotide–gated channels
HCO_3^+	Bicarbonate
hr	Hour
Hz	Hertz
IB	Intrinsic bursting
IFSECN	International Federation of Societies for EEG and Clinical Neurophysiology
I_h	Hyperpolarisation activated cation current
I_{Kca}	Ca^{2+} dependent hyperpolarising K^+ current
IN	Interneuron
ING	Interneuronal network gamma
IPSC	Inhibitory postsynaptic current

IPSP	Inhibitory postsynaptic potential
I_T	Low-threshold calcium current
iGluR	Ionotropic glutamate receptor
K^+	Potassium ion
KA	Kainic acid/kainate
KAR	Kainic acid receptor
KCC2	Potasssium chloride co-transporter
KO	Knock-out
L I	Layer 1
L II	Layer 2
L III	Layer 3
L IV	Layer 4
L V	Layer 5
L VI	Layer 6
LFP	Local field potentials
LTD	Long term depression
LTP	Long term potentiation
LTS	Low threshold spiking
LY 341495	(2S)-2-Amino-2-[(1S,2S)-2-carboxycycloprop-1-yl]-3-(xanth-9-yl) propanoic acid
LY 379268	(1R,4R,5S,6R)-4-Amino-2-oxabicyclo [3.1.0] hexane-4,6-dicarboxylic acid
M1	Primary motor cortex
M2	Secondary motor cortex
mAchR	Muscarinic acetylcholine receptor
MEG	Magnetoencephalography
mGluR	Metabotropic gutamate receptor
MSNs	Medium spiny neurons (MSNs)
MI	Modulation Index
min	Minute
MK-801	(5S,10R)-(+)-5-Methyl-10,11-dihydro-5H-dibenzo[a,d]cyclohepten-5,10-imine maleate
mM	Millimolar
MPEP	2-Methyl-6-(phenylethynyl) pyridine
Ms	Millisecond
MSNs	Medium spiny neurons
MTEP	3-((2-Methyl-1,3-thiazol-4-yl) ethynyl)pyridine hydrochloride

mV	Millivolt
NA	Noradrenaline
Na^+	Sodium ion
NE	Norepinephrine
NKCC	Sodium and potassium coupled co-transporter
NMDAR	N-methyl-D-aspartate receptor
NREM	Non-rapid eye movement
OLM	Oriens lacunosum moleculare
PAC	Phase-amplitude coupling
PDPC	Phase-dependent power correlations
PD	Parkinson's disease
PET	Positron emission tomography
PFC	Prefrontal cortex
PI	Phosphoinositole/phosphoinositide
PING	Pyramidal-interneuron network gamma
PIR	Pirenzepine
PLC	Phospholipase C
PO	Posterior thalamic nucleus
PPC	Phase-phase coupling
PPN	Pedunculopontine nucleus
PTX	Picrotoxin
PV+	Parvalbumin positive interneurons
r	Radius
REM	Rapid eye movement
RMP	Resting membrane potential
RS	Regular Spiking
RSNP	Regular spiking non-pyramidal cell
RT/RTN	Reticular nucleus of thalamus
s	Second
S1	Primary sensory cortex
S2/Par2	Secondary somatosensory/parietal area
SC	Superior colliculus
SCH 23390	(R)-(+)-7-Chloro-8-hydroxy-3-methyl-1-phenyl-2,3,4,5-tetrahydro-1H-3-benzazepine hydrochloride
SKF96365	1-[2-(4-Methoxyphenyl)-2-[3-(4-methoxyphenyl) propoxy]ethyl-1H-imidazole

SO	Somatostatin
SWO	Slow wave oscillations
SYM2206	(±)-4-(4-Aminophenyl)-1,2-dihydro-1-methyl-2-propylcarbamoyl-6,7-methylenedioxyphthalazine
TLE	Temporal lobe epilepsy
TRPC	Transient receptor potential cation channels
UBP 304	(S)-1-(2-Amino-2-carboxyethyl)-3-(2-carboxythiophen-3-ylmethyl) pyrimidine 2,4-dione
UBP 310	(S)-1-(2-Amino-2-carboxyethyl)-3-(2-carboxy-thiophene-3-yl-methyl)-5-methylpyrimidine-2,4-dione
V_e	Electrical potential
VIP	Vasoactive intestinal polypeptide
VL	Ventrolateral nucleus of thalamus
ZI	Zona inserta
ZOL	Zolpidem
A	Alpha
β	Beta
γ	Gamma
θ	Theta
δ	Delta
π	Pi
ρ	Rho
T	Tau

1 Introduction

1.1 Brain rhythms

Brain rhythms are voltage fluctuations of electrical activity of neuronal assemblies and are shaped by geometry and alignment of those assemblies (Buzsaki, 2006). Hans Berger first recorded rhythmic electric signal in humans in 1929 using the electroencephalograph (EEG) device. The reliable nature of the EEG device attracted both clinicians and scientists, which lead to research into brain rhythms, their mechanisms, origin, and roles in health and disease. Nowadays, neuronal voltage changes can be measured by EEG or indirectly via magnetoencephalography (MEG) on the scalp and intracranially with subdural electrodes (electrocorticography) *in vivo*. Extracellular local field potential recordings (LFPs; mechanisms detailed below) can also detect these rhythms and this approach is widely used *in vitro* alongside single-cell electrophysiology techniques. Brain rhythms are categorized depending on frequency band (number of cycles per second, units: Hertz (Hz)). Different types of rhythms include: very slow oscillations (<1 Hz), delta (2-4 Hz), theta (4-11 Hz), alpha (8-13 Hz), mu (7-10 Hz) beta (13-30 Hz), gamma (30-100 Hz) and very fast oscillations (>100 Hz) (Steriade *et al.,* 1993; Curio *et al.,* 1994). In LFP experiments, activity at different frequency band is measured by their relative power (amplitude of the power spectrum). It is evident that brain rhythms are associated with specific brain functional activity. For example, research suggests roles in physiological functions such as sleep & wakefulness (delta rhythm), memory formation (theta and gamma rhythms) and consolidation (delta), cognitive processing and integration (gamma activity; Thallon and Bertrand, 1999; Singer, 1999) and in diseases such as Parkinson`s disease, schizophrenia, epilepsy, and Alzheimer`s disease (Brown *et al.,* 2001; Herrmann and Demiralp, 2005).

1.1.1 Neuronal contribution to the LFP

Local field potential recording (electric potential V_e) is generated by the summation of currents flowing in and out (sink and source respectively) of neuronal elements (synapses, dendrites and somata) and across the extent of extracellular recording site. The amplitude and frequency of LFP activity depends upon contributions from these various current sources as well as properties of the brain tissue. Amplitude is inversely proportional to the distance (r) between recording site and source. Hence, larger the distance between the source and recording site the less information obtained from LFP (see review Buzsaki *et al.,* 2012). The most important contributor to LFP is synaptic activity. The overlapping activity of several similar compartments induces a measurable signal, which is made possible by kinetically slow events like synaptic currents (Elul 1971; Logothetis, 2004 Niedermayer *et al.,* 2005). Hence, the tree-like structure of neurons formed by soma and dendrites with electrically excitable properties affected by several thousand synapses provides the basis of LFP signals.

Synaptic NMDA and AMPA receptors mediate excitatory events by enabling the flow of calcium and sodium ions respectively. Influx of these cations (Ca^{2+} and Na^+) to intracellular space from extracellular space creates an extracellular current sink. To achieve electrical balance, this sink is balanced by a source. Passive current flows along the neurons as an opposing ion flow from intracellular to extracellular space which, together with the original sink, forms a dipole. Synaptic $GABA_A$ receptors mediate inhibitory currents involving the flow of Cl^- which creates an active source in the extracellular space and need an intracellular sink to achieve electrical balance. However, it is difficult to determine if the identified source or sink is active or passive unless the type of synapse is known (Buzsaki *et al.,* 2003, 2006, 2012). Since the chloride ion equilibrium potential is near to resting membrane potential, inhibitory events are assumed to contribute very little to the LFP (Bartos *et al.,* 2007; Koch 1999). However, inhibitory currents can induce transmembrane hyperpolarising currents in fast spiking neurons (when the membrane gets depolarised) and are known to contribute to LFP in generating fast oscillations in hippocampus (Trevelyan *et al.,* 2009; Glickfeld *et al.,* 2009; Oren *et al.,* 2010; Bazelot *et al.,* 2010). Pyramidal neurons also generate strong dipoles owing to the separation distance between active sink or source and the return current, and have been suggested to contribute greatly to the LFP (Buzsaki *et al.,* 2012). Nevertheless, interneurons are significant contributors to LFP where the contribution from pyramidal neurons is paced and controlled via inhibitory interneurons, di-synaptically. This was reported in invasive studies in cortex of human and monkey (Telenczuk *et al.,* 2017) and is consistent with data from hippocampal slices (Bazelot, 2010). Spike waveform features such as shape of the spike has enabled the classification of inhibitory (narrow spikes) and excitatory (broad spikes) neurons (Peyrache *et al.,* 2012) but exceptions do exist such that non-fast spiking interneurons display a broad waveform spike (Fuentealba *et al.,* 2008) whilst some excitatory neurons in motor cortex display narrow spikes (Vigneswaran *et al.,* 2011). Intracellular and extracellular recordings at synaptic sites of excitatory (e.g. NMDAR) and inhibitory (GAB_AR) receptors are illustrated in figure 1.1.

Figure 1.1 An illustration of field potentials at an excitatory and inhibitory at both synaptic and non-synaptic sites.

Intracellular and extracellular recordings shows a rapid EPSP/IPSP at a synaptic site on dendrite but a slower and smaller EPSP/IPSP at soma. **(A)** Source (positive) flows outward and inward (negative) sink at synaptic site whilst the opposite is true for inhibitory synapse **(B)** Note the source at synaptic site and sink at soma.
Source: http://clinicalgate.com/electroencephalography/.

Strong currents that are generated across extracellular space are fast action potentials that are detected as spikes or 'units' (e.g. Koch, 1999). Despite the high amplitude V_e generating ability of Na^+ spikes, they were thought not to contribute greatly to LFP or EEG (Niedermeyer *et al.,* 2005; Nunez *et al.,* 2006) due to their short duration (<2 ms). However, synchronous firing from many neurons (population) is known to play a role in high frequency activity (Buzsaki *et al.,* 2012) suggesting a role of action potentials in LFP (Pettersen *et al.,* 2008).

Voltage dependent Ca^{2+} spikes are often triggered by a back-propagating action potential to distal dendrites (Iakram *et al.,*2009) or because of excitatory post synaptic potentials (EPSPs) mediated by NMDA receptors (Hirsch *et al.,* 1995; Schiller *et al.,* 2000; Polsky *et al.,* 2004; Larkum *et al.,* 2009). Due to their long-lasting nature (10-100 ms) and large power (10-50 mV) dendritic Ca^{2+} spikes are considered to play a role in the LFP (Wong *et al.,* 1979; Llinas *et al.,* 1988; Schiller *et al.,* 2000; Stuart *et al.,* 2008). Other non-synaptic contributors include voltage dependent intrinsic currents (I_h and I_T) in resonance (neuronal ability to respond to a frequency band) (Llinas, 1998) and gap junctional potentials.

1.2 Gamma oscillations

Gamma oscillations were first designated as beta-like waves (35-45 Hz) (Jasper and Andrews, 1938). Later, they began to be referred to as 40 Hz oscillation (Das and Gastaut, 1955). Then, in the late 19th century, gamma rhythms were named based on the frequency range (30-70 Hz) of oscillations (Bressler and Freeman, 1980) and they have since become the most commonly studied type of oscillation in various regions of brain. Many studies have been carried out in hippocampus (*in vitro* and *in vivo*) due to its clear laminar organization and densely packed pyramidal neurons that give rise to high amplitude gamma oscillations spontaneously *in vitro* (Modebadze, 2014, Shah, 2016).

1.2.1 Mechanistic aspects of gamma oscillatory activity

In vivo studies have reported that there are two rhythm-generating structures in hippocampus: dentate gyrus and CA3 (Csicsvari *et al.,* 2003). *In vitro* pharmacological induction methods of gamma oscillations have been demonstrated using approaches such as hypertonic potassium solution and tetanic stimulation but the most commonly used method is the bath application of cholinergic agonist, carbachol (CCh) and/or kainate receptor agonist, kainic acid (KA) or metabotropic glutamate receptor agonist (CHPG) (Whittington *et al.,* 1995; Fisahn *et al.,* 1998; Fisahn *et al.,* 2004; Hajos and Paulsen, 2009). Gamma oscillations have been reported in various regions: in hippocampus (CA3 and CA1) (Buzsaki *et al.,* 1983; Whittington 1995; ; Bragin *et al.,* 1995; Fisahn *et al.,* 1998 ;Gillies *et al.,* 2002; Mann *et al.,* 2005), somatosensory cortex (Buhl *et al.,* 1998) striatum (Berke *et al.,* 2004; Tort *et al.,* 2008) entorhinal cortex (Cunningham *et al.,* 2003), amygdala (Sinfield and Collins, 2006), cerebral cortex (Middleton *et al.,* 2008), olfactory bulb (Adrian, 1942, Freeman, 1975) and primary motor cortex (Johnson *et al.,* 2017). However, the time required to induce activity and concentrations of KA and CCh varies with the region and slice preparation. ING (interneurons network gamma) (Whittington, 1995; Traub *et al.,* 1996a) and PING (pyramidal-interneuron network gamma) are the two models proposed as mechanisms of gamma oscillations *in vitro* as illustrated in figure below (Whittington *et al.,* 2010) both depending on interneuron populations in cortex. (McCormick, 1996; Wang, 1993; Wang 1999; Minlebaev *et al.,* 2011).
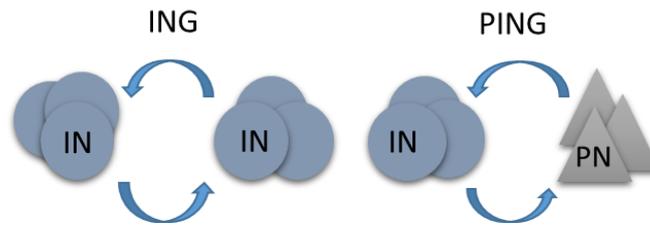
Figure 1.2 Schematic representation of acting models of ING and PING.

1.2.2 ING

Interneuronal gamma (ING) arises from a neuronal population consisting of only inhibitory interneurons in which the important factors include: mutually connected interneurons, a time constant mediated by $GABA_AR$, driving current to initiate interneuron spiking in the absence of fast phasic excitatory drive (Wang & Rinzel 1992; Whittington *et al.,* 1995; Wang & Buzsáki 1996; Traub *et al.,* 1996b;). During ING (figure 1.2), one population (group 1) of interneurons fire action potentials (AP), generating IPSC in another connected population of interneurons (group2). When the required net excitation of interneurons is available then group 2 generates rebound spikes with IPSCs in group 1 and the cycle repeats. This recurrent chain of events suggest inhibition to be essential for synchronisation (Van Vreeswijk *et al.,* 1994). Oscillatory frequency is strongly determined by the IPSC decay time kinetics (Wang and Buzsaki, 1996; Tiesinga and Jose, 2000; Buzsaki and Wang, 2012). Hence, a $GABA_AR$ modulator, pentobarbital, decreases the frequency of oscillations via increased IPSC decay time, confirming the critical role of IPSC kinetics in determining the frequency (Segal and Baker, 1984; Fishan *et al.,* 2004). Nevertheless, there is no clear understanding of where the source of exciatation in ING model.

1.2.3 PING

Pyramidal-Interneuronal gamma (PING) is a mechanism of gamma oscillations based on reciprocal interactions between populations of pyramidal and inhibitory neurons (Wilson and Cowan, 1972; Freeman, 1975; Leung, 1982; Ermentrout & Kopell, 1998; Borgers and Kopell, 2003; Brunel & Wang, 2003; Geisler *et al.,* 2005). These oscillations rely upon phasic excitation and inhibition to synchronise (Roopun *et al.,* 2009; Fisahn *et al.,* 1998). These oscillations have been suggested to be more persistent than ING like oscillations due to their alternative fast excitation and delayed inhibition that occurs in a cyclic manner (Buzsaki and Wang, 2012). Like ING model, enhancing IPSC kinetics using pentobarbital reduced the frequency and oscillations were abolished upon addition of $GABA_AR$ antagonist. Hence, $GABA_AR$ mediated IPSC decay time determines the frequency of the oscillations (Freeman, 1975, Leung, 1982) which is now known to be a characteristic feature of PING both *in vivo* and *in vitro* (Mann *et al.,* 2005; Hájos and Paulsen, 2009; Bragin *et al.,*

1995; Csicsvari *et al.,* 2003; Hasenstaub *et al.,* 2005; Tiesinga and Sejnowski, 2009). Unlike ING model, PING like oscillations were found to be dependent on AMPAR due to the reliance on excitatory drive (Cunningham *et al.,* 2003). Interestingly, pharmacological manipulation of IPSC kinetics has shown to have comparatively more impact on frequency of ING, suggesting the stability of the network was enhanced upon the recruitment of pyramidal cells in PING (Whittington *et al.,* 2000).

1.2.4 Evidence for ING and PING *in vivo* and *in vitro*

In vitro ING-like mechanism was first observed in CA1 in the presence of the metabotropic glutamate receptor agonist, DHPG or high potassium solution plus blockade of ionotropic glutamate receptors (Whittington *et al.,* 1995; Traub, 1996; LeBeau *et al.,* 2002; Whittington *et al.,* 2010) and also by bath application of KA (Fisahn *et al.,* 2004). Cholinergically induced PING like mechanisms have also been identified in hippocampal and cortical slices (Fisahn *et al.,* 1998) and KA and CCh also induced the same (Whittington, 2010; Modebadze, 2014; Nicholas, 2016). Further studies (Fuchs *et al.,* 2007) have shown that the amplitude of gamma oscillations was decreased when AMPAR expression was genetically knocked down, presumably due to disturbed interaction between pyramidal and interneuron cells. Depolarising cortical interneurons by optogenetically exciting ChR2 channels *in vivo* has shown an increase in gamma amplitude when recording extracellularly whilst a decrease in gamma power was observed by hyperpolarising interneurons via halorhodopsin (Sohal *et al.,* 2009). It was also reported that when random light pulses were used to drive interneurons *in vivo*, power in the gamma frequency range was enhanced in comparison to other frequency bands (Cardin *et al.,* 2009). However, many studies suggest ING to be an artefact since the source of excitation is unknown which needs further exploration.

1.3 Theta oscillations

Theta rhythm with a frequency range of 4-10 Hz has been the subject of many investigations in the rodent hippocampus (Bland, 1986; Bland *et al.,* 2002; Cunningham *et al.,* 2003; Jacobs, 2010; Jacobs, 2014). Previous studies have defined hippocampal 1-4 Hz as delta (Clemens *et al.,* 2013), as theta (Fell *et al.,* 2003) and also theta/delta (Mormann *et al.,* 2008) and discrepancies still exist. Despite these issues relating to frequency banding, hippocampal 1-4 Hz and 4-8 Hz oscillations found in human and rodents respectively have been reported to have functional similarities in that they exhibit an activation during navigation and memory tasks and show analogous coupling pattern with gamma oscillations (Ekstrom *et al.,* 2005; Jacobs, 2014).

Hippocampal theta in rodents can be divided into two types: atropine sensitive theta (4-9 Hz) which is associated with automatic movement and atropine insensitive theta (6-12 Hz)

which is found during voluntary movements (Vanderwolf, 1969; Kramis *et al.,* 1975). Since Local field potential is the summation of EPSPs and IPSPs on the soma and dendrites of pyramidal cells it is assumed that theta activity is the interplay between two different dipoles (current generators). One being the excitatory input received by pyramidal cells and the other being inhibitory input from GABAergic neurons (Buzsaki, 2002). The role of theta oscillations in spatial memory was demonstrated by behavioural studies in which specific pattern at theta frequency corresponds to firing of place cells corresponding to visual cues (O`Keefe, 1976) and the phase relationship between spiking and theta activity of place cells was identified to shift depending on the location (O`Keefe and Reece, 1993), suggesting that location was encoded by phase precession.

1.4 Phase-amplitude coupling (PAC)

Studies have demonstrated that certain brain functions such as cognition are achieved by simultaneous activity in multiple frequency bands (Schutter and Knyazev, 2012). It is evident that each frequency band plays a specific role in functional aspects like perception and cognition (Cohen, 2008) but further insight may be provided by uncovering the relation and interaction *between* different frequency band oscillations (Jensen and Colgin, 2007). Such interaction is termed cross-frequency coupling (CFC) which has received greater interest in recent years in the field of neuroscience. CFC has been identified in signals obtained from LFP, electroencephalogram, electrocortigram recordings (Bragin *et al.,* 1995; Lakatos *et al.,* 2005; Canolty *et al.,* 2006; Demiralp *et al.,* 2007; Jensen and Colgin, 2007; Cohen, 2008; Kramer *et al.,* 2008; Young and Eggermont 2009).

CFC was categorised in two forms: phase-amplitude coupling (PAC) and phase-phase coupling (PPC). The former is the type of CFC investigated in this thesis. PAC is also known as nested oscillations in which the phase of low frequency oscillations (example: theta) determines the power or amplitude of high frequency oscillations (example: gamma). Thus, amplitude of high frequency oscillation (nested) is synchronised with the phase of low frequency oscillation (nesting) (Palva *et al.,* 2005). This type of CFC enables observation of the inter-frequency relationship aspects that correspond to low frequency and the amplitude of higher frequency components of local cortical circuit (Canolty and Knight, 2010). Behavioural studies have suggested that PAC is involved in sensory integration, attentiveness and memory organisation (Lisman and Idiart, 1995; Lisman, 2005; Schroeder and Lakatos, 2009; Voytek *et al.,* 2010). Several brain regions have been reported to show PAC, including hippocampus (Bragin *et al.,* 1995), neocortex (Canolty *et al.,* 2006) and basal ganglia (Cohen *et al.,* 2008) and PAC is evident in rodents (Bragin *et al.,* 1995; Tort *et al.,* 2008), sheep (Nicol *et al.,* 2009) and monkeys (Lakatos *et al.,* 2005) as well as in

humans (Cohen *et al.,* 2008), Schematic representation is shown in figure 1.3. Note from the figure that the amplitude of fast oscillations is always greatest at a certain phase of low frequency oscillation, this is called the coupling phase.

Figure 1.3 Representative PAC

Top trace is the sum of both (fast and slow) oscillations in which the amplitude of fast oscillations corresponds to the phase of slow oscillation.
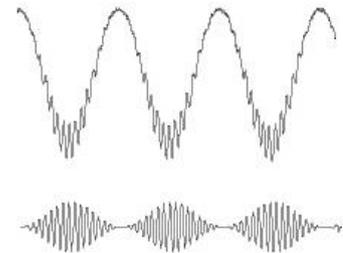
Figure 1.4 Illustration of phase-amplitude coupling analysis with different modulation indices (cases 1-4).

(A) Left traces are the example summation of fast and slow oscillations (top traces) and filtered data of coupling strength (bottom traces), right traces are the corresponding phase-amplitude analysis graphs **(B)** bar graph of corresponding modulation index of all cases (1-4). Note greater the coupling strength greater the modulation index. Obtained from Tort *et al.,* 2010 for illustration purposes.

Several methods of measuring PAC have been reported (Canolty *et al.,* 2006; Tort *et al.,* 2010) but each of them have advantages and disadvantages. The figure 1.4 illustrates phase amplitude coupling analysis and corresponding modulation index of theta and gamma taken as an example. In this thesis, the method and Matlab scripts provided by Tort *et al.,* 2010 were used for PAC analysis (see results chapter 3).

1.5 Oscillatory patterns during sleep

Various sleep stages were first described by Loomis *et al.,* (1937) who demonstrated the spectrum of EEG from wakefulness to deep sleep. In the 1950, REM (Rapid Eye Movement) stage was distinguished and sleep stages were reclassified as NREM (Non-Rapid Eye Movement) and REM stage (Dement and Kleitmen, 1957). Various rhythmic patterns were described in thalamocortical systems during sleep stages, including infra-slow: 0.02-0.1 Hz, slow (0.2-1 Hz), delta (1-4 Hz), spindle (12-14 Hz) theta (3-7 Hz), and fast: 20-60 Hz and ultra-fast: 100-600 Hz (Bazhenov and Timofeev, 2006).

Aston University

Illustration removed for copyright restrictions

Figure 1.5 Elucidating the EEG recordings during various stages from awake to deep sleep stages and the associated oscillations during each stage.

Low amplitude but high frequency oscillations were identified in wakeful stages and REM stages whereas, high amplitude low frequency oscillations were characterized in deep sleep stages. Source: Hockenbury and Hockenbury 2010.

Five stages of sleep cycle were characterized in humans. The first four stages are grouped as (NREM) sleep stage with last deepest one (stage 4) is punctuated by episodes of REM (Rechtschaffen and Kales, 1968) as illustrated in figure 1.5.

The sleep cycle is known to progress in following order, N1-N2-N3-N4-REM (Feinberg and Floyd, 1979). Stage 1 is a transitional stage between sleep and waking and is associated with low voltage EEG with mixed frequencies at alpha (4-7 Hz) and theta (7-10 Hz) band. Alpha oscillations are often seen in this relaxed state (Carskadon and Dement, 2011) and this stage lasts about 1-7 minutes, constituting about 2% of the sleep cycle. Stage 2 comprises sleep spindles (10-17 Hz), K^+ complexes, typically constitutes about 45-55% in adults (even more in young adults) of sleep cycle and lasts about 20-30 minutes. Stage 3 consists of a mixture of theta and delta waves of frequency 0.1-1 and 1-4 Hz. Stage 3 occurs

longer periods during initial sleep cycles. This stage is characterized by the lowest breathing rate and blood pressure with increased dreaming (Carskadon and Dement, 2011) and delta activity. Stage 4 is defined by high amplitude delta oscillations (2-4 Hz). Stage 3 and 4 are often described as slow-wave or delta sleep stage and represents 15-20% of sleep cycle. EEG recordings revealed that these stages are characterised by 'up' and 'down' states of cortex in which neurons in cortex are depolarised in 'up' state and may fire action potentials whilst 'down' state is when the cells are hyperpolarised and do not fire (Steriade *et al.,* 1991, 1993a, 1993b, 2001; Contreras and Steriade, 1995; Werth *et al.,* 1996; Timofeev *et al.,* 2000a, 2000b, 2001; Molle *et al.,* 2002; Clemens *et al.,* 2007). Stage 5 (REM stage), which lasts for 5-15 minutes is an indication of end of NREM stages and is characterized with rapid eye movements, loss of muscle tone and dreaming. It is thought that sleep stages always begin with NREM stages (lasts about 50-70 minutes) followed with REM (5-25 minutes) stage in a cyclic manner for about four times every night (Rechtschaffen and Kales, 1968; Amzica and Steriade 1998; Carskadon and Dement, 2011). REM sleep was found to be dominant during later cycles of sleep whilst N3 and 4 are dominant in earlier cycles (Aeschbach and Borbely, 1993).

1.6 Delta oscillations and sleep

The delta rhythm was first described by Walter in 1936 as a specific slow wave recorded during an EEG investigation of pathological tumours. The frequency range for delta wave activity is between 0 and 4 Hz as implicated in International Federation of Societies for Electroencephalography and Clinical Neurophysiology (IFSECN) (1974). However, frequency ranges such as 1-4 Hz (Ursin, 1968), 0.5-4 Hz (Frost and Kellaway *et al.,* 1966), 0.5-5 Hz (Gibbs and Gibbs, 1951) and 0.1-3.5 Hz (Niedermeyer 1999) are often mentioned in the literature. A wide range of research has been carried out to disclose the relation between the EEG and cellular mechanisms (Creutzfeldt *et al.,* 1966; Frost and Kellaway *et al.,* 1966; Rappelsberger *et al.,* 1982). There is more than one phenomenon in the frequency range of 0-4 Hz which includes slow oscillations (<1 Hz) and delta (1-4 Hz) oscillations. Several studies are available demonstrating the origins of slow-wave oscillations (<1 Hz) in thalamus (Crunelli and Hughes, 2010) neocortex (Compte *et al.,* 2003; Shu *et al.,* 2003; Hasenstaub *et al.,* 2005; Haider *et al.,* 2006), in cortex (Sanchez-Vives and McCormick, 2000) yet very little is known about delta oscillations in terms of origin and mechanism underlying the rhythm at 2-4 Hz, though it is assumed that there are at least two types such as thalamic and cortical delta oscillations, depending on the source of origin.

1.6.1 Thalamic delta oscillations

Thalamic delta oscillations were characterized *in vivo* in motor, sensory, association and intralaminar thalamic nuclei of cats (Steriade *et al.,* 1991b; Dossi *et al.,* 1992) and *in vitro* in neurons of the rodent lateral geniculate (LG) (McCormick and Pape, 1990; Leresche *et al.,* 1990). The rhythmicity in these oscillations is generated intrinsically as a result of interplay between two inward currents of thalamic relay neurons: low-threshold Ca^{2+} current (I_T) and hyperpolarisation activated cation (Na^+ and K^+) current (I_h). Long-lasting hyperpolarisation, below -65 mV in a neuron of thalamus activates slow I_h, which causes depolarisation of membrane potential which activates I_T, generating a Ca^{2+} spike which in turn triggers a burst of high frequency Na^{2+} action potentials. I_h is deactivated and I_T is inactivated during the burst of spikes and burst termination is followed by hyperpolarising overshoot mediated by a Ca^{2+}-dependent afterhyperpolarising K^+ current (IK_{Ca}). During bursts, both I_h and I_T are deactivated and inactivated because of voltage dependency and transient nature respectively. The post-burst after hyperpolarisation (AHP) activates I_h and starts the next cycle of oscillations (McCormick and Pape, 1990). This mechanism is illustrated in figure 1.6.

Aston University

Illustration removed for copyright restrictions

Figure 1.6 Intracellular mechanism of thalamic delta oscillations (adapted from McCormick and Pape 1990).

I_h is sensitive to both voltage and Ca^{2+} concentration, the fluctuations in Ca^{2+} concentration can alter the strength of I_h. This converts delta activity into a waxing/waning pattern which is like that of thalamocortical neurons in intact cat (Dossi *et al.,* 1992) and changes to clock-like after neocortex removal (Timofeev *et al.,* 2000). Moreover, similar activity of rebound bursts at delta range was also noticed in thalamic slice preparations (McCormick and Pape,

1990; Leresche *et al.,* 1990; Soltesz *et al.,* 1991) and in single neurons of computer models (Toth and Crunelli, 1992; Destexhe *et al.,* 1993; Wang, 1994).

1.6.2 Cortical delta oscillations

Early studies reported delta oscillations in isolated cortex of cats (Frost and Kellaway *et al.,* 1966) and of neocortical origin after thalamectomy (Villablanca and Salinas-Zeballos, 1972; Villablanca, 1974). In addition, Ball *et al.,* demonstrated that the delta oscillations emerge in between II/III and V layers of cortex (Ball *et al.,* 1977). Cortical delta is far less well understood than thalamic delta. Some studies suggest that thalamic delta is independent of cortical delta rhythm as it existed after decortication (Steriade *et al.,* 1985; Pare *et al.,* 1987). On the other hand, delta oscillations were desynchronised after decortication proving that the thalamic delta is synchronised by long-range cortical connections (Timofeev and Steriade, 1996). These controversial reports suggest the need for further investigation of cortical delta rhythm. Nevertheless, a recent study in slices containing secondary somatosensory/parietal area S2/Par2 has enabled pharmacological induction of delta oscillations first time *in vitro* by maintaining a neuro-modulatory state equivalent to that of sleep (Carracedo *et al.,* 2013).

1.7 Primary motor cortex (M1)

The primary motor cortex (M1) contributes greatly to the execution of voluntary movements and motor learning (Rioult-Pedotti *et al.,* 1998). In early studies, Penfield and Boldrey used low intensity micro-stimulation of M1 in human surgical patients to show its organization in a somatotopic manner of leg, arm, head and face, which was termed the "Motor Homunculus" (Penfield and Boldrey, 1937). The homunculus elucidates a somatotopic M1 map with each area and corresponding body parts (see figure 1.7). In 1968 Stoney *et al.,* (1968) followed up the studies in M1 using the intra-cortical electrical stimulation method. This technique enabled various researches to investigate and prove the topographic organization in M1, where the microelectrode was inserted into M1 and moved in small steps across the area (Asanuma and Ward, 1971; Kwan *et al.,* 1978; Donoghue *et al.,* 1992). However, areas associated with body parts showed overlap and were also widely spread and/or were present in multiple representations (Nudo *et al.,* 1992; Sane and Donoghue, 2000). This functional overlapping was further established by various imaging techniques (positron emission tomography (PET) and functional magnetic resonance imaging (fMRI)) (Colebatch *et al.,* 1991) and, hence, the homunculus is perhaps too simple a representation of motor somatotopy. Pyramidal cells form 70% of the neuronal population in M1 (Sloper *et al.,* 1979). Moreover, a greater diversity in size of pyramidal cell is observed in M1 than in any other cortical area. For instance, there is a fourfold range of pyramidal cell body area in precentral gyrus compared to a tenfold range of pyramidal cell body area

in M1 (Jones and Wise, 1977). M1 is oriented in vertical columnar pattern which comprises of five horizontal layers: superficial (I,II&III) and deep (V,VI) layers.

Figure 1.7 Somatotopic representation of the sensory and motor cortical representation of body regions.

Note the extensive representation of the hands in the motor map. Source: Joseph R (2000) http://brainmind.net/BrainLecture5.html.

1.7.1 Layer I

Layer I (LI) is termed as the plexiform layer, and is known to be devoid of excitatory pyramidal neurons (Chu *et al.,* 2003). Hence, it is mostly comprised of inhibitory interneurons (Gabbott and Somogyi, 1986) which provide inhibitory input to pyramidal cells in other layers (Chu *et al.,* 2003). Douglas and Martin identified two structurally different interneurons such as Retzius-Ccajal neurons and small neurons in LI. This layer possesses axons from LII-VI and receives inputs from other cortical areas and thalamus (Douglas and Martin, 2004).

1.7.2 Layer II/III

Layer II (LII) and Layer III (LIII) are termed as external granular layer and external pyramidal layer respectively. Both pyramidal and non-pyramidal cells were characterised in LII/III. Pyramidal cells receive inputs from S1 and send axon collaterals either to LV or are confined to LII/III. Non-pyramidal cells do not possess apical dendrites and are categorised into fast spiking (FS), late spiking (LS), low threshold spiking (LTS), and regular spiking non-pyramidal cells (RSNP) (Kawaguchi, 1995) in these layers. Douglas and Martin reported that cells LII/III have dense thalamic axonal inputs and bear receptors for various neuromodulators including 5-HT, dopamine, and noradrenaline (Douglas and Martin, 2004).

1.7.3 Layer IV

M1 has always been considered to be agranular (Brodmann, 1909; Shipp, 2005; Bastos *et al.,* 2012; Shipp *et al.,* 2013) due to the apparent absence of an anatomically definable LIV (Donoghue and Wise, 1982; Beaulieu, 1993; Zilles *et al.,* 1995) which makes it unique compared to other cortical regions. However, several recent studies (Krieg, 1946; von Bonin, 1949; Caviness, 1975; Deschênes *et al.,* 1979; Skoglund *et al.,* 1997; Cho *et al.,* 2004, Kuramoto *et al.,* 2009; Rowell *et al.,* 2010; Mao *et al.,* 2011; Kaneko, 2013; García-Cabezas and Barbas, 2014; Yamawaki *et al.,* 2014) suggest the existence of connectivity patterns that are like those of LIV in other sensory regions, despite the lack of cyto-architectural visibility of this layer. The cells present in a thin area between LIII and LVa in mouse have been identified to have synaptic connections like LIV which includes: excitatory projections from thalamus, long range corticocortical projections and excitatory projections to LII/III (Yamawaki *et al.,* 2014). Interestingly, LIV of M1 does not contain stellate cells that were present in sensory regions but instead have pyramidal type neurons across a thin laminar zone (Yamawaki *et al.,* 2014; Barbas *et al.,* 2015).

1.7.4 Layer V

Layer V (LV) is called the internal pyramidal layer and is characterised by the presence of large, special cells called Betz cells (Betz, 1894) which is the unique feature of LV in M1 (but like the large Meynert cells of deep primary visual cortex (V1)). Betz cells occupy a large volume in deep layers of M1 and have giant cell bodies (Meyer 1987) and make up 12% of the pyramidal cell assemblies (Rivara *et al.,* 2003). Also, these cells are heterogeneous in structure and therefore exist not just pyramidal form but also triangular and spindle like forms (Braak, 1976). The smaller pyramidal cells are known to possess prominent apical dendrites which project to the pial surface and have terminations in superficial layers of M1 (Cho *et al.,* 2004) whilst the axons from these cells projects to spinal cord. Those large cells in LVa project their axons to basal ganglia (BG) (Lei *et al.,* 2004) and their apical dendrites receive input from LII/III (Kaneka *et al.,* 2000).

1.7.5 Layer VI

Layer VI is called the fusiform layer. It has been demonstrated that many of pyramidal cells in this layer have their inputs from, and projections to thalamus (Kaneka *et al.,* 2000). Colossal interneurons form a source of input to pyramidal and non-pyramidal cells in this layer (Karayannis *et al.,* 2007). Parvalbumin (PV) positive interneurons are also prominently identified in this layer.

1.8 Cortico-cortical and sub-cortical connections

Major cortico-cortical connections (as represented in figure 1.8) in rats are granular S1 (transfers contralateral and ipsilateral sensorimotor signal), S2-PV region somatosensory cortex (dysgranular) of both same and contralateral cerebral hemisphere (White and DeAmicis, 1977; Porter and White, 1983; Welker *et al.,* 1988) contralateral M1 had callosal connections. Sub-cortical reciprocal connections (as indicated in Fig 3B) are found with motor thalamus (Ventral lateral thalamus), reticular thalamic nucleus, central lateral nucleus (cerebello-thalamic pathway) and Zona inserta (regulatory inputs in and out M1) (Donoghue and Parhan, 1983; Koralek *et al.,* 1990; Reep *et al.,* 1990; Fabri and Burton, 1991; Rouiller *et al.,* 1993; Izraeli and Porter, 1995; Hoffer *et al.,* 2013).

Aston University

Illustration removed for copyright restrictions

Figure 1.8 Cortical and subcortical connections of M1 in rats and mice

A) Representation of cortical connections. S1-somatosensory cortex, dysgranular somatosensory cortex, PP-posterior parietal cortex, S2-second somatosensory area, PV-parietal ventral somatosensory cortex, M2-second motor area, V1-primary visual cortex. B) Subcortical connections of M1 in rats and mice. VL-Ventral lateral nucleus, CL-central lateral nucleus, RT-reticular nucleus, ZI-Zona inserta. Other connections to spinal cord and brain stem. Arrows indicate reciprocal connections. Adapted from: Young N *et al.,* 2012 Motor cortex. The mouse nervous system.

1.9 Intrinsic laminar organisation of M1 in rats

It is thought that the major ascending pathway is LVa to LII/III and the dominant descending pathway is from LII/LIII to L Va (Weiler *et al.,* 2008). It is assumed corticocortical connectivity is obtained from cells in both deep and superficial layers whereas thalamocortical output is onto deep layers. Photo-stimulation techniques recently revealed excitatory circuits (Weiler *et al.,* 2008) connecting to various regions. Synaptic transmission is regulated by calcium binding protein containing interneurons which include parvalbumin (PV), calbindin (CB), and calretinin (CR) expressing cells in rats and mice (Celio 1990; Van Bredrode *et al.,* 1991;

Resibois and Rogers 1992; Mucignat-Caretta *et al.,* 2002) most of these neurons appear in two bands which correspond to LII/III and LV/VI. In spite of well-established long-range connections between M1 and other regions of cortex as well as M1 and sub-cortical connections in rodents, far less is known about intrinsic circuit organization in rat M1 compared to other cortical regions.

1.10 Primary somatosensory cortex (S1)

Brain architecture studies were started in 20th century (Broadmann, 1909; Vogt and Vogt, 1919; Von Economo, 1929) but only in the middle of this century were various sensory parts of the brain like auditory cortex, visual cortex, and somatosensory cortex described (Woolsey *et al.,* 1946, 1958). Primary somatosensory cortex (S1) which is also called a Broadmann Area 3b and consists of a mediolateral strip of cortex that extends from the medial wall of the cerebral hemisphere towards the lateral sulcus, where it curves anterior and ends on the ventral surface of the frontal cortex. S1 is known to share a similar anatomical structure within various species except the absence of barrel cortex in humans.

1.10.1 Layer I

L1 of S1 is known to contribute to modulating feed forward transfer of information from thalamus (Galazo *et al.,* 2008) but does not contain pyramidal cells (Ren *et al.,* 1992). Also, known to have reciprocal connections with the arborizing pyramidal tufts of LII (Zhu and Zhu, 2004).

1.10.2 Layer II/III

LII and III have high proportion of pyramidal cells, densely packed but no apical dendrites in LII whilst there are apical dendrites in LIII that extend to LI. Inputs to LII are from LIV and LV whereas LIII inputs are only from LIV (Lefort, 2009), but outputs extend to LVa and LVI. LII is known to process long range connections to M1 (Alloway, 2008)

1.10.3 Layer IV

LIV also known as Barrel cortex in rodents contains star pyramidal cells and spiny stellate cells. Input projections are known to be from lemniscus thalamus (Gibson *et al.,* 1999; Bureau *et al.,* 2006) and from neurons within same column (Feldmeyer *et al.,* 1999; Petersen and Sakmann, 2000) besides intracolumnar projections and trans-columnar projections form LIV (Schubert *et al.,* 2003; Egger *et al.,* 2008; Staiger *et al.,* 2009;). Doughlas and his colleagues described "canonical microcircuit" which is a closed loop comprising of series of excitatory feed forward connection, which were innervated by thalamus LIV via the lemniscal pathway which in turn projects to LII and LIII (Douglas *et al.,*

1989). In rodents, every whisker is characterised by well-structured arrangement almost similar to whisker layout (Woolsey and Vander Loos, 1970).

1.10.4 Layer V

LV receives feedback from LVI (Mercer *et al.,* 2005). LVa constitutes medium principal neurons projecting to M1 and striatum (Alloway, 2008), connections have been reported from the layer itself as well as LIV. LVb contains very large pyramidal cells (Schubert *et al.,* 2001) and IB neurons which are involved sub-cortical connections (de Kock and Sakmann, 2008). Projections from this layer have been identified to be thalamus to trigeminal nucleus and spinal cord.

1.10.5 Layer VI

Layer VI in S1 is characterised as LVIa and b. whilst the former contain spiny pyramidal neurons LVIb contains fewer neurons and is known to intermingle with horizontal pathways (Clancy and Cauller, 1999). Input projections to this layer are from LV and LIV (Mercer *et al.,* 2005; lefort *et al.,* 2009) and output projections are reciprocally connected to thalamus, reticular nucleus and ventrobasal nucleus (Ledergerber and larkum, 2010)

1.11 Sensorimotor circuit

Mao *et al.,* managed to sketch a vibrissal sensorimotor loop in mice (Mao *et al.,* 2011) by assembling their long-range connections with local cortical circuits (Lefort *et al.,* 2009; Sato and Svoboda, 2010; Hooks *et al.,* 2011) and thalamocortical circuits (Lu and Lin, 1993; Bureau *et al.,* 2006; Petreanu *et al.,* 2009; Meyer *et al.,* 2010b). When some external input triggers sensory neurons in trigeminal ganglion activity passes via the brain stem, VPM and to LIV of S1 (Petersen 2007; Sato and Svoboda, 2010). LIV projections activate LII/III which in turn activates LVb (Armstrong-James and Fox, 1987; Brecht and Sakmann, 2002; Brecht *et al.,* 2003; Manns *et al.,* 2004; Lefort *et al.,* 2009; Hooks *et al.,* 2011). Projections from LII/III and LVa connect to M1 with strong targets mostly in upper layers such as LII/III and LVa but also have weak projections to LVb and LVI (Mao *et al.,* 2011). LII and LVa which receive strong input from S1 reciprocate projections back to S1 unto LII/III, LVa and strong synapses were found in LVb (Petreanu *et al.,* 2009) making a dual synaptic feedback loop (S1, L2/3/5A $\longleftrightarrow$ M1, L2/3/5A) creating connection between M1 and S1 as described in figure 1.9.

Figure 1.9 Sensorimotor circuit representing reciprocal and long-range connections.

Trans-cortical projections from M1 to S1 are represented in purple and red for projections from S1 to M1. Intra-cortical projections are denoted in blue, LII/III to LVa, LII/LIII to LVa and LVb in M1, LIV to LII/III, LII/III to LVb, LVa to LII/III in S1. Thickness of the lines represent connection strength. Targets of M1 include (LVb and LVI to PO (posterior thalamic nucleus) magenta, brainstem nuclei (LVb to BS, green), superior colliculus (LVa and LVb to SC, cyan), Zona inserta (LVa and LVb to ZI, orange). Adapted from Mao *et al.,* 2011.

1.12 Types of cells in cortex

Neurons in cortex are categorised as excitatory (glutamatergic/principal) pyramidal or stellate cells (pyramid or star-like like morphology) and inhibitory (GABAergic) non-pyramidal interneurons cells. In cortex, principal cells constitute about 80 % (Gao and Zheng, 2004; Halabisky *et al.,* 2006) whilst the rest comprises interneurons which play a critical role in regulating cortical activity and rhythmogenesis (Beaulieu *et al.,* 1992).

1.12.1 Pyramidal cells constitute most of the neuronal population and are known to be prime output cells in M1 (Sloper *et al.,* 1979). These cells also contribute to excitatory inputs within the local circuit in M1 due to the presence of axonal collaterals (Douglas and Martin, 2004). Electrophysiological studies in rats revealed two types of pyramidal cells in sensorimotor slices (Connors *et al.,* 1982; McCormick *et al.,* 1985; Van Brederode and Snyder; 1992; Chen *et al.,* 1996). Intrinsically bursting (IB) neurons are identified by their bursts of spikes followed by non-adapting and low frequency action potentials. In contrast to regular spiking (RS), pyrmaidal cells show adaptation in spike frequency (Chen *et al.,* 1996).

Layer V of M1 is characterised with specialised large, pyramidal cells called Betz cells like Meynert cells in visual cortex (Betz, 1874). Betz cells are 20 times the size of other

pyramidal cells in deep layers of cortex and constitute up to 12 % of total pyramidal population (Rivara *et al.,* 2003). Betz cells are classified into two types depending upon their projections. Type I cells have thick, tufted apical dendrites and perform intrinsic burst firing activity (Molnar and Cheung 2006) and have their projections to striatum, superior colliculus, spinal cord and basal pons. Type ll Betz cells are always regular spiking and have slender and obliquely aligned apical dendrites (Molnar and Cheung, 2006). These cells have their projections to ipsilateral striatum or contralateral hemisphere. Betz cells are further categorised depending on the increase or decrease of firing rate upon the injection of hyperpolarising current (Spain 1991a, 1991 b, 1994). Betz cells are larger but fewer in the superficial region (LVa) than in deep area (LVb).

1.12.2 Interneurons constitute a minority of the population yet are crucial for controlling network activity by forming short range connections and are known to inhibit the target cells by releasing GABA (McBain and Fishan, 2001; Somogyi and Klausberger 2005). Interneurons are often categorised based on morphology, physiology, histology but it is rather difficult to categorise them using electrophysiological methods due to overlapping characteristics (Kawaguchi, 1993; Jones, 1993; McBain and Fisahn, 2001). Broadly speaking, however, electrophysiological classification in M1 has revealed four types of interneurons: low threshold spiking (LTS), fast spiking cells (FS), regular spiking non-pyramidal cells (RSNP) and late spiking cells (LS) (Kawaguchi and Kubota, 1997) as described in table below.

Cell type	RMP (mV)	Spike width (ms)	Neurochemical substances	Morphological type	Synaptic targets
FS	-77.4- -73.0	0.43-0.59	parvalbumin, cholecystokinin	basket, chandelier	soma, AIS, thick dendrites
RSNP	-66.0- -60.06	0.75-1.06	somatostatin	Martinotti	thin dendritic branches
LTS, BSNP	~-57.5	0.94	VIP, calrectin, NPY	double bouquet	dendrites, soma
LS	~-67.2	0.77	calbindin	neurogliaform	dendritic spines

Table 1.1 Types of interneurons that M1 may contain and their properties

Various types of cells based on electrophysiological properties: FS (fast spiking), RSNP (regular spiking non-pyramidal), LTS (low threshold spiking), LS (late spiking). Neurochemical classification (immune positive to): parvalbumin, cholecystokinin, somatostatin, calrectin, calbindin. Morphological classification (based on the shape): Basket, chandelier, Martinotti, double bouquet, Neurogliaform. RMP: resting membrane potential (mV) FS<LS<RSNP<LTS, and spike width (ms), FS<LS≤RSNP<LTS. (Kawaguchi, 1995; Halasy *et al.,* 1996; Kawaguchi and Kubotoa, 1997; Cauli *et al.,* 1997).

Fast spiking cells (FS) are basket and chandelier type which fire at high frequency (non-adapting) upon depolarising current. They exhibit short half-width action potentials (AP) but large afterhyperpolarisation (AHP). FS cells are immunopositive for parvalbumin and cholecystokinin proteins (Kawaguchi, 1993a, 1993b; Kawaguchi, 1995; Kawaguchi and Kubota, 1997; Galarreta and Hestrin, 2002). Late spiking (LS) are neurogliaform cells with symmetrical dendrites. They show a delay in onset of action potential preceded by slow ramp to threshold level (Chu *et al.,* 2003). Firing can be generated from hyperpolarised and depolarised states and they also show non-adapting patterns of firing. These cells are immunopositive to calbindin. (Kawaguchi, 1995; Kawaguchi and Kubota, 1996). Low threshold spiking (LTS) are double bouquet-like cells, immunopositive for calretinin. These cells show multiple spike behaviour on current injection (Kawaguchi and Kubota, 1997; McBain and Fisahn, 2001). Regular spiking non-pyramidal cells (RSNP) are different to those that are described above. Regular and adapting spike behaviour was noticed

displaying two groups based on the "notch" after spike behaviour upon application of depolarising current (Kawaguchi and Kubota, 1996, 1997 and 1998).

1.12.3 Inhibition in cortex

Synaptic inhibition in cortex is present in diverse groups of GABAergic interneurons (as described above in 1.12.2 section) and are classified based on their morphology, chemical and electrical properties (Fishell and Rudy, 2011). There are distinct subtypes of interneurons based on the chemical they produce which include: Parvalbumin (PV) neurons, somatostatin (SOM) neurons, vasoactive intestinal polypeptides (VIPs) producing neurons and calbindin (CB) in mouse neocortex (Xu *et al.,* 2010). PV neurons are identified to target cell bodies and proximal dendrites of pyramidal cells to control pyramidal activity (Thomson and Lamy, 2007, Tanaka *et al.,* 2011). The mutual connections between basket shaped fast spiking neurons have also been reported to be primarily on soma and proximal dendrites in majority of populations by performing paired recording experiments and light microscopic analyses (Gupta *et al.,* 2000; Tamas *et al.,* 2000). However, immunoreactivity for connexin36 protein has revealed that gap junctions were distributed not just on proximal but the distal dendrites in rat neocortex (Fukuda and Kosaka, 2003; Fukuda *et al.,* 2006). Martinotti cells which are SOM producing cells target distal dendrites of pyramidal cells (Kawaguchi and Kubota, 1997). VIP+ and CR+ neurons have known to modulate local SOM+ cells enabling dendritic disinhibition to pyramidal neurons in cortex (Lee *et al.,* 2013) and this disinhibition was found to be engaged in specific behavioural states. The activity of VIP+ cells was high in S1 during whisking (Lee *et al.,* 2013)

1.13 Neurotransmitters, receptors and mechanism of action in cortex

1.13.1 GABA

γ-Aminobutyric acid (GABA) is the main inhibitory neurotransmitter in the mammalian central nervous system (CNS) (Bormann, 2000) which controls neuronal firing, network oscillation and regulates excitability of neurons (Kullmann *et al.,* 2012). GABA was identified in brain tissue in 1950 (Roberts, 1950; Awapara, 1950) but the inhibitory action of GABA was only identified in 1956 by Takashi Hayashi and Nagai (Hayashi and Nagai, 1956; Hayashi, 1956). L-glutamic acid decarboxylase is an enzyme that promotes the synthesis of GABA in presynaptic neurons which is stored in synaptic vesicles (Jin *et al.,* 2003). GABA is released at the synapse from vesicles upon neuronal activation. A number of GABA are released from a single vesicle fusion into synaptic cleft, raising the concentration of GABA in millimolar range (Mody *et al.,* 1994; Mozrzymas *et al.,* 2003; Mozrzymas 2004) which can act either on post synaptic receptors or on extra synaptic receptors by diffusing to

extracellular space. GABA transporters take up GABA away from postsynaptic receptors (Cherubini 2001; Deken *et al.,* 2003). The balance between GABA release from synaptic vesicles and uptake of GABA by transporters regulate the extracellular GABA levels (Deken *et al.,* 2003). Mode of action of GABA can be via fast acting ionotropic GABA$_A$ and GABA$_C$ receptors or slow acting metabotropic GABA$_B$ receptors (Bormann 2000). Ionotropic GABA$_A$ receptors are predominant type of GABA$_A$Rs (Bowery *et al.,* 1987) which are known to constitute about 20-50% synapses in the brain (Nutt and Malizia, 2001).

1.13.2 GABA$_A$R are pentameric ion channels consisting of 21 distinct subunits (α1-8, β1-3, γ1-3, δ, ε, π, θ and ρ1–3) and a central pore which is permeable to anions (Cl$^-$ and HCO$_3^+$) (Bormann, 1987; Kaila, 1994; Wafford *et al.,* 1996; Whiting *et al.,* 1997; Wafford *et al.,* 2005; see figure 1.10). The combination of various subunit binding sites creates ligand specific sites for benzodiazepines and barbiturates (Mohler, 1992; Wafford *et al.,* 1993; Graham *et al.,* 1996). GABA$_A$Rs have been identified both pre-and post-synaptic neurons in various regions in the brain. In rats these receptors are found more in LII/III than in LV and are implicated to play a role in cortico-cortical connections (Jones and Wise, 1977; Jones *et al.,* 1986). Moreover, GABA$_A$R expression was found to be denser in sensory regions than motor regions (Zilles *et al.,* 1995).

In most mature neurons, equilibrium potential of Cl$^-$ becomes more negative than resting membrane potential via KCC2 (potassium chloride co transporter) activity which enables receptor activation with an influx of Cl$^-$ and response is measured as IPSP (inhibitory post synaptic potential). This hyperpolarisation effect and increase in conductance shunt excitatory inputs which in turn decreases the probability of action potential generation (Payne *et al.,* 2003; Farrant and Nusser, 2005). However, hyperpolarising GABA input is not always functionally inhibitory as recovery from deep hyperpolarisation may sometimes activate excitatory conductances which generate rebound spikes (Chavas *et al.,* 1994; Llinas *et al.,* 1988). Similarly, when the concentration of Cl$^-$ is higher inside the cell, opening of GABA receptors may cause efflux of the anion, thereby generating action potentials (Staley, 1992; Owens *et al.,* 1996). Interestingly, GABA response is depolarising in most immature neurons due to the lack of KCC2 and presence of NKCC1 (sodium and potassium coupled co-transporter) (Riwera *et al.,* 1999; Riwera *et al.,* 2005). The depolarising action of GABA is also seen in some mature neurons (Chavas *et al.,* 2003; Stein *et al.,* 2003), however, in mature cells under normal circumstances activation of GABA$_A$R generates inhibition in two ways described below.
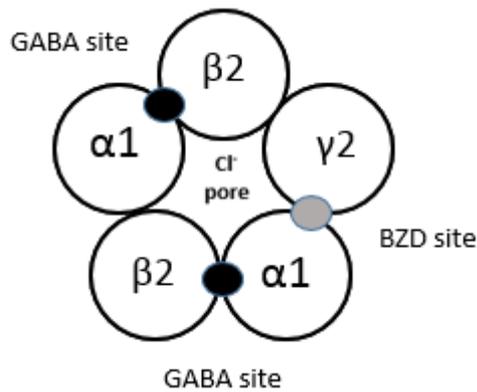
Figure 1.10 Representation of a typical GABAAR structure.

A pentameric structure which consists of two GABA binding sites (black) between α and β subunits whilst the benzodiazepine site (grey) exists between α and γ subunits with a central pore for Cl⁻ transmission.

1.13.3 Types of Inhibition

1.13.3.1 Phasic Inhibition

Phasic inhibition is rapid (short lasting) and precise transmission mediated by synchronous activation of small number of GABA$_A$R at synapses. The mechanism involves the presynaptic calcium influx which initiates the fusion of vesicles that contain GABA upon arrival of an action potential. Each vesicle is known to release several thousand GABA molecules (with a synaptic concentration in mM) onto a few hundred receptors located on post synaptic neurons. These receptors witness large number of molecules for a short duration enabling synchronous opening of the pore for Cl⁻ travel across the membrane generating IPSPs (Edwards *et al.,* 1990; Mody *et al.,* 1994; Nusser *et al.,* 1997; Brickley *et al.,* 1999). Studies using low affinity competitive antagonist revealed that decay of GABA concentration and GABA binding occurs at time constants of < 500 μs (Overstreet, 2002) and about 100 μs (Mozrzymas *et al.,* 2003; Mozrzymas *et al.,* 2004) respectively which inputs to short duration and fast diffusion from synapse. The occupancy of various receptors varies between synapses on a single neuron or on multiple neurons. Vesicle size, nature of fusion, geometry of synapse, arrangement of GABA transporters and postsynaptic receptor expression and conformational changes of receptors during ion transition are the various factors that contribute to phasic inhibition (Frerking *et al.,* 1996; Nusser *et al.,* 1997; Perrais *et al.,* 1999; Hajos *et al.,* 2000; Mozrzymas *et al.,* 2003) leading to decrease in number of IPSCs and amplitude.

1.13.3.2 Tonic Inhibition

Tonic inhibition is long lasting transmission by activating non-synaptic $GABA_A R$ (Connolly and Wafford, 2004), often via spilling of extracellular GABA causing diffusion away from the synaptic cleft which then activates receptors on extra- and peri-synaptic sites that contain alpha6 or delta subunits, which display a high affinity for GABA binding (Farrant and Nusser, 2005). This type of inhibition was reported in rat cerebellar granule cells in voltage clamp recording (Kaneda *et al.,* 1995a), then in hippocampus (Semyanov *et al.,* 2003), dentate gyrus (Nusser and Mody, 2002), pyramidal cells in LV of somatosensory cortex (Keros and Hablitz *et al.,* 2005; Yamada *et al.,* 2007). It was identified that pyramidal neurons may require an additional increase in GABA concentrations whilst interneurons are thought to display tonic inhibition without any external GABA (Seymanov *et al.,* 2003; Scimemi *et al.,* 2005). It was evident that tonic activation was noticed in embryonic neurons prior to synapse formation (Valeyev *et al.,* 1993; LoTurco *et al.,* 1995; Owen *et al.,* 1999; Demarque *et al.,* 2002). Several studies revealed that reduction of spontaneous IPSCs as well as decrease in holding current suggesting the reduction in conductance due to the decrease in open $GABA_A R$ channels (Kaneda *et al.,* 1995b; Brickely *et al.,* 1996; Tia *et al.,* 1996; Wall *et al.,* 1997). Ambient GABA may be enough to activate persistent tonic conductance which was thought to be nM to mM concentration range (Tossman, 1986; Lerma *et al.,* 1986; Kennedy *et al.,* 2002; Xi *et al.,* 2003). Tonic currents play a role in setting the frequency of neuronal network oscillations, hence tonic NMDAR activity on interneurons in mouse CA3 increase the frequency of gamma oscillations while delta subunit containing $GABA_A R$ mediated tonic inhibition decreases gamma frequency (Mann and Mody, 2010). Therefore, the balance between tonic inhibition and tonic excitation is critical for modulating gamma oscillations via progressive interneuronal synchronisation (Mann and Mody, 2010).

1.13.4 $GABA_B R$ are G-protein coupled metabotropic receptors (Hill and Bowery, 1981, Bowery *et al.,* 1983, Bowery, 2002) which acts via intracellular transduction cascades by regulating calcium and potassium channels and are expressed in both presynaptic and postsynaptic neurons (Axmacher and Draguhn, 2004). Reversal potential of slow IPSP mediated by $GABA_B R$ is -100 mV. Pre-synaptically, they have been implicated in inducing membrane hyperpolarisation or shunting the action potential by inhibiting the opening of voltage gated Ca^+ channels leading to inhibition of GABA release. Post-synaptically, they generate long lasting hyperpolarisation by activating inwardly rectifying K^+ channels (GIRK channels) (Gage, 1992; Kulik, 2006). $GABA_B Rs$ can be pharmacologically isolated by activation via baclofen and blocked by 2-OH-saclofen (Terunuma *et al.,* 2010).

1.14 Glutamate

Glutamate is a crucial excitatory neurotransmitter in CNS and has been known to play a significant role in several functions (Hollmann and Heinemann, 1994; Monaghan *et al.,* 1989). Glutamate acts on two different type of receptors: ionotropic and metabotropic (Pin and Duvosin, 1995). Ionotropic receptors (iGluR) are further divided (based on the agonist sensitivity) in to AMPA (α-amino- 3-hydroxy-5-methyl-4-isoxazole-propionic acid), NMDA (N-methyl-d-aspartate) and KA (Kainate) receptors (Watkins and Evans, 1981). Metabotropic receptors (mGluR) are categorised to three groups (I, II and III) which are G-protein coupled receptors (Nakanishi, 1994).

1.14.1 AMPAR are tetrameric, either homo or heteromeric (Nakanishi *et al.,* 1990; Rosenmund *et al.,* 1998) structures formed of different combination of subunits: GluA1-4 (Keinanen *et al.* 1990; Hollmann, 1999; Dingledine, 1999). AMPARs are activated directly by glutamate leading to postsynaptic membrane potential by allowing the influx of Na^+ and K^+. Therefore, the reversal potential EPSP mediated via non-NMDAR (AMPA) is 0 mV. Different combinations of AMPAR subunits have significant impact on receptor functions as the receptor kinetics and ion selectivity are dependent on subunit compositions (see review Traynelis *et al.,* 2010). For instance, slow gating properties have been identified in a receptor containing GluA2 subunit compared to one that lack GluA2 subunit (Lomeli *et al.,* 1994; Swanson *et al.,* 1997) and increased receptor kinetics was identified in receptors containing GluA4 subunit (Swanson *et al.,* 1997). PV-positive hippocampal interneurons are known to express low GluA2 and high GluA4 (Geiger *et al.,* 1995; Pelkey *et al.,* 2015) resulting in rapid EPSPs and high Ca^{2+} permeability (Geiger *et al.,* 1995; Lawrence and McBain, 2003) when compared to pyramidal cells (Hestrin, 1993). GluA2 subunit containing AMPAR have been found to be Ca^{2+} impermeable whilst the other subunits combine to form a Ca^{2+} permeable receptors (Hollmann *et al.,* 1991; Verdoorn *et al.* 1991). The expression of fast acting Ca^{2+} permeable AMPAR on fast spiking interneurons was found to be a requirement for control of oscillatory activity (Bartos *et al.,* 2007, Hu *et al.,* 2014). Also, PV-positive interneurons of cortex have shown a correlation between action potential timing and EPSCs which are AMPAR mediated (Helm *et al.,* 2013). Moreover, over expression of GluA2 subunit in GAD67-positive interneurons has shown significant disruption in long range synchronization (Fuchs *et al.,* 2001). Furthermore, GluA1 and A4 subunit KO on PV-positive interneurons altered gamma oscillations and hippocampal memory (Fuchs *et al.,* 2007). These studies (above) suggest a role of subunit combination in network entrainment and a need for new subunit specific targets.

Rapid kinetics of AMPAR produces fast EPSPs which enables rapid synaptic transmission in CNS. Gamma oscillations have been found to decrease in power in rats upon the application of AMAPAR antagonists or by genetically reducing AMPA currents implying a significant role of this receptor in the maintenance of gamma oscillations (Cunningham *et al.,* 2003, 2004; Palhalmi *et al.,* 2004; Fuchs *et al.,* 2007). In contrast, a study by Fisahn *et al.,* (2004) on mice demonstrated that AMPAR antagonist did not alter oscillation suggesting AMPAR do not contribute to gamma oscillations. These contradicting reports of AMPAR sensitivity could be due to the species like rat vs mouse, the area of experiment: hippocampus (AMPAR-sensitive) or entorhinal cortex (insensitive) and AMPAR antagonists used (SYM2206, GYKI 53655).

1.14.2 NMDAR are tetramers, consists of GluN1 and GluN2 (A-D) subunits (Hollmann, 1999; Dingledine, 1999) with GluN1 being the obligatory subunit for functional receptors and most receptors comprising combinations of GluN1 and GluN2 subunits of various subtypes. When the pore is open, Ca^{2+} influx is initiated by which various intracellular process such as second messenger signalling cascades in the post-synaptic neuron are activated due to rather slow activation and deactivation kinetics of NMDARs when compared to AMPAR. But, the permeability of these receptors at hyperpolarised membranes (negative membrane potentials) is limited due to the block of the receptor pore by Mg^{2+}. Hence, the activation of NMDAR requires depolarisation (>40 mV) (Mayer, 1984; Nowak, 1984). NMDAR expression varies across various brain regions and is known to be regulated by development and disease conditions (Watanabe *et al.,* 1992; Monyer *et al.,* 1994; Akbarian *et al.,* 1996; Purcell *et al.,* 2001; The pharmacological properties of these receptors have been known to be determined by subunit compositions (McBain and Mayer, 1994; Traynelis *et al.,* 2010). NMDARs containing GluN2A generate rapid kinetics whilst those containing GluN2B have slower kinetics and GluN2C and GluN2D even slower kinetics. The slowest decay (т ~ 2s) was identified in receptors with di-heteromeric receptors of GluN1 and GluN2D subunits (Vicini *et al.,* 1998). Knockout mice studies revealed that slow gating GluN2B and GluN2D are highly expressed in early development stages, whilst, GluN2A is highly expressed at later stages which enhance the synaptic responses in hippocampus (von Engelhardt *et al.,* 2015).

Earlier findings assumed that NMDARs have minimal contribution to fast synaptic transmissions in interneurons when compared to pyramidal cells. However, various studies after extensive research suggested that NMDAR contribution depend on subunit composition and type of interneuron. NMDAR mediated EPSPs have been documented at low levels of Mg^{2+} (Bekkers and Stevens, 1989; Watt *et al.,* 2000; Myme *et al.,* 2003) or at depolarised potentials (McBain and Dingledine, 1992). It is interesting to note that NMDAR

correlates with AMPAR expressed on same neuron (McBain and Dingledine, 1993, Monyer *et al.,* 1994; Matta *et al.,* 2013; von Engelhardt *et al.,* 2015). When NMDA mediated currents were pharmacologically blocked synapses containing AMPA/NMDAR has shown a significant decrease in summation of EPSPs and hence reduction in action potential firing irrespective of ratios of AMPA/NMDARs (Lei and McBain, 2002). Augmented activation of NMDAR has been observed in stroke and trauma (Nicoletti *et al.,* 1996) also in neuro-degenerative disease like Parkinson`s and Huntington`s (Shaw, 1993).

1.14.3 KAR are homo or heteromeric structured, consisting of following subunits: GluK1 (GluR5) (Bettler *et al.,* 1990), GluK2 (GluR6) (Egebjerg *et al.,* 1991), GluK3 (GluR7) (Bettler *et al.,* 1992), GluK4 (KA1) or GluK5 (KA2) (Werner *et al.,* 1991; Herb *et al.,* 1992, Lerma, 2001; for review see Traynelis *et al.,* 2010 and Akgul and McBain, 2016). KARs were expressed widely in the brain both on pyramidal neurons and interneurons (Wisden and Seeburg, 1993). Higher expression of GluK1, 2 and 4 have been identified on interneurons that regulate both pre- and post-synaptic activity (Fisahn *et al.,* 2004; Lein *et al.,* 2007; see review Carta *et al.,* 2014). Post-synaptic KAR are known to modulate neuronal excitability by integrating only excitatory synapses, due to their slow kinetics (Frerking and Nicoll, 2000; Pinheiro *et al.,* 2013). However, KARs located pre-synaptically regulate NT release at both inhibitory and excitatory synapses (Cossart *et al.,* 2001; Lerma and Marques, 2013). Exogenous application of micromolar concentration of KA pre-synaptically reduced inhibitory effects of CA1 interneurons on to principal cells (Fisher and Alger, 1984; Kehl *et al.,* 1984; Rodriguez-Moreno *et al.,* 1997). Various pharmacological and genetic experiments have revealed conflicting results due to poor receptor specific pharmacology as well as lack of specific targets (Mulle *et al.,* 2000; Fishan *et al.,* 2004). KAR, like AMPAR are activated by glutamate release but are known to have much slower kinetics (decay t ~10 ms) and low amplitude EPSCs (Cossart *et al.,* 2002; Goldin *et al.,* 2007). KAR, sometimes act via metabotropic mechanisms without depending on depolarisation (Rodriguez-Moreno and Lerma, 1998; Frerking *et al.,* 2001). In a study by Frerking and Ohliger-Frerking (2002) revealed that AMPAR induce transient, variable membrane depolarisations, whilst KARs trigger tonic depolarisations with low variability.

Application of nano molar concentration of KA (and/or CCh) has generated persistent gamma oscillations *in vitro* in primary motor cortex (Johnson, 2016), somatosensory cortex (Buhl *et al.,* 1998; Cunningham *et al.,* 2003), hippocampus (Hajos *et al.,* 2000, Hormuzdi *et al.,* 2001, Fisahn *et al.,* 2001, Modebadze, 2014). GluK1 and K2 KO mice experiments performed have revealed a critical role of these subunits since it was not possible to induce gamma oscillations (Fisahn *et al.,* 2004). It was assumed in this study that GluK1 KARs were localised on the axons of interneurons and did not contribute to oscillatory activity

whilst GluK2 subunit containing KARs were located on somato-dendritic area of interneurons and pyramidal cells which enhanced action potential firing upon activation, which enabled GABA and glutamate release. However, it was not possible to induce oscillatory activity in the presence of GluK1 antagonists suggesting the role of this subunit in maintaining gamma oscillations (Stanger *et al.,* 2008). Moreover, KARs have been implicated in spike entrainment at theta frequencies in oriens lacunosum-moleculare (OLM) cells (Goldin *et al.,* 2007) suggesting a significant role of KARs in oscillatory activity. Furthermore, KARs have implicated to contribute to slow wave oscillations SWO, as SWO was abolished upon the application of the GluK1-slective KAR antagonist, UBP302 (Cunningham *et al.,* 2006; Sheroziya *et al.,* 2009). Interestingly, KAR also plays a critical role in epilepsy since systemic administration of KA has been used as a widely accepted model for investigating seizures like those observed in temporal epilepsy (TLE) (Ben-Ari *et al.,* 1985).

iGluRs are known to play a significant role in synchronising network activity by recruiting inhibitory interneurons. Recent subunit knockout studies (Akgul and McBain *et al.,* 2016) revealed the sub-unit composition expressed on type of interneurons were involved in the network oscillations (some examples are shown in table below).

sub-unit knockout	Interneuron subtype	physiological effect	oscillatory effect	reference
AMPAR (GluR$_{1-4}$)	PV (PV-Cre), GAD67	decrease in AMPA mediated EPSPs, altered firing	altered gamma oscillations, disrupted long range synchrony	Fuchs *et al.,* 2007
NMDAR (N$_{2C}$, N$_{2D}$)	GAD67, Ppp1r2-Cre	increased EPSP amplitude,decreased frequency	Reduced synchronous activity	Kelsch *et al.,* 2012, Belforte *et al.,* 2010
KAR (GluK$_{1-2}$)	Global	does not increase IPSC frequency	disrupted/enhanced kainate induced gamma oscillations	Mulle *et al.,* 2000, Fishan *et al.,* 2004

Table 1.2 Role of iGluR subunits in various physiological and oscillatory activity Adapted from Akgul and McBain *et al.,* 2016

1.14.4 mGluR are classified in to three groups based on the subunit sequence homology. Postsynaptically expressed, group I (mGluR1, mGluR5) are positively coupled to phosphoinositide (PI) which increases cyclic AMP (cAMP) via second messenger cascades and are known to enhance neuronal excitation. In contrast, presynaptically expressed group II (mGluR2, mGluR3) and III (mGluR4, mGluR6, mGluR7, mGluR8) mGluRs are negatively coupled to adenylyl cyclase and inhibits cAMP which accounts for the reduction in synaptic transmission (decrease in excitation). Group II and III also regulate glutamate release by acting as auto receptors in presynaptic neurons (Schoepp *et al.,* 1992; Shigermoto *et al.,* 1997) playing a role in both LTP (upregulate glutamate release) and LTD (downregulate glutamate release) (Holscher *et al.,* 1999). However, peri-synaptic expression of group I mGluR often regulate the excitability of neurons via iGluR channels (Shigermoto *et al.,* 1993; Baude *et al.,* 1993; Shigermoto *et al.,* 1997). mGluRs have been implicated in many process like neuronal development, neurodegeneration, synaptic plasticity, learning and memory (Nakanishi, 1994; Pin and Bockaert, 1995; Pin and Duvosin, 1995; Conn and Pin, 1997; Dale *et al.,* 2003).

1.15 Dopamine

Dopamine (DA), a catecholamine present in the brain, was identified as a neurotransmitter in 1972 (Brown and Maknman, 1972; Kebabian *et al.,* 1972). Pharmacological evidence revealed the presence of more than one binding sites for DA DA receptors can be classified as D1-like and D2-like based on their differential coupling to AC (Kabebian and Calne, 1979). D1 (D1 and D5) receptors activate Gαs/olf family of G-proteins and thus enhance cAMP. (Dearry *et al.,* 1990; Monsma *et al.,* 1990; Zhou *et al.,* 1990) and D1R are found exclusively on post synaptic neurons such as medium spiny neurons (MSNs) in striatum. D2 (D2, D3, D4) receptors unlike D1, are expressed in both pre- and postsynaptic terminals and known to be negatively coupled to AC via Gαi/o family of G proteins (Sokoloff *et al.,* 2006; Rankin *et al.,* 2010; Rondou *et al.,* 2010). It is evident that DA induces long lasting effect via different mechanisms (reviewed in Jay 2003; Luft and Schwarz, 2009) which include: intracellular Ca^{2+} levels (via L-type channels) increase and decrease upon activation of D1 and D2 receptors respectively (Neve *et al.,* 2004), increased cAMP due to the activation of D1R (but not D2R) activates (protein kinase A) PKA which in turn enhances the currents mediated by AMPA and NMDA receptors (Snyder *et al.,* 1998; Gurden *et al.,* 2000; Wang and O`Donell, 2001) as illustrated in the figure 1.10.

Aston University

Illustration removed for copyright restrictions

Figure 1.11 Representation of various signal transduction mechanisms of action D1-like and D2-like receptors.

D1-like receptors are positively coupled to AC whilst the opposite is true for D2-like receptors and their corresponding effects on K^+ channels, Arachinoid acid, Na^+/H^+ exchange, Na^+-K^+-ATPase. + indicates positively coupled and – indicates negative coupling, AC-adenylate cyclase, PLC- phospholipase C (adapted from Missale *et al.,* 1988).

The physiological roles of DA include (but are not limited to) sleep, immune system, renal functions and sympathetic regulatory function (Snyder *et al.,* 1970; Missale *et al.,* 1998; Sibley, 1999; Carlsso, 2001; Iversen and Iversen 2007). On the other hand, several studies have implicated a role of DA in pathological conditions such as Parkinson`s disease from loss of dopaminergic innervation (Ehringer and Hornykiewicz, 1960), Schizophrenia (Snyder *et al.,* 1970; Creese *et al.,* 1976; Seeman *et al.,* 1976; Carlsson *et al.,* 2001) and associated with drug abuse (Hyman *et al.,* 2006; Di Chiara and Bassareo, 2007; Koob and Volkow, 2010).

Network activity in primary motor cortex (M1) has been shown to be modulated by DA (Alexander *et al.,* 1986). D1 and D2 receptors have a crucial role in direct and indirect pathways associated with Parkinson`s disease (Ueki *et al.,* 2006). D1R is more abundant than D2R in rat cortex (Boyson *et al.,* 1986). M1 and PFC (pre-frontal cortex) show similar organization of DR although M1 expresses fewer DR than PFC (Lidow *et al.,* 1989). The laminar distribution of both receptors is found to correspond to dopaminergic terminals in M1 which are predominately in deep layers (LV and LVI) (Martes *et al.,* 1985; Dawson *et al.,* 1986).

Additionally, recent studies have indicated that DA modulates tonic currents in various regions of brain (Aman *et al.,* 2006; Yague *et al.,* 2013; Liang *et al.,* 2014) and may directly inhibit GABA-R (Hoerbelt *et al.,* 2015). These novel activities of DA may impel new definitions of dopaminergic signalling in the brain.

1.16 Aims and Objectives

The primary objective of this thesis is to explore the oscillatory cortical dynamics at different frequencies that were induced by various pharmacological manipulations. Given the inadequate *in vitro* research, we aimed to explore delta, nested theta and gamma oscillations in primary motor and sensory cortices in rat brain slices. Studies have implicated M1 in execution of voluntary movements and S1 in sensory information from both local network *in vitro* and whole brain *in vivo* perspectives and interactions between these two regions are known to play critical roles in motor learning and control skills (Asanuma and Arissian, 1984; Asanuma and Pavlides, 1997) which forms the basis for choosing M1 and S1 in our study.

Objectives:

- To explore oscillatory activity in primary motor cortex (M1) and primary sensory cortex (S1) using KA and CCh using extracellular, local field potential (LFP) recordings from control rats.
- To induce and characterise the origin and mechanisms involved in delta oscillations in M1 and S1 using pharmacological manipulations.
- To investigate interactions between rhythms in M1 and S1.
- To examine the role of dopamine in tonic and phasic inhibition by using single cell patch clamp technique.

2 Methods

2.1 Animals and ethical approval

All the experiments were carried out in accordance with the Animals (Scientific Procedures) Act 1986 UK, European Communities Council Directive 1986 (86/609/EEC) and the Aston University ethical review document.

2.2 Slice preparation

Sagittal slices containing primary motor cortex (M1) and somatosensory cortex (S1) were obtained from male Wistar rats (50-70 g). Initially, rats were anesthetized by placing them in a chamber containing 2% Isoflurane and N_2/O_2 and then by injecting pentobarbital (600 mg/kg) subcutaneously (SC). Xylazine (100 mg/kg) was administered through the intramuscular route and when pedal reflexes were completely lost transcardial perfusion was performed with ice-cold sucrose based artificial cerebrospinal fluid (aCSF). aCSF contained (mM): 180 sucrose, 2.5 KCl, 10 $MgSO_4$, 25 $NaHCO_3$, 1.25 NaH_2PO_4, 0.5 $CaCl_2$, 10 glucose, 1 L-ascorbic acid, 2 N-acetyl-L-cysteine, 1 taurine, 20 ethyl pyruvate. Neuroprotectants such as 0.04 indomethacin, 0.3 uric acid and 0.2 aminoguanidine were also added and aCSF was saturated with carbogen (95% O_2, 5% CO_2). The brain was carefully extracted and sagittal slices of 450 μm thickness for extracellular recordings and 350 μm thickness for intracellular recording were prepared using a vibrating microtome (Campden Instruments, UK) using the same solution at room temperature. Prepared slices for extracellular recording were then stored in an interface chamber (Scientific System Design Inc., Canada) whereas slices for intracellular recording were submerged in aCSF which was constantly bubbled with carbogen at room-temperature and was composed of glucose-based aCSF containing (mM): 126 NaCl, 3 KCl, 1.6 $MgSO_4$, 26 $NaHCO_3$, 1.25 NaH_2PO_4, 2 $CaCl_2$, 10 glucose. 0.04 of indomethacin (a cyclooxygenase inhibitor) and 0.3 of uric acid were added as neuro-protectants to improve cell viability (Pakhotin *et al.,* 1997; Rice *et al.,* 1994). Slices for extracellular recordings were then immediately transferred carefully unto a recording chamber (Scientific System Design Inc., Canada), where they were perfused with glucose-based aCSF at a flow rate of 2 ml/min for an hour before recording. PTC03 proportional temperature controller (Scientific System Design Inc., Canada) was used to maintain 33-34 °C. Slices for intracellular recording were placed in submerged holding chamber for an hour prior to being placed into a submerged recording chamber and allowed to settle for 15 minutes prior to recording.
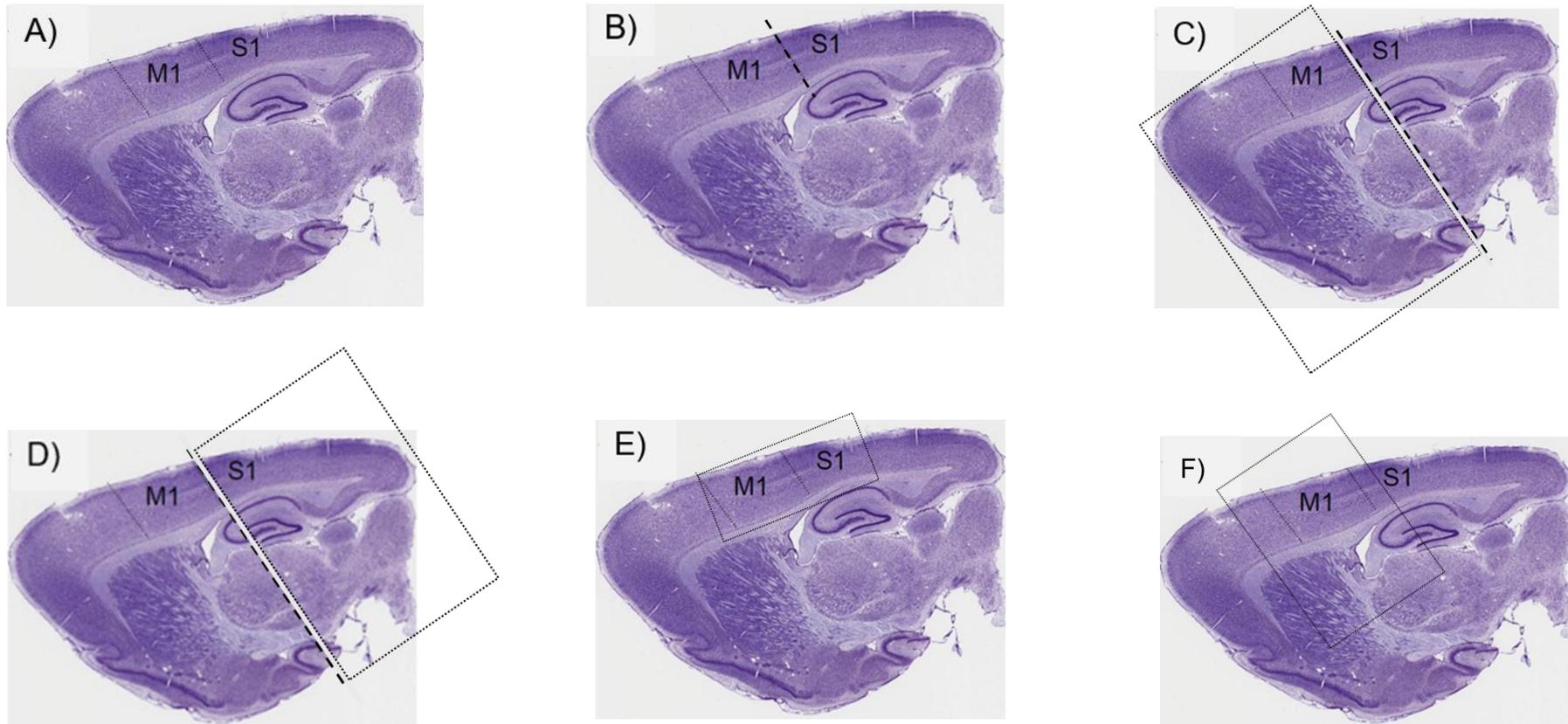
Figure 2.1 Representation of various types of rat brain slice preparations used for extracellular and intracellular recordings.

Nissl stained sagittal sensory motor slice locating Primary motor cortex (M1) and primary somatosensory cortex (S1). Adapted from The Rat Brain Atlas (Paxinos and Waston, 1998). **A)** Sensory motor sagittal slice with both M1 and S1 intact, areas of each region were represented by lines. **B)** Sensory motor sagittal slice with a micro-cut made between M1 and S1 regions only, which was represented by a dashed line. **C)** Primary motor cortex sagittal slice (boxed area) segregated from sensory motor slice. **D)** Primary somatosensory cortex (boxed area) segregated from sensory motor slice. Cut was made all through the slice separating M1 and S1 which was represented by dashed line in C and D. **E)** micro slice with just M1 and S1, isolated from rest of the slice (boxed area). **F)** M1 slice isolated from a sensory motor slice with surroundings intact. This type of slice was used for intracellular recordings whereas all the other types of slices were used for extracellular recordings.

The M1 region of the cortex was identified as being dorsal to the lateral ventricle and the caudal extent of the striatum and S1 being adjacent to M1 dorsal to hippocampus. With the aid of The Rat Brain Atlas (Paxinos and Waston, 1998) various types of slices were prepared based on regions of interest as illustrated in figure 2.1. These different types of slices were used to perform region-specific studies and correlation studies. Type A slices were 450 μm in thickness used for extracellular recordings. This type of slice contain intact M1 and S1 and recordings were made from one region or simultaneously from both regions. Type B slices are the same as type A except a cut (dashed line in figure 2.1) was made between M1 and S1 using a surgical scalpel blade and were carefully transferred on to the recording chamber where they were settled for an hour before recording. Simultaneous recordings were made from this type of slice which was used to determine the correlation between rhythms in the two regions. Type C slices were again 450 μm thick and were used for extracellular recordings. M1 was isolated from sensory motor slice by cutting all through the slice and boxed region from the figure C was used for region-specific recording. Type D slices were same as type C but this type has S1 isolated (boxed region) from the sensory motor slice. Type E slices were also 450 μm thick and were used for extracellular recordings but this type is a micro slice with just M1 and S1 isolated from rest of the sensory motor slice. This isolation was made diligently with surgical scalpel blade and were transferred to the recording chamber. Type F slices were 350 μm thick and were used for intracellular recordings. This type of slice had M1 with surroundings intact (boxed region in figure 2.1). These slices were carefully transferred to and submersion chamber to settle before experiments. All the recordings were made from layer V of both M1 and S1 (unless otherwise stated) which was located through visual inspection using microscope (Olympus BX51W1, Japan) unless otherwise stated.

2.3   Extracellular recordings

Local Field Potentials (LFPs) of neuronal network activity were recorded using an extracellular field potential technique. LFPs reflect local neuronal network mechanisms of a specific brain region and are known to arise from activity within approximately 250 μm at the tip of electrode. These recordings are often used to investigate synchronous activity of neuronal networks (Logothesis, 2003; Mitzdorf, 1985; 1987; Rasch *et al.,* 2007). A Flaming-Brown micropipette puller (Sutter Instruments, CA) was used to pull borosilicate glass microelectrodes with open tip resistance of 2-3 MΩ which were placed into Layer V of M1 and/or S1 using the rat brain atlas of Paxinos and Watson (Paxinos and Waston, 2012) as a reference by viewing under a LEICA MZ6 field microscope. The activity was recorded using an EXT amplifier head-stage (NPI electronics GMBH, Germany) mounted on to a

manually operated micromanipulator (MM-33; Narishige, Japan). The signal was amplified 10 x using an LHBF-48X preamplifier/signal conditioner (NPI, Germany) set to band-pass filter between 700 Hz and 0.1 Hz and then amplified a further 100 times using EXT-102F amplifier (NPI, Germany). Humbugs (Quest Scientific, Canada) signal conditioners were used to eliminate low amplitude (<100 μV p-p) 50 Hz noise. The signal was simultaneously digitised using a CED 1401 digital converter in to a disk using Spike2 software (figure 2.2).
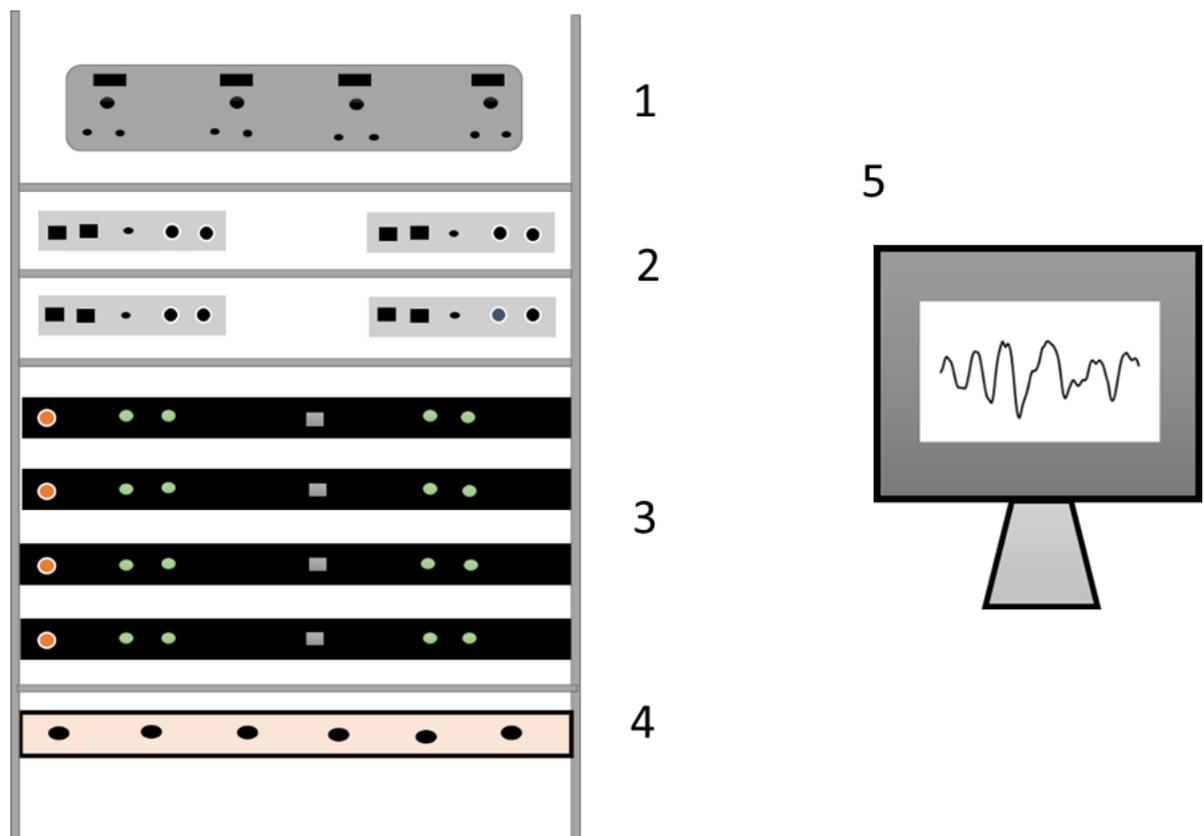
Figure 2.2 The extracellular local field potential recording setup

The signal from micro-electrode which was mounted onto head stage was amplified 100x by EXT 10-2F amplifier (1), 50 Hz noise was eliminated by humbugs (2), signal was further amplified (x10) and high and low pass filtered by LHBF-48X amplifiers (3) signals was then converted from analogue to digital signal by CED 1401 digitizer (4) recordings were made and saved on a PC (5).

2.3 Intracellular recordings

Patch clamp technique was used to make whole cell recordings of synaptic currents. A Flaming-Brown micropipette puller (Sutter Instruments, CA) was used to pull borosilicate glass microelectrodes of 4-6 MΩ. The tip of the electrode filled with internal solution (composition below) was then carefully placed on the surface of the neurons located visually using infra-red video microscopy with differential inference contrast (DIC) optics (Olympus, BX51WI) which enabled the visibility of neurons located in deep surface of the slice. Cells with smooth edges tends to give successful patch recordings. Slight positive pressure was applied from inside the electrode to maintain the resistance of the electrode by keeping off contamination. The tip of the electrode was advanced onto the chosen cell. Pipette offset was reset to zero and signs for slight rise in resistance and indentation of the cell membrane were examined, which indicates the electrode tip was on the neuron surface. As soon as the tip was confirmed to have contacted the membrane, positive pressure was turned off and a natural suction was noticed, after which gentle mouth suction was applied to seal the tip onto the membrane. At this stage pipette capacitance was compensated. When gigaseal (>1 GΩ as measured using a 5 mV step injected at line frequency) was observed, a gentle suction was applied to rupture the membrane under the patch electrode tip, with the pipette holding current set to -70 mV. A sudden appearance of large capacitance transients at the leading and trailing edges of the pulse is an indication of successful breakthrough.

2.3.1 Voltage clamp

Voltage clamp technique was used to characterise phasic and tonic inhibitory currents in the layer V of M1 the rat brain atlas of Paxinos and Watson as a reference. In this technique membrane potential was held constant (-70 mV) so that the current flow resulting from ion channel opening was measured in pA in the form of Inhibitory Post Synaptic currents (IPSCs). Electrodes used for this purpose were filled with internal solution containing (in mM): 100 CSCl (blocks K^+ channels), 40 HEPES (buffering agent, maintains pH), 1 Qx-314 (voltage activated Na^+ channel blocker), 0.6 EGTA (calcium chelator), 5 MgCl2 (salt), 10 TEA-Cl (blocks K^+ channels), 80ATP-Na, GTP-Na and 1 IEM 1460 (AMPA blocker) (titrated with CsOH (to adjust pH =7.25) at 290-295 mOsm. This solution was maintained in ice-cold conditions as ATP and GTP degrade at room temperature and was stored at -20 degrees in aliquots until required. This chloride based solution (which has a Cl^- equilibrium potential around 0 mV) enables the IPSCs to be recorded as apparent inward currents at -70 mV using Axopatch 700A amplifier (Molecular Devices, USA). Frequent measurements of series resistance (Rs) were made using the capacitance transient on a line-frequency voltage step (5 mV) during recording. Sampling rate of the recording was 10 KHz, filtered (8-pole low-pass Bessel filter) at 2 KHz which was digitised using a Digidata 1440A (figure

2.3). Under these conditions of high internal Cl⁻ concentration, IPSCs were recorded as downward deflections ranging in amplitude from 10-500 pA. Since IPSC parameters were only compared prior to and following drug addition, whole cell capacitance and electrode series resistance were monitored, but not compensated. Recording in which series resistance (as measured at the peak of the capacitance transient recorded in response to seal test at 5 mV) changed by >25% were routinely rejected from analysis.
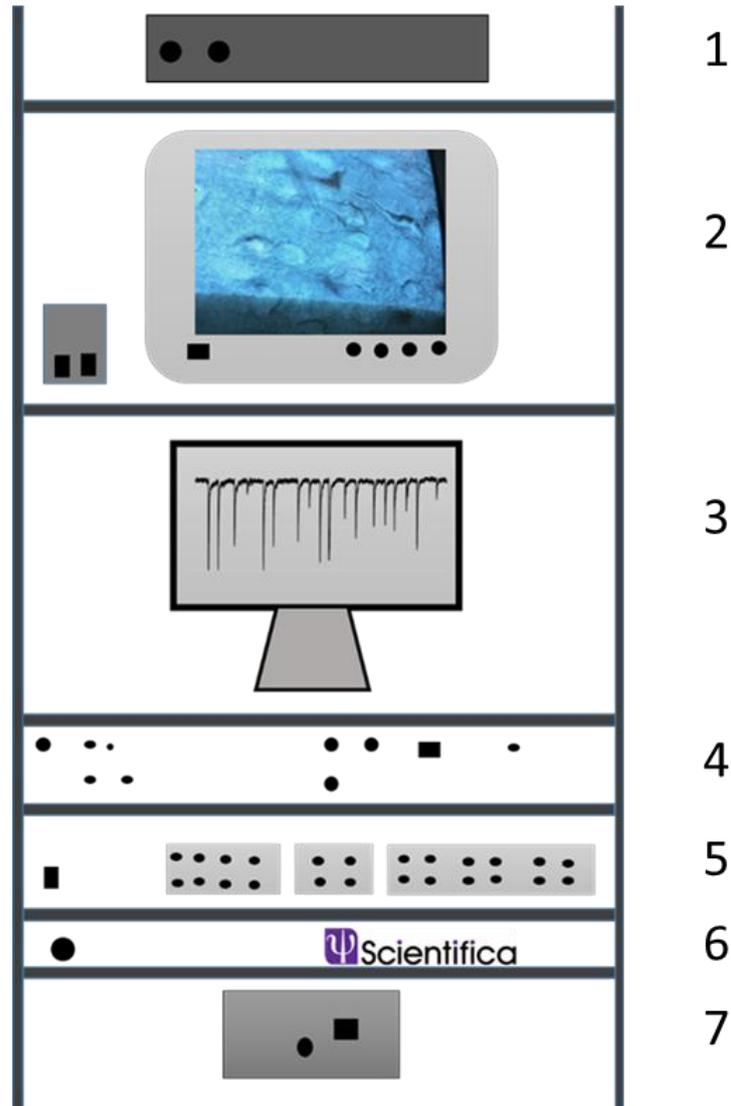
Figure 2.3 The patch clamp recording setup.

Slices were observed under microscope with differential interference (Nomarski) optics and a contrast enhancer (BRSL CE-4) (1), cells were visualised on a basic video monitor (Panasonic) (2), head stage on which microelectrode was mounted was connected to a manipulator which enables movement (Scientifica device) (6), Axopatch 700A amplifier (Molecular Devices, USA (4), signal was digitised using Digidata 1440A (Axon Instruments, Molecular devices) (5). Digitised data were recorded and saved on a standard PC (3). Water heater circulator C-85A (7).

2.5 Drugs

All drugs were obtained from Tocris, Sigma-Aldrich, Abcam, Actavis, Thermo Fisher Scientific and Sigma-Aldrich. Powdered drugs were diluted into 1-100 mM stock solutions using suitable solvents which were then stored at -20ºC until use. Depending on the experimental design the drugs were added directly to perfusing aCSF in required amounts at desired concentration. The concentrations used throughout this thesis are both empirical and theoretical (literature).

2.6 Data collection and analysis

2.6.1 Extracellular (LFP) analysis

Data were analysed offline using Spike2 v7.1 software (Cambridge electronic design). To reconstruct the original signal below 200 Hz, the sampling rate was chosen to be 10 KHz based on Nyquist sampling theorem (Axon guide). The sampling frequency must be more than twice the frequency of the input signal to enable proper reconstruction of digital signal. Time-frequency analysis was performed to create power spectra using Fast Fourier Transform (FFT) algorithm where the waveform was divided to frequency components against power. The FFT block size used for theta and gamma oscillations was 8192 (0.983 s), results showed frequencies 0 to 4166.67 Hz in 4096 bins with a resolution of 1.01 Hz. For delta oscillations, 16384 (1.966 s), results showed frequencies 0 to 4166.67 Hz in 8192 bins with a resolution of 0.050 Hz. The obtained data were copied to Graph-Pad Prism 5 and 7 (GraphPad Software, Inc. USA) for further analysis. 60 second epochs were used to analyse rhythms. 2 seconds' raw data presented in the figures throughout this thesis was filtered using a band pass second order Infinite impulse response (IIR) Bessel digital filter between 1 and 6 Hz for delta, between 5 and 13 Hz for theta, between 4 and 8 Hz for slow theta, between 22 and 30 Hz for beta and between 30 and 40 Hz for gamma oscillations. Filtering was performed on wider range for example in between 1 and 6 Hz for delta than corresponding frequency range (2-4 Hz) so that the data were not lost due to `rolling off` effect from using IIR filters.

2.6.2 Intracellular analysis

Spontaneous IPSCs (sIPSCs) were recorded using Clampex10.2, viewed using Clampfit 10.2 (Molecular Devices, USA) and were analysed in the Mini-analysis programme (synaptosoft, USA).

2.6.3.1 Tonic current analysis

The method of Nusser and Mody (2002) was used to measure tonic currents to exclude confounding effects of IPSCs overlapping. A baseline current amplitude (pA) of a 5-ms epoch was taken every 100 ms. The mean and SD of the averaged baseline points were calculated for 10 s (~100 averaged baseline points) at three distinct times of the recordings (for example: periods A, B, and C). Two changes in the baseline current were calculated between the three periods. The first (DBL) was the value of the difference during recording periods A and B, both taken during the control period and reflecting baseline fluctuation. The second (DDrug) was the value of the difference during recording periods C and B, and reflecting drug induced changes to the holding current. The two baseline changes (DBL and DDrug) were then statistically compared (paired t-test). Raw traces were shown to illustrate changes in baseline in control and drug conditions which were made using PowerPoint.

2.6.3.2 Phasic current analysis

The Mini Analysis programme (synaptosoft, USA) was used. Minimum 200 events were taken from the recordings to calculate the amplitude and the inter event interval of the IPSCs. Double events were also scanned and were considered in analysis. The cumulative probability distributions were plotted for sIPSC amplitude and inter event interval (IEI) to compare control and drug conditions using Graph Pad Prism 5 and 7 (GraphPad Software, Inc. USA). Raw traces were shown to illustrate the changes in IPSCs amplitude and IEI in control and drug conditions (after 15 min of drug application) which were made using PowerPoint.

2.6.1 Statistical analysis

For extracellular recordings, pooled data are presented as mean ± SEM. Wilcoxon (non-parametric) signed rank test (ns, not significant, $p > 0.05$; * significant $0.05 > p > 0.01$; ** very significant, $0.01 > p > 0.001$, *** extremely significant) was used to determine statistical significance for one drug (example: PTX). The Friedman test (*$p > 0.05$, **$p > 0.01$, ***$p > 0.001$) was used to detect significant differences for multiple drug applications (example: Zolpidem).

For intracellular recordings, pooled data are presented as mean ± SEM. Significance of changes in tonic currents were determined using paired t-tests and Dunn`s multiple comparisons using Graph Pad prism software and are designated by p values and *.

For Phasic currents, a cumulative probability distribution was plotted for sIPSC amplitude and inter event interval (IEI) during control and drug conditions. The significance between

these two distributions are determined by two sample Kolmogorov-Smirnov test using Graph Pad prism software.

2.6.2 Correlation analysis

Correlation analysis is a measure of linear relationship of variables with correlation coefficient values in between -1 and 1 which was performed in Spike2.

Auto correlation function of a signal is defined with respect to the signal itself. This means that the signal is being compared (for similarity) with a time shift. Mathematically, its function is the average of the sequence x(t) with a time shift of m within itself which measure periodicity of a signal in time domain format. This analysis was used to identify signals at various frequency bands (delta, theta, and gamma) to determine the level of correlation.

Cross correlation function of a signal is correlation of two independent signals with a time shift in one of the two independent signals. This analysis was used to determine temporal relationship between two independent signals x(t) and y (t) to estimate the degree to which two waveforms are correlated which ranges from -1 to +1. +1 indicates positive correlation, -1 indicated negative correlation whilst zero (0) implies no correlation.

2.6.3 Linear regression analysis

Linear regression is the most commonly used predictive analysis. Regression analyses are used to describe data and to explain the relationship between a dependent variable and one or more independent variables. This analysis assembles the data as a single line through a scatter plot. The simplest form with one dependent and one independent variable is defined by the formula $y = c + b*x$ (y = estimated dependent, c = constant, b = regression coefficients, and x = independent variable). Linear regression analysis was performed in Graph Pad Prism software to determine the significance of the elevation or trend (y-intercepts) of two data sets.

2.6.4 Phase amplitude coupling analysis

Phase amplitude coupling (PAC), is a type of cross frequency coupling (CFC). PAC analysis was performed to determine the coupling of phase of low frequency oscillations and amplitude of high frequency oscillations by using a customised MATLAB script 'CalleRoutine3' developed by Tort *et al.,* 2010. To measure PAC, the low (theta) and high (gamma) frequency data of 60 s with a sampling rate of 1000 Hz were band pass filtered in the range of 3-15 Hz and 30-45 Hz respectively. To remove any phase distortion, the filters

were applied to the original time series in the forward and then the reverse direction using MATLAB's function 'filtering.m'. These zero-phase filtered data were then used to conduct PAC studies based on a Hilbert transform. Amplitudes were normalized by subtracting the temporal mean and dividing the result by the temporal standard deviation to create the set of normalized band-passed signals. Normalization was performed to facilitate comparison between different frequency bands (Tort *et al.,* 2010).

The degree of PAC between theta and gamma oscillations were measured by modulation index (MI) in the desired frequency bands: (theta) phase modulating and (gamma) amplitude modulated and was represented by bi-dimensional cross-frequency coupling in frequency domain in which high coupling was represented by hot (red) colours. Several other hotspots observed in some PAC plots could account for harmonic activity or artefacts.

3 Characterisation of pharmacologically induced theta and gamma oscillations in LV of M1 and S1

3.1 Introduction

3.1.1 Oscillations in M1 and S1

The use of *in vitro* electrophysiological techniques has enabled a greater understanding of neuronal activity, primarily through the use of the brain slice preparation (Yamamoto and McIlwain, 1966; Andersen *et al.,* 1972). Over the last 20 years, this preparation has provided insight into the mechanisms underlying oscillations at various frequency ranges. Understanding the electrical and neuropharmacological properties of brain networks using selective receptor modulators in native tissue enables comparison with such properties with those in disease models (e.g. epilepsy and PD). *In vivo* and *in vitro* studies have reported M1 in execution of voluntary movements and, from both local network *in vitro* and whole brain *in vivo* perspectives, M1 has shown to generate oscillatory activity at beta frequency (Murthy and Fetz, 1992; Baker *et al.,* 1997, Jensen *et al.,* 2005; Yamawaki, 2008, Prokic, 2011, 2015). However, MEG studies in human have also revealed nested rhythms at theta and gamma frequencies (Cheyne *et al.,* 2008) like those of rat hippocampus (Bragin *et al.,* 1995) and *in vivo* studies also confirm slow wave oscillations in somatosensory cortex including delta and theta band activity (Steriade, 2006). Whilst gamma oscillations have been reported *in vitro* in somatosensory cortex (Buhl *et al.,* 1998), this has not since been followed up with detailed mechanistic studies. To date, rhythms in other bands, such as delta, theta and alpha frequencies, have not been demonstrated in somatosensory and motor cortices *in vitro* and hence their mechanisms remain unexplored.

Using a modified sagittal plane slice preparation (Prokic *et al.,* 2015; Johnson *et al.,* 2017; Ozkan *et al.,* 2017), with aCSF containing neuro-protectants, we have greatly improved brain slice viability, enabling the generation and study of dual rhythms (theta and gamma oscillations) in the *in vitro* sensorimotor slice in the presence of KA and CCh (Johnson *et al.,* 2017) and enabling production of theta-gamma and delta waves *in vitro* for the first time. Over the next 3 chapters, this thesis describes the physiology and pharmacology of these various rhythms in rat sensorimotor cortex *in vitro*.

3.1.2 Significance of gamma oscillations

Gamma oscillations have been identified to play critical role in cognitive integration in brain (Herrmann *et al.,* 2004). They have found to be involved in attention (Tiitinen *et al.,* 1993) sensory and motor functions, learning and memory (Hopfield *et al.,* 1995; Lisman and Idiart, 1995; Buzsaki and Chrobak, 1995; Lisman, 1999) arousal (Struber *et al.,* 2000), language perception, focussed attention, recognition (Bouyer *et al.,* 1981; Sheer *et al.,* 1989; Murthy and Fetz, 1992; Pfurtscheller and Neuper, 1992) and memory formation, processing and retrieval (Buzsaki, 1989; Fell *et al.,* 2001; Kaiser *et al.,* 2003). Besides these role of gamma

oscillations in healthy brain, they have been implicated too in disease conditions such as hyperactivity disorder (Yordanova *et al.,* 2001), Alzheimer`s disease (Stam *et al.,* 2007) and epilepsy (Willoughby *et al.,* 2003), autism (Brock *et al.,* 2002). Gamma oscillations have also been found to be profoundly altered in schizophrenia (Moghaddam *et al.,* 2003; Lewis *et al.,* 2005) and high-frequency gamma oscillations were reported in cortex before and after the onset of epileptic seizures (Allen *et al.,* 1992; Fisher *et al.,* 1992).

3.1.3 Significance of theta oscillations

The occurrence of theta rhythm is mostly associated with REM sleep, locomotor activity (Jouvet, 1969; Vanderwolf, 1969) and learning and memory (Vertes, 1997; Buzsaki, 2002; kowalczyk *et al.,* 2013). It has been suggested that theta oscillations play a major role in synchronising long-range circuits, facilitating transfer of information between distant brain regions (Sirota *et al.,* 2008; Gordon, 2011; Buzsaki and Watson, 2012). Theta oscillations are known to be synchronised with the activity in amygdala, pre frontal cortex, and medial septum during cognitive functions (Seidenbecher *et al.,* 2003; DeCoteau *et al.,* 2007; Adhikari *et al.,* 2010; Benchenane *et al.,* 2010; Hernandez-Perez *et al.,* 2015) and furthermore, gamma oscillations in hippocampus and other cortical regions like M1 are often phase-locked to theta rhythm (Bragain, 1995; Canolty *et al.,* 2006; Sirota *et al.,* 2008; Montgomery *et al.,* 2009; Colgin *et al.,* 2009; Johnson *et al.,* 2017), suggesting functional interactions between theta and gamma rhythms. Hence, theta oscillations contribute to both local network function as well as widely dispersed cortico-cortical, and sub-cortical circuits (Hernandez-Perez *et al.,* 2015). *In vitro* studies demonstrate that theta can be pharmacologically induced in hippocampus (Kowalczyk *et al.,* 2013) and in cortex (Lukatch and MacIver, 1997) using CCh.

3.1.4 Significance of theta and gamma coupling

Neuronal network oscillations do not function as single-frequency representations of network states, rather, they exist as complex activity patterns that appear to code information in cross-frequency relationship between the phase, amplitude and frequency components of the various waves. For example, evidence exists that phase-amplitude coupling (PAC) contributes to sensory signal detection (Handel and Haarmeier, 2009), and memory processes (Tort *et al.,* 2009; Axmacher *et al.,* 2010), maintenance of working memory (Lisamn and Idiart, 1995), sequential memory organisation (Lisamn, 2005), attentional selection (Schroeder and Lakatos, 2009). According to theoretical models (Lisman, 2005), PAC has a functional role in cognitive functions (Lakatos *et al.,* 2008; Tort *et al.,* 2008, 2009; Cohen *et al.,* 2009a, b; Axmacher *et al.,* 2010). PAC has been reported *in vivo* in rodent hippocampus (Bragin *et al.,* 1995; Buzsaki *et al.,* 2003; Hentschke *et al.,* 2007; Tort *et al.,* 2008; Tort *et al.,* 2009; Wulff *et al.,* 2009), rodent basal ganglia (Tort *et al.,*

2008), macaque neocortex (Lakatos *et al.,* 2005) and in various cortical and sub-cortical regions in humans (Bragin *et al.,* 1995; Buzsaki *et al.,* 2003; Bruns and Eckhorn, 2004; Vanhatalo *et al.,* 2004; Mormann *et al.,* 2005; Canolty *et al.,* 2006; Hentschke *et al.,* 2007; Demiralp *et al.,* 2007; Osipova *et al.,* 2008; Monto *et al.,* 2008;Tort *et al.,* 2008; Penny at al., 2008; Wulff *et al.,* 2009; Tort *et al.,* 2009; Cohen *et al.,* 2009a, 2009b; 2009c; Handel and Heermeier, 2009; He *et al.,* 2010; Axmacher *et al.,* 2010; Sadaghiani *et al.,* 2010; Voytek *et al.,* 2010). A recent study in our own laboratory, (Johnson *et al.,* 2017) has reported PAC in primary motor cortex slices of rats *in vitro* and this is the first demonstration of PAC in cortex *in vitro.*

3.1.5 M1 and S1 interactions

Both regions (M1 and S1) have similar laminar structure, though some studies suggest absence of LIV in M1 (Donoghue and Wise, 1982; Beaulieu, 1993; Zilles *et al.,* 1995) which makes it unique compared to other cortical regions. However, several studies (Krieg, 1946; von Bonin, 1949; Caviness, 1975; Deschênes *et al.,* 1979; Skoglund *et al.,* 1997; Cho *et al.,* 2004, Kuramoto *et al.,* 2009; Rowell *et al.,* 2010; Mao *et al.,* 2011; Kaneko, 2013; García-Cabezas and Barbas, 2014; Yamawaki *et al.,* 2014) suggest the existence of connection patterns that are similar to that of LIV in other sensory regions. Topographic maps of both M1 and S1 are well established (Brooks *et al.,* 1961, Woolsey 1952, Li and Waters 1991) and interactions between these two regions are known to play critical roles in motor learning and control skills (Asanuma and Arissian, 1984; Asanuma and Pavlides, 1997). Recovery of motor function after a brain injury requires changes in structure and function (Bornschlegl and Asanuma, 1987) and these changes may be mediated by inter-cortical interactions between M1 and S1 (Paperna and Malach, 1991). Changes in motor function due to the projections from S1 have been reported in several species and vice versa. In cats, LTP in M1 is generated by exciting the neurones that project from S1 and thalamus to M1 (Iriki *et al.,* 1989). In humans and rodents, somatosensory entrainment enhances the excitability of M1 (Luft *et al.,* 2002; Kaelin and Lang *et al.,* 2002). Disrupting S1 projections in primates causes disturbances in chewing (Lin *et al.,* 1993, 1998; Hiraba *et al.,* 2000), muscle contraction, motor coordination and ability to carry heavy objects (Rothwell *et al.,* 1982; Johansson and Westling, 1984; Hikosaka *et al.,* 1985; Brochier *et al.,* 1999). It is evident that neurones in S1 fire prior to the onset of actual movement in rhesus macaques (Soso and Fetz, 1980) and also in non-human primates (Nelson, 1987). This phenomenon, in which somatosensory integration plays a critical role in voluntary movements, is termed as efference copy (EC) which was used to distinguish between sensory inputs obtained from internal and external stimuli (Wolpert *et al.,* 1995; Helmholtz, 2011). Physiological properties of individual regions have been well characterised but inter-

cortical connectivity remains less explored despite its clear functional significance. Sensorimotor integration has been studied *in-vivo* (Wannier *et al.,* 1991; Smith *et al.,* 1983) but this does not enable a full understanding of the pathways and local network interactions.

We have recently developed a novel slice preparation method (details in section 3.3) based upon use of numerous neuroprotectants to aid preservation of inhibitory neurons critical for maintenance of rhythmic network activity. Using this modified preparation, dual theta-gamma oscillations could reliably be induced in M1 (Johnson *et al.,* 2017.) and S1. We determined to use the same slice preparation to induce theta-gamma activity and to explore rhythms generated in both M1 and S1, with a view to exploring potential interactions between M1 and S1 in the functionally connected sagittal cortical slice.

3.2 Results

3.2.1 Induction of theta and gamma oscillations in M1 and S1

M1 and S1 are adjacent to each other and when simultaneous extracellular LFP recordings were performed in deep layers of M1/S1 in the absence of exogenously applied neuronal excitants we found no spontaneous oscillatory activity. Subsequently, KA and CCh were used to induce oscillations both in M1 and S1. Sagittal sensory motor slices were used in these experiments as it was easy to locate M1 and S1 and functional connectivity is well preserved (Woodhall, unpublished observations). Since there seems to be greater oscillatory power in deeper layers (Yamawaki, 2008) than in superficial, recordings were made from LV of both M1 and S1 simultaneously or non-simultaneously from slice type A in this section 3.2 (unless otherwise stated) located using the rat brain atlas of Paxinos and Watson (Paxinos and Waston, 2012).

Co-application of 150 nM of KA and 10 µM CCh reliably induced theta (6-11 Hz) and gamma (30-40 Hz) oscillations in both M1 and S1 (figure 3.1) which were stable for 3-4 hrs. Mean values: theta (M1 7.5 ± 0.2 Hz; S1 7.7 ± 0.3 Hz, n=40) and gamma (M1 33.4 ± 1.2 Hz; S1 33.7 ± 1.8 Hz, n=40). Whilst, most of the recordings have high gamma power but there are some recordings with high theta power (example: Figure 3.10). Therefore, noemalised values are used for analysis. Various receptor modulators were bath applied to perform pharmacological studies to determine the mechanisms involved in these oscillations. `Control` (normalised to 100%) in experiments in this chapter indicates stable theta and gamma oscillations where there was no change noticed in frequency and amplitude over 20 min period. The effect of drug was measured after 40 min of bath application (unless otherwise stated) which was compared with control.
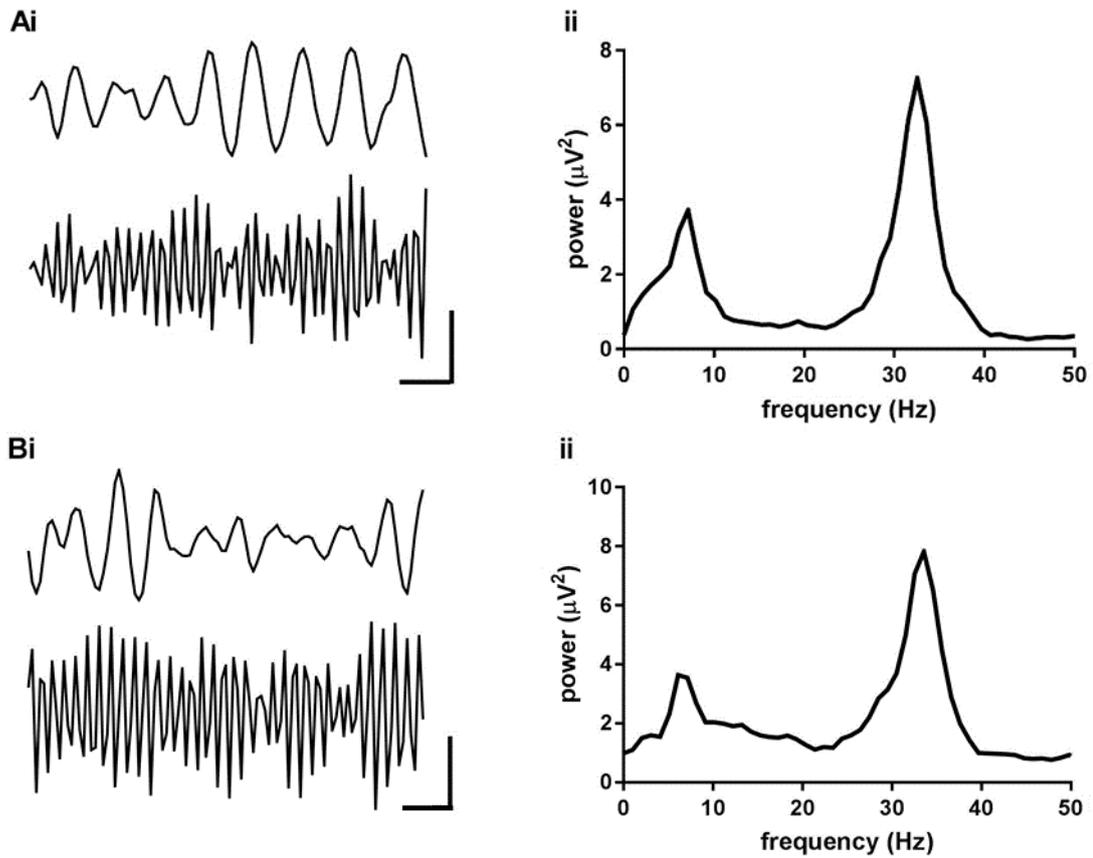
Figure 3.1 Theta and gamma oscillations were induced both in M1 and S1 in the presence of KA and CCh.

(Ai) raw data of 60 s LFP recording of theta and gamma oscillations in LV of M1 (scale: 20 µV vs 200 ms) **(Bi)** in LV of S1 filtered using Bessel IIR filter (scale: 20 µV vs 200 ms). **(ii)** A typical representative power spectrum of 60 s extracellular recording of M1 and S1 (8 Hz and 32 Hz) and S1 (7 Hz and 33 Hz).

3.2.2 GABA$_A$R modulation of theta and gamma oscillations in M1 and S1

To uncover the dependence of theta and gamma oscillations on inhibitory mechanisms, gabazine (GBZ), a competitive GABA$_A$R antagonist was applied to the solution perfusing the slices. 250 nM GBZ significantly attenuated the synchronous activity of gamma oscillations but increased the amplitude of theta oscillations both in M1 and S1. In M1, GBZ increased the power of theta oscillations to 146 ± 9% of control (n=8, $p<0.01$ and significantly decreased the power of gamma oscillations to 38 ± 2% (n=8, $p<0.001$) (figure 3.2A). In S1, GBZ increased the power of theta oscillations to 122 ± 4% of control (n=8, $p<0.05$) and significantly decreased the power of gamma oscillations to 24 ± 3% (n=8, $p<0.001$) (figure 3.2B).
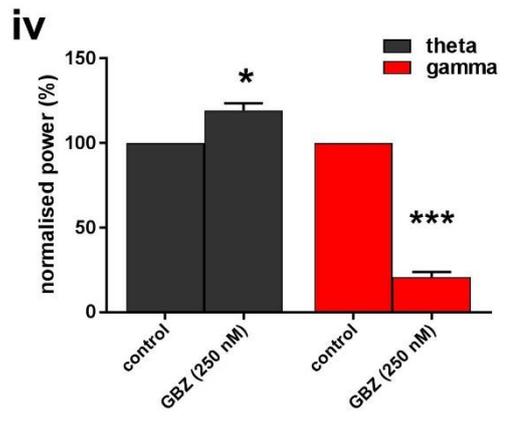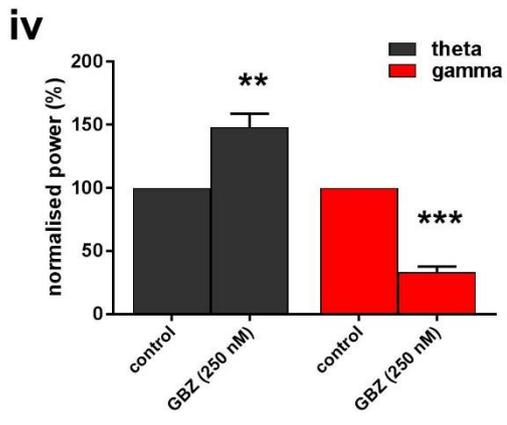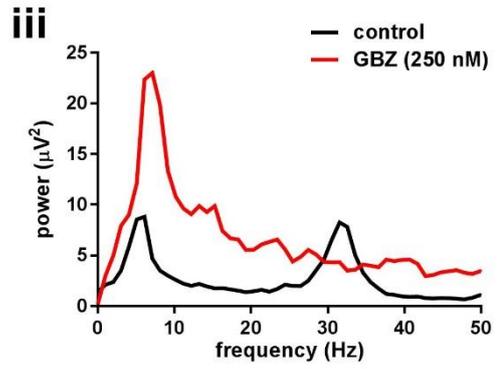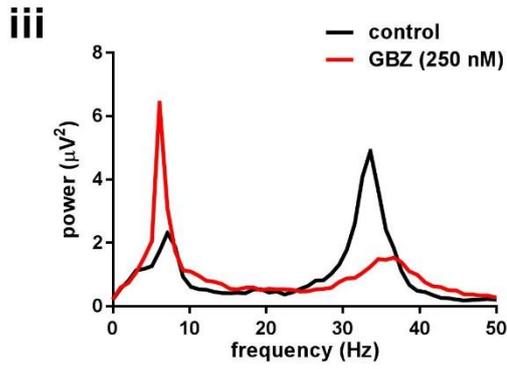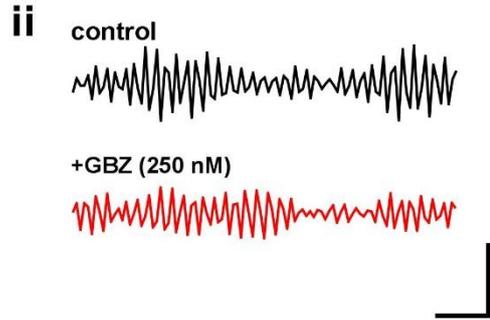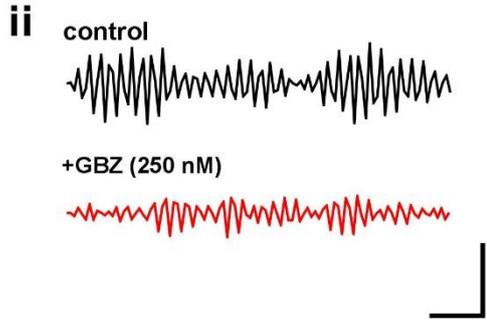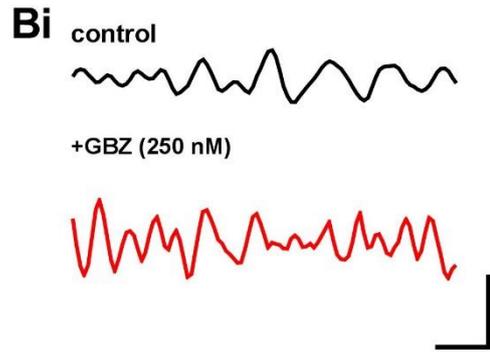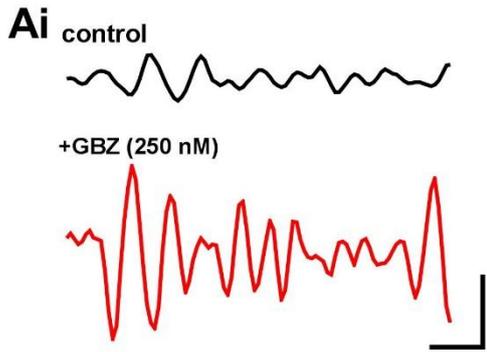
Figure 3.2 GABA$_A$R receptor block increases theta oscillatory power whilst decreasing gamma oscillatory power in M1 and S1.

(A) Effect of gabazine (250 nM) on theta and gamma oscillations in M1 **(i)** Raw data showing the changes in oscillatory activity before (black) and after (red) drug application of theta (top) and gamma (bottom) (scale: 20 µV vs 200 ms) **(iii)** Representative power spectra of 60s of extracellular recording showing peak power before (black) and after (red) gabazine **(iv)** Bar graphs showing pooled peak oscillatory power of theta (grey bars) and gamma (red bars) oscillations normalised to control (**p<0.01, *** p<0.001; n=8).

(B) Effect of gabazine (250 nM) on theta and gamma oscillations in S1 **(i)** Raw data showing the changes in oscillatory activity before (black) and after (red) drug application of theta (top) and gamma (bottom) (scale: 10 µV vs 200 ms) **(iii)** Representative power spectra of 60s of extracellular recording showing peak power before (black) and after (red) gabazine **(iv)** Bar graphs showing pooled peak oscillatory power of theta (grey bars) and gamma (red bars) oscillations normalised to control (*p<0.05, *** p<0.001; n=8).

3.2.3 iGluR modulation of theta and gamma oscillations

3.2.3.1 AMPAR modulation of theta and gamma oscillations in M1 and S1

To investigate whether AMPAR are involved in the generation of theta and gamma oscillations in M1 and S1, SYM2206 (a specific AMPAR antagonist) was applied to bath. 20 µM of SYM2206 decreased the gamma activity whilst increasing theta activity both in M1 and S1. In M1, SYM2206 increased theta activity to $225 \pm 12\%$ of control (n=8, $p<0.001$) and significantly decreased gamma oscillations to $32 \pm 2\%$ of control (n=8, $p<0.001$) (figure 3.3A). In S1, theta oscillations were significantly increased to $301 \pm 8\%$ of control (n=8, $p<0.001$) and decreased gamma oscillations to $41 \pm 6\%$ (n=8, $p<0.01$) (figure 3.3B).
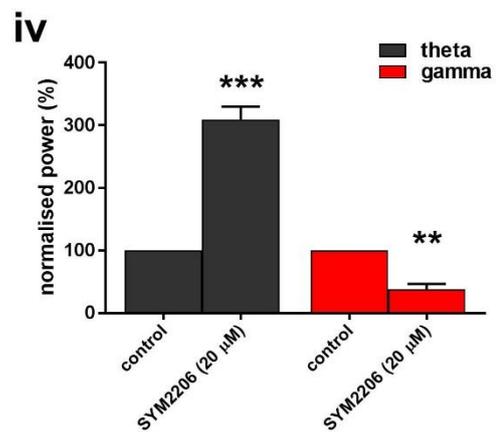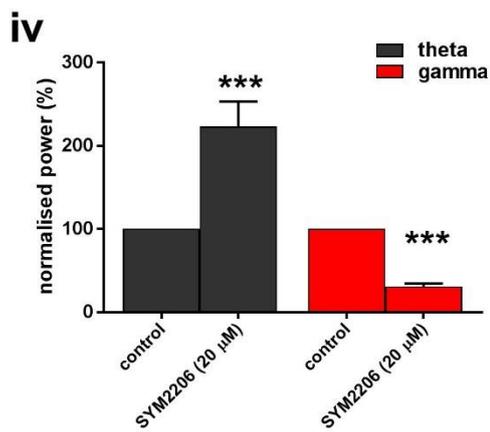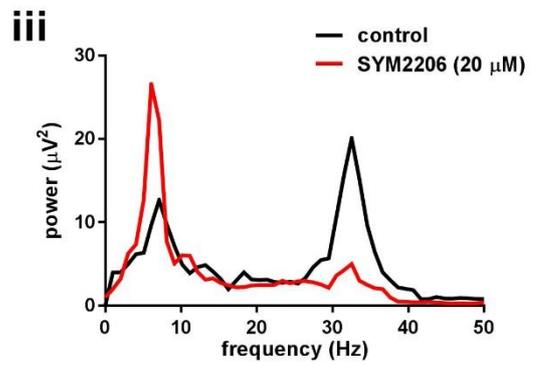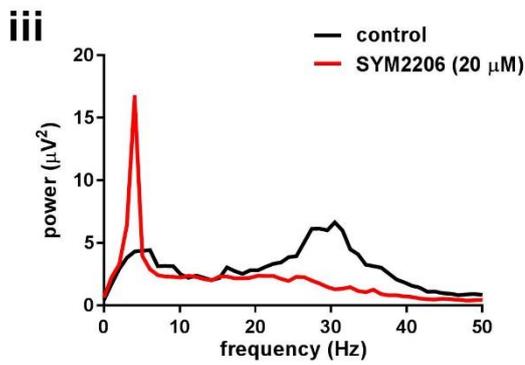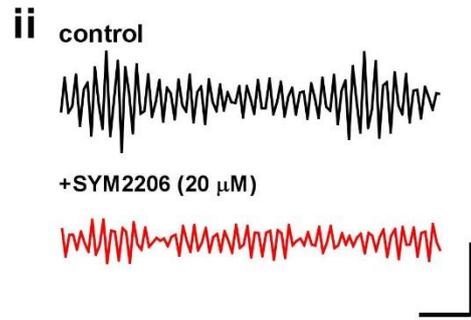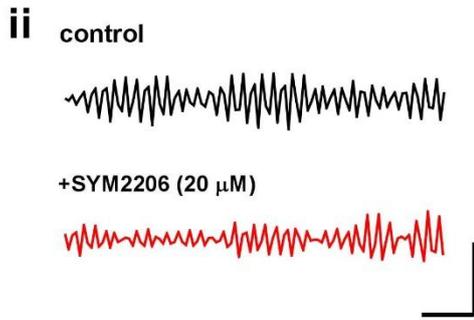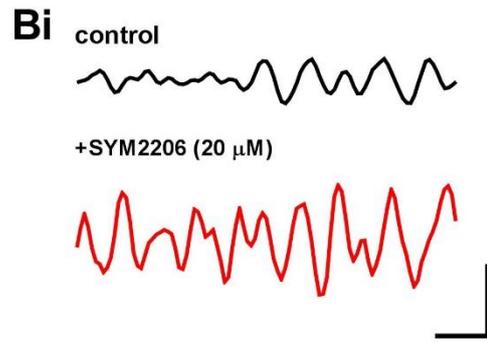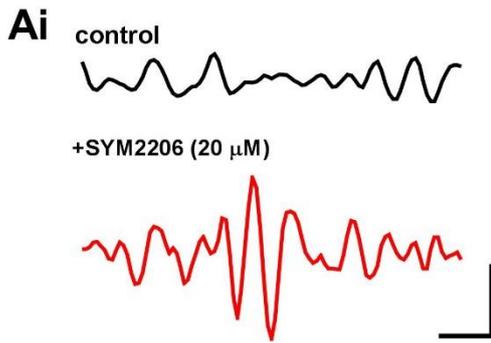
Figure 3.3 AMPA receptor block increases theta oscillatory power whilst increasing gamma oscillatory power in M1 and S1.

(A) Effect of SYM2206 (20 μM) on theta and gamma oscillations in M1 **(i)** raw data showing the changes in oscillatory activity before (black) and after (red) drug application of theta (top) and gamma (bottom) (scale: 10 μV vs 200 ms) **(iii)** Representative power spectra of 60s of extracellular recording showing peak power before (black) and after (red) SYM2206 **(iv)** Bar graphs showing pooled peak oscillatory power of theta (grey bars) and gamma (red bars) oscillations normalised to control (**$p<0.01$, *** $p<0.001$; n=8).

(B) Effect of SYM2206 (20 μM) on theta and gamma oscillations in S1 **(i)** raw data showing the changes in oscillatory activity before (black) and after (red) drug application of theta (top) and gamma (bottom) (scale: 10 μV vs 200 ms) **(iii)** Representative power spectra of 60s of extracellular recording showing peak power before (black) and after (red) SYM2206 **(iv)** Bar graphs showing pooled peak oscillatory power of theta (grey bars) and gamma (red bars) oscillations normalised to control (**$p<0.01$, *** $p<0.001$; n=8).

3.2.3.2 KA/AMPAR modulation of theta and gamma oscillations in M1 and S1

After confirming the significance of AMPAR in generation of theta and gamma oscillations in M1 and S1 by using SYM2206, CNQX (a KAR/AMPAR antagonist) was used to examine the combined impact of KAR and AMPAR on these oscillations. 25 µM of CNQX decreased the gamma activity whilst increasing theta activity both in M1 and S1. In M1, CNQX increased the power of theta oscillations to $189 \pm 14\%$ of control (n=8, p<0.001) and significantly decreased the power of gamma oscillations to $44 \pm 4\%$ (n=8, p<0.01) (figure 3.4A). In S1, CNQX increased the power of theta oscillations to $194 \pm 16\%$ of control (n=8, p<0.001) and significantly decreased the power of gamma oscillations to $58 \pm 3\%$ of control (n=8, p<0.01) (figure 3.4B) suggesting a role of both KA and AMPA receptors. Specific KAR antagonists, UBP 304 and UBP 310 would be beneficial.
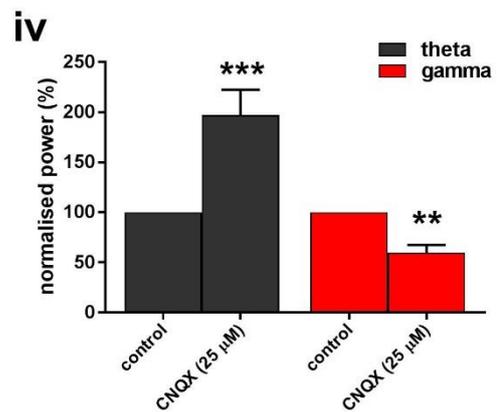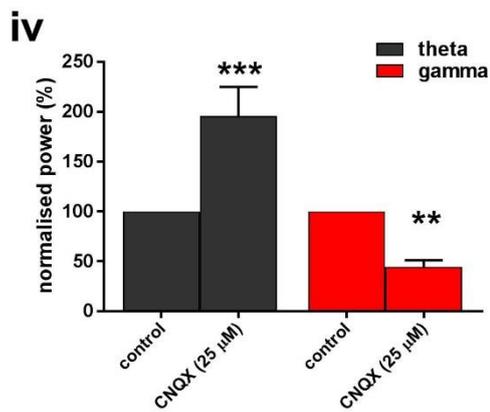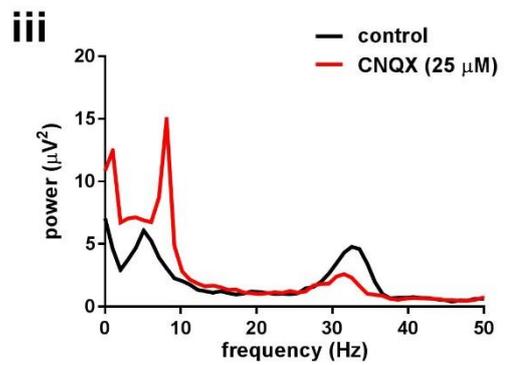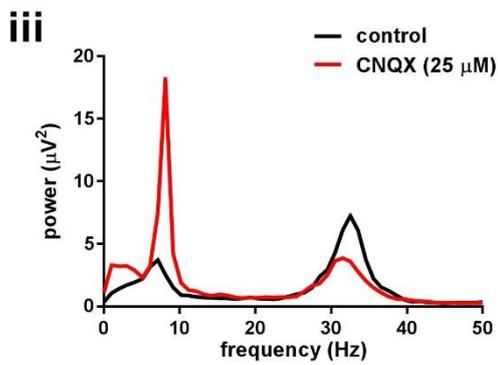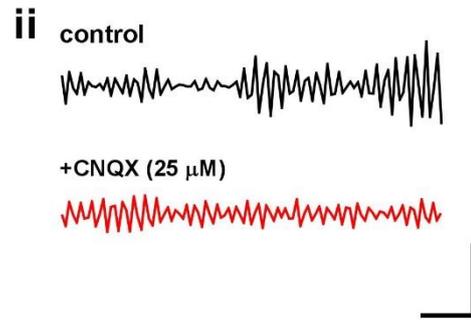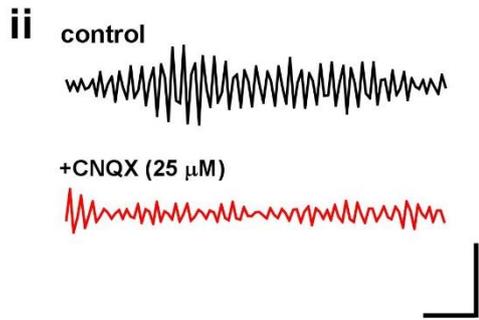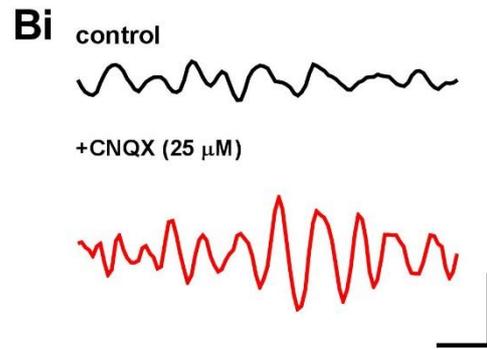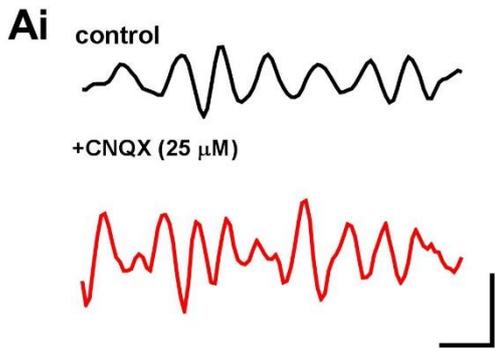
Figure 3.4 AMPA/KA receptor block increases theta oscillatory power whilst increasing gamma oscillatory power in M1 and S1.

(A) Effect of CNQX (25 µM) on theta and gamma oscillations in M1 **(i)** raw data showing the changes in oscillatory activity before (black) and after (red) drug application of theta (top) and gamma (bottom) (scale: 10 µV vs 200 ms) **(iii)** Representative power spectra of 60s of extracellular recording showing peak power before (black) and after (red) CNQX **(iv)** Bar graphs showing pooled peak oscillatory power of theta (grey bars) and gamma (red bars) oscillations normalised to control (**$p<0.01$, *** $p<0.001$; n=8).

(B) Effect of CNQX (25 µM) on theta and gamma oscillations in S1 **(i)** raw data showing the changes in oscillatory activity before (black) and after (red) drug application of theta (top) and gamma (bottom) (scale: 10 µV vs 200 ms) **(iii)** Representative power spectra of 60s of extracellular recording showing peak power before (black) and after (red) CNQX **(iv)** Bar graphs showing pooled peak oscillatory power of theta (grey bars) and gamma (red bars) oscillations normalised to control (**$p<0.01$, *** $p<0.001$; n=8).

3.2.3.3 NMDAR modulation of theta and gamma oscillations in M1 and S1

To investigate the dependence of theta and gamma oscillations on NMDAR mechanisms, 2-AP5, a competitive NMDAR antagonist was applied to bath solution perfusing the slices. 50 µM of 2-AP5 significantly enhanced the synchronous activity of gamma oscillations but had differential effects on amplitude of theta oscillations in M1 and S1. In M1, 2-AP5 had no significant effect on the power of theta oscillations (n=8, $p>0.05$) but significantly increased the power of gamma oscillations to $174 \pm 7\%$ of control (n=8, $p<0.001$) (figure 3.5A). In S1, 2-AP5 decreased the power of theta oscillations to $80 \pm 3\%$ of control (n=8, $p<0.05$) and significantly increased the power of gamma oscillations to $180 \pm 8\%$ (n=8, $p<0.001$) (figure 3.5B). Although the power spectrum in the figure (Aiii) shows a decrease in peak frequency it is not significant when data were pooled.
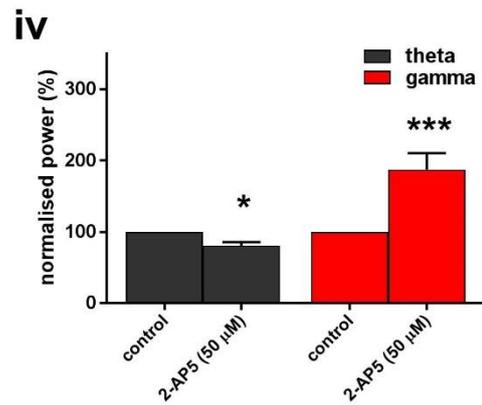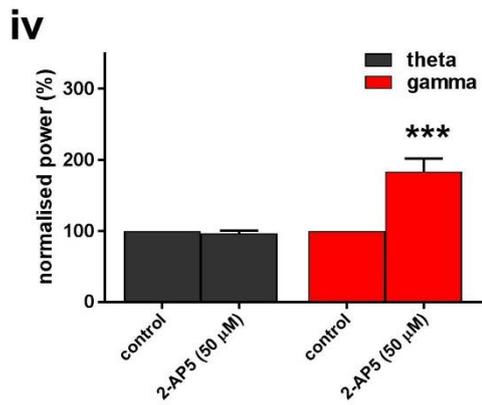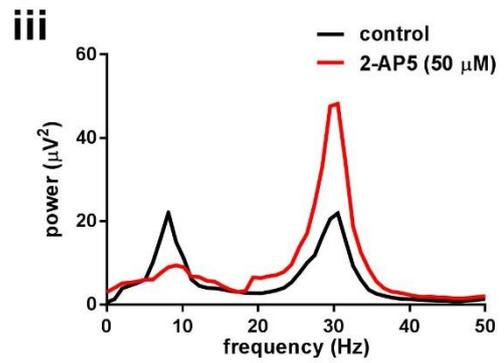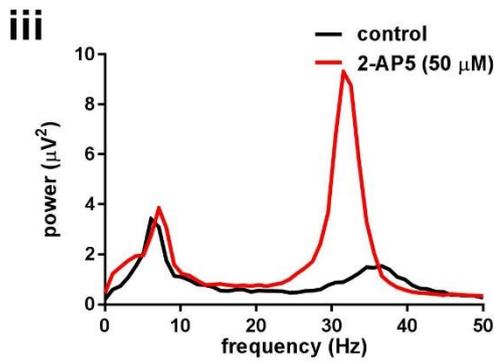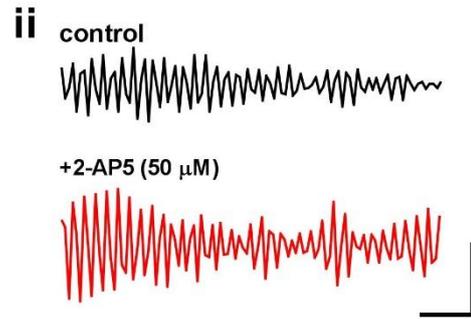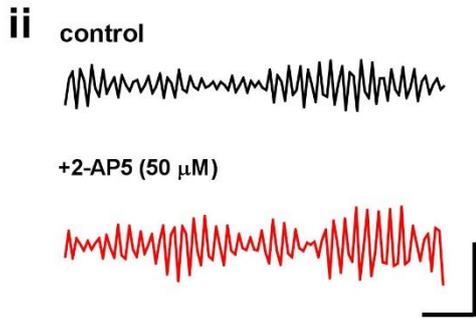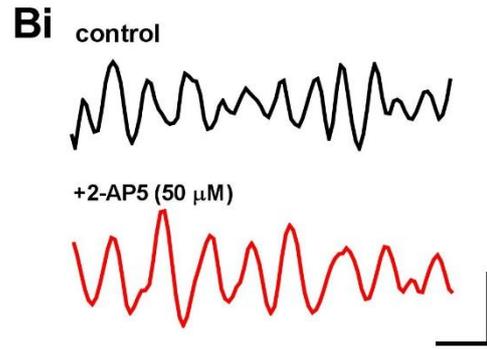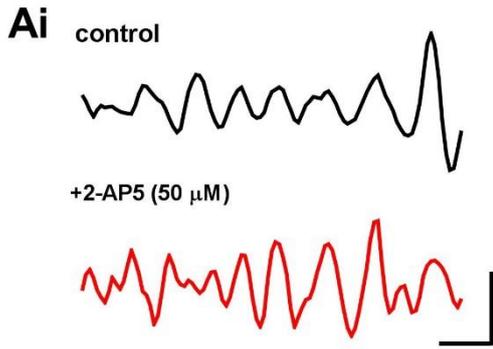
Figure 3.5 NMDA receptor block has differential effects on theta oscillatory power whilst increasing gamma oscillatory power in M1 and S1.

(A) Effect of -2-AP5 (50 µM) on theta and gamma oscillations in M1 **(i)** raw data showing the changes in oscillatory activity before (black) and after (red) drug application of theta (top) and gamma (bottom) (scale: 10 µV vs 200 ms) **(iii)** Representative power spectra of 60s of extracellular recording showing peak power before (black) and after (red) 2-AP5 **(iv)** Bar graphs showing pooled peak oscillatory power of theta (grey bars) and gamma (red bars) oscillations normalised to control (**p<0.01, *** p<0.001; n=8).

(B) Effect of -2-AP5 (50 µM) on theta and gamma oscillations in S1 **(i)** raw data showing the changes in oscillatory activity before (black) and after (red) drug application of theta (top) and gamma (bottom) (scale: 20 µV vs 200 ms) **(iii)** Representative power spectra of 60s of extracellular recording showing peak power before (black) and after (red) 2-AP5 **(iv)** Bar graphs showing pooled peak oscillatory power of theta (grey bars) and gamma (red bars) oscillations normalised to control (*p<0.05, *** p<0.001; n=8).

3.2.4 Dopamine modulation of theta and gamma oscillations in M1 and S1

3.2.4.1 DAR modulation of theta and gamma oscillations

DA was bath applied along with 250 µM ascorbic acid to prevent DA oxidation (Hastings *et al.,* 1996) to determine the effect of DAR in generation of theta and gamma oscillations in M1 and S1. 30 µM DA enhanced the synchronous oscillatory activity of theta and gamma oscillations both in M1 and S1. In M1 DA increased theta to $120 \pm 2\%$ of control (n=8, p<0.01) and gamma to $148 \pm 4\%$ of control (n=8, p<0.001) (figure 3.6A). In S1, DA significantly increased the theta activity to $153 \pm 5\%$ of control (n=8, p<0.01) and gamma oscillation to $160 \pm 6\%$ of control (n=8, p<0.01) (figure 3.6B) suggesting a role in these oscillations.
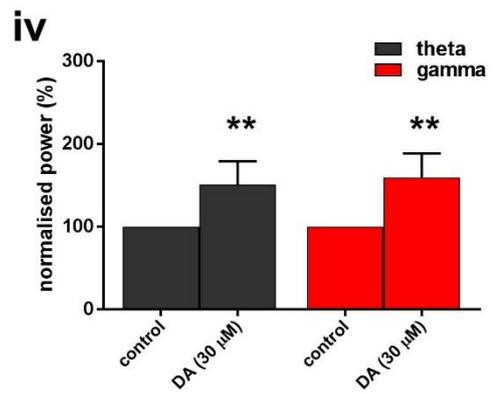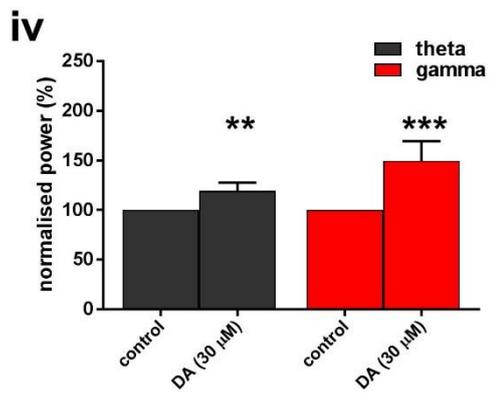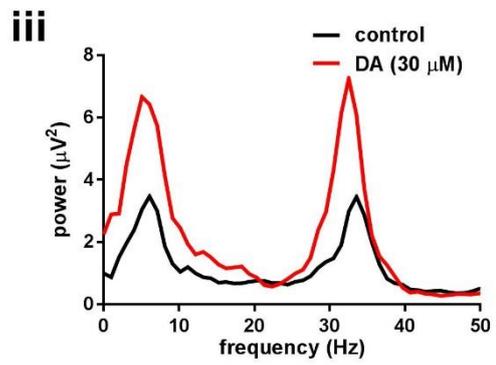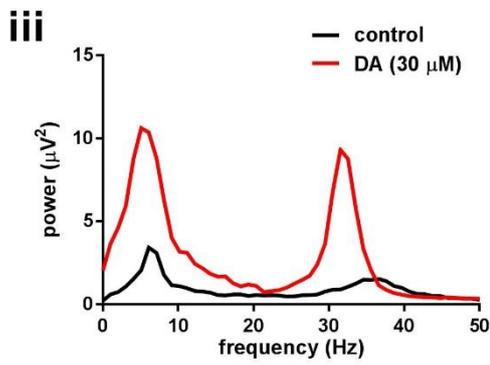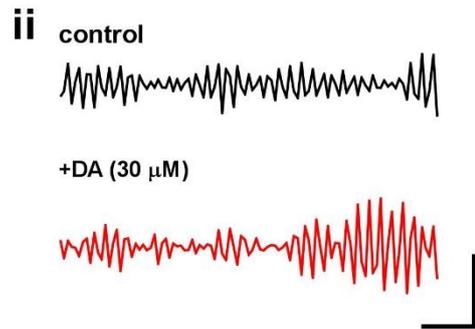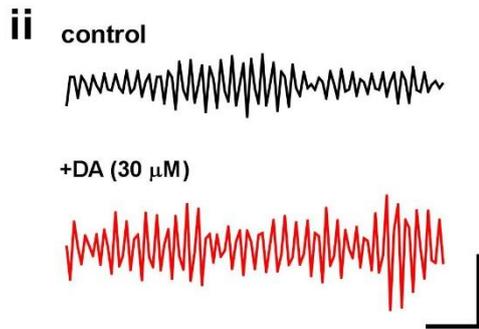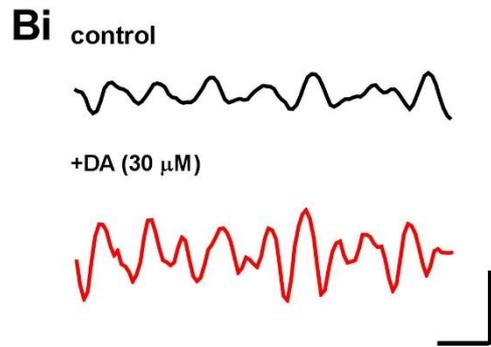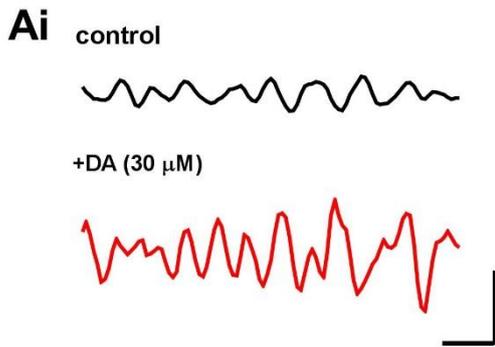
Figure 3.6 Dopamine increases both theta and gamma oscillatory power in M1 and S1.

(A) Effect of DA (30 µM) on theta and gamma oscillations in M1 **(i)** raw data showing the changes in oscillatory activity before (black) and after (red) drug application of theta (top) and gamma (bottom) (scale: 10 µV vs 200 ms) **(iii)** Representative power spectra of 60s of extracellular recording showing peak power before (black) and after (red) DA **(iv)** Bar graphs showing pooled peak oscillatory power of theta (grey bars) and gamma (red bars) oscillations normalised to control (**$p<0.01$, *** $p<0.001$; n=8).

(B) Effect of DA (30 µM) on theta and gamma oscillations in S1 **(i)** raw data showing the changes in oscillatory activity before (black) and after (red) drug application of theta (top) and gamma (bottom) (scale: 10 µV vs 200 ms) **(iii)** Representative power spectra of 60s of extracellular recording showing peak power before (black) and after (red) DA **(iv)** Bar graphs showing pooled peak oscillatory power of theta (grey bars) and gamma (red bars) oscillations normalised to control (**$p<0.01$; n=8).

3.2.4.2 AMPH modulation of theta and gamma oscillations in M1 and S1

It may be argued that application of micromolar concentrations of dopamine is not physiological, and we decided to investigate the effect of endogenously released DA. To this end, we applied amphetamine sulphate, which is known to release DA from vesicles by direct displacement, as well as to block DA transport across the neuronal membrane. 20 µM of AMPH was bath applied. AMPH in M1 enhanced the synchronous oscillatory activity of theta and gamma oscillations both in M1 and S1. In M1, AMPH had significantly increased theta to 171 ± 11% of control (n=8, $p<0.001$) and gamma to 213 ± 5 % of control (n=8, $p<0.001$) (figure 3.7A). In S1, AMPH significantly increased the theta activity to 196 ± 8% of control (n=8, $p<0.001$) and gamma oscillation to 164 ± 15 % of control (n=8, $p<0.001$) (figure 3.7B).
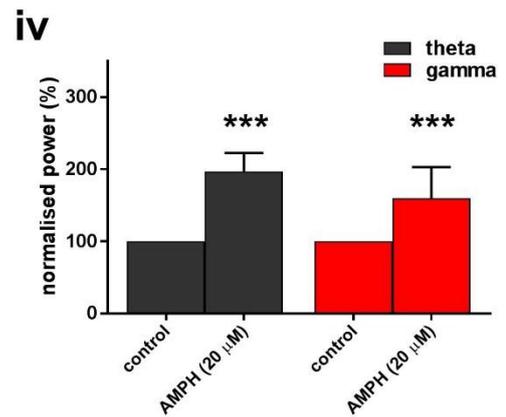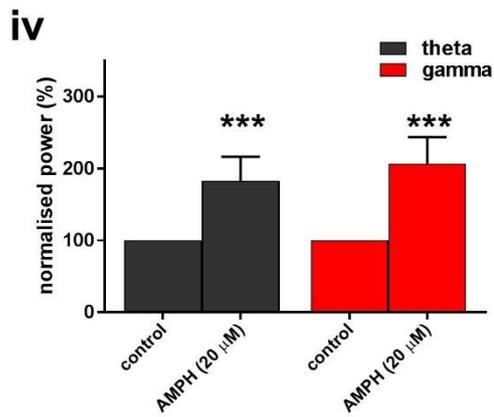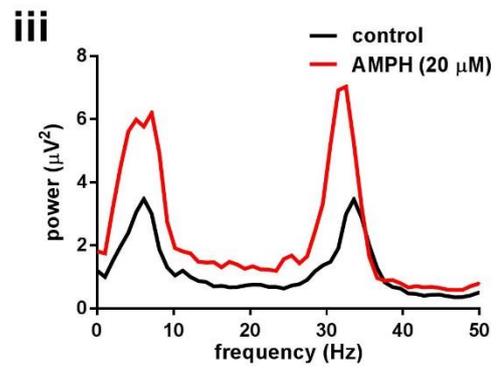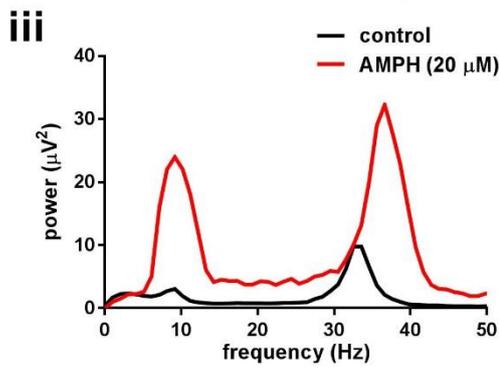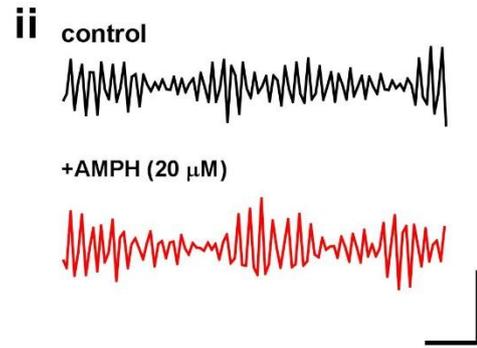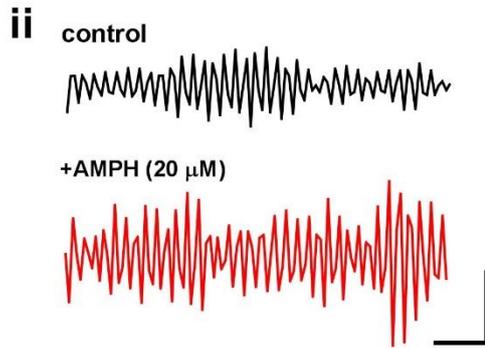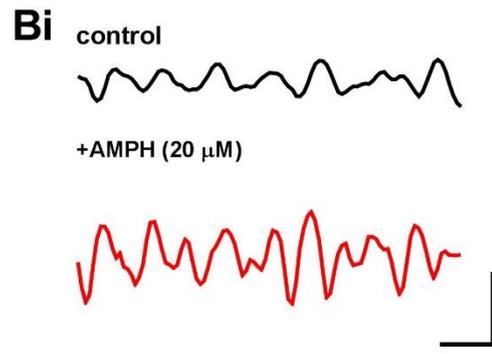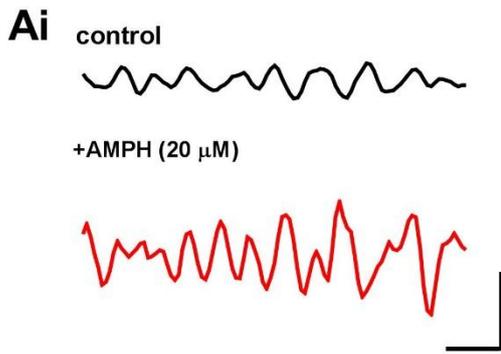
Figure 3.7 AMPH increases both theta and gamma oscillatory power in M1 and S1 via DA release.

(A) Effect of AMPH (20 µM) on theta and gamma oscillations in M1 **(i)** raw data showing the changes in oscillatory activity before (black) and after (red) drug application of theta (top) and gamma (bottom) (scale: 20 µV vs 200 ms) **(iii)** Representative power spectra of 60s of extracellular recording showing peak power before (black) and after (red) AMPH **(iv)** Bar graphs showing pooled peak oscillatory power of theta (grey bars) and gamma (red bars) oscillations normalised to control (*** $p<0.001$; n=8).

(B) Effect of AMPH (20 µM) on theta and gamma oscillations in S1 **(i)** raw data showing the changes in oscillatory activity before (black) and after (red) drug application of theta (top) and gamma (bottom) (scale: 10 µV vs 200 ms) **(iii)** Representative power spectra of 60s of extracellular recording showing peak power before (black) and after (red) AMPH **(iv)** Bar graphs showing pooled peak oscillatory power of theta (grey bars) and gamma (red bars) oscillations normalised to control (***$p<0.001$; n=8).

3.2.5 Summary of results

The pharmacology of theta and gamma oscillations in M1 and S1 is summarised in the table below.

Drug (concentration)	Region	% Change in Control		N	Significance
		Theta	gamma		
gabazine (250 nM) [GABAR antagonist]	M1	146 ± 9	38 ± 2	8	**, ***
	S1	122 ± 4	24 ± 3	8	*, ***
SYM2206 (20 µM) [AMPAR antagonist]	M1	225 ± 12	32 ± 2	8	***, ***
	S1	301 ± 8	41 ± 6	8	***, **
CNQX (25 µM) [KAR+AMPAR antagonist]	M1	189 ± 14	44 ± 4	8	***, **
	S1	194 ± 16	58 ± 3	8	***, **
2-AP5 (50 µM) [NMDAR antagonist]	M1	ns	174 ± 7	8	ns, ***
	S1	80 ± 3	180 ± 8	8	*, ***
Dopamine (30 µM)	M1	120 ± 2	148 ± 4	8	**, ***
	S1	153 ± 5	160 ± 6	8	**, **
AMPH (20 µM) [endogenous DA release	M1	171 ± 11	213 ± 13	8	***, ***
	S1	196 ± 8	164 ± 15	8	***, ***

Table 3.1 Pharmacology of theta and gamma oscillations in LV of M1 and S1

Peak power changes after application of various receptor modulators is represented as mean ± SEM when compared to control (normalised to 100%). N= number of recordings (obtained from 3 different animals), significance: ns, $p > 0.05$, * $p < 0.05$, **$p < 0.01$, ***$p < 0.001$.

3.3 Correlation and Phase-amplitude coupling studies

As noted above, oscillations at different frequencies coexist and interact with each other in *in vivo* networks. The ability to investigate such interaction in the *in vitro* slice preparation would, therefore, be invaluable in answering mechanistic questions about cross-frequency interactions. To this end, correlation analysis was performed to determine the relation between theta and gamma activity in M1 and S1 *in vitro*, to examine intra and inter regional interactions across and between different frequency bands. Auto-correlation analysis was conducted for theta and gamma oscillations in M1 and S1 to determine the frequency of oscillations. To explore the potential for cross-frequency interactions, cross-correlation analysis was performed between theta in M1 and theta in S1, between gamma in M1 and gamma in S1 and between theta and gamma oscillations. Analysis of phase-amplitude coupling (PAC) was performed between theta and gamma oscillations, with theta frequency (3 –12 Hz) as phase and gamma frequency (25-50 Hz) as amplitude that was driven by low frequency using a script developed by Tort *et al.,* 2010. PAC was performed on 60 s epochs of data in various slice types (refer methods section) and was represented as Modulation Index (MI) which indicates the degree of coupling that existed between two oscillations. As shown above, results obtained from autocorrelation, as expected, revealed the frequency of low frequency in theta range and high frequency in gamma range explaining internal positive correlation between each frequency range in a time series. Cross correlation analysis showed that theta and gamma oscillatory activity was phase delayed by 5.5 ± 1 ms and 1 ± 0.3 ms respectively to that of in S1. Average MI of theta and gamma oscillations in M1 was found to be $1.6 \times 10^{-4} \pm 0.8 \times 10^{-4}$ (n=5) whilst in S1 it is $1.1 \times 10^{-4} \pm 0.5 \times 10^{-4}$ (n=5). MI in M1 was higher than of S1 in this intact slice preparation (figure 3.8). However, there is no correlation within theta or gamma oscillations between M1 and S1 in slice type B (figure 3.10) in which there was a cut made between two regions. Average MI of theta and gamma oscillations in M1 was found to be $2.4 \times 10^{-4} \pm 1.4 \times 10^{-4}$ z (n=5) whilst in S1 it was $2.1 \times 10^{-4} \pm 1.3 \times 10^{-4}$ (n=5). MI was found to be slightly higher in M1 than in S1 (figure 3.11).

Phase lag that was noticed in M1 with reference to S1 in intact slice suggests that theta and gamma oscillations originated in S1 (figure 3.8 G, H), however, further investigations revealed that when M1 was isolated from S1, both regions produced theta and gamma oscillations suggesting the existence of independent local rhythm generators (figures 3.12, 3.14). In slice type C, the average MI of theta and gamma oscillations was found to be $4.2 \times 10^{-4} \pm 1 \times 10^{-4}$ (n=5) (figure 3.13). In slice type D, average MI of theta and gamma oscillations was found to be $3.6 \times 10^{-4} \pm 0.9 \times 10^{-4}$ (n=5) (figure 3.15). Overall, high coupling was found in slice types C and D in which M1 and S1 are isolated along with adjacent regions.

3.3.1 Correlation and PAC studies of theta and gamma oscillations in slice type A
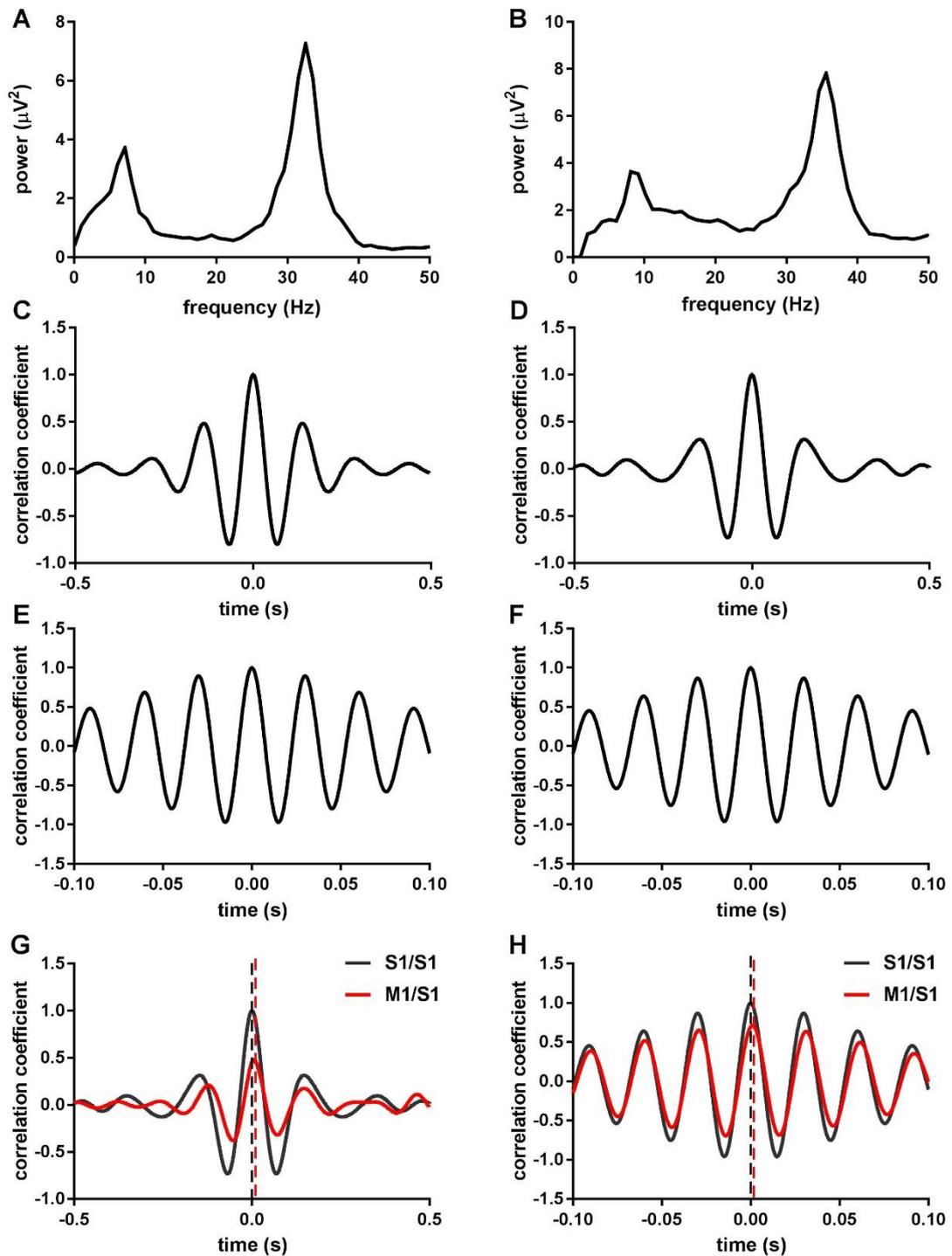
Figure 3.8 Theta and gamma oscillations are phase delayed in M1 when compared to S1 in slice type A.

(A) Representative power spectrum of theta and gamma oscillations of 60 s extracellular recording from LV of M1 and **(B)** of S1 **(C)** auto-correlation analysis of theta oscillation in M1 and **(D)** in S1 **(E)** auto-correlation analysis of gamma oscillations in M1 and **(F)** in S1. **(G)** cross-correlation analysis of theta oscillations between S1/S1 (black) and M1//S1 (red) **(H)** cross-correlation analysis of gamma oscillations between S1/S1 (black and M1/S1 (red).
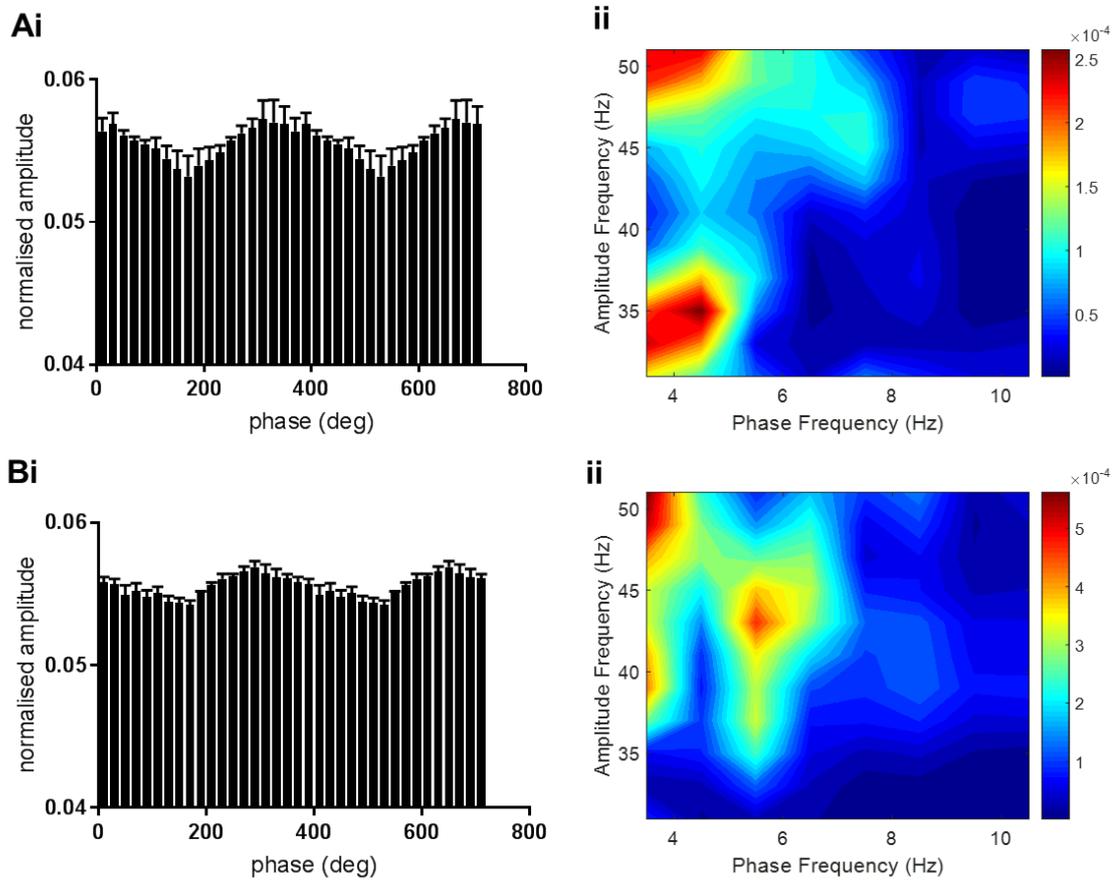
Figure 3.9 Phase amplitude coupling exists between theta and gamma oscillations both in M1 and S1 in slice type A

(Ai) pooled phase amplitude coupling (PAC) graph of theta and gamma oscillations in M1 **(Bi)** of S1 **(Aii), (Bii)** representative comodulogram showing the cross frequency coupling in frequency domain, areas of high modulation are in red in M1 (MI=4.08x10^{-4}) and S1 (MI=1.3x10-4) respectively.

3.3.2 Correlation and PAC studies of theta and gamma oscillations in slice type B
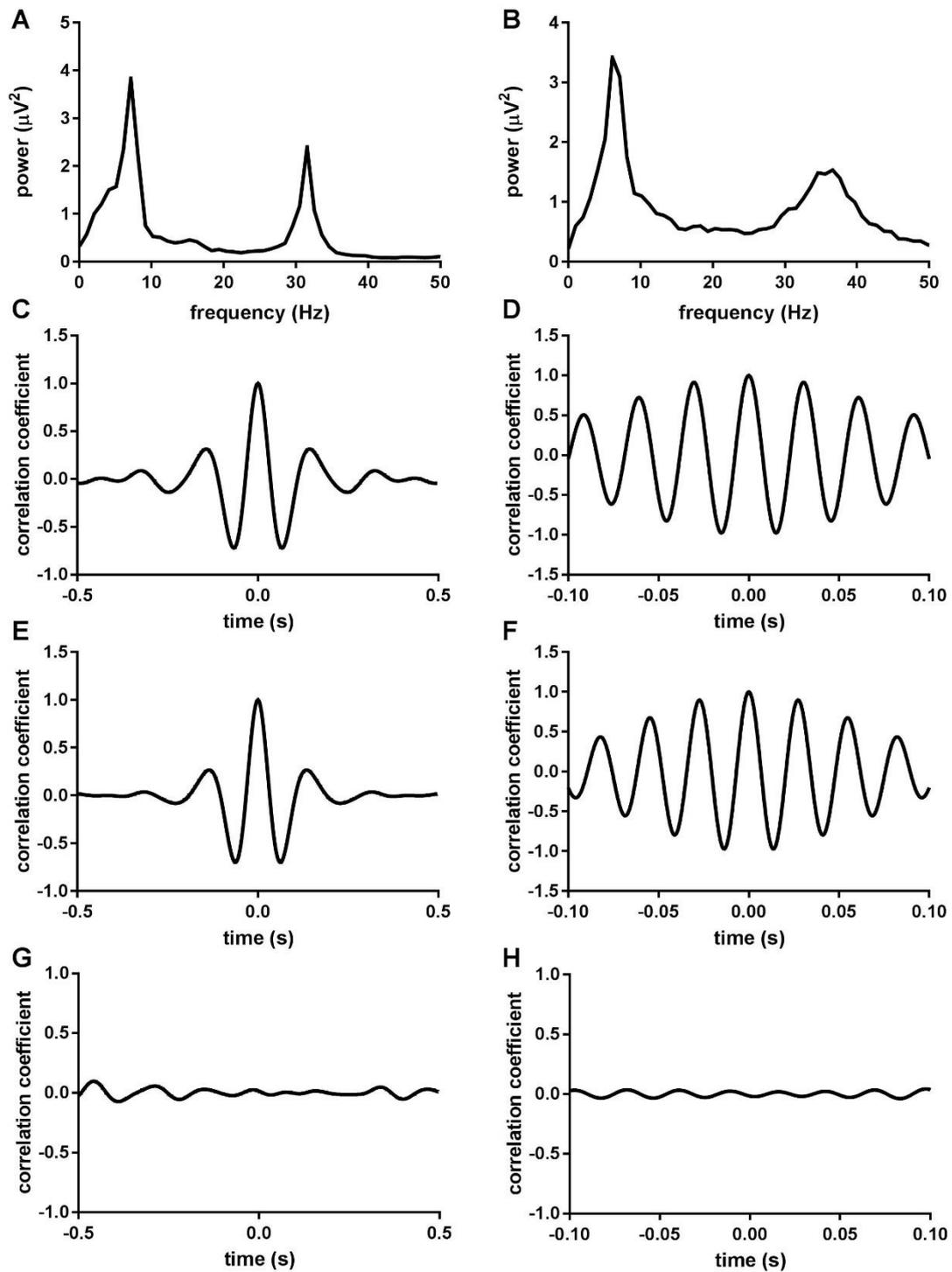
Figure 3.10 No correlation exists between theta and gamma oscillations between M1 and S1 in slice type B.

(A) Representative power spectrum of theta and gamma oscillations of 60 s extracellular recording from LV of M1 and **(B)** of S1 **(C)** auto-correlation analysis of theta oscillation in M1 and **(E)** in S1 **(D)** auto-correlation analysis of gamma oscillations in M1 and **(F)** in S1. **(G)** cross-correlation analysis of theta oscillations in M1 and S1 **(H)** cross-correlation analysis of gamma oscillations in M1 and S1.
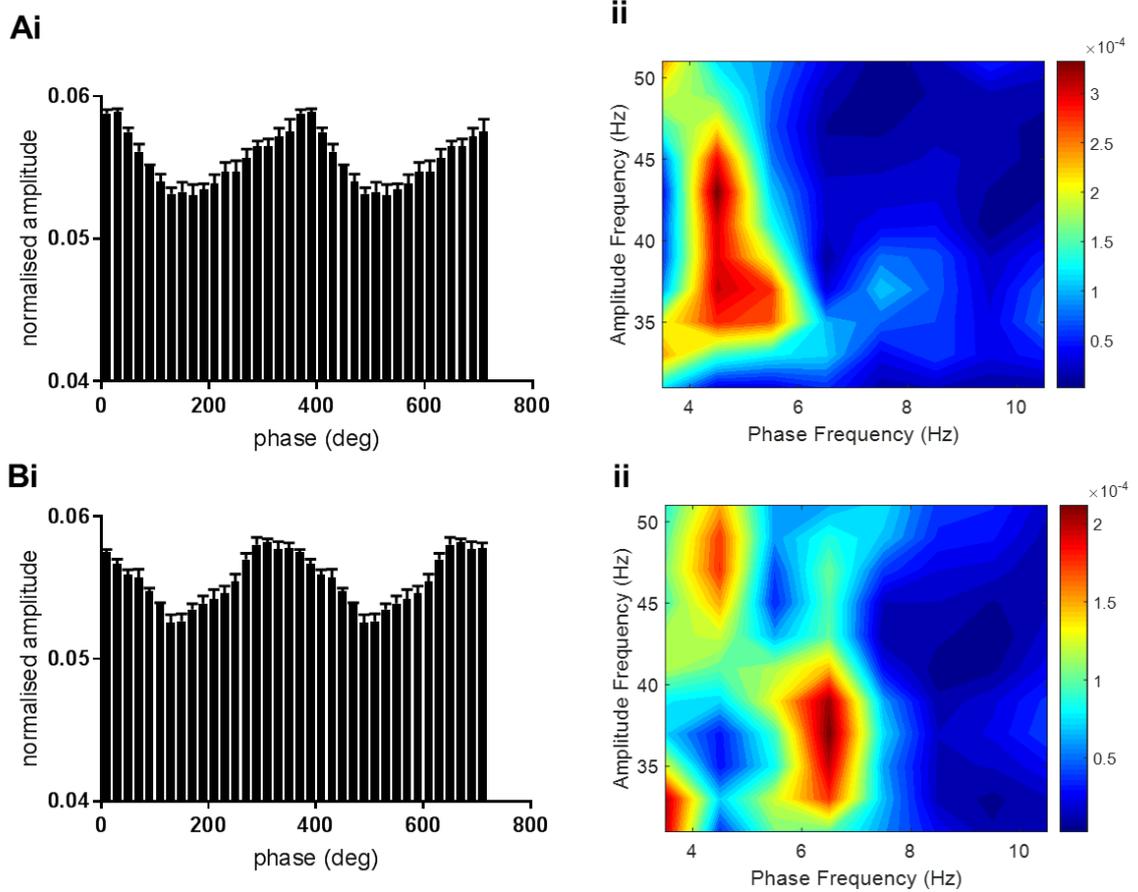
Figure 3.11 Local phase amplitude coupling exists between theta and gamma oscillations both in M1 and S1 in slice type B

(Ai) pooled phase amplitude coupling (PAC) graph of theta and gamma oscillations in M1 **(Bi)** of S1 **(Aii), (Bii)** representative comodulogram showing the cross frequency coupling in frequency domain, areas of high modulation are in red in M1 (MI=6.06x10^{-4}) and S1 (MI=1.4x10^{-4}) respectively.

3.3.3 Correlation and PAC studies of theta and gamma oscillations in slice type C
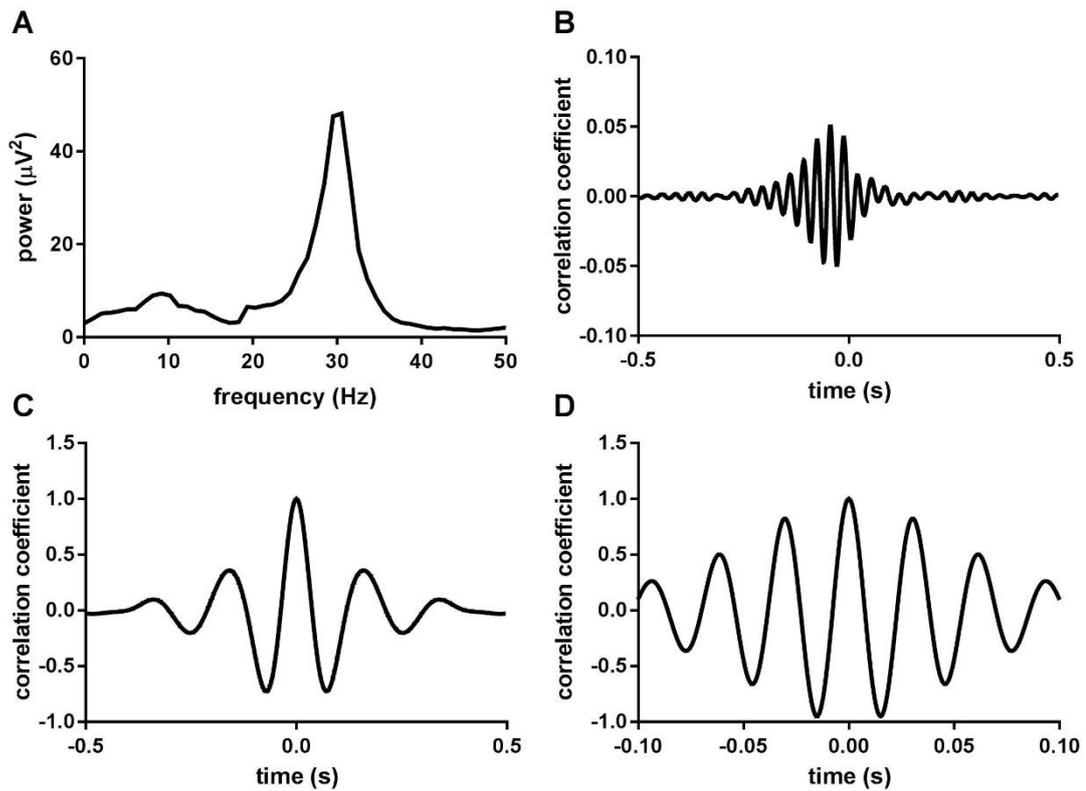
Figure 3.12 No correlation exists between theta and gamma oscillations in (M1) slice type C

(A) Representative power spectrum of theta and gamma oscillations of 60 s extracellular recording from LV of M1 **(B)** cross-correlation analysis of theta and gamma oscillations. **(C)** auto-correlation analysis of theta oscillation in M1 **(D)** auto-correlation analysis of gamma oscillations in M1.
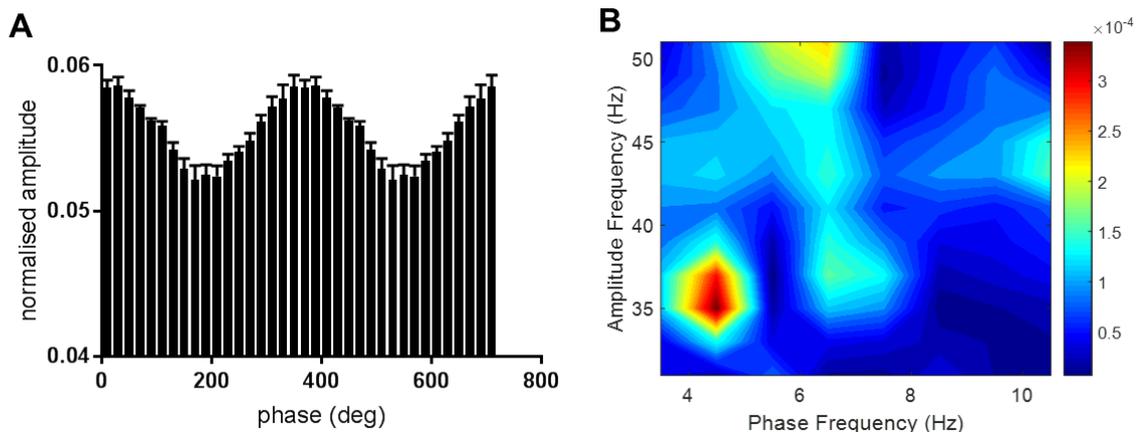
Figure 3.13 Local phase amplitude coupling exists between theta and gamma oscillations in M1 slice type C

(A) pooled phase amplitude coupling (PAC) graph of theta and gamma oscillations in M1 **(B)** representative comodulogram showing the cross-frequency coupling in frequency domain, areas of high modulation are in red (MI=3.19x10^{-4}).

3.3.4 Correlation and PAC studies of theta and gamma oscillations in slice type D
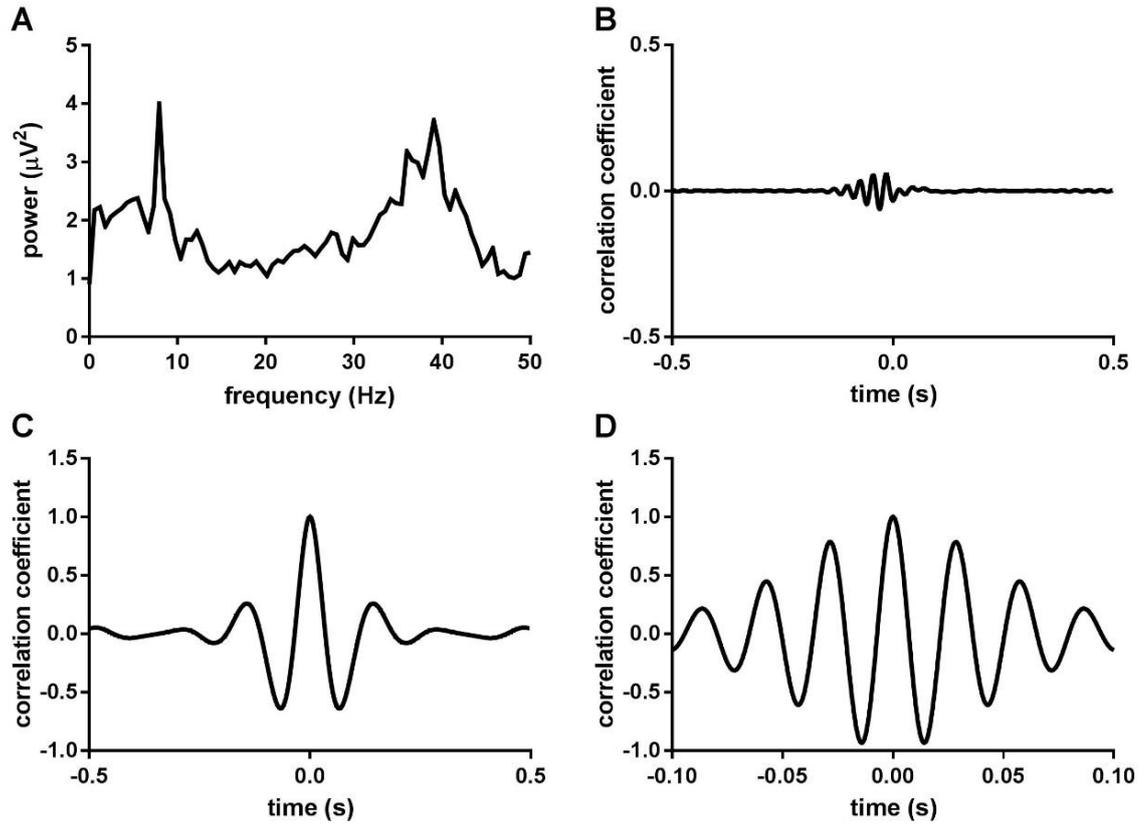
Figure 3.14 No correlation exists between theta and gamma oscillations in (S1) slice type D

(A) Representative power spectrum of theta and gamma oscillations of 60 s extracellular recording from LV of S1 **(B)** cross-correlation analysis of theta and gamma oscillations. **(C)** auto-correlation analysis of theta oscillation in S1 **(D)** auto-correlation analysis of gamma oscillations in S1.
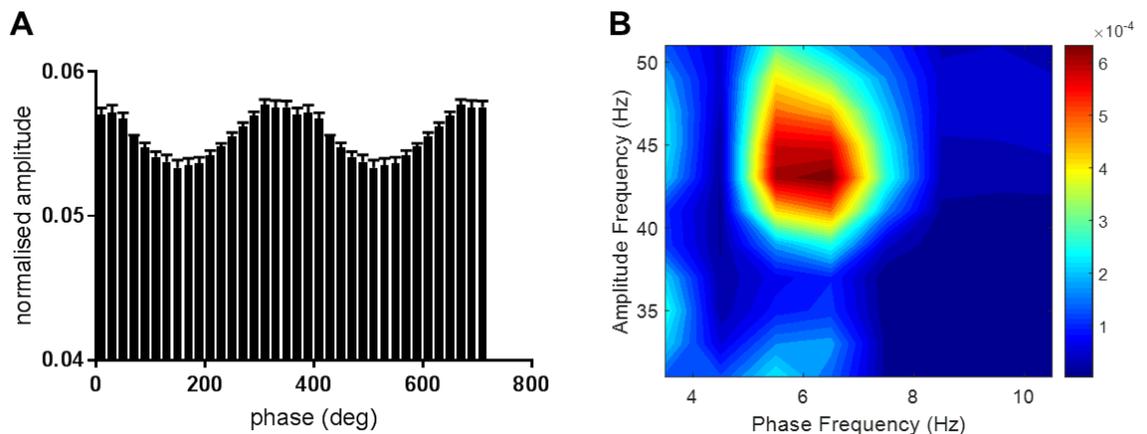
Figure 3.15   Local phase amplitude coupling exists between theta and gamma oscillations in S1 slice type D

(A) pooled phase amplitude coupling (PAC) graph of theta and gamma oscillations in S1 **(B)** representative comodulogram showing the cross-frequency coupling in frequency domain, areas of high modulation are in red (MI=1.62×10^{-4}).

3.3.5 Correlation and PAC studies of theta and gamma oscillations in slice type E

In this type of micro slice where only M1 and S1 were isolated from rest of the regions, there was no activity noticed in the presence of KA (150 nM) and CCh (10 µM). Application of double concentrations of KA and CCh also did not induce any oscillatory activity, probably because of many cuts that were made in slice preparation as well as suggesting local networks are essential for neuronal activity within M1 or/and S1 (data not shown).

3.3.6 Comparison of modulation index in various slice types

Bar graph below represents MI in various slice types. Note the significant differences between M1 in intact slice (A) and M1 only slice (C) (**, $p<0.01$, n=5), S1 in intact (A) and S1 only slice (D) (**, $p<0.01$, n=5), S1 in intact (A) and M1 only slice (C) (***, $p<0.001$, n=5), S1 in cut slice (B) and M1 only slice (C) (*, $p<0.05$, n=5).

Taken together (table below), high percentage (74%) of coupling was observed in slice type C, then in slice type D (66%) followed by slice type B (41%) and A (36%). This could probably mean the biological differences in each slice obtained daily however needs further investigations of the mechanisms behind the coupling.
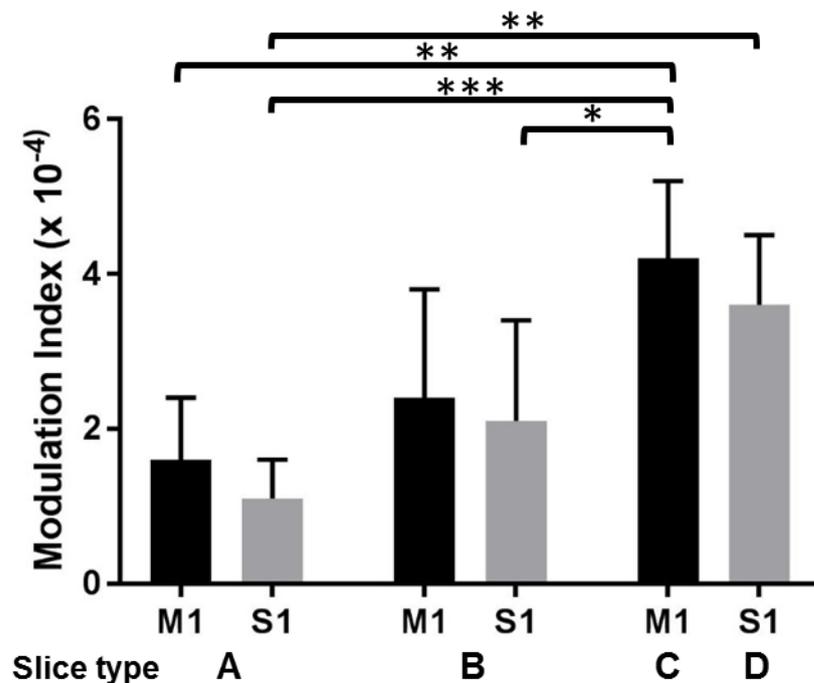
Figure 3.16 Bar chart representing modulation index (MI) in various slice types.

MI (Mean+SEM) of theta and gamma oscillations coupling in M1 and S1 in slice types A, B, C and D.

Slice preparation type	Modulation Index (MI) x 10^{-4} mean+SEM (n=5)		% of slices showing coupling
	M1	S1	
(A) Intact M1&S1	1.6 ± 0.8	1.1 ± 0.5	36
(B) Cut M1/S1	2.4 ± 1.4	2.1 ± 1.3	41
(C) only M1	4.2 ± 1	-	74
(D) only S1	-	3.6 ± 0.9	66

Table 3.2 Mean modulation index of theta and gamma oscillations in M1 and S1 and the percentage of coupling in various slice types.

3.3 Discussion

Initial investigations in the lab (Yamawaki, 2008) using coronal sensorimotor slices that are obtained from decapitated animals using standard storage glucose-based aCSF and the cutting aCSF was sucrose-based (Aghajanian and Rasmussen, 1989). aCSF in these studies contained neuro-protectants such as indomethacin (cyclooxygenase inhibitor, 450 µM) (Pakhotin *et al.,* 1997). There was no spontaneous activity in these slices, however, bath application of KA (400 nM) and CCh (50 µM) (as used by Buhl *et al.,* 1998) induced beta oscillations with a mean frequency of 27.8 ± 1.1 Hz which was in consistent with previous *in vivo* studies (Murthy and Fetz, 1992; Baker *et al.,* 1997; Jensen *et al.,* 2005). Beta oscillations in M1 were reported to originate in layer V and were dependent on GABAR, NMDAR, M_1R as well as gap junctions (Yamawaki, 2008). It was only in subsequent years it was identified that the slices were less viable and only a very low percentage of slices showed oscillatory activity (Prokic, 2011), possibly due to the damage that occurred during preparation of slices. Numerous studies have explored this issue and it was indicated that addition of neuro-modulators to standard sucrose-based aCSF solutions would enable increased viability of slices (Hajos and Mody, 2006). Ascorbic acid is known to be abundant in cerebral cortex (up to 500 µM) (Rice, 2000) which was found to be depleted during slice preparation. Hence, addition of 1 mM Ascorbate was used to compensate any loss. Taurine has been identified to play a role in cell viability (Boldyrev *et al.,* 1999), mitochondrial function (Palmi *et al.,* 1999) and intracellular calcium levels (Wu and Prentice, 2010) and NAC has been suggested to revive the functioning of mitochondria during brain injury (Xiong, Peterson and Lee 1999). Therefore, we (Prokic *et al.,* 2011) decided to modify the standard aCSF (see methods chapter for full composition of modified aCSF) by adding ascorbate (1 mM), taurine (1 mM) and NAC (2 mM). Also, indomethacin (22.5 µM), uric acid (400 µM) and ascorbic acid (300 µM) and aminoguanidine (200 µM) were added to modified aCSF as neuro-protectants (Griffiths *et al.,* 1993; Rice *et al.,* 1994; Pakhotin *et al.,* 1997). Storage aCSF also contained indomethacin (22.5 µM) and uric acid (400 µM). Slices were stored on a storage chamber before recording to enable the above-mentioned neuro-protectants to be washed off. Also, several studies in the past have suggested that slices required an hour of recovery period due to the structural damage that occurred during slicing (Hajos *et al.,* 1989; Kirov *et al.,* 1999). Recordings made from slices immediately after slicing did not enable the generation of oscillatory activity even in the presence of KA and CCh confirming the need for recovery period before recording.

Pietersen *et al.,* has showed that trans-cardial perfusion using sucrose-based aCSF has increased the generation of spontaneous gamma oscillations in hippocampus (Pietersen *et al.,* 2009). These modifications and additions to aCSF along with trans-cardial perfusion has enabled a better cell viability and improved oscillatory activity to greater extent (about

60%) (Prokic, 2011) when compared to original work in the lab (Yamawaki, 2008). Recordings made from these slices revealed no spontaneous activity. However, an increase in frequency to 29.9 ± 1.0 Hz in coronal plane whilst, 32.66 ± 0.89 Hz in sagittal plane in the presence of KA (100-150 nM) and CCh (5-10 µM) was observed since high concentration used previously (400 nM) and CCh (50 µM) (Buhl *et al.,* 1998; Yamawaki, 2008) induced seizure like activity. This reduced requirement of KA and CCh could be accounted for by the modified solutions as well as sagittal plane slicing which aided in better preservation of network connections (Prokic, 2011; Johnson, 2016).

3.3.1 KA and CCh induced oscillations in M1 and S1

KA has been shown to induce oscillatory activity in sensory cortex (Roopun *et al.,* 2006), hippocampus (Fishan *et al.,* 1998; Modebadze, 2014) and entorhinal cortex (Cunningham *et al.,* 2003). Wang and Buzsaki have reported that increasing excitatory drive by application of KA or CCh induced high power and high frequency gamma oscillations when compared to spontaneous gamma in hippocampus (Wang and Buzsaki, 1996). KA alone failed to induce oscillations in mouse somatosensory cortex (Buhl *et al.,* 1998). However, co-application of muscarinic receptor agonist in micro-molar concentration has enabled oscillatory activity at gamma frequency (Buhl *et al.,* 1998). Various concentrations of CCh (4-60 µM) has enabled the generation of delta, theta and gamma oscillations (Fellous and Sejnowski, 2000; Tiesinga *et al.,* 2001). Currently, nested rhythms have become of more interest in electrophysiology and may have a role in memory processing, sensory information and coding (Lisman and Jensen, 2013). Theta and gamma oscillations were observed previously in hippocampus (Soltesz and Deschenes, 1993; Bragin *et al.,* 1995; Colgin *et al.,* 2009; Belluscio *et al.,* 2012). Co-application of KA and CCh was found to be essential to generate oscillatory activity in M1 (Yamawaki, 2008, Prokic, 2011, Johnson, 2017).

Co-application of KA and CCh reliably induced theta and gamma oscillations in both M1 and S1 and which were stable for 3-4 hrs in line with other *in vitro* studies (Dickinson *et al.,* 2003). Beta was initially defined as 25-35 Hz (Murthy and Fetz, 1992) but was redefined as 20-40 Hz (Murthy and Fetz, 1996 a, b), then as 20-30 Hz (Baker *et al.,* 1999) and the others defined as 15 Hz (Traub *et al.,* 1996). It was then considered as low (15-20 Hz) and high beta (20-30 Hz). These frequencies overlap with gamma which is either 25 Hz above or 35 Hz and above (Whittington *et al.,* 1995). The classification of frequency ranges has always been in conflict between several studies. Nevertheless, theta was defined as 6-10 Hz and gamma as 30-40 Hz in this study.

3.3.2 Role of KA and CCh in oscillatory activity

KA enables neuronal excitation and synaptic transmission (Contractor *et al.,* 2011). It was established that KA acts via direct pre-synaptic effect (Cossart *et al.,* 2001) as it enhances AP-independent miniature (m) IPSC frequency (Cossart *et al.,* 1998; Frerking *et al.,* 1998). Moreover, KA was known to activate KAR by resulting in enhancing the excitability of neurons. Furthermore, nanomolar concentrations of KA have been identified to increase both sEPSPs and mEPSPs recorded from pyramidal cells (Campbell *et al.,* 2007) by postsynaptic depolarisation of excitatory synapses. Nevertheless, *in vivo* studies in rats revealed that low concentrations of KA cause a reduction in GABA mediated inhibition (Lerma, 1997) and KA when used in higher concentration can induce seizures (Smolders *et al.,* 2002).

CCh was co-applied along with KA to induce oscillatory activity in M1 and S1. CCh activates muscarinic mACh receptors. These receptors are known to be post synaptically expressed and are G-protein coupled (Muller and Misgeld, 1986). This receptor depolarises by regulating various K^+ channels which include leak K^+ current ($I_{K\text{-leak}}$), Ca^{2+} dependent K^+ current (I_{AHP}), rectifying outward current (I_M) (Lucas-Meunier *et al.,* 2003). Moreover, mAchR modulates I_h currents which are known to play a critical role in oscillatory activity (Traub *et al.,* 2000; Fishan *et al.,* 2002). Furthermore, CCh acts by increasing glutamate release first in interneurons by fast hyperpolarisation and then in pyramidal cells via slow depolarisation (McCormick and Prince, 1986; Lucas-Meunier *et al.,* 2003). Pirenzepine, a mAChR antagonist, was found to abolish CCh induced gamma oscillations (Fishan *et al.,* 1998; Fishan *et al.,* 2002).

3.3.3 GABA$_A$R modulation

GABA$_A$ receptors are ligand gated ion channels. These receptors act by increasing the membrane permeability of anions (Cl^- and HCO_3^- ions) which hyperpolarises the membrane resulting in inhibition (Rivera *et al.,* 1999). Theta oscillations and gamma oscillations have suggested to be dependent on GABAR in several studies (Gokebiewski *et al.,* 1996; Konopacki *et al.,* 1997; Buhl *et al.,* 1998; Fisahn *et al.,* 1998; Cunningham *et al.,* 2003; Cardin *et al.,* 2009) Theta oscillations were increased upon application of gabazine. The increase in power of theta oscillations could attributed to disinhibition (inhibiting the inhibitory inputs) generated by theta-off neurons in cortex (Lukatch and MacIver, 1997). Gamma oscillations were abolished upon the application of GABAR antagonists in line with previous studies in hippocampus, CA3 and cortex (Fisahn *et al.,* 1998; Fisahn *et al.,* 2004; Palhalmi *et al.,* 2004; Cunningham *et al.,* 2003; Pietersen *et al.,* 2009). Frequency of gamma oscillations were known to be dependent on decay time constant of GABA$_A$R mediated IPSCs (Traub

et al., 1996). Pentobarbital has shown a decrease in hippocampal gamma frequency owing to prolonged IPSC decay kinetics (Segal and Barker, 1984; Modebadze, 2014). Moreover, fast spiking interneurons are known to be essential for gamma oscillations in cortex (Cardin *et al.,* 2009). However, it was not possible to investigate interactions between pyramidal neurons and adjacent interneurons due to experimental limitations in the current study. Dependence of theta and gamma oscillations on GABA$_A$R implies the requirement of inhibitory currents in M1 and S1 like in hippocampal brain regions (Whittington *et al.,* 1995; Fishan *et al.,* 1998, Modebadze, 2014). It is however assumed from the above results that gamma oscillations may originate from synaptic mechanisms whilst theta oscillations reflect non-synaptic mechanisms since the power of theta increased upon application of GABAAR antagonist unlike gamma oscillations (decreased in power). A colleague in the lab has recently reported that high concentration (2.5 µM) of GBZ has shown a similar effect as low concentration (Johnson *et al.,* 2017) implying the blockade of synaptically driven oscillations enhances the non-synaptically driven oscillation (Roopun *et al.,*2006).

3.3.4 Glutamate modulation

Excitatory currents have been identified to contribute to network oscillatory activity in M1 including delta, theta, gamma and beta oscillations (Yamawaki, 2008; Prokic, 2011; Johnson, 2016, Carrecedo *et al.,* 2013), somatosensory cortex of mouse (Buhl *et al.,* 1998) and in hippocampus (Fisahn *et al.,* 1998; Modebadze, 2014).

SYM2206, an AMPAR antagonist (Pelletier *et al.,* 1996) abolished gamma oscillations, whilst increasing theta oscillations in M1 and S1. When CNQX, a KAR/AMPAR antagonist was bath applied, similar effects to that of SYM2206 were observed. Requirement of KAR and AMPAR mediated excitation for the generation of gamma oscillations has been previously reported in various studies in hippocampus (Whittington *et al.,* 2000; Cunningham *et al.,* 2003; Pietersen *et al.,* 2009). Gamma oscillations in M1 and S1 represent PING-like oscillations based on their reliance on phasic excitatory transmission (Whittington *et al.,* 2000) and are not comparable to beta oscillations in M1 which were insensitive to AMPAR block (Yamawaki, 2008). Gamma oscillations have been shown to be altered upon the reduction of AMPAR mediated EPSPs in GluA3 and A4 subunits (expressed on PV+ interneurons) KO experiments suggesting a role of specific sub-unit expression on interneurons in oscillatory activity (Fuchs *et al.,* 2007). Increases in the power of theta oscillations is in consistent with a study performed in the conditions of decreased AMPAR activity in hippocampus (Gillies *et al.,* 2002) and it was suggested that a subset of interneurons have set this theta frequency. This could mean the existence of neuronal population with similar intrinsic properties to that of in hippocampus that are being recruited in the conditions suppressing AMPA currents. Further investigations of neuronal populations in M1 and S1 using optogenetic or labelling studies would be beneficial.

It was previously reported that NMDAR blockade induced an increase of beta frequency oscillatory power in M1 (Yamawaki, 2008). We found the NMDAR antagonist, 2-AP5, increased gamma oscillations in M1 and S1 whilst decreasing theta power in S1, but no effect on theta oscillations in M1. NMDAR have shown differential effect on gamma oscillations in various studies. For instance, no significant change was identified in KA induced gamma oscillations (Fishan *et al.,* 2004). In contrast, spontaneous gamma oscillations were decreased, and KA induced activity was increased in the presence of NMDAR antagonist, AP-5 (Pietersen *et al.,* 2009). CCh induced gamma oscillations have been reported to be enhanced upon NMDAR suppression (Modebadze, 2014) in hippocampal slices. Similar results were identified with NMDAR modulators at delta frequency in M1 and S1 as well (see chapter 4 and 5). GluN1 subunit played a significant role in neuronal activity as knocking out this specific subunit has increased firing rate of pyramidal neurons and decreased synchrony in cortex (Belforte *et al.,* 2010). It was also evident that, increase in theta oscillations, decrease in the gamma oscillations and altered theta and gamma coupling have been identified in PV+ interneurons using GluN1 KO mice experiments (Korotkova *et al.,* 2010) suggesting NMDAR that is localised on GABAergic interneurons drive them to spike at gamma frequency (Borgers and Kopell, 2003). Increase in theta power in S1 could mean that there are more cells available to entrain at theta frequency and no change in M1 could be attributed to the region-specific organisation suggesting a need for various subunit expression investigations using KO studies. However, theta oscillations were found to be increased when non-competitive antagonists MK-801 and ketamine were bath applied by a colleague in lab (Johnson *et al.,* 2017) which contrasts with an in vivo study in hippocampus has shown a reduction of theta oscillations using ketamine (Sabolek *et al.,* 2009) in accordance with Gillies *et al.,* (2002) suggesting a need for further studies using various receptor modulators.

3.3.5 DA and AMPH modulation

D1-like receptors have identified to be abundantly expressed on pyramidal neurons in deep layers of M1 (Vitrac *et al.,* 2014) with D1R located on soma and D5R on apical dendrites (Awenowicz and Porter, 2002). However, Both D1 and D2 like receptors are known to be localised on PV+ interneurons that are present in deep layers (Le Moine and Gasper, 1995). DA plays a critical role in network activity in M1 (Alexander *et al.,* 1986). Exaggerated beta oscillations (12-30 Hz) have been reported in DA depleted conditions associated with PD (Bevan *et al.,* 2002). DA is known to oxidise which was noticed by colour change. Hence, Ascorbic acid was added to prevent this. Ascorbic acid on it own at the concentrations used in our study did not affect oscillations. Ozkan *et al.,* (2017) demonstrated that "bath application of DA resulted in a decrease in gamma power with no change in theta power.

However, application of either the D1-like receptor agonist SKF38393 or the D2-like agonist quinpiroleco increased the power of both theta and gamma suggesting that the DA-mediated inhibition of oscillatory power is by action at other sites other than classical DA receptors". In the current study, when DA was bath applied, it increased the power of both theta and gamma in M1 and S1 respectively. There could be several possible mechanisms as to why DA enabled the excitation as following: *In vivo* studies have revealed that administration of DA in to M1 of awake rat enhanced excitability (Storozhuk *et al.,* 2004) in accordance with previous work in LV of primate M1 in which DA increased the spontaneous activity of the neurons (Sawaguchi *et al.,* 1986). Activation of D1 receptors on pyramidal neurons or D2 receptors in interneurons (by inhibiting the inhibitory drive) could be the basis for excitation. Similarly, there is evidence that D2 antagonists, but not D1 receptor antagonists decreased the excitability of pyramidal neurons in motor cortex of rats (Hosp *et al.,* 2009). Also, α-adrenergic receptors have shown to contribute to DA mediated responses (Yang *et al.,* 2014). Moreover, D1R, via PKA cascades has reported to directly influence the function and trafficking of iGluRs. For instance, PKA increases the surface expression of NMDA and AMPA receptors (Snyder *et al.,* 2000; Hallett *et al.,* 2006) trafficking could be a result of direct interaction between D1 and NMDAR (Lee *et al.,* 2002; Scott *et al.,* 2006). Furthermore, it was evident from recent years that DA directly modulates $GABA_A R$ (Hoerbelt *et al.,* 2015) which could form the grounds for increase in power of theta and gamma oscillations in M1 and S1. The mechanism involved here could be disinhibition in which increase in GABA would increase inhibiton on inhibitory interneurons which is enhancing the power through consequent increased excitation of principal cells. Given the ubiquity of $GABA_A Rs$, it might be beneficial to perform investigations using selective and specific drugs that target DA-GABA mechanisms. Amphetamine sulphate, a potent CNS stimulant, when bath applied has shown a significant increase in power of theta and gamma oscillations to in M1 and S1 similar to that was observed upon DA application. AMPH enhances DA levels by inhibiting DA uptake via (dopamine transporter) DAT, facilitates the release of DA from vesicles to cytoplasm and by enabling the DAT mediated reverse transit from cytoplasm to extracellular space (synaptic cleft) independent of action potential mediated vesicular release (Richfield *et al.,* 1989; Fleckenstein *et al.,* 2007) which was termed as DA efflux enabling increased locomotion (German *et al.,* 2015; Kopra *et al.,* 2017) in line with a study suggesting extracellular dopamine levels have indicated to be higher after AMPH administration in rats (O`Leary *et al.,* 2016.). This may explain DA mediated effects of AMPH. Auto-radiographic investigations have shown that deep layers (LV and LVI) of motor areas (M1 and S1/2) have been identified to be innervated by dopamine (Descarries *et al.,* 1987; Berger *et al.,* 1988) which may suggest a robust disruption of M1 and S1 interactions in PD pathophysiology caused due to DA depletion suggesting a requirement for further research.

3.3.6 Possible mechanism of theta and gamma oscillations in M1 and S1.

Co-application of KA and CCh at very low concentrations (150 nM and 10 μM CCh) compared to earlier studies (Buhl *et al.,* 1996, Yamawaki, 2008) reliably induced theta and gamma oscillations both in M1 and S1. Basic pharmacology performed using various receptor modulators has revealed the contribution of $GABA_A R$, NMDAR, AMPAR as well as DAR. Gamma oscillations were decreased by $GABA_A R$ antagonists (gabazine and picrotoxin) and also by AMAPAR antagonist (SYM2206), whilst increasing theta power in these cases. $GABA_B R$ antagonist (CGP55845), GABA positive modulators such as diazepam, zolpidem, NMDAR antagonist (MK 801) and mGluR antagonists have shown an increase in both oscillations (Johnson *et al.,* 2017). Theta and gamma oscillations were found to be reliant on gap junctions as the activity was abolished when carbenoxolone, a gap junction blocker was bath applied (Johnson *et al.,* 2017) which in consistent with beta oscillations in M1 (Yamawaki *et al.,* 2008) and delta oscillations (chapter 4). Dependence of oscillatory activity of mAchR in M1 reflects the incidence of oscillatory activity using CCh (Johnson *et al.,* 2017) along with KA and was proved by bath application of mAchR antagonist. Atropine abolished both theta and gamma oscillations (Johnson *et al.,* 2017) in consistent with various studies (Konopacki *et al.,* 1987; Lukatch and MacIver, 1997; Buhl *et al.,* 1998; Fisahn *et al.,* 1998).

3.4 M1 and S1 interactions in various types of slice preparations

3.4.1 Correlation studies

It is evident that the relation between sensory inputs and movements is facilitated by interactions within primary motor and primary sensory cortices. Exploration of environment by whisker movements and this feedback from sensory inputs aids further movements as seen in rodents (Nguyen and Kleinfeld, 2005) as well as in primates (Murthy and Fetz, 1996) suggesting a critical role of sensory motor circuits in integration and synchronising activity. Sensorimotor areas also show an association with several other regions like cerebellum (Popa *et al.,* 2013), cerebral cortex, spinal cord and basal ganglia in order to aid voluntary movements (Wichmann and DeLong, 1999). Anatomical studies have reported that M1 receives sensory input from S1 and thalamus (Zin-Ka-Leu and Arnault, 1998; Miyachi *et al.,* 2005). The reciprocal connections between M1 and S1 have been known to be well preserved by optimum plane sensorimotor slice preparation developed by Rocco *et al.,* (2007). Auto correlation studies revealed the frequencies of the above described dual rhythm to be in theta and gamma range. Theta in between two regions have shown a

significant correlation and so did gamma between M1 and S1. However, both theta and gamma frequencies have revealed a significant phase delay in M1 to that of S1 suggesting S1 to be the possible origin of oscillatory activity of this dual rhythm (theta and gamma). This is in accordance with several electrophysiological investigations which suggested that neuronal network activity of M1 was regulated by S1 (Kosar *et al.,* 1985; Zarzecki *et al.,* 1989; Kaneko *et al.,* 1994; Farkas *et al.,* 1999; Kelly *et al.,* 2001). Interestingly, cross-correlation studies performed in M1 and S1 at beta frequency (Prokic, 2011) has revealed near synchrony since there were no significant phase differences. However, there was a delay in desynchronising oscillatory activity in M1 suggesting that activity in S1 preceded that of M1 based on the fact that sensory information is being transferred to M1 from S1 (Ferezou *et al.,* 2007) and that the connections from S1 to M1 dominate (Izraeli and Porter, 1995; Welker *et al.,* 1998). It was found that oscillatory activity in S1 was first abolished followed by M1 when zolpidem was bath applied reflecting the dominant projections from S1 to M1 and could also mean that S1 sets the rhythm and M1 follows (Prokic, 2011).

Interestingly, in slice type B, there was absolutely no correlation between M1 and S1 suggesting the loss of crucial connections between M1 and S1 with the cut made in this type of slice between two regions based on the fact that there are direct connections between the two regions in rodents and cats (Asunama *et al.,* 1981; Donoghue and Parham, 1983; Porter and Sakamoto, 1988; Izraeli and Porter, 1995). Although there were intra and inter-cortical connections between M1 and S1, those between LVa of S1 to L2/3 and LVa of M1 and reciprocal connections to S1 from LVa and LVb are probably the two most important connections (Mao *et al.,* 2011) and the cut that was made was is assumed to have disrupted these connections. It was suggested that onset of movements have occurred upon S1 stimulation, both in healthy and pathological states (Johansson *et al.,* 1993; Hamdy *et al.,* 1998; Kaelin-Lang *et al.,* 2002) as well as prevention of sensory inputs using local anaesthesia has disrupted motor control (Edin and Johansson, 1995) and complex motor skills (Sakamoto, 1989). Also, activity in M1 was eliminated upon the inactivation of S1 (Anderson, 1995) suggesting that connections between M1 and S1 has functional significance. In isolated slice types C (M1 only) and D (S1 only), dual oscillations (theta and gamma) have been induced using KA and CCh suggesting the ability of individual regions to generate oscillatory activity independent of each other. The local networks seem to be sufficient for this dual rhythm generation. However, these slices were intact with neighbouring regions and to investigate the role of regions surrounding both M1 and S1, slice type E was used. This slice is a segregated micro slice of just M1 and S1 isolated from every possible surrounding region, which did not enable any oscillatory activity probably due to several cuts made to obtain this slice or the involvement of sub cortical connections in generating oscillatory activity, which may need further exploration.

3.4.2 Phase-amplitude coupling (PAC) studies

Interactions between two different types of oscillations is defined as cross-frequency coupling (CFC) and has been identified in EEG, ECog and LFP recordings (Bragin *et al.,* 1995; Lakatos *et al.,* 2005; Canolty *et al.,* 2006; Demiralp *et al.,* 2007; Jensen and Colgin, 2007; Cohen, 2008; Kramer *et al.,* 2008; Young and Eggermont, 2009). Phase amplitude coupling between theta and gamma oscillations, where the phase of low frequency (theta) oscillations modulates the amplitude of high frequency (gamma) oscillations has been of a particular interest in recent years (Bragin *et al.,* 1995; Canolty *et al.,* 2006; Demiralp *et al.,* 2007; Hentschke *et al.,* 2007; Jensen and Colgin, 2007; Kramer *et al.,* 2008; Cohen, 2008; Cohen *et al.,* 2009a,b; Handel and Haarmeier, 2009; Lakatos *et al.,* 2005, 2008; Schroeder and Lakatos, 2009; Tort *et al.,* 2008, 2009; Wulff *et al.,* 2009; Young and Eggermont, 2009; Axmacher *et al.,* 2010; McGinn and Valiante, 2014; Lega *et al.,* 2016; Sotero, 2016; Chehelcheraghi *et al.,* 2017; Johnson *et al.,* 2017).

In the current study, PAC was performed between theta and gamma oscillations, with theta frequency (3 –14 Hz) as phase and gamma frequency (25-50 Hz) as amplitude that was driven by low frequency using a MATLAB script developed by Tort *et al.,* 2010. PAC was performed on 60 s epochs of data in various slice types (refer methods section) and was represented as Modulation Index (MI) which indicates the degree of coupling that existed between two oscillations. It was interesting to note that not every slice has shown a coupling and the percentage of slices that exhibited coupling varied according to slice type. High MI was found in slice types C and D in which M1 and S1 are isolated along with adjacent regions. Low MI was observed intact slice (type A) than in cut slice (type B) suggesting that there are connections between two regions in intact slices that are involved in suppression of PAC. Although the MI equation was first applied (to our knowledge) to neuroscience studies in 1998 (Tass *et al.,* 1998), it was not until 2008 that it was applied to phase-amplitude coupling analysis (Tort *et al.,* 2008) in which the phase-amplitude distributions were analysed. Comodulograms is a bidimensional colour map used to measure coupling as described by Tort *et al.,* (2010) and was previously performed by various studies (Canolty *et al.,* 2006; Tort *et al.,* 2008; Tort *et al.,* 2009; Colgin *et al.,* 2009). Coupling was found to vary with each slice. This could probably mean the biological differences such as viability of each slice, receptor expression, interneurons and pyramidal cell expression in each slice obtained daily however, the need for further investigations is high to uncover possible mechanisms behind the coupling.

Modulation of gamma oscillations by theta oscillations has been reported previously in hippocampus in *in vitro* (Fisahn *et al.,* 1998) and *in vivo* studies (Bragain *et al.,* 1995; Penttonen *et al.,* 1998; Csicsvari *et al.,* 2003) and this may be due to the contribution of two distinct sets of interneurons. A study reported that, during gamma oscillations O-LM cells

fire at theta frequency (every 4-5 gamma periods), whereas basket cells fire at each gamma cycle (Gloveli *et al.,* 2005b).

PV+ interneurons could form the basis for high coupling in M1 based on the evidence that PV+ interneurons contribute to generation and coupling of theta and gamma oscillations since selective removal of fast synaptic inhibition from PV+ cells using transgenic mouse protocols (Wulff *et al.,* 2009) effectively abolished theta-gamma rhythmogenesis. This suggests fast synaptic inhibition could form the basis for cross frequency coupling (Bragin *et al.,* 1995; Buzsaki *et al.,* 2002; Bartos *et al.,* 2002; Gloveli *et al.,* 2005a; Tort *et al.,* 2007). Since each subtype fire at distinct patters (phase) each subtype of interneurons probably has a unique role in entraining nested rhythms in various regions.

Moreover, McGinn and Valiante have reported that inter-laminar (deep and superficial layers) synchrony within human cortex is linked to the degree of coupling between the theta and gamma oscillations (PAC) (MacGinn and Valiante, 2014) which is inconsistent with a study in rat cortex and striatum (von Nicolai *et al.,* 2014). Theta frequency displays phase differences between deep and superficial layers which are not uniform (Florez *et al.,* 2013) and these oscillations are coordinated between layers. To further investigate this, McGinn and Valiante performed phase-dependent power correlations, and phase coherence (PDPC) studies (Womelsdorf *et al.,* 2007) which revealed that "both theta power and theta synchrony are related to one another between [deep and superficial] cortical laminae. At the population level, increases in theta power within the LFP may arise from increased synchrony and/or number of theta generating elements (i.e., neurons or small circuits; Buzsaki *et al.,* 2012) and possibly increased spiking (Reimann *et al.,* 2013)" (MacGinn and Valiante, 2014). They have also demonstrated that significant correlation existed between PAC and PDPC mostly within theta band (4-12 Hz) and is particularly strong in deep layers suggesting PAC increases with increase in theta synchrony between the layers. Given the dominance of cortico-cortical projections (Douglas and Martin, 2004) in superficial layers and output to subcortical regions in deep layers, theta oscillations may repesent a mechanism of coordinating cortical outputs. Inter-laminar synchrony at theta frequency may have been well preserved in slices with isolated cortical regions such as M1 and S1 (sub-cortical connections being cut off) and this could probably reflect high coupling in isolated slices compared to intact slices and also providing scope for further investigations.

Pharmacological agents such as ketamine have been reported to influence PAC (Caixeta *et al.,* 2013). In their study, an NMDAR antagonist, ketamine, has shown a dose dependent effect on theta and gamma coupling with an increase in PAC at low dose and decrease in PAC at high doses. Therefore, it is essential to perform PAC before and after various receptor modulators or even throughout the recording to identify how various receptors are

contributing to PAC. This is not explpored in our study but gives plenty of room for future work.

Interestingly, human hippocampus and cortex exhibited different properties in that PAC in hippocampus was the strongest at the phase of slow theta band (2.5-5 Hz) and both low (35-70 Hz) and high gamma (70-130 Hz) whilst, the phase of high theta band (4-9 Hz) was preferred with low gamma exhibiting greater coupling in cortex (Lega *et al.,* 2016). This observation may prove the difference between hippocampal theta oscillations among humans (< 5Hz) and rats (6-12Hz) (Lega *et al.,* 2012; Watrous *et al.,* 2013; Jacobs *et al.,* 2014). It would be beneficial to apply these frequency specific studies in the PAC data that was observed in M1 and S1 of rat slices.

3.5 Final conclusions

Trans-cardial perfusion, sagittal slice preparation, modified aCSF solution as well as addition of neuro-protectants have greatly increased slice viability. Co-application of KA and CCh induced persistent theta and gamma oscillations. This dual rhythm was identified to be led by S1 in an intact slice but both M1 and S1 have individual rhythm generators. These nested oscillations seem to have distinct mechanisms and were identified to be coupled from PAC analysis. However, the percentage of coupling varied in various types of slice preparations with high modulation index (MI) in M1 only slice followed by S1 only slice when compared to intact slice preparations.

4 Characterisation of pharmacologically induced delta oscillations in LV of primary motor cortex (M1)

4.1 Introduction

4.1.1 Neurochemical aspects of the sleep-wake cycle

The sleep-wake cycle is associated with electrical and chemical changes that enable the transition between various sleep and awake states. However, overall orchestrated co-ordination of these electrical and chemical processes in specific brain regions have yet to be explored. We now know that neurons in various regions in the brain such as hypothalamus and brain stem undergo transitions between states via regulated release of various neuromodulators in cortex and thalamus and these are discussed below:

Acetylcholine (ACh) has been identified to play a role in both sleep and awake states. Cholinergic neurons fire at high frequency in the awake state whilst showing no activity in REM sleep. The NREM state has been shown to have an intermediate cholinergic tone (Hobson *et al.,* 2003; Espana and Scammell, 2004; Jones, 2005). Interestingly, ACh neurons in pedunculopontine (PPN), have been identified to have high firing rates both in wake and REM sleep (Wake-ON) more in REM than wake or non-REM sleep (REM-ON) in which the increased firing was observed 20-60 s prior to state change. This shift in patterns has been suggested to underpin the role of PPN in desynchronizing the cortex during awake and REM states (Steriade *et al.,* 1990).

Dopamine (DA) plays a key role in arousal and sleep states. DA has been implicated in awake-associated behaviours such as movement, cognition and arousal as lesioning dopaminergic innervations has shown to decrease arousal. In Parkinson's, a neuro-degenerative disease with symptoms caused by depletion of DA, sufferers show difficulty in active awake-state maintenance. CNS stimulants such as amphetamines and cocaine act on dopaminergic systems which enhances arousal, increased vigilance and attention either by stimulating DA release or by inhibiting re-uptake. Interestingly, compounds like caffeine, that does not act via DA systems, may also influence DA release in the synaptic cleft (Schultz and Miller, 2004; Boutrel and Koob, 2004; Espana and Scammell, 2004; Wisor, 2005; Jones, 2005). Despite the above evidence that DA is critical for arousal, it has not traditionally been grouped with the reticular activating system based on the fact that DA neurons fire at equal rates both in awake and sleep states (Trulson *et al.,* 1981).

Histamine (HA) was found to be wake promoting from the fact that histaminergic neurons fire at higher rates in awake state while remaining silent during REM and NREM sleep (Takahashi *et al.,* 2006), which was revealed in electrophysiological recordings. Furthermore, increased sleepiness is an unwanted side effect of some anti-histamines (Hobson *et al.,* 2003; Jones, 2005).

Serotonin (5-HT) also has been implicated in wake promoting since serotonergic cells fire at a maximum rate in awake state with progressive decline in activity in NREM sleep and no activity in REM sleep. However, the activity was found to be resumed prior to the end of REM episodes (McGinty and Harper, 1976; Trulson and Jacobs, 1979). Although evidence supports the role of 5-HT in the awake state, there is controversy over its role in sleep (Jones, 2005; Espana and Scammell, 2004). Studies suggest this confusion is probably due to many receptor subtypes as well as many activities attributed to 5-HT (Espana and Scammell, 2004; Jones, 2005).

GABA concentration was found to be the highest in cortex during NREM sleep and is reduced in REM sleep in comparison to awake state (NREM>awake>REM) (Vanini *et al.,* 2011). Increased levels of extracellular GABA may indeed enhance synaptic inhibition whereby balancing synaptic inhibition and excitation in slow wave sleep (Haider *et al.,* 2006; Rudolph *et al.,* 2007). However, several studies have identified co-release of GABA with ACh and HA suggesting decreased levels of GABA in NREM sleep (Saunders *et al.,* 2015; Yu *et al.,* 2015).

4.1.2 Significance of delta oscillations

Delta oscillations have been implicated both in deep sleep state and awake states performing cognitive tasks. This apparent contradiction was explained by the existence of some type of inhibition during task that would inhibit the non-relevant neuronal activity (Vogel *et al.,* 1968) known as behavioural inhibition (Kamarajan *et al.,* 2004; Knyazev, 2007; Putman, 2011). Behavioural studies on humans showed that delta oscillations which are prevalent in deep sleep may mediate an enhancement in declarative memory (Huber *et al.,* 2004; Aeschbach, 2009). Rotation adaption tasks on human subjects performed in this study showed a greater correlation between increases in the 1-4 frequency range and improved task performance after sleeping in EEG of cerebral cortex (Huber *et al.,* 2004). Sleep has been suggested to facilitate memory consolidation by strengthening and stabilising memories (Gais *et al.,* 2000; Stickgold *et al.,* 2000; Maquet, 2001; Walker and Stickgold, 2006; Rasch and Born, 2013). It was demonstrated that better performance was observed in a group that were allowed to sleep after learning compared to a group that were awake after learning. Besides consolidation of previously acquired memories sleep also plays a role in acquisition of new memories (Van Der Werf *et al.,* 2009) which was proved in a study where short period of sleep preceding learning has enabled a greater capacity to encode information (Mander *et al.,* 2011). Also, it has been reported that the synaptic plasticity associated with low frequency oscillations during sleep contribute to memory consolidation processes (Steriade and Timofeev, 2003). Interestingly, some studies have suggested a role for the phase component of delta oscillations in decision making and signal detection (Basar-Eroglu *et al.,* 1992) by rhythmically modulating the rate of sensory

information received over time (Wyart *et al.,* 2012) and in many cognitive processes (Basar *et al.,* 2001). Delta oscillations are also known to play a critical role in pathological conditions: decreased synchronous delta activity was observed in schizophrenic patients (Ford *et al.,* 2008), reduced delta amplitude and coherence in Alzheimer's patients (Guntekin *et al.,* 2008; Yener and Basar *et al.,* 2010) increased delta power in Parkinson`s patients under medication (Kryzhanovskii *et al.,* 1990) and disrupted delta activity in epilepsy (Tao *et al.,* 2011; for review see Harmony, 2013).

Despite its functional significance, cellular mechanisms of cortical delta rhythmogenesis and its mechanistic origin have not yet been explored. There is a hypothesis that the cortical delta rhythm was mediated by intrinsically bursting neurons (Amzica and Steriade, 1998) however, in that study the usage of depolarising current pulse (intercellular injections) did not match with long lasting hyperpolariaation conditions during sleep reported in cortex (Steriade *et al.,* 2001; Timofeev *et al.,* 2000). This leads to further discrepancies regarding the mechanism underlying cortical delta rhythm. A recent study in slices containing secondary somatosensory/parietal area (S2/Par2) has revealed generation of delta oscillations *in vitro* by maintaining neuro-modulatory state equivalent to deep sleep state (Carracedo *et al.,* 2013). Our current study performed on LV of M1 demonstrates the generation of delta oscillations by pharmacological manipulations and investigates the contribution of various receptors involved in the rhythm generation and the pharmacological equivalent awake state. Characterisation of delta rhythm in control slice preparations may facilitate understanding of the mechanisms underlying various pathological conditions like Alzheimer's disease.

4.2. Pharmacology of delta oscillations in M1.

4.2.1 Pharmacological induction of delta oscillations in M1

It is evident that there was no spontaneous activity in M1, however, it was possible to induce activity by pharmacological manipulations. Theta (6-10 Hz) and gamma (30-37 Hz) oscillations were induced by co-application of 150 nM of KA and 10 µM of CCh (see chapter 3 for details). Delta (2-4 Hz) oscillations were induced by mimicking the neuromodulatory state of deep sleep via low dopaminergic and cholinergic tone. KA (150 nM) and CCh (10 µM) was added half an hour prior to recording as this gave time for slices to settle into rhythmic activity. Theta (6-10 Hz) and gamma (30-37 Hz) oscillations emerged after half an hour. At this point, a bath solution (aCSF) which contained KA (150 nM) and CCh (10 µM) was changed to the one that contained: KA (150 nM), CCh (2 µM), SCH23390 (10 µM) and Haloperidol (10 µM). Application of either D1 or D2 antagonist along with low CCh did not induce delta oscillations indicating the need for both D1 and D2 receptor antagonists to induce delta activity. There was a transition from fast oscillations: Theta (6-10 Hz) and gamma (30-37 Hz) to slow oscillations: slow theta (5-7 Hz) and beta oscillations (25-30 Hz) before a high amplitude delta oscillation (2-4 Hz, ~400 µV^2, n=200) with mean frequency 3.1 ± 0.2 Hz emerged (figure 4.1, 4.2).
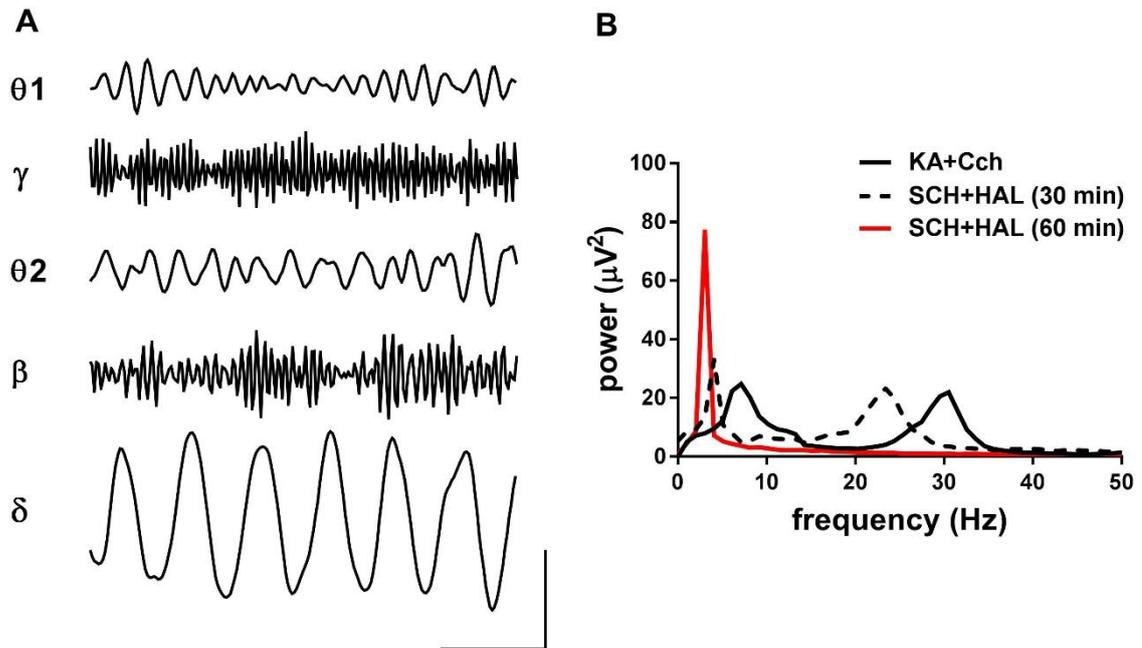
Figure 4.1a Pharmacological induction and transition of delta oscillations (2-4 Hz).

(A) Representative extracellular voltage recordings of activity during development of delta rhythm in SCH23390 & haloperidol. Gamma (30-40 Hz), beta (25-29 Hz), theta-1 (6-10 Hz), theta-2 (5-7 Hz) and delta (2-4 Hz) oscillations (scale: 20 µV x 500 ms). **(B)** Power spectra of oscillatory activity during application of SCH23390 & haloperidol in 30 min (dotted line), in 60 min (red line). Note how gamma-theta activity gradually shifted into beta and slow theta (5-7 Hz) oscillations (dotted), before a high amplitude (20-400 μV^2) delta rhythm (red) emerged.)
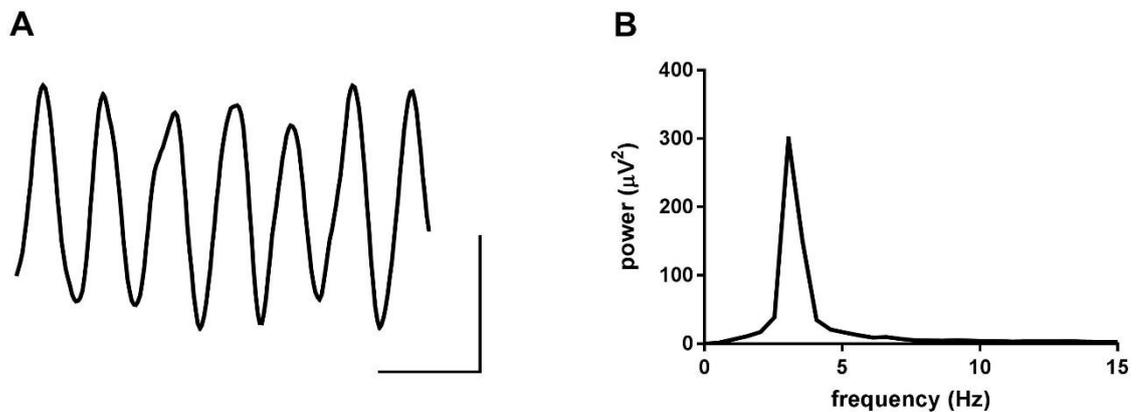
Figure 4.1b. Representative typical delta oscillation in LV of M1 (2-4 Hz)

(A) Raw data of an example typical delta oscillation recorded from LV of M1 **(B)** representative power spectrum of pharmacologically induced delta activity in neuromodulatory state (low dopaminergic and low cholinergic tone).

At the beginning of this project, low cholinergic and low dopaminergic states were induced only after prior induction of theta and gamma oscillations, hence, delta oscillations appeared relatively late into experiments. In order to save time and to keep slices viable, later experiments were started off by bath application of low CCh, KA, D1 and D2 antagonists and this was also found to reliably induce delta oscillations (stable for 2-3 hr) in 73% of slices. This approach enabled me to perform pharmacological studies using various receptor modulators. In the following report, 'control' (normalised to 100%) refers to a period where stable delta oscillations were present and there was no change noticed in frequency and amplitude over 20 min period. The effect of drug was then measured after 40 min of bath application (unless otherwise stated) which was then compared with control.

4.2.2 Laminar studies of delta oscillations through M1

Investigations were performed in sagittal slice preparation as it contained intact M1-S1 connections as well as easily identifiable gross anatomy. All layers except Ll showed delta activity however, relative power reduced from deep to superficial layers. To address this, simultaneous recordings across the layers (Lll, Llll, LV, LVI) were examined. Figure 4.2 A, B shows the power in various layers with LV being normalised to 100%. To further investigate if LV was the source of origin for delta oscillatory activity, recordings were made by placing a reference electrode in LV and 'walking' a second electrode up the layers V to ll. The data obtained from each layer were analysed by performing cross-correlation analysis with data from LV as reference point. These cross-correlation studies showed that oscillatory activity in LII and Lllll was phase delayed to that of LV. The average time lag was found to be 2.4 ± 0.4 and 2.3 ± 0.6 ms for Lll and Llll respectively. However, delta oscillatory activity in LVI was found to precede to that of LV by 2.1 ± 1 ms. (figure 4.2 C, D, E). Due to the difficulty in identifying the exact boundary between LV and LVI, cross correlation analysis was performed between deep (LV/LVI) and superficial layers (LII/LIII) in which superficial layers showed an average phase lag of 2.6 ± 0.7 ms (figure 4.2 F). This suggests the origin of delta oscillations to be deep layers and hence the subsequent recording were being made from deep layers especially from LV due to its salient feature of the presence of Betz cells.
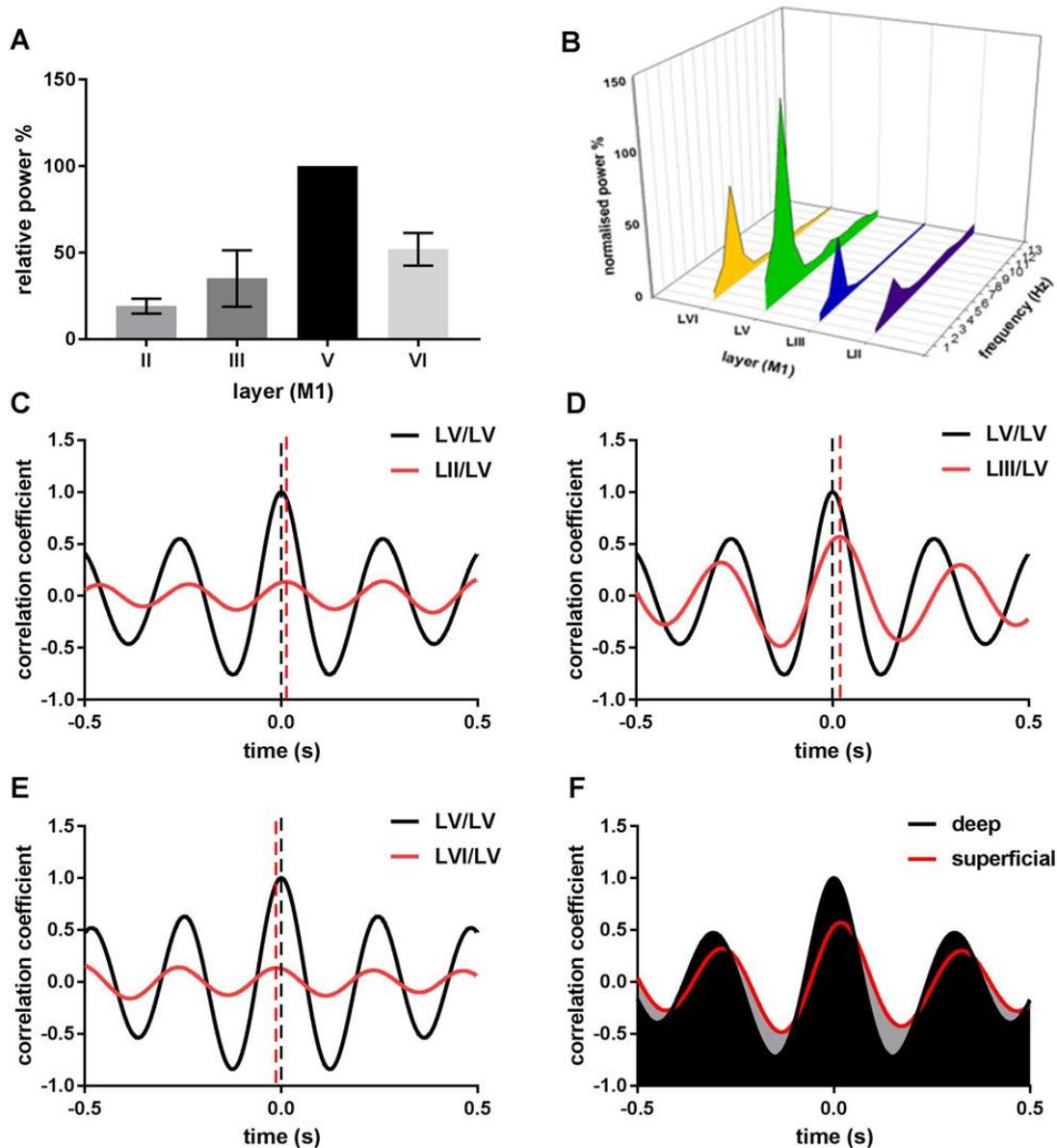
Figure 4.2 Deep layers are the origin of delta oscillation in M1

(A) Relative peak power changes in LII, LIII, LVI (grey) with respect to LV (black) activity (normalised to 100%) **(B)** Power spectrum of normalised oscillatory activity in each layer, LII, LIII, LVI, LV (100%) in a single slice. **(C)** cross-correlation analysis between LII/LV (red) and LV/LV (black). **(D)** cross-correlation analysis between LIII/LV (red) and LV/LV (black). **(E)** cross-correlation analysis between LVI/LV (red) and LV/LV (black). **(F)** cross-correlation analysis between superficial (red) and deep layers (black).

4.2.3 Cholinergic modulation of delta oscillations

To determine the role of CCh in delta oscillations whether it is via muscarinic acetylcholine receptors, general mAChR antagonists, atropine (AT) and pirenzepine (PIR) were bath applied. AT (5 µM) significantly desynchronised delta activity and the amplitude was decreased to 23.8 ± 5% of control (p< 0.001, n=8). PIR (10 µM) also significantly decreased delta power to 21.5 ± 7.5% of control (p< 0.001, n=8) indicating the action of muscarinic receptors is M1 specific. PIR showed significant reduction in power within 10 min of bath application (figures 4.3A-B) implying delta oscillations are reliant on M1 mAChRs.
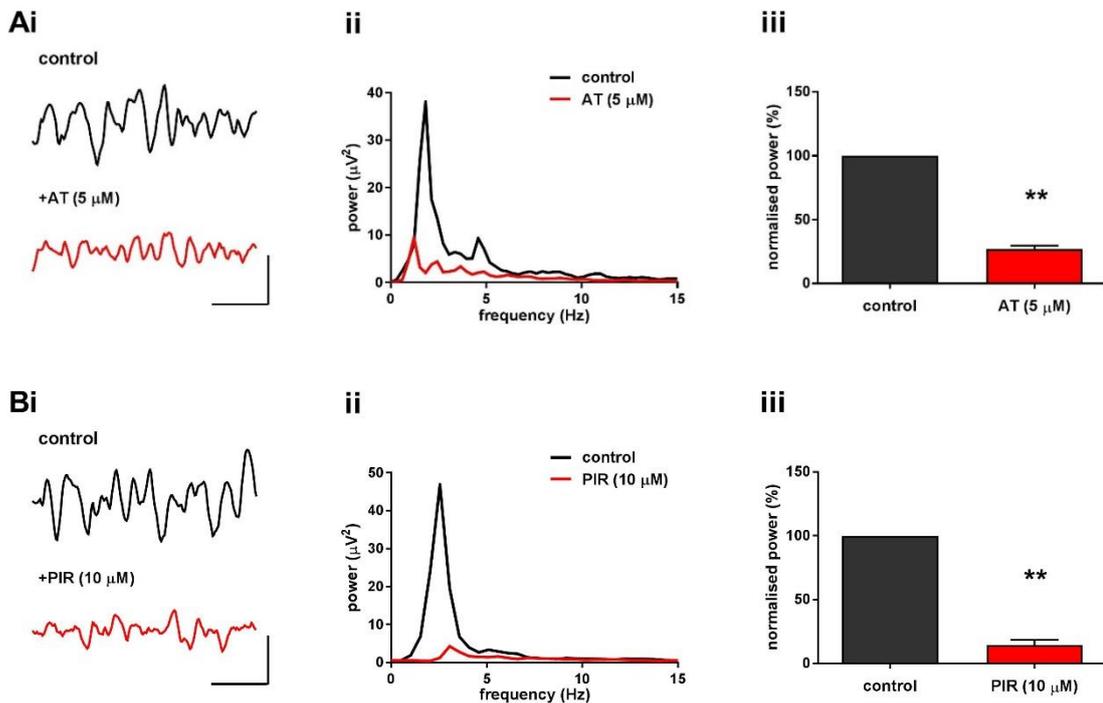
Figure 4.3 Muscarinic receptor block decreases delta oscillatory power

(A) Effect of atropine (10 µM) on delta oscillations. **(i)** Raw data showing the changes in oscillatory activity before (black) and after (red) drug application (scale: 20 µV vs 1 min). **(ii)** Representative power spectra of 60s of extracellular recording demonstrating peak responses before (black) and after (red) AT **(iii)** Bar graphs showing peak oscillatory power of oscillations before (grey) and after (red) drug application normalised to control. ** p<0.01, n=8. **(B)** Effect of pirenzepine (10 µM) on delta oscillations. **(i)** Raw data showing the changes in oscillatory activity before (black) and after (red) drug application (scale: 20 µV vs 1 min). **(ii)** Representative power spectra of 60s of extracellular recording demonstrating peak responses before (black) and after (red) PIR **(iii)** Bar graphs showing peak oscillatory power of oscillations before (grey) and after (red) drug application normalised to control. ** p<0.01, n=8.

4.2.4 Gap junction modulation of delta oscillations

To examine the involvement of gap junctions in incidence of delta oscillations, the gap junction blocker, carbenoxolone (CBNX) was added. CBNX (200 μM) abolished the synchronous activity after two hours of application. Peak power was reduced to 4.5 ± 0.5% of control (n=6, P<0.01) suggesting a significant role of gap junctions in delta oscillation generation in Layer 5 of M1 (figure 4.4)
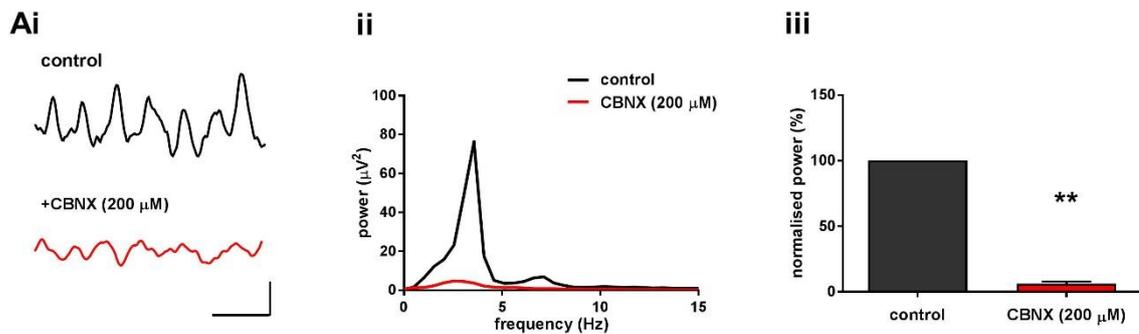
Figure 4.4 Gap junction block decreases delta oscillatory power

(A) Effect of carbenoxolone (200 μM) on delta oscillations **(i)** Raw data showing the changes in oscillatory activity before (black) and after (red) drug application (scale: 50 μV vs 500 ms). **(ii)** Representative power spectra of 60s of extracellular recording demonstrating peak responses before (black) and after (red) CBNX **(iii)** Bar graphs showing peak oscillatory power of oscillations before (grey) and after (red) drug application normalised to control. ** p<0.01, n=8

4.2.5 GABA$_A$R modulation of delta oscillations

Contribution of GABA$_A$R on pharmacologically induced delta oscillations in layer V of M1 was investigated by perfusing GABA$_A$R agonists and antagonists and comparing the activity before and after the application of drug.

Zolpidem, a benzodiazepine site agonist was bath applied at a concentration of 10 nM, 30 nM and 50 nM. As Fig. 4.5 shows, delta activity is exquisitely sensitive to benzodiazepine site modulation. Hence, 10 nM of Zolpidem increased the peak power of delta oscillations to 123 ± 9 % of control whilst at 30 and 50 nM peak power of delta activity was reduced to 44 ± 4% and 11 ± 3% respectively.
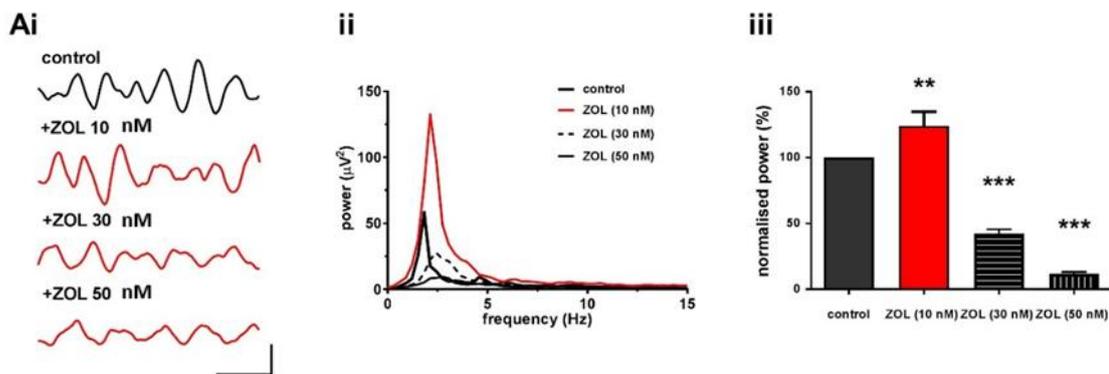
Figure 4.5 GABA$_A$R receptor agonist shows concentration dependent differential effects on delta oscillatory power

(A) Effect of Zolpidem (10 nM, 30 nM and 50 nM) on delta oscillations **(i)** Raw data showing the changes in oscillatory activity before (black) and after (red) drug application (scale: 50 µV vs 500 ms). **(ii)** Representative power spectra of 60s of extracellular recording showing peak power before (black), after 10 nM (red), 30 nM (dotted line) and 50 nM (solid line) of Zolpidem. **(ii)** Bar graphs showing peak oscillatory power of oscillations before (grey) and after 10 nM (red), 30 nM (lined) and 50 nM (lined) of drug application normalised to control. *** p<0.001, p<0.01, n=8.

In order to investigate the role of the GABA at the orthosteric binding site of the GABA$_A$R, gabazine (GBZ), a competitive GABA$_A$R antagonist was applied at 250nM and 2.5 µM concentrations. Both concentrations significantly reduced synchronous delta activity to

26.50 ± 5% and 11.7 ± 4% of control respectively (n=8, p<0.001) (figure 4.6A), suggesting roles for both synaptic and extra-synaptic receptors. The effect of picrotoxin (PTX), a non-competitive channel blocker which acts by preventing the entry of Cl^- ions into the neuron was examined. 5 µM PTX significantly reduced the synchronous activity to 25.50 ± 13% of control (n=8, P<0.01) (figure 4.6B). Taken together, these data suggest delta activity depends on inhibitory $GABA_AR$ receptors in layer V of M1.
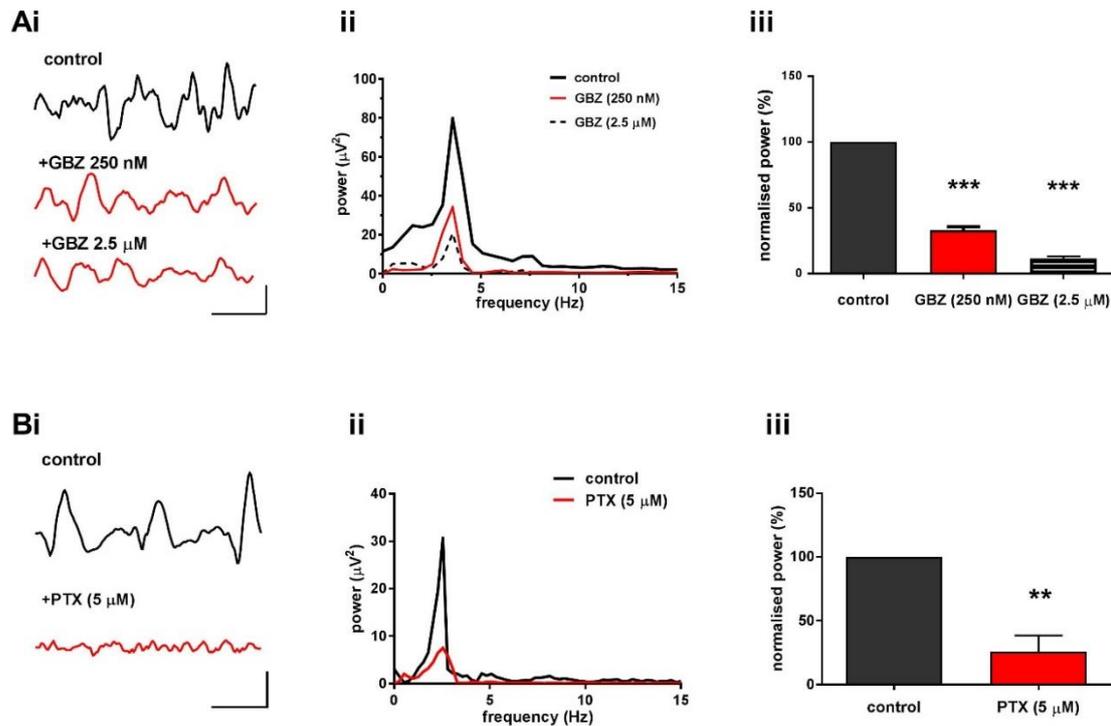
Figure 4.6 GABA$_A$ receptor block decreases delta oscillatory power

(A) Effect of gabazine (250 nM and 2.5 µM) on delta oscillations **(i)** Raw data showing the changes in oscillatory activity before (black) and after (red) drug application (scale: 40 µV vs 500 ms) **(ii)** Representative power spectra of 60s of extracellular recording showing peak power before (black) and after 250 nM (red) and 2.5 µM (dotted line) gabazine. **(ii)** Bar graphs showing peak oscillatory power of oscillations before (grey) and after (red) drug application normalised to control. *** p<0.001, n=8.

(B) Effect of picrotoxin (50 µM) on delta oscillations **(i)** Raw data showing the changes in oscillatory activity before (black) and after (red) drug application (scale: 20 µV vs 500 ms). **(ii)** Representative power spectra of 60s of extracellular recording demonstrating peak responses before (black red) and after picrotoxin (red) **(iii)** Bar graphs showing peak oscillatory power of oscillations before (grey) and after (red) drug application normalised to control. **p<0.01, n=8.

4.2.6 GABA$_B$R modulation of delta oscillations

To investigate if pharmacologically induced delta oscillations require the activation of GABA$_B$R, CGP55845, a competitive GABA$_B$R antagonist was bath applied. 5 µM of CGP55845 significantly decreased the delta synchronisation to 71.50 ± 14% of control (n=8, P<0.01) suggesting a small but significant GABA$_B$R contribution to the power of delta oscillations (figure 4.7).
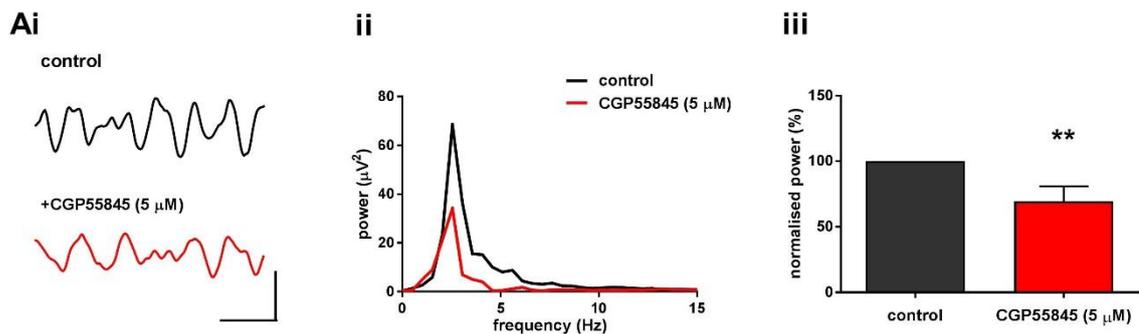
Figure 4.7 GABA$_B$ receptor block decreases delta oscillatory power

(A) Effect of CGP55845 (5 µM) on delta oscillations **(i)** Raw data showing the changes in oscillatory activity before (black) and after (red) drug application (scale: 30 µV vs 500 ms). **(ii)** Representative power spectra of 60s of extracellular recording demonstrating peak responses before (black) and after CGP55845 (red) **(iii)** Bar graphs showing peak oscillatory power of oscillations before (grey) and after (red) drug application normalised to control. **p<0.01, n=8.

4.2.7 iGluR modulation of delta oscillations

KAR modulation of delta oscillations: To investigate the role of kainate receptors and to confirm the action of KA is through kainate receptors, UBP310 (a GluK1/3 antagonist) and UBP 304 (a GluK1-selective antagonist) were bath applied. 10 µM of UBP304 and 3 µM of UBP310 significantly decreased the power of delta activity to 14.50 ± 4% of control (n=8, p<0.01) and 29.0 ± 0.5% of control (n=8, p<0.001) respectively (figures 4.8A-B). These data suggest an important role for KAR in delta oscillogenesis given that KA is used to evoke oscillations.
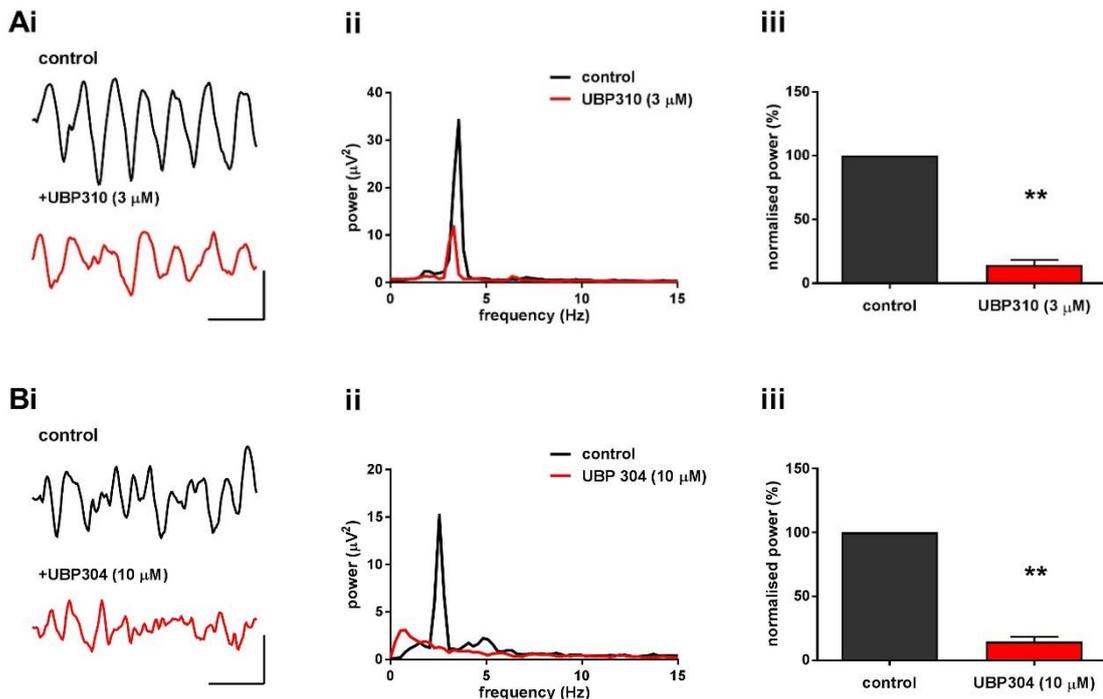
Figure 4.8 Kainate receptor block decreases delta oscillatory power

(A) Effect of UBP310 (3 µM) on delta oscillations **(i)** Raw data showing the changes in oscillatory activity before (black) and after (red) drug application (scale: 30 µV vs 500 ms). **(ii)** Representative power spectra of 60s of extracellular recording demonstrating peak responses before (black) and after (red) UBP310 **(iii)** Bar graphs showing peak oscillatory power of oscillations before (grey) and after (red) drug application normalised to control. *** p<0.001, n=8. **(B)** Effect of UBP304 (10 µM) on delta oscillations **(i)** Raw data showing the changes in oscillatory activity before (black) and after (red) drug application (scale: 20 µV vs 1 min). **(ii)** Representative power spectra of 60s of extracellular recording demonstrating peak responses before (black) and after (red) UBP304 **(iii)** Bar graphs showing peak oscillatory power of oscillations before (grey) and after (red) drug application normalised to control. **p<0.01, n=8.

4.2.7.1 AMPAR modulation of delta oscillations

The dependence of delta oscillations on AMPAR was investigated by using SYM2206, a specific AMPAR antagonist. Application of 20 µM of SYM2206 significantly desynchronised the delta activity. It reduced the power to 29.50 ± 6% of control (n=8, p<0.01) (figure 4.9A). In order to assess the contribution of combined AMPAR/KAR activity, we applied 25 µM CNQX, a KAR/AMPAR antagonist. CNQX significantly reduced the synchronous delta activity (figure 4.9B) to 15.50 ± 6% of control (n=8, P<0.001) revealing the role of both KA and AMPA receptors in generation of delta oscillations but stronger role for KAR.
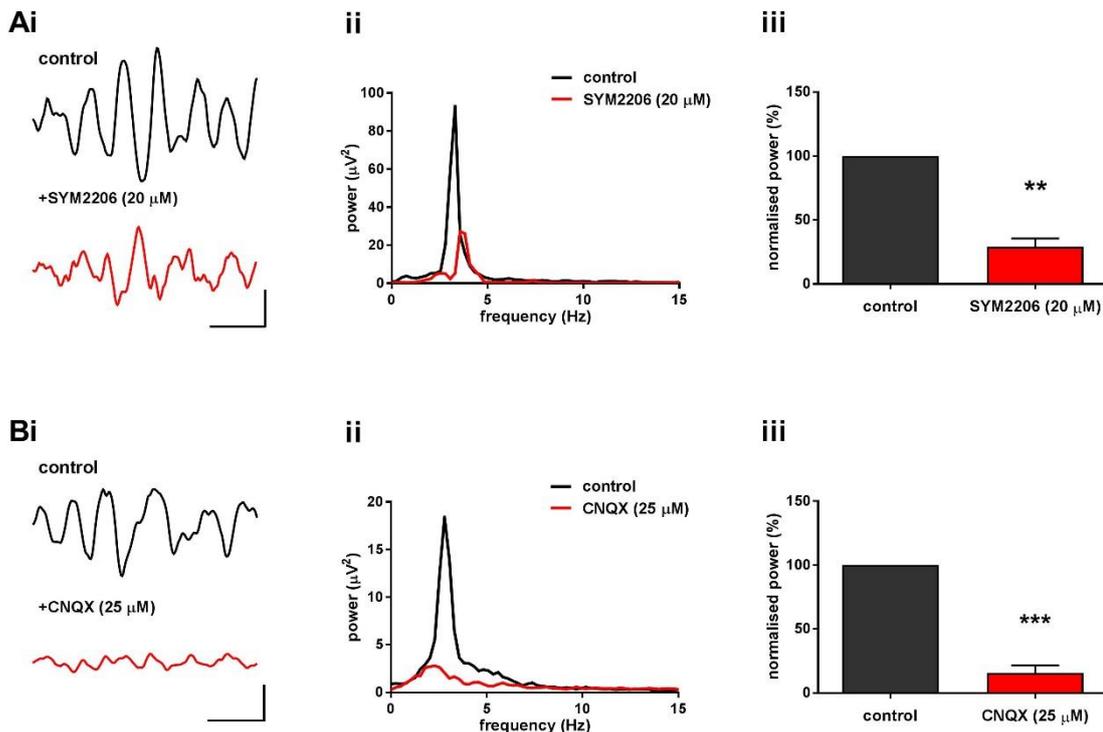
Figure 4.9 AMPA receptor block decreases delta oscillatory power

(A) Effect of SYM2206 (20 µM) on delta oscillations **(i)** Raw data showing the changes in oscillatory activity before (black) and after (red) drug application (scale: 70 µV vs 500 ms). **(ii)** Representative power spectra of 60s of extracellular recording demonstrating peak responses before (black) and after (red) SYM2206 **(iii)** Bar graphs showing peak oscillatory power of oscillations before (grey) and after (red) drug application normalised to control. **p<0.01, n=8.

(B) Effect of CNQX (25 µM) on delta oscillations **(i)** Raw data showing the changes in oscillatory activity before (black) and after (red) drug application (scale: 40 µV vs 500 ms). **(ii)** Representative power spectra of 60s of extracellular recording demonstrating peak responses before (black) and after (red) CNQX **(iii)** Bar graphs showing peak oscillatory power of oscillations before (grey) and after (red) drug application normalised to control. *** p<0.001, n=8

4.2.7.2 NMDAR modulation of delta oscillations

The role of NMDA receptors was tested using 2-AP5, a competitive NMDAR antagonist. 50 µM 2-AP5 did not alter the delta peak (95.5 ± 17 % of control, n=8, P>0.05) (figure 4.10A). To confirm this lack of reliance of delta oscillations on NMDAR, a selective non-competitive antagonist, MK-801 was bath applied. Application of MK-801 had no significant effect on peak delta power (n=8, P>0.05, figure 4.10B)
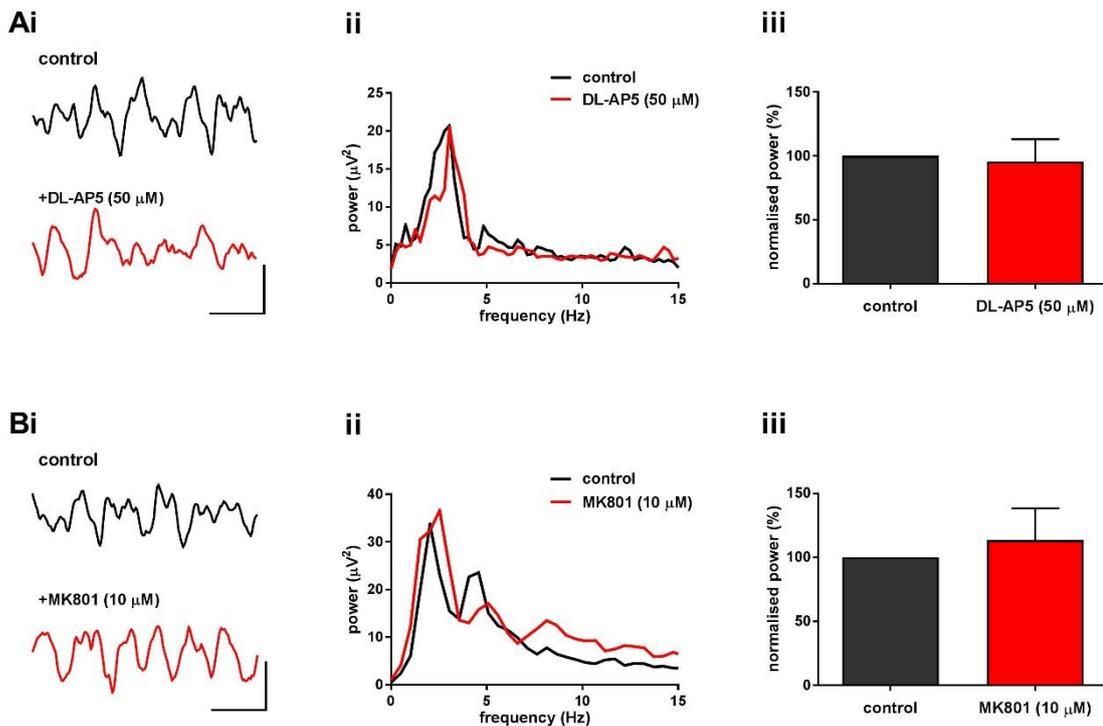
Figure 4.10 NMDA receptor block has no effect on delta oscillatory power

(A) Effect of 2-AP5 (50 µM) on delta oscillations **(i)** Raw data showing the changes in oscillatory activity before (black) and after (red) drug application (scale: 60 µV vs 500 ms). **(ii)** Representative power spectra of 60s of extracellular recording demonstrating peak responses before (black) and after (red) 2-AP5 **(iii)** Bar graphs showing peak oscillatory power of oscillations before (grey) and after (red) drug application normalised to control. ns p>0.05, n=8. **(B)** Effect of MK801 (10 µM) on delta oscillations **(i)** Raw data showing the changes in oscillatory activity before (black) and after (red) drug application (scale: 20 µV vs 500 ms). **(ii)** Representative power spectra of 60s of extracellular recording demonstrating peak responses before (black) and after (red) MK801 **(iii)** Bar graphs showing peak oscillatory power of oscillations before (grey) and after (red) drug application normalised to control. ns p>0.0, n=8.

4.2.8 mGluR modulation of delta oscillations

The contributions of mGluR to delta activity was investigated by using positive and negative receptor modulators of group I, group II and group III mGluRs. Agonists generally decreased the peak power whilst antagonists increased peak delta power.

Group I modulation of delta oscillations: Application of the mGluR group I agonist DHPG (10 µM) did not show any significant effect ($p>0.05$, n=8). Consistently, the non-competitive mGluR1 antagonist CPCCOet (25 µM) had no effect on delta oscillations ($p>0.05$, n=8) whereas as mGluR5 specific antagonist MPEP (20 µM) and potent mGluR5 antagonist MTEP (100 nM) significantly increased the activity to $187 \pm 22.5\%$ of control and $189 \pm 29\%$ (n=8, $p<0.01$) of control (n=8, $p<0.01$) respectively (figures 4.11 A-D), suggesting a role for mGluR5, rather than mGluR1 in modulation of delta power.
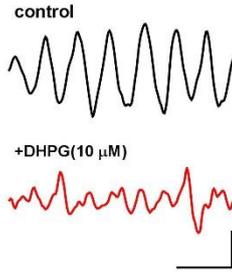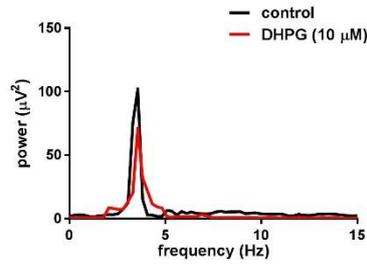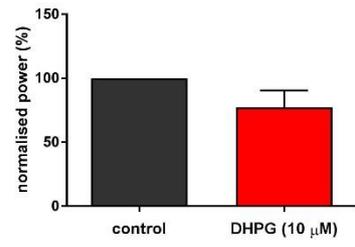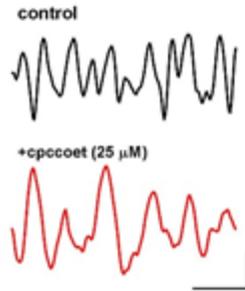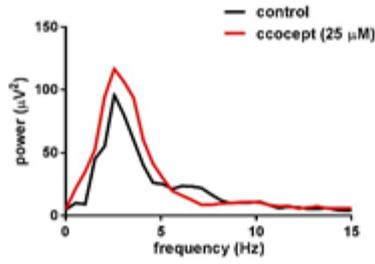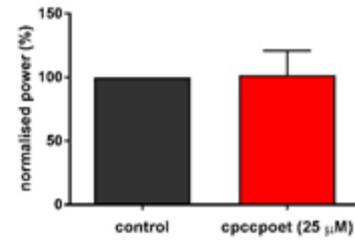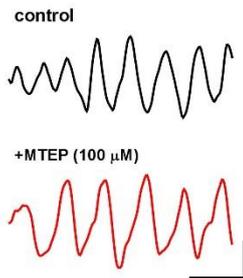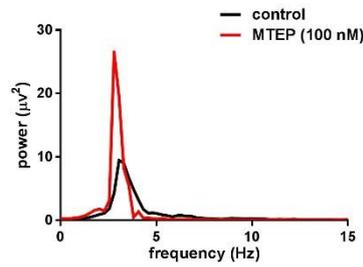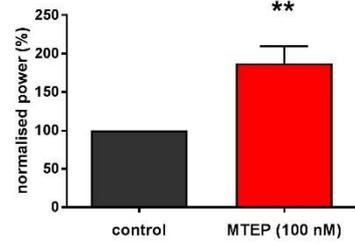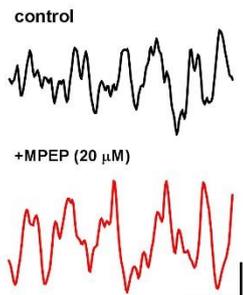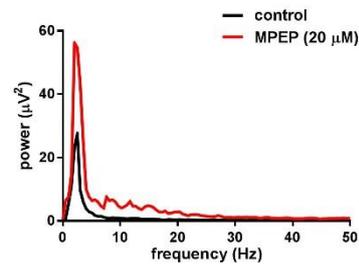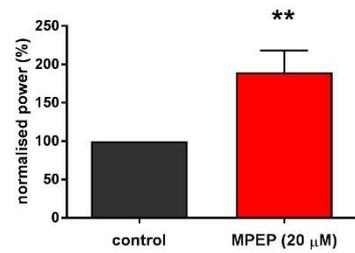
Figure 4.11 Effect of group I, mGlu receptor modulators on delta oscillatory power

(A) Effect of DHPG (10 μM) on delta oscillations **(i)** Raw data showing the changes in oscillatory activity before (black) and after (red) drug application (scale: 50 μV vs 500 ms). **(ii)** Representative power spectra of 60s of extracellular recording demonstrating peak responses before (black) and after (red) DHPG **(iii)** Bar graphs showing peak oscillatory power of oscillations before (grey) and after (red) drug application normalised to control. ns $p > 0.05$, n=8.

(B) Effect of cpccoet (25 μM) on delta oscillations **(i)** Raw data showing the changes in oscillatory activity before (black) and after (red) drug application (scale: 50 μV vs 500 ms). **(ii)** Representative power spectra of 60s of extracellular recording demonstrating peak responses before (black) and after (red) cpccoet **(iii)** Bar graphs showing peak oscillatory power of oscillations before (grey) and after (red) drug application normalised to control. ns $p > 0.05$, n=8.

(C) Effect of MTEP (100 nM) on delta oscillations **(i)** Raw data showing the changes in oscillatory activity before (black) and after (red) drug application (scale: 30 μV vs 500 ms). **(ii)** Representative power spectra of 60s of extracellular recording demonstrating peak responses before (black) and after (red) MTEP **(iii)** Bar graphs showing peak oscillatory power of oscillations before (grey) and after (red) drug application normalised to control. ** $p < 0.01$, n=8.

(D) Effect of MPEP (20 μM) on delta oscillations **(i)** Raw data showing the changes in oscillatory activity before (black) and after (red) drug application (scale: 40 μV vs 500 ms). **(ii)** Representative power spectra of 60s of extracellular recording demonstrating peak responses before (black) and after (red) MPEP **(iii)** Bar graphs showing peak oscillatory power of oscillations before (grey) and after (red) drug application normalised to control. ** $p < 0.01$, n=8.

Group II modulation of delta oscillations: The group ll (mGluR3) agonist, LY379268 (1 μM) showed a significant reduction in synchronous delta activity to 41.80 ± 10 % of control (p<0.01, n=8). mGluR2 antagonist LY341495 (100 nM) and mGlu-R2/3 antagonist LY341495 (1 μM) did not show any significant effect on peak power of delta oscillations (p>0.05, n=8) (figure 4.12 A-B). Please note that the figure Aii shows an effect on frequency however this effect was not significant when data were pooled.
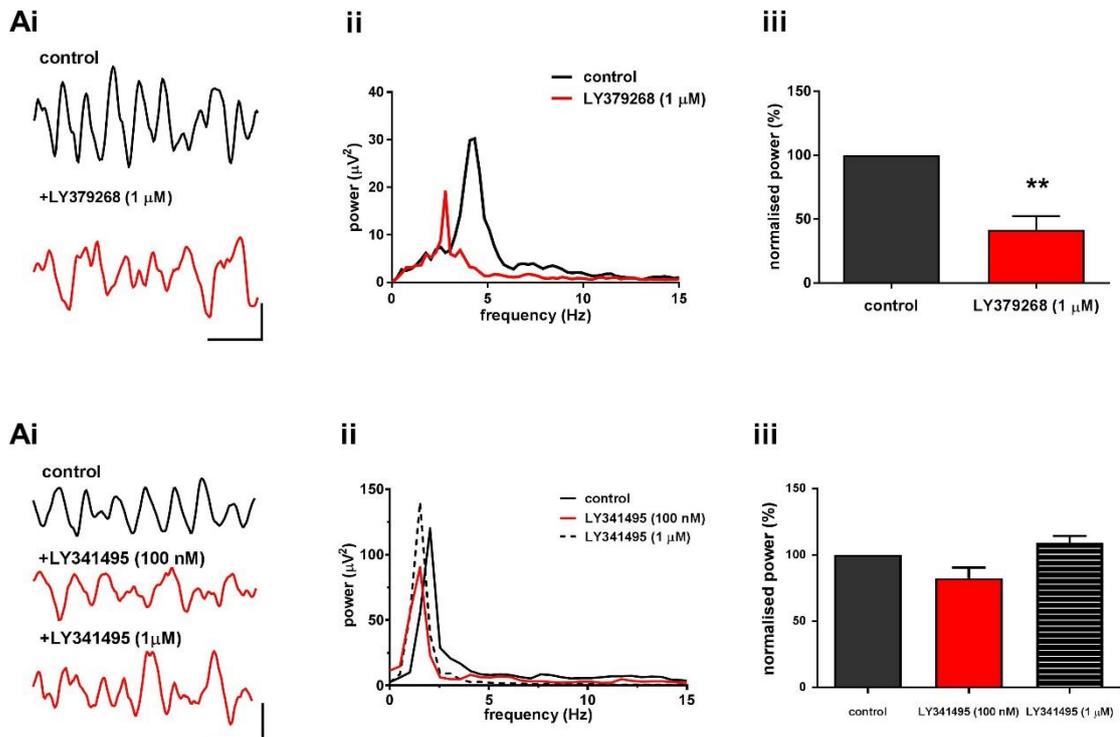
Figure 4.12 Effect of group II, mGlu receptor modulators on delta oscillatory power

(A) Effect of LY379268 (1 μM) on delta oscillations **(i)** Raw data showing the changes in oscillatory activity before (black) and after (red) drug application (scale: 40 μV vs 500 ms). **(ii)** Representative power spectra of 60s of extracellular recording demonstrating peak responses before (black) and after (red) LY379268 **(iii)** Bar graphs showing peak oscillatory power of oscillations before (grey) and after (red) drug application normalised to control. ** p<0.01, n=8.

(B) Effects of LY341495 (100 nM and 1 μM) on delta oscillations **(i)** Raw data showing the changes in oscillatory activity before (black) and after (red) drug application (scale: 100 μV vs 500 ms). **(ii)** Representative power spectra of 60s of extracellular recording showing peak power before (black) and after 100 nM (red) and 1 μM (dotted line) LY341495. **(ii)** Bar graphs showing peak oscillatory power of oscillations before (grey) and after (red) drug application normalised to control. ns p>0.5, n=8.

Group III modulation of delta oscillations: L-AP4 (50 µM), an agonist and an antagonist CPPG (10 µM), an antagonist, did not show any significant effect on peak power of delta oscillations (p>0.05, n=8) (figures 4.13 A-B).
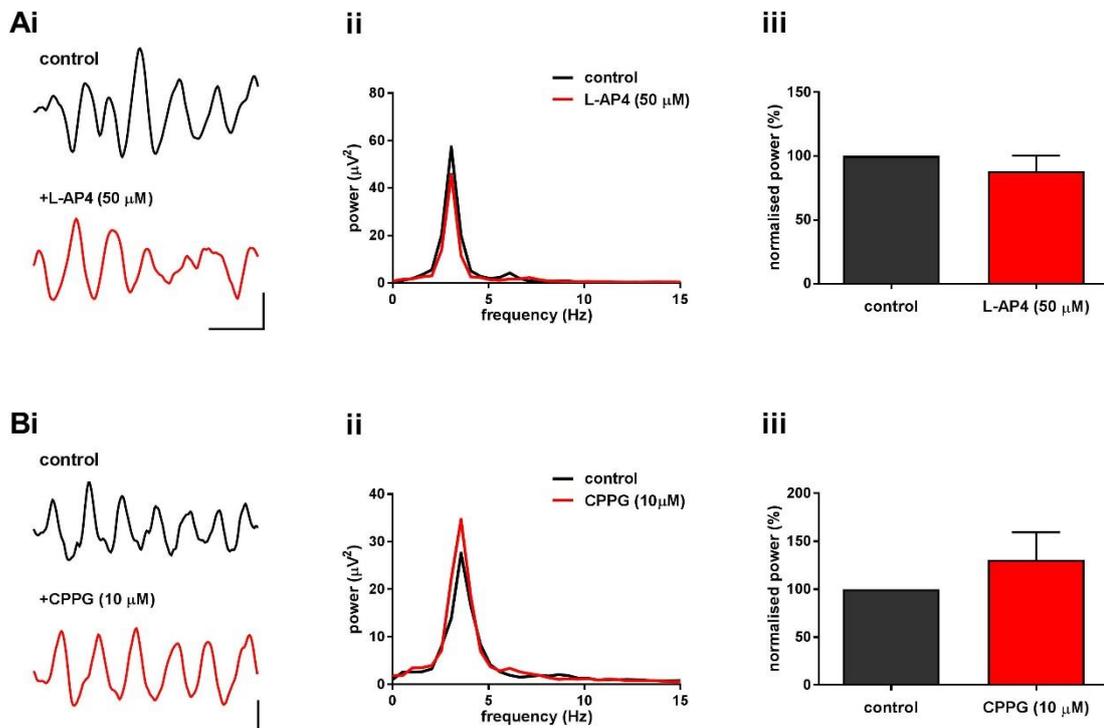
Figure 4.13 Effect of group III, mGlu receptor modulators on delta oscillatory power

(A) Effect of L-AP4 (50 µM) on delta oscillations **(i)** Raw data showing the changes in oscillatory activity before (black) and after (red) drug application (scale: 40 µV vs 500 ms). **(ii)** Representative power spectra of 60s of extracellular recording demonstrating peak responses before (black) and after (red) L-AP4 **(iii)** Bar graphs showing peak oscillatory power of oscillations before (grey bars) and after (red bars) drug application normalised to control. ns p>0.05, n=8. **(B)** Effect of CPPG (10 µM) on delta oscillations **(i)** Raw data showing the changes in oscillatory activity before (black) and after (red) drug application (scale: 30 µV vs 500 ms). **(ii)** Representative power spectra of 60s of extracellular recording demonstrating peak responses before (black) and after (red) CPPG **(iii)** Bar graphs showing peak oscillatory power of oscillations before (grey) and after (red) drug application normalised to control. ns p>0.05, n=8.

4.2.9 Pharmacological equivalent awake state: delta reversal protocol

Having investigated the pharmacology of persistent delta activity in M1, we determined to attempt to mimic the switch to awake-state neurochemistry. This section details the various pharmacological equivalent awake state protocols that were used to try and reverse the delta which was pharmacologically induced. All the recordings form this section were made from LV of M1.

4.2.9.1 Effect of KA+CCh (wash) on delta oscillations:

To investigate if delta induced by bath application of KA (150 nM), CCh (2 µM), SCH23390 (10 µM) and Haloperidol (10 µM), perfusing solution (aCSF) was changed to the one that contained KA (150 nM), CCh (10 µM). There was no significant change either in power or in frequency. Concentrations of KA and CCh were doubled to observe any change but there was not any change confirming the stable and persistent nature of the delta oscillations ($p > 0.05$, n=8) (figure 4.14).
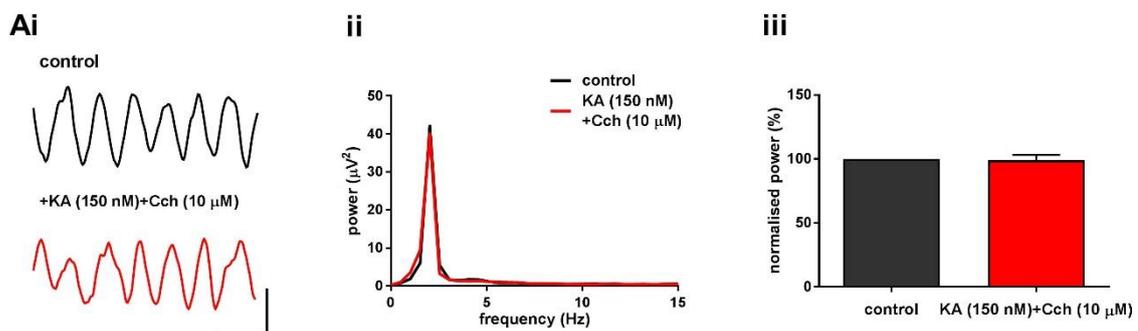
Figure 4.14 No significant change was noticed in frequency and power of delta oscillations in wash

(A) Effect of wash (150 nM KA+10 µM CCh) on delta oscillations **(i)** Raw data showing the changes in oscillatory activity before (black) and after (red) wash (scale: 70 µV vs 500 ms). **(ii)** Representative power spectra of 60s of extracellular recording demonstrating peak responses before (black) and after (red) wash **(iii)** Bar graphs showing peak oscillatory power of oscillations before (grey) and after (red) wash normalised to control. ns $p > 0.05$, n=8.

4.2.9.2 Effect of high KA on delta oscillations

To determine the effect of high concentrations of KA on delta oscillations, 250 nM, 350 nM, 500 nM KA were bath applied. Since all the concentrations showed similar effect, only the highest is reported here. KA at 500 nM induced seizure like activity with very high power 1350 ± 600% of control with frequency range of 0.5-1 Hz (n=8, figure 4.15) which is different to that of induced delta oscillations of 2-4 Hz frequency range. However, delta oscillations were found to be intact when traces were filtered but were potentially masked by high amplitude and low frequency activity. The power of the activity was reduced to 69 ± 4 % of control.
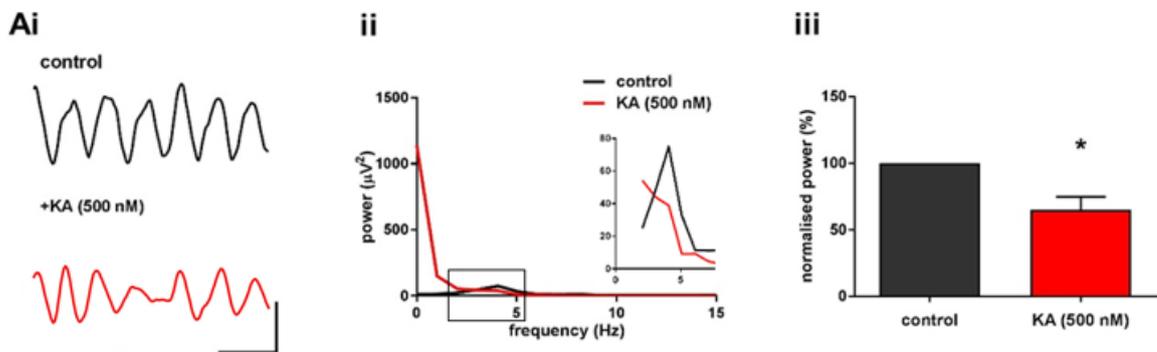
Figure 4.15 Seizure like activity was induced in the presence of high KA with intact delta

(A) Effect of high KA (500 nM) on delta oscillations **(i)** Raw data showing the changes in oscillatory activity before (black) and after (red) high KA (scale: 150 µV vs 500 ms). **(ii)** Representative power spectra of 60s of extracellular recording demonstrating peak responses before (black) and after (red) wash **(iii)** Bar graphs showing delta oscillatory power of oscillations before (grey) and after (red) high KA normalised to control. ns p>0.05. The boxed area represents the expanded graph at 2-5Hz.

4.2.9.3 Effect of high CCh on delta oscillations

To investigate if enhancing the cholinergic drive (dominance in awake state) would enable the reversal of induced delta oscillation, high concentrations of CCh were bath applied. When 100 µM was bath applied, seizure activity was induced with a high power 2150 ± 300% of control with low frequency of about 0.5-1 Hz, different to actual delta oscillations (2-4 Hz) (figure 4.16). Interestingly, delta oscillations were found to be intact but were possibly masked by high amplitude and low frequency oscillations similar to that of high KA. The power of delta oscillations was significantly reduced to 52 ± 3 % of control.
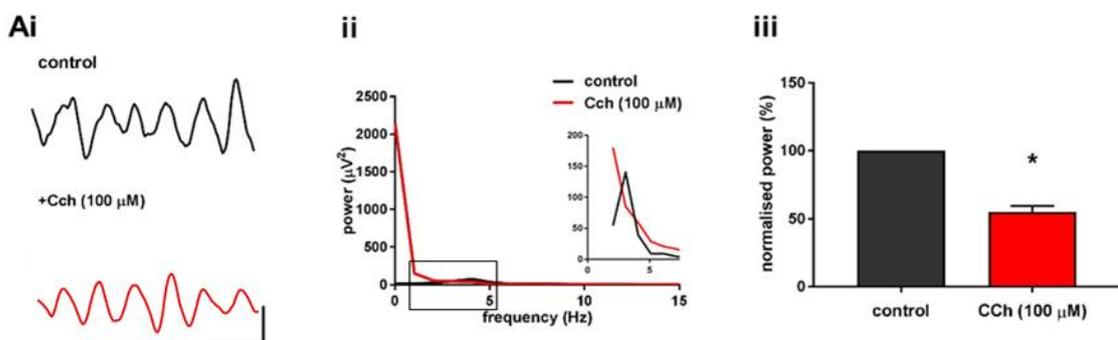
Figure 4.16 Seizure like activity was induced in the presence of high CCh with delta intact

(A) Effect of high CCh (100 µM) on delta oscillations **(i)** Raw data showing the changes in oscillatory activity before (black) and after (red) high CCh (scale: 200 µV vs 500 ms). **(ii)** Representative power spectra of 60s of extracellular recording demonstrating peak responses before (black) and after (red) wash **(iii)** Bar graphs showing delta oscillatory power of oscillations before (grey) and after (red) high CCh normalised to control. ns p>0.05, n=8. The boxed area represents the expanded graph at 2-5Hz.

4.2.9.4 Effect of DA on delta oscillations

To examine if dopaminergic drive would reverse slow oscillations (2-4 Hz) to faster oscillations since low dopaminergic state was used to induce delta oscillations. DA was bath applied along with 250 µM of ascorbic acid to prevent DA from oxidising (Hastings *et al.,* 1996) since DA is an unstable molecule (Graham, 1978). 30 µM DA (data not shown) did not show any significant effect in terms of amplitude and frequency whilst 50 µM of DA slightly enhanced the power of delta oscillations to $110 \pm 10\%$ ($p<0.05$) but showed no effect on frequency (figure 4.17).
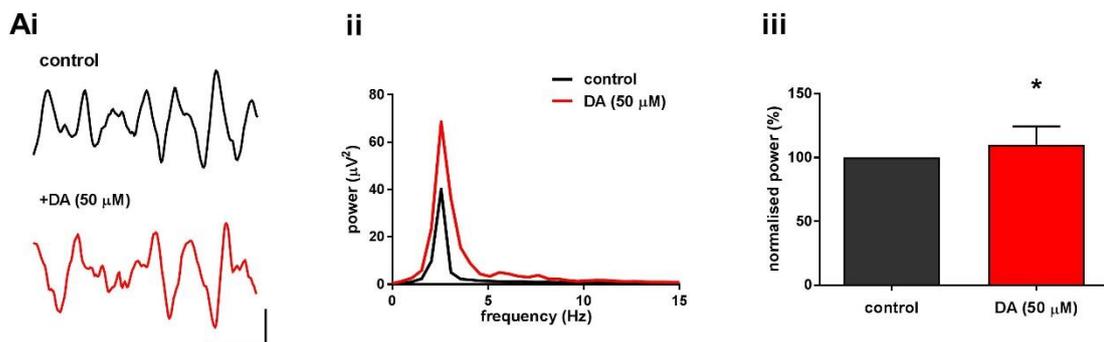
Figure 4.17 DA increases the power of delta oscillations but no effect on frequency

(A) Effect of DA (50 µM) on delta oscillations **(i)** Raw data showing the changes in oscillatory activity before (black) and after (red) DA (scale: 60 µV vs 500 ms). **(ii)** Representative power spectra of 60s of extracellular recording demonstrating peak responses before (black) and after (red) wash **(iii)** Bar graphs showing peak oscillatory power of oscillations before (grey) and after (red) DA normalised to control. ns $p<0.05$, n=8.

4.2.9.5 Effect of HA on delta oscillations

Histamine (HA) was bath applied to investigate if histaminergic drive (associated with awake state) would change the low frequency delta oscillations to faster oscillations. 200 µM of HA, when applied to bath, significantly increased the peak power to $116 \pm 4\%$ (p<0.05, n=8) but frequency range remained the same (figure 4.18).
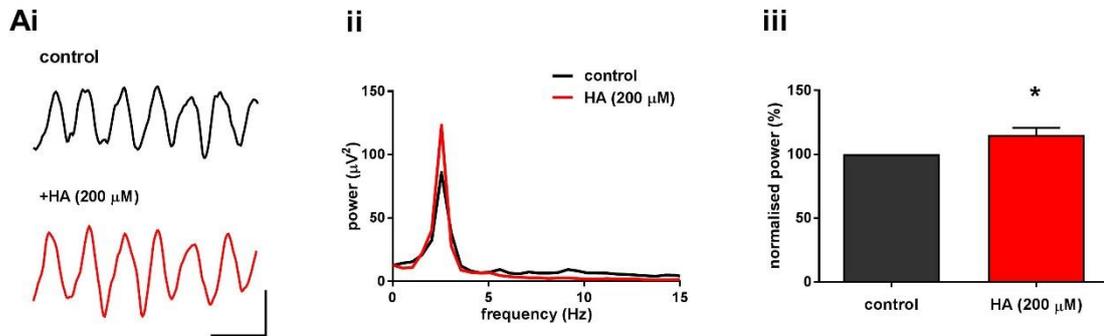
Figure 4.18 HA increases the power of delta oscillations but no effect on frequency

(A) Effect of HA (200 µM) on delta oscillations **(i)** Raw data showing the changes in oscillatory activity before (black) and after (red) HA (scale: 70 µV vs 500 ms). **(ii)** Representative power spectra of 60s of extracellular recording demonstrating peak responses before (black) and after (red) wash **(iii)** Bar graphs showing peak oscillatory power of oscillations before (grey) and after (red) HA normalised to control. ns p<0.05, n=8.

4.2.9.6 Effect of combined awake-state drugs on delta oscillations

Neuromodulators (without any dopamine antagonists) (KA (150 nM), CCh (10 µM), GABA (1 µM), DA (50 µM), HA (200 µM) and 5-HT (1 µM) that are prevalent in awake state are bath applied to examine if this mixture would enable the reversal of pharmacologically induced delta oscillations. Ascorbic acid (250 µM) was bath applied along with the mixture above to prevent DA oxidation (Hastings *et al.,* 1996). When bath was applied with this mixture, delta peak power was increased significantly to 170 ± 9% of control (n=8, p<0.01) but again wihtout change in frequency range (figure 4.19).
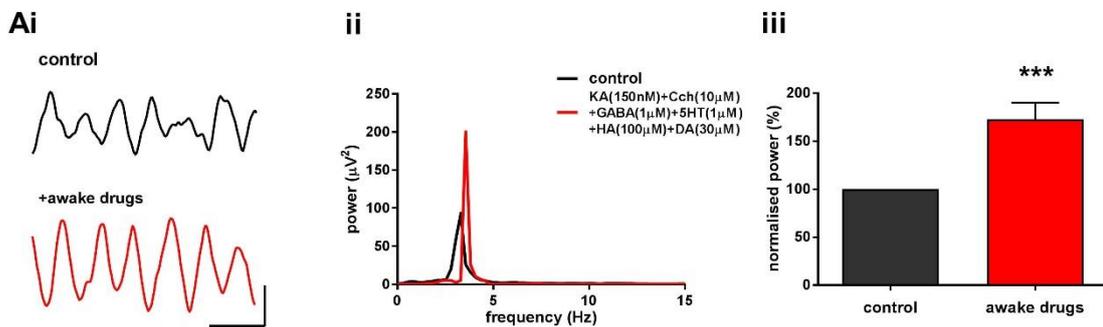
Figure 4.19 Awake drug mixture increases the power of delta oscillations but no effect on frequency

(A) Effect of awake drug mixture ((KA (150 nM), CCh (10 µM), GABA (1 µM), DA (50 µM), HA (200 µM), 5-HT (1 µM)) on delta oscillations **(i)** Raw data showing the changes in oscillatory activity before (black) and after (red) awake mixture (scale: 70 µV vs 500 ms). **(ii)** Representative power spectra of 60s of extracellular recording demonstrating peak responses before (black) and after (red) awake drug mixture **(iii)** Bar graphs showing peak oscillatory power of oscillations before (grey) and after (red) awake mixture normalised to control. ns p<0.001, n=8.

4.2.9.7 Effect of waking-state pharmacology before inducing delta oscillations

To investigate if this drug mixture ((KA (150 nM), CCh (10 µM), GABA (1 µM), DA (50 µM), HA (200 µM), 5-HT (1 µM), Ascorbic acid (250 µM)) had any impact on induction of delta oscillations, this mixture was bath applied on theta and gamma oscillations which were induced when bath applied KA and CCh. This drug mixture significantly increased the power of theta and gamma oscillations. These fast oscillations graduated to slow oscillations and to delta oscillations upon application of KA (150 nM), CCh (2 µM), SCH23390 (10 µM) and Haloperidol (10 µM) (n=8, figure 4.20)
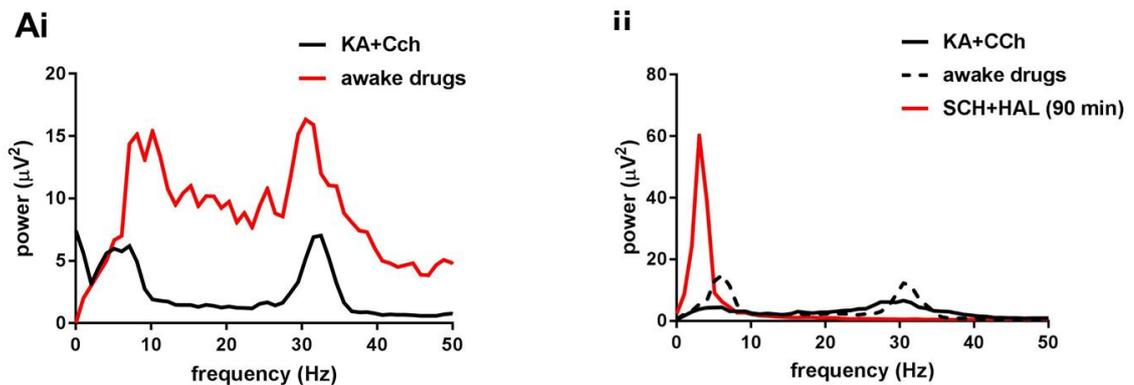
Figure 4.20 Induction of delta oscillations in the presence of awake drug mixture

(A) Effect of awake drug mixture ((KA (150 nM), CCh (10 µM), GABA (1 µM), DA (50 µM), HA (200 µM), 5-HT (1 µM), Ascorbic acid (250 µM)) on induction delta oscillations **(i)** Representative power spectra of 60s of extracellular recording demonstrating peak responses before (black) and after (red) awake drug mixture on theta and gamma oscillations **(iii)** Representative power spectrum illustrating the transition of fast oscillations (black) to slow oscillations (dotted line) and to delta oscillations (red) in the presence of awake drug mixture (n=8).

4.2.9.8 Effect of AMPH on delta oscillations

To investigate if CNS stimulants would change the frequency range, amphetamine sulphate (AMPH) was bath applied. Application of 20 µM and 40 µM increased the peak delta power to 123 ± 6% of control (n-8, p<0.01) but no effect on frequency range (figure 4.21).
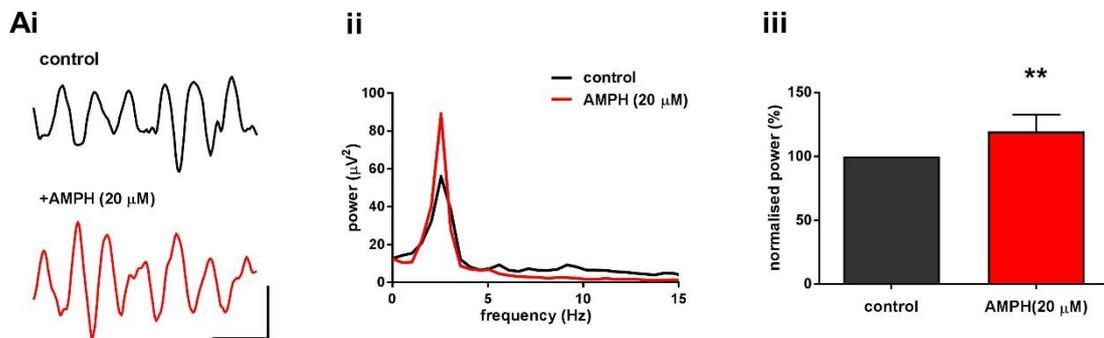
Figure 4.21 AMPH increases the power of delta oscillations but no effect on frequency

(A) Effect of AMPH (20 µM) on delta oscillations **(i)** Raw data showing the changes in oscillatory activity before (black) and after (red) AMPH (scale: 50 µV vs 500 ms). **(ii)** Representative power spectra of 60s of extracellular recording demonstrating peak responses before (black) and after (red) wash **(iii)** Bar graphs showing peak oscillatory power of oscillations before (grey) and after (red) AMPH normalised to control. ns p<0.05, n=8.

4.2.9.9 Effect of AMPH before inducing delta oscillations

The effect of AMPH on induction of delta oscillations was examined by bath application of AMPH on theta and gamma oscillations. When 20 µM of AMPH was bath applied, there was a significant increase in the peak power of theta and gamma oscillations. However, there is no transition to delta oscillations upon application of KA (150 nM), CCh (2 µM), SCH23390 (10 µM) and Haloperidol (10 µM) even after 2 hours of observation. (n=8, figure 4.22) but to our surprise it revealed an increase in theta power (mean frequency: 7.9 ± 0.6 Hz).
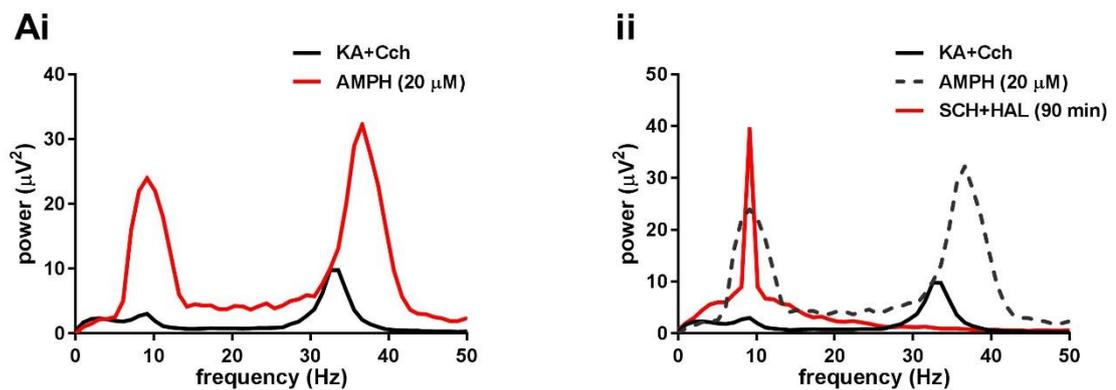
Figure 4.22 Delta was not induced in the presence of AMPH

(A) Effect of AMPH (20 µM) on induction delta oscillations **(i)** Representative power spectra of 60s of extracellular recording demonstrating peak responses before (black) and after (red) AMPH on theta and gamma oscillations **(iii)** Representative power spectrum illustrating the transition of fast oscillations (black) to slow oscillations (dotted line) and to theta oscillations (red) in the presence of awake drug mixture (n=8). Note: No delta was induced in the presence of AMPH.

4.2.10 Summary of results

Pharmacology of delta oscillations in LV of M1 was summarised in table below.

Drug (concentration)	% Change of Control	N	Significance
atropine (5 µM) [mAch antagonist]	23.8 ± 5	8	**
pirenzepine (10 µM) [mAch antagonist]	21.5 ± 7.5	8	**
Carbenoxolone (200µM) [Gap junction blocker]	4.5 ± 0.5	8	**
zolpidem (10 nM,30 nM,50 nM) [GABAAR agonist]	123±9,41±4,11±3	8	**, ***, ***
gabazine (250 nM,25 µM) [GABAAR antagonist]	26.6 ± 5, 11.7 ± 4	8	***
picrotoxin (5 µM) [GABAAR antagonist]	25.9 ± 13	8	**
CGP55845 (5 µM) [GABABR antagonist]	71.48 ± 14	8	**
UBP310 (3 µM) [KAR antagonist]	29.27 ± 4	8	***
UBP304 (10 µM) [KAR antagonist]	14.5 ± 4	8	**
SYM2206 (20 µM) [AMPAR antagonist]	29.15 ± 6	8	**
CNQX (25 µM) [KA/AMPAR antagonist]	15.77 ± 6	8	***
2-AP5 (50 µM) [NMDAR antagonist]	N/A	8	ns
MK801 (10 µM) [NMDAR antagonist]	N/A	8	ns
DHDG (10 µM) [groupI mGluR agonist]	N/A	8	ns
cpccoet (25 nM) [gI mGluR antagonist]	N/A	8	ns
MTEP (100 µM) [gI mGluR antagonist]	187 ± 23	8	**
MPEP (20 µM) [gI mGluR antagonist]	189 ± 29	8	**
LY 379268 (1 µM) [groupII mGluR agonist]	41.8 ± 11	8	**
LY 341495 (100 nM,1 µM) [gII mGluR antagonist]	N/A	8	ns
L-AP4 (50 µM) [groupIII mGluR agonist]	N/A	8	ns
CPPG (10 µM) [gIII mGluR antagonist]	N/A	8	ns

Table 4.1 Pharmacology of delta oscillations in LV of M1
Peak power changes after application of various receptor modulators is represented as mean ± SEM when compared to control (normalised to 100%). N= number of recordings (obtained from 3 different animals), significance: ns p>0.05, * p<0.05, **p<0.01, ***p<0.001.

Delta reversal protocol was summarised in table below. Note delta was found to be irreversible as there was no change in frequency of the oscillations but there was changes in peak power of delta oscillations.

Drug (concentration)	%Change of Control	N	significance
KA (150 nM)+CCh (10 µM)	ns	8	Ns
high KA (500 nM)	ns	8	Ns
high CCh (50 µM)	ns	8	Ns
dopamine (50 µM)	110 ± 10	8	*
histamine (200 µM)	116 ± 4	8	*
amphetamine Sulphate (20 µM)	123 ± 6	8	**
awake mixture (150 nMKA+10 µM CCh+1 µM GABA+1 µM 5HT+50µM DA+200 µM HA+250 µM Ascorbic Acid)	170 ± 9	8	***

Table 4.2 Various delta reversal protocols

Peak power changes after application of various receptor modulators is represented as mean ± SEM when compared to control (normalised to 100%). N= number of recordings (obtained from 3 different animals), significance: ns p>0.05, * p<0.05, **p<0.01, ***p<0.001.

4.3 Discussion

Initial LFP recordings revealed the absence of spontaneous oscillatory activity in M1 and S1 in consistent with previous work (Yamawaki, 2008; Johnson, 2016). Co-application of KA and CCh reliably induced beta oscillations (Yamawaki, 2008; Prokic, 2011) in old slice preparations whereas, theta and gamma oscillations were identified both in M1 and S1 (Johnson *et al.,* 2016) with new slice preparation (refer chapter 3 for details). To further investigate the low frequency neuronal network activity in M1 and S1, experiments were performed to induce delta (2-4 Hz) oscillations which are known to be associated with deep sleep stages especially NREM3 and NREM4 stages. Although a number of studies demonstrated the origin of delta oscillations (1-4 Hz) in thalamus (Amzica *et al.,* 1992), relatively less is known about cortical based delta oscillations. A delta rhythm of purely cortical origin has been implicated in *in vivo* studies (Amzica and steriade, 1998; Fell *et al.,* 2002) but the mechanisms underlying were not as clear as those in thalamic origin (Pirchio *et al.,* 1997; Hughes *et al.,* 1999; 2002). Additionally, it has been suggested that cortical delta oscillations are generated in a use-dependent manner, in that the cortical circuits that are active during awake states generate these oscillations in the succeeding sleep (Kattler *et al.,* 1994; Huber *et al.,* 2004) and in a region specific way, implying a self-organising property of local neuronal networks (Krueger and Oba´l, 1993; Vassalli and Dijk, 2009; Vyazovskiy *et al.,* 2011). Frontal and parietal cortical regions are known to be delta generators in human cortex during sleep with a possibility of local delta generators for each region (Mormann *et al.,* 2008; Ioannides *et al.,* 2009). A recent *in vitro* study has indicated delta oscillations in secondary somatosensory cortex/parietal area, S2/Par2 slices prepared from male Wistar rats (Carracedo *et al.,* 2013). None of these studies have indicated the mechanisms and origin of cortical delta rhythm probably because it is challenging to induce delta oscillations unlike gamma oscillations, which can be identified spontaneously or with minimal pharmacological manipulations in regions like CA3, M1, S1, V1 etc. A recent study has revealed that transition of NREM2 to NREM3&4 stages required the neuromodulatory action of cortex itself but not thalamus (Krishnan *et al.,* 2016). We have assumed that the origin of delta oscillations could possibly be primary motor and sensory cortices with these regions being primary projection sites for thalamus, hence the term 'primary'.

4.3.1 Generation of delta oscillations

Induction of delta oscillations requires a state that mimics the physiologically equivalent deep sleep state. In order to achieve this neuromodulatory state we have tried various protocols using sleep related neurochemicals. Initially 150 nM KA and 10 µM CCh was bath applied to activate the slices since there is no spontaneous activity observed in M1 and S1. Co-application of KA and CCh induced theta and gamma oscillations (see chapter 3). When

GABA$_A$ positive modulator, pentobarbital (10-30 µM) was bath applied at this stage, the oscillations have been desynchronised and very slow oscillations (< 1Hz) were identified which was different to what was expected (2-4 Hz) (data not shown). It was not surprising to see pentobarbital affect frequency with no change in power based on the fact that it acts via phasic inhibition, by opening GABA$_A$R for longer time. Increased IPSC decay has enabled the decrease in frequency (Segal and Baker, 1984). The reciprocal interaction model suggested that the awake state has aminergic dominance and REM sleep state has cholinergic dominance whereas NREM state of sleep has intermediate tone (McCarley and Hobson, 1975). To investigate if low cholinergic tone would induce delta oscillations, aCSF with standard KA (150 nM) and CCh (10 µM) was replaced to that which contained same KA but low concentration of CCh (2 µM – 1/5th of what is generally required for cortical activation). Reduction in ACh levels has shown increased excitatory connection strength via AMPA conductance, as well as increased leak (K$^+$) currents. This decreased ACh levels have proved to be essential for transition to deep sleep stages (Krishnan *et al.,* 2016). There has been research that suggests CCh when injected bilaterally promoted sleep *in vivo* (George *et al.,* 1964). This has decreased the power of theta and gamma oscillations but did not induce delta oscillations probably because low cholinergic tone alone was not enough. Since dopamine plays a critical role in promoting arousal, it was suspected whether ambient dopamine in the slices was too high to enable delta induction. This was examined by perfusing the slices with D2 antagonist (Haloperidol 10 µM) besides KA and CCh based on the evidence that D2 blocking properties has enabled NREM 3 and 4 sleep whilst decreasing awake state (Monti and Monti, 2007). This still did not induce delta oscillations but reduced the frequency of oscillations. To mimic low cholinergic and low dopaminergic state, 150 nM KA, 2 µM of CCh, D2 antagonist; Haloperidol and D1 antagonist; SCH23390 was bath applied simultaneously. In this condition, it was possible to induce persistent delta oscillations at 2-4 Hz frequency. Interestingly, delta oscillations were not generated either by blocking D1 receptors or D2 receptors on their own which is contrary to recent *in vitro* work on delta rhythm in rat slices containing secondary somatosensory/parietal area, S2/Par2 (Carracedo *et al.,* 2013) suggesting a physiological difference in the origin of M1 delta rhythm. Changes in power (increase) and frequency (decrease) in the generation of delta meant the involvement pre (phasic) and post-synaptic (tonic) currents. Activation of D1 receptors disturbs long-term depression and increases (spike time dependent) long-term potentiation (Xu and Yao *et al.,* 2010). Furthermore, evidence exists that application of D1 antagonist (SCH 23390) prevented arousal (Trampus *et al.,* 1993) hence, the decrease in D1 tone may be a critical aspect of the current study.

4.3.2 Origin of delta oscillations

All the layers of M1 exhibited delta activity with same mean frequency but Layer V was thought to be the source of origin since the power of delta oscillations was found to be progressing from deep to superficial layers. This is consistent with human invasive electrode *in vivo* delta studies (Cserca *et al.,* 2010) and also *in vitro* delta studies that were carried out in rat parietal cortex and human frontal cortical tissue (Carracedo *et al.,* 2013). *In vivo* awake and sleep delta have been thought to originate mostly from the deep layers of frontal cortex (Knyazev, 2012). Additionally, beta oscillations (Murthy and Fetz, 1996; Donoghue *et al.,* 1998; Yamawaki, 2008) have also been reported to have highest power in Layer V as well as theta and gamma oscillations (Johnson *et al.,* 2017). Theta oscillations in human neocortex slices have shown temporal delays in superficial layers relative to deep layers, suggesting deep layers to be the origin of activity (Florez *et al.,* 2013). In accordance with the idea that deep layers drive slow oscillations, RS neurons in LV have been found to drive pyramidal neurons in superficial layers at low theta range (Carracedo *et al.,* 2013). Initiation of activity in LV was proved by local application of tetrodotoxin (TTX) whilst recording from LII/III and LV. 10 µM of TTX showed no effect on oscillatory activity of LV when locally applied to superficial layers whereas the oscillatory activity was abolished in LII/III when TTX was locally applied in deep layers (LV) (Yamawaki *et al.,* 2008). Correlation studies were performed on simultaneous recordings across each layer (II, III, V, VI) with a reference electrode in LV. These revealed that delta band oscillatory activity in LII and LIII was phase-delayed compared to that of LV however, delta activity in LVI was found to precede to that of LV. As the peak power of delta activity is greater in LV than in LVI, it might be assumed that LV would drive the activity, however, the fact that LVI leads LV suggest the latter as a driver. Unfortunately, it was not possible to isolate deep layers due to experimental difficulties in finding the precise boundary and so we could not directly test the ability of LVI alone to generate delta oscillations. There could be several possible grounds as to why LV may be assumed to drive oscillatory activity. Firstly, the morphological aspects; as it contains high density pyramidal cells in deep layers and also the presence of the Betz cells that were characteristic feature of LV of M1. Betz cells in M1 have extensive projections across all layers up to LI with a huge cell body (Molnar and Cheung, 2006). Secondly, the physiological properties of the interneuron populations that are present in LV which are responsible for neuronal oscillatory activity at delta frequency (not explored in this study). A strong drive onto vasoactive intestinal peptide-positive (VIP+) cells was identified in M1 and S1 (Lee *et al.,* 2013) and these cells have been identified to receive greater input from LV (Xu and Callaway, 2009) based on the anatomical evidence that layer V projections are more widely diffused than that of superficial layers (Markov *et al.,* 2014). Also, as seen in up/down states of mice sleep state *in vivo* and *in vitro* studies, network activation involves

intrinsically bursting (IB) neurons with cell bodies located in LV (Beltramo *et al.,* 2013; Carrecedo *et al.,* 2013). IB cells relate to excitatory synapses and gap junctions which could form the basis for high oscillatory activity in LV (Mercer *et al.,* 2006; Lefort *et al.,* 2009). Current source density studies in human recordings have revealed more synaptic input in superficial layers indicating enhancing the excitation onto distal dendrites in deep layers (LV) (Csercsa *et al.,* 2010). This excitatory output to deep layers from superficial layers have indicated in local circuits (Thomson and Morris, 2002). Previous studies on local circuits have suggested the existence of strong excitatory inputs to LV from other layers (Weiler *et al.,* 2008; Yu *et al.,* 2008; Anderson *et al.,* 2010; Hooks *et al.,* 2011;). Gap junctions between interneurons are known to increase network synchronisation (Gibson *et al.,* 1999; Galarreta and Hestrin, 1999; Traub *et al.,* 2000, 2001, 2003). Also, gap junctions between pyramidal axons have been implicated to enhance output activity of these cells (Schmitz *et al.,* 2001; Traub *et al.,* 2003). Moreover, the existence of most common gap junction subunit, connexion 36 was identified to be densely expressed in deep layers when compared to superficial layers which could be the basis for high amplitude oscillations in LV (Condorelli *et al.,* 2000; LeBeau *et al.,* 2003).

However, LV can not be considered the sole origin of network activity since LVI also contains various cell types that may contribute to generation of oscillatory activity. Cells in LVI receive direct thalamo-cortical input as well as forms an output layer to many thalamic nuclei. The major types of pyramidal cells that were identified in LVI which are distinguished based on shape include: CT (cortico-thalamus) cells that project to thalamus are short, narrow and vertically oriented towards LIV and LV. CC (cortico-cortical) cells that are present only within cortical regions with different shapes from short upright to bipolar neurons (see review Thompson, 2010). But, the functional characterisation of each type remains unexplored (Gonchar *et al.,* 2007). Nevertheless, LVI was reported to provide significant excitatory input to LV pyramidal cells in a paired recording study (Mercer *et al.,* 2005) besides the strong reverse connection from LV to LVI. It is challenging to identify the boundary between LV and LVI in our experiments, therefore we have recorded from deep layers (LV) with it being large area and was easily identified under microscope. A better way to delineate between LV and LVI would be beneficial.

4.3.3 Muscarinic receptor modulation

Application of CCh was essential to induce network activity in M1. Gamma oscillations were desynchronised when muscarinic receptor antagonists were bath applied (Fisahn *et al.,* 1998). Action of CCh was proved to be pre-dominantly via M1 receptors (mACh) as the delta oscillations were desynchronised when pirenzepine, an M1 receptor antagonist was applied to bath which is similar to delta oscillations in *in vitro* in other brain region like secondary somatosensory/parietal area (S2/Par2) (Carracedo *et al.,* 2013).

4.3.4 Gap junctions

Neuronal network activity is known to be dependent on electrical coupling via gap junctions (Draguhn *et al.,* 1998; Galarreta and Hestrin, 1999; Traub *et al.,* 2000, 2001, 2003*)* Gap junctions also have a critical role in high frequency oscillations generation and synchronization (Buhl *et al.,* 2003; Hormuzdi *et al.,* 2001) especially in the gamma frequency range (Kopell and Ermentrout, 2004; Hormuzdi *et al.,* 2001). Investigations of (Draguhn *et al.,* 1998) axo-axonal (pyramidal-pyramidal) gap junctions has revealed that action potentials propagate from one cell to another (Draguhn *et al.,* 1998; Schmitz *et al.,* 2001); cortex (Grenier *et al.,* 2001). Connexion-36 subunit knockout experiments revealed a role of axonal gap junctions in initiation of oscillatory activity whilst dendritic (interneuron-interneuron) gap junctions contribute to oscillation coherence (Traub and Bibbig, 2000). When gap junctions were blocked using carbenoxolone, delta oscillations were abolished in M1 after about 2 hours of drug application. The slow action of carbenoxolone is similar to that observed during EEG recordings *in vivo*, where oscillatory activity at theta frequency was only abolished after 60 min of perfusion (Konopacki *et al.,* 2004). Various gap junction blockers such as octanol (1 mM), CBX (0.2 mM), quinine (0.2 mM) and 18β-glycyrrhetinic acid has shown to decrease or abolish delta oscillations in slices containing secondary somatosensory/parietal area (S2/Par2) (Carracedo *et al.,* 2013) as well as gamma oscillations in other brain regions (Traub and Bibbig, 2000; Cunningham *et al.,* 2004). This evidence suggests the role of gap junction in generation and maintenance of delta oscillations. However, it is critical to note that gap junction modulators are non-specific and could act through mechanisms that are independent of gap junctions (Nakahiro *et al.,* 1991; Rouach *et al.,* 2003). Carbenoxolone is highly non-specific and has indicated to act through various mechanisms that include (but not limited to): block post synaptic NMDAR, reduce IPSCs via GABA$_A$R, suppress action potentials, blocks calcium channels, and reduces seizure activity besides blocking gap junctions (Rekling *et al.,* 2000; Rouach *et al.,* 2003; Vessey, 2004; Tovar *et al.,* 2009; Connors, 2012) yet still was used in current experiments due to its water-soluble nature and the lack of better alternatives (Konopacki *et al.,* 2004).

Further specific subunit KO experiments would be essential as well as developing selective blockers.

4.3.5 GABA modulation

$GABA_A$ receptors are ligand gated ion channels. These receptors act by increasing the membrane permeability of anions (Cl^- and HCO_3^- ions) which hyperpolarises the membrane resulting in inhibition (Rivera *et al.,* 1999). $GABA_AR$ antagonists, GBZ and PTX, reduced the power of delta oscillations with no change in frequency range. Dependence of delta oscillations on $GABA_AR$ implies the requirement of inhibitory currents in M1 like in hippocampal brain regions (Whittington *et al.,* 1995). It is known that the competitive antagonist, GBZ, at low concentration (250 nM) inhibits phasic synaptic currents but not extracellular tonic currents (Farrant & Nusser, 2005) due to the differential affinity of tonic (high affinity) and phasic (low affinity) $GABA_A$ receptors. Hence, high concentration GBZ (2.5 µM) was bath applied to surpass extra-synaptic tonic currents (Stell and Mody, 2002). 250 nM and 2.5 µM significantly reduced the synaptic synchronous delta activity revealing the role of both synaptic and extra-synaptic receptors in delta rhythm generation. Further investigations were made using a non-competitive channel blocker. PTX (5 µM) acts by binding inside the receptor ionophore which prevents the flow of Cl^- (Krishek *et al.,* 1996). PTX reduced the power of delta oscillations. Since pharmacological manipulation of IPSC kinetics using antagonists has meant the change (reduction) in power, tonic inhibition is responsible for delta rhythm initiation (Traub and Whittington, 2010). Surprisingly, these results contrasts with that of in rat secondary somatosensory/parietal area whose delta is $GABA_AR$ insensitive, suggesting a distinct mechanism between two regions (Carracedo *et al.,* 2013). This may be due to the subunit expression in various regions that are responsible for delta oscillations.

Zolpidem, a benzodiazepine site agonist showed differential effects at various concentrations and was previously demonstrated on beta oscillations in M1 (Prokic *et al.,* 2015). At beta frequency, Zolpidem stabilises a tonic current in a kinetically-slow state, meaning it cannot be desensitised and it therefore acts to hyperpolarise the GABA neurons, reducing oscillatory power. At higher concentrations, there is no slow state and zolpidem enhances power by augmenting inhibition. Interestingly, delta oscillations have shown an increase in delta power at 10 nM and decreased in the power at higher concentrations suggesting the $GABA_AR$ are not working in the same manner as it they were during beta or gamma activity (Prokic *et al.,* 2015). This could depend on the population of cells and receptor subtypes with different kinetic properties that are recruited for generation of delta oscillations in M1.

The GABA$_B$ receptors are metabotropic G-protein coupled receptors, which act by inhibiting presynaptic calcium release via adenylyl cyclase (Dunlap and Fischbach, 1981; Hill 1985; Newberry and Nicoll, 1985). On one hand, a study reported that GABA$_B$R do not contribute to oscillatory activity induced by CCh (Williams and Kauer, 1997). On the other hand, a study by Whittington *et al.,* has revealed the role of these receptors in determining the duration of gamma oscillations (Whittington *et al.,* 1995). CGP55845 (5 µM), GABA$_B$R antagonist reduced the power of synchronous delta oscillations which is in line with hippocampal and cortical gamma and beta oscillations (Yamawaki, 2008; Dugladze *et al.,* 2013) and similar to delta in secondary somatosensory/parietal area (Carracedo *et al.,* 2013) demonstrating the role of slow acting GABA$_B$R in delta rhythm generation.

4.3.6 Glutamate modulation

Excitatory currents have been identified to contribute to network oscillatory activity in M1 including theta, gamma and beta oscillations (Yamawaki, 2008, Prokic, 2011, Nicholas, 2016). To investigate iGluR involvement in delta rhythm generation, various receptor antagonists were bath applied. CNQX desynchronised delta oscillations by blocking both KA/AMPAR indicating the requirement of KAR or/and AMPAR. SYM2206, a potent AMPAR antagonist reduced the synchronous activity of delta oscillations GluA1-4 (APAMR) subunit KO studies revealed decrease in AMPA mediated EPSPs, changes in firing properties which in turn disrupted long range synchronisation (Fuchs *et al.,* 2001). KAR antagonists: UBP310 (GluK1/3) and UBP304 (GluK1) also blocked the activity. Kainate receptors were identified to be critical for rhythm generation as well as stabilisation. However, the delta induced in parietal cortex did not show significant effect to AMPA or KA receptors on their own but desynchronised the delta power when both receptors were blocked using CNQX (KA/AMPA blocker) suggesting a distinct mechanism (Carracedo *et al.,* 2013).

It is interesting to note that unlike the generation of beta oscillations in LV of M1 (Yamawaki, 2008), delta oscillations do not require NMDAR, which was in contrast to what was demonstrated both *in vitro* (Carracedo *et al.,* 2013) and *in vivo* studies (Hunt and Kasicki, 2013). *In vitro* studies in rat parietal cortex observed that synchronous delta oscillations were reduced when NMDAR antagonist 2-AP5 was added to bath whereas *in vivo* studies on freely moving rats proved that the delta power was increased in various cortical regions as demonstrated by various studies in the past (Mattia and Moreton, 1986; Marquis *et al.,* 1989; Feinberg and Campbell, 1998). These controversial findings imply further investigation on NMDAR associated with the delta rhythm. Since 2-AP5 is a competitive NMDAR antagonist, MK801 which is a selective non-competitive antagonist was bath applied. However, both drugs showed no effect on delta oscillations. There could be several reasons as to why pharmacologically induced delta oscillations are NMDA insensitive which may include experimental protocol, types of cells expressed in the region recordings were

made, receptor subunit composition and neuronal populations recruited for the rhythm. Moreover, Specific subunit KO experiments revealed that GluN1 KO increased firing rate thereby altering the synchrony (Belforte *et al.,* 2010), GluN2B (Kelsch *et al.,* 2014) KO reduced frequency and amplitude of EPSPs and knocking out GluN2C and D (Von Engelhardt *et al.,* 2015) had no change in NMDA mediated EPSPs in hippocampal interneurons. Therefore, comparatively greater expression of GluN2C and D subunits in layer V of M1 could also form the basis for this. Further investigations however are needed to address this by using subunit specific receptor modulators and KO studies.

mGluRs are known to influence rhythmic activity of transient gamma oscillations induced by tetanic stimulation as demonstrated by Whittington *et al.,* (1995). It has been reported that s activation of group I mGluRs by DHPG induced gamma oscillations in CA3 which are different to those induced by KA and CCh in CA3 (Palhalmi *et al.,* 2004). However, these receptors showed little contributions to synchronous activity of pharmacologically induced delta oscillations in M1. Moreover, they showed no contribution on pharmacologically induced beta oscillations in same area (Yamawaki, 2008). Only mGlu-R$_3$, mGlu-R$_5$ amongst three groups have been found to contribute to delta rhythm generation. None of the other receptors appeared to be involved in delta in M1. Minor but significant reduction in synchronous delta oscillations was noticed when mGlu-R$_3$ agonist LY379268 was bath applied whilst mGlu-R$_5$ antagonists MTEP and MPEP showed a significant increase in delta oscillations.

4.3.7 Pharmacological equivalent awake state: delta reversal protocol

Neurotransmitters play a critical role not only in sleep and awake states but also in transition state. It was evident that acetylcholine (ACh), histamine (HA), GABA, serotonin (5-HT), dopamine (DA) and nor-epinephrine (NE) are involved in sleep wake mechanisms. High levels of ACh, HA, NE are found in NREM2&3 stages whilst GABA was found to be lowest in these stages when compared to awake state (Aston-Jones and Bloom, 1981; McCormick, 1992; Vazquez and Baghdoyan, 2001; Lena *et al.,* 2005; Vanini *et al.,* 2011). It was interesting that, in REM sleep, ACh levels were found to increase but HA, NE and GABA were observed to decrease (Baghdoyan and Lydic, 2012). The reciprocal interaction model suggested that the awake state has aminergic dominance and REM sleep state has cholinergic dominance whereas NREM state of sleep has intermediate tone (McCarley and Hobson, 1975). Delta oscillations (2-4 Hz) were reliably induced by mimicking neuromodulatory deep sleep (low cholinergic and low dopaminergic) state. This state was obtained by pharmacological manipulation by bathing the slices in 150 nM of KA, 2 µM CCh, 10 µM SCH23390, 10 µM Haloperidol. Subsequent experiments were performed to reverse this state to a pharmacologically equivalent awake state. Since theta and gamma oscillations were identified upon application of KA and CCh, it was assumed that washing the slices in the same would reverse delta oscillations to faster frequency range but no change was observed confirming the persistent nature of delta oscillations. Increased ACh would mean the decrease in AMPA conductance based on experimental findings (Gil *et al.,* 1997; Kimura *et al.,* 1999; Hsieh *et al.,* 2000) which would not influence frequency of oscillations. High concentrations of KA and CCh were bath applied and both lead to seizure like activity which was not surprising as KA and CCh increase the rate of firing whereby inducing seizure like activity as observed in various studies (Ben-Ari *et al.,* 1985; Brudzynski *et al.,* 1995; Stivers *et al.,* 1998; Ben-Ari and Cossart, 2000). Interestingly, when we investigated experiments in high KA and CCh, we found delta intact, but masked by very low frequency and high amplitude activity. High levels of DA has shown an increase in wakefulness in dopamine transporter (DAT) knock out mice (Wiser *et al.,* 2001). Also, application of D1 agonist, SKF38393 increased wakefulness and decreased sleep and a simultaneous block of D1 receptors using an antagonist (SCH23390) prevented arousal (Trampus *et al.,* 1993). Subsequent experiments were carried out using dopamine and histamine assuming the increase in aminergic tone would enable the transition from deep sleep state to awake state but both HA and DA showed an increase in power with no effect on frequency of delta oscillations. High levels of HA has led to effect I_h current by positively shifting activation curve (McCormick and Williamson, 1991) with no effect on network activity. Moreover, awake drug mixture [KA (150 nM), CCh (10 µM), GABA (1 µM), DA (50 µM), HA (200 µM), 5-HT (1 µM), Ascorbic acid (250 µM)] was used but no change in

frequency range was noticed. This mixture contains ascorbic acid as a neuro-protectant since DA is an unstable molecule (Graham, 1978) and easily gets oxidised to free radicals and reactive quinones (Hastings *et al.,* 1996). However, a massive increase in power of delta oscillations was observed suggesting all the above wake promoting compounds have strengthened the neuronal network synchronisation in M1. Furthermore, amphetamine sulphate, a potent CNS stimulant which is critical for monoamine regulation via trace amine-associated (G-protein coupled) receptor (TAAR1) was bath applied to investigate if this would enable wakeful state (Miller, 2011).

On an interesting note, both awake drug mixture and amphetamine sulphate, when bath applied before delta incidence have shown a significant increase in power of theta and gamma oscillations yet, only the former has enabled delta induction whilst the latter did not. AMPH reverses the DA transit from cytoplasm to extracellular space via DAT which was termed as DA efflux enabling increased locomotion (German *et al.,* 2015; Kopra *et al.,* 2017) in accordance with a study suggesting extracellular dopamine levels have indicated to be higher after AMPH administration in rats (O`Leary *et al.,* 2016). This hyper dopamine levels explains the prevention of delta oscillations which requires low dopaminergic state. Reduction in power of gamma oscillations upon subsequent addition of delta drugs could account for the cytotoxicity caused due to auto-oxidation of high levels DA upon AMPH application (as seen in Carvalho *et al.,* 2012).

Recently, Krishnan *et al.,* (2016) has developed an *in silico* model that was sufficient to cater the needs to study sleep-wake cycle characteristics which included populations of interneurons (IN) and pyramidal cells (PY) in cortex, thalamic reticular nucleus (RE) and thalamic relay neurons from thalamus based on the previous evidence from literature (Bazhenov *et al.,* 1998, 1999; Timofeev *et al.,* 2000; Bonjean *et al.,* 2011; Chen *et al.,* 2012; Wei *et al.,* 2016). In their study, Krishnan et al show transition from NREM2 to deep sleep (NREM3 & 4) stages required neuromodulatory actions within cortex itself and thalamus was not required. In our own study, we saw delta in slices containing cortex only, confirming the *in silico* results of Krishnan *et al.*, however, it is not possible for transition to awake states from sleep stages within cortex in our experiments. We speculate that the role of thalamo-cortical connections is critical to reversal of the sleep-like state in our *in vitro* preparation. This may explain why it was possible to induce delta oscillations in M1 and S1 slices but not possible to reverse it to equivalent awake state. Slice preparations containing various regions involved in sleep, including thalamus, would be helpful to address this issue however, this was currently not possible due to time limitations.

4.3.8 Possible mechanism of delta oscillations in M1

In the current study, we have shown KA and CCh induced theta and gamma oscillations simultaneously which is comparable to previous work in the lab. Delta oscillations are pharmacologically induced in layer V of Primary motor cortex (M1) by maintaining low cholinergic and low dopaminergic tone which is the characteristic feature in deep sleep stages and we have illustrated the transition from fast (gamma and theta) oscillations to slow (mu and beta) oscillations before a high amplitude delta rhythm emerged. Delta rhythm was characterised using various receptor modulators to determine the role of various receptors in the rhythm generation. Current study suggests that these delta oscillations are dependent on GABAR, AMPAR, KAR, mAChR and gap junctions but are independent of NMDAR. mGluRs do not seem to show much contribution to the generation of delta rhythm however mGluR agonists showed a general reduction in the activity whilst the antagonists showed an increase in the activity which is significant only in case of group I mGluR antagonists (MPEP & MTEP). These suggestions were based on the pharmacology performed using various receptor modulators and comparing them with control.

4.3.9 Final conclusions

To our knowledge, this is the first demonstration of motor cortical delta oscillation *in vitro* and was identified to have a distinct mechanism to that of delta in secondary somatosensory/parietal area (S2/Par2) (also *in vitro)* (Carracedo *et al.,* 2013). These extracellular studies could prove significant in investigating neuronal network oscillations in pathological states such as PD, AD by using animal models that can enable the comparison of mechanisms. Delta oscillations were induced by KA, CCh, D1 and D2 antagonists and are reliant on both inhibitory and excitatory network activity. AMPAR contribute to overall excitation of the cells, CCh to activate the cells and GABAR to the set the frequency similar to that of gamma oscillations except delta are found independent of NMDAR both in M1 and S1. Based on suggestion that cortical delta oscillations are generated in a use-dependent manner, in that the cortical circuits that are active during awake states generate these oscillations in the succeeding sleep (Kattler *et al.,* 1994; Huber *et al.,* 2004) and in a region specific way, implying a self-organising property of local neuronal networks (Krueger and Oba´l, 1993; Vassalli and Dijk, 2009; Vyazovskiy *et al.,* 2011) reflecting previously prevalent gamma oscillations then become delta oscillations. Pharmacologically induced delta oscillations were found to be irreversible since the frequency of the oscillations had not changed when pharmacologically equivalent awake state was maintained possibly due to experimental limitations. A slice preparation with both cortex and thalamus preserved and also using various wake promoting compounds such as caffeine, adenosine, and orexin would probably enable delta reversal.

5. Characterisation of delta oscillations in S1 and interaction between M1 and S1 at delta frequency.

5.1 Introduction

In some studies (Werth *et al.,* 1997; Finelli *et al.,* 2001), the appearance of slow wave activity was found to follow an ascending pattern from anterior to posterior regions in cerebral cortex, with highest power in frontal areas. This was identified to be promising in the first NREM sleep suggesting a role of frontal regions such as M1 and S1 in sleep management. This was found to be evident in the vibratory stimulation study performed in awake state enhanced the power of delta oscillations in somatosensory cortex during the first cycle of sleep (Kattler *et al.,* 1994) and gradually decreased in subsequent cycles. S1 was chosen based on the fact that it is the primary source of sensory information in rats (Burwell *et al.,* 1995). The term 'primary' is used to describe sensory cortex that receives unimodal input directly from the thalamus.

Anatomical studies have shown that M1 receives input from S1 and thalamus (Zin-Ka-Leu, 1998; Miyachi *et al.,* 2005) and the highly reciprocal nature of functional connections between M1 and S1 have been demonstrated in an optimum plane sensorimotor slice preparation developed by Rocco *et al.,* (2007). Similarly, studies using voltage-sensitive dye imaging (VSD) and anterograde and retrograde tracers or viral vectors provide strong evidence that sensory input and whisker movement are related in rats (Ferezou *et al.,* 2007) and inactivation of S1 results in altered chewing (Lin *et al.,* 1993; Hiraba *et al.,* 2000), muscle contractions and motor co-ordination (Rothwell *et al.,* 1982; Hikosaka *et al.,* 1985, Johansson and Westling, 1984). These reports suggest the role of sensory input from S1 in modulating motor output from M1. Topographical organisation of S1 was found to be similar to that of M1 (Huffman and Krubitzer, 2001) and have close association with M1 via reciprocal connections. Axonal projections of LIII of S1 (otherwise known as area 3a) have been identified to terminate throughout the cortical column of M1 (Porter 1991, 1992, 1996; Porter and Sakamoto, 1988) by performing retrograde labelling studies. These studies have also revealed LII and LVI of M1 send projections to S1 (Porter, 1991, 1993).

Sensorimotor integration has been studied *in vivo* (Smith *et al.,* 1983; Wannier *et al.,* 1991) but this does not enable the full understanding of the pathways. However, sensorimotor slice preparation by Rocco *et al.,* enables to investigate further on sensorimotor connections *in vitro* (Rocco *et al.,* 2007). Detailed information and significance of M1 and S1 interactions were discussed in chapter 3 (section 3.3).

This chapter deals with pharmacology of delta oscillations in LV of S1 and compared to delta oscillations in M1. To determine the origin of delta oscillations, various sagittal slice preparations were made (see Methods section 2.2 for details). Experiments in the first part (5.2) of this chapter was performed in LV of a sensorimotor slice (slice type A) with both regions and surroundings intact. The following section (5.3) utilised the various types of

slice preparation (as seen in Methods 2.2 section) with a view towards identifying whether M1 and S1 have their own delta rhythm generator or if one region was leading the other or if there was any thalamic dependence for rhythm generation.

Previous studies on local circuits have suggested the existence of strong excitatory inputs to LV from other layers (Weiler *et al.,* 2008; Yu *et al.,* 2008; Anderson *et al.,* 2010; Hooks *et al.,* 2011). Based on the fact that high amplitude oscillations were recorded from layer V of M1 as shown in laminar studies (section 4.2.2) in 4th chapter as well as structural similarities (Huffman and Krubitzer, 2001), all experiments in this chapter were performed in deep layer (LV) of either M1 and/or S1.

5.2 Pharmacology of delta oscillations in S1

5.2.1 Pharmacological induction of delta oscillations in LV of S1

Primary somatosensory cortex (S1) is adjacent to primary motor cortex (M1) and shares structural similarities with it. Investigations were made to examine the ability of S1 to generate delta oscillations. All recordings in this chapter are made from LV of S1 unless otherwise stated. In the presence of KA (150 nM) and (10 µM), theta and gamma oscillations were induced (see chapter 3 for details). In the intact sensorimotor slice containing M1, S1 and surrounding regions, a transition similar to that of in M1 was identified. When perfused with aCSF containing KA (150 nM), CCh (2 µM), SCH23390 (10 µM) and Haloperidol (10 µM), fast oscillations, theta (6-11 Hz) and gamma (30-37 Hz) gradually shifted to slow oscillations: slow theta (5-7 Hz) and beta oscillations (25-30 Hz) before high amplitude delta oscillations (2-4 Hz, ~300 µV^2, n=50) with a mean frequency of 3.2 ± 0.7 Hz emerged (figures 5.1, 5.2).
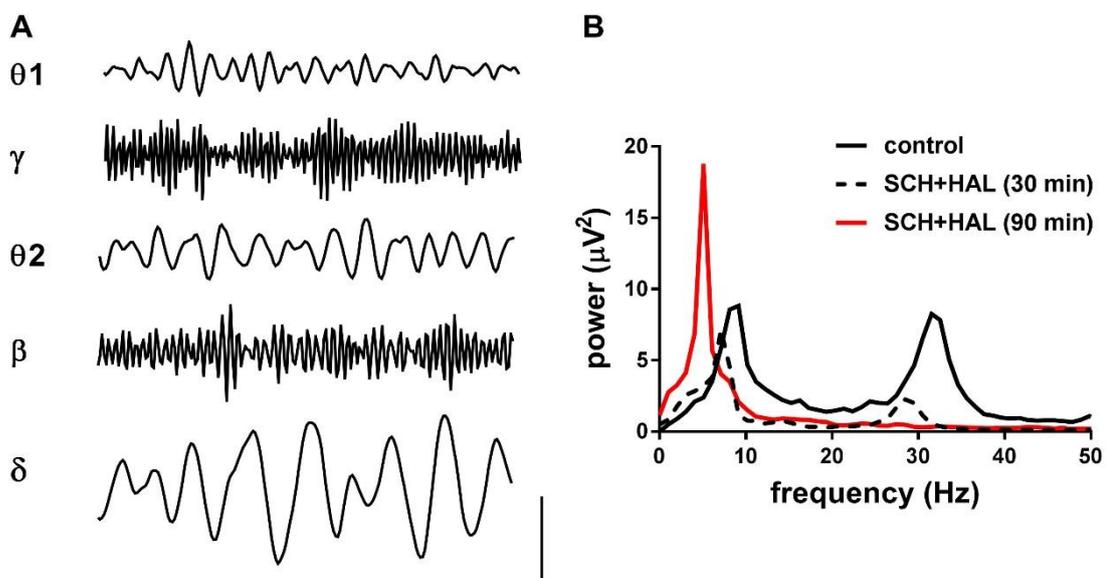
Figure 5.1 Pharmacological induction and transition of theta-gamma to delta oscillations (2-4 Hz) in LV of S1

(A) Representative extracellular voltage recordings of activity during development of delta rhythm in SCH23390 & haloperidol. Gamma (30-40 Hz), beta (25-29 Hz), theta-1 (7-14 Hz), theta-2 (5-7 Hz) and delta (1-4 Hz) oscillations (scale: 20 µV x 250 ms). **(B)** Power spectra of oscillatory activity during application of SCH23390 & haloperidol at 30 min (dotted line) and at 90 min (red line). Note how gamma-theta activity gradually shifted into beta and slow theta (5-7 Hz) oscillations (dotted), before a high amplitude (20-400 µV^2) delta rhythm (red) emerged.

Pharmacological studies were performed using various receptor modulators. Control for each recording was normalised to 100% and in experiments of this chapter, stable delta oscillations were characterised as showing no change noticed in frequency and amplitude over 20 min period. The effect of a drug was measured just after 40 min of bath application of the drug (unless otherwise stated) which was compared to control.
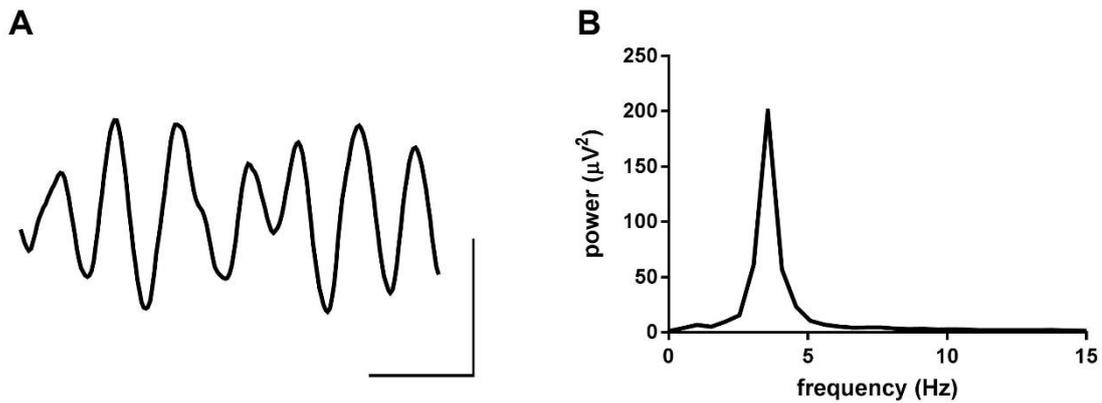
Figure 5.2 Representative typical delta oscillation in LV of S1 (2-4 Hz)

(A) Raw data of an example typical delta oscillation recorded from LV of S1 (scale: 50 μV x 500 ms) **(B)** representative power spectrum of pharmacologically induced delta activity in 'sleep' neuromodulatory state (low dopaminergic and low cholinergic tone).

5.2.2 Cholinergic modulation of delta oscillations in LV of S1

To examine the effect of CCh was through muscarinic acetylcholine receptors, pirenzepine (PIR), an mAch antagonist was bath applied when oscillations were stable for 20 min. 10 µM of PIR significantly decreased the peak delta power to 23 ± 1% of control (normalised to 100%) suggesting a role of mAch receptors in generation of delta oscillations in LV of S1 as in M1 (n=8, p<0.001) (figure 5.3)
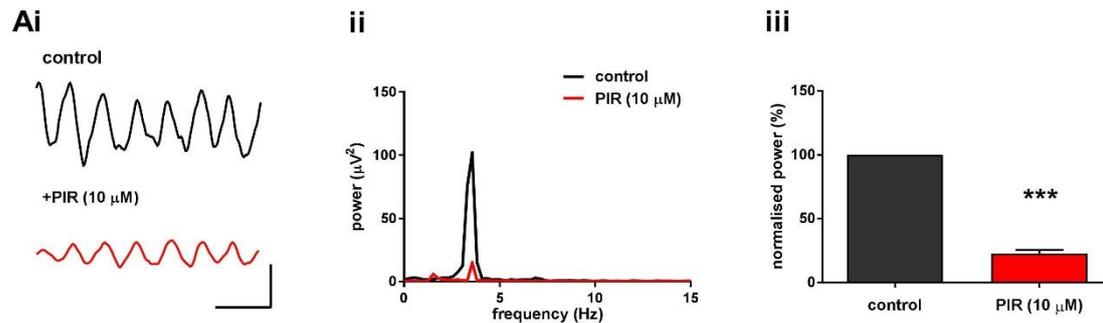
Figure 5.3 Muscarinic receptor block decreases delta oscillatory power

(A) Effect of pirenzepine (10 µM) on delta oscillations. **(i)** Raw data showing the changes in oscillatory activity before (black) and after (red) drug application (scale: 100 µV vs 500 ms). **(ii)** Representative power spectra of 60s of extracellular recording demonstrating peak responses before (black) and after (red) PIR **(iii)** Bar graphs showing peak oscillatory power of oscillations before (grey) and after (red) drug application normalised to control. ** p<0.01, n=8.

5.2.3 GABA$_A$R modulation of delta oscillations in LV of S1

To determine the involvement of inhibitory GABA$_B$R, a competitive GABA$_A$R antagonist gabazine (GBZ) and a non-competitive channel blocker picrotoxin (PTX) were bath applied. Application of GBZ at 250nM and 2.5 μM significantly reduced the synaptic synchronous delta activity to 36.50 ± 3% and 22 ± 5% of control respectively (n=8, p<0.001) (figure 5.4A). 5 μM of PTX significantly reduced the delta synchronous activity to 38 ± 5% of control (n=8, P<0.01) (figure 5.4B).
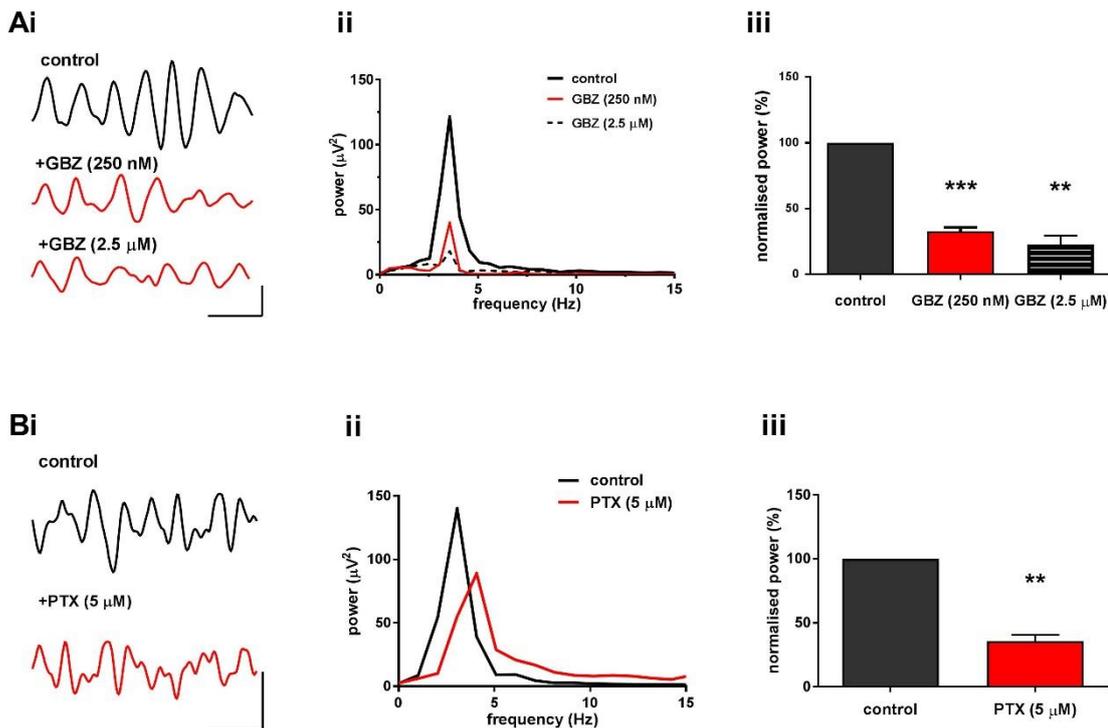
Figure 5.4 GABA$_A$ receptor block decreases delta oscillatory power

(A) Effect of gabazine (250 nM and 2.5 μM) on delta oscillations. **(i)** Raw data showing the changes in oscillatory activity before (black) and after (red) 250 nM, 2.5 μM drug application (scale: 60 μV vs 500 ms). **(ii)** Representative power spectra of 60s of extracellular recording demonstrating peak responses before (black), after GBZ 250 nM (red) and GBZ 2.5 μM (dashed line) **(iii)** Bar graphs showing peak oscillatory power of oscillations before (grey) and after (red) drug application normalised to control. **p<0.01, n=8.

(B) Effect of picrotoxin (5 μM) on delta oscillations. **(i)** Raw data showing the changes in oscillatory activity before (black) and after (red) drug application (scale: 100 μV vs 500 ms). **(ii)** Representative power spectra of 60s of extracellular recording demonstrating peak responses before (black) and after picrotoxin (red) **(iii)** Bar graphs showing peak oscillatory power of oscillations before (grey) and after (red) drug application normalised to control. **p<0.01, n=8.

5.2.4 iGluR modulation of delta oscillations in LV of S1

5.2.4.1 AMPAR modulation of delta oscillations

The dependence of delta oscillations on AMPAR was investigated by using SYM2206, a specific AMPAR antagonist. Application of 20 µM of SYM2206 significantly desynchronised the delta activity. It reduced the power to 49 ± 4% of control (n=8, p<0.01) (figure 5.5A).

Bath application of 25 µM CNQX, KAR/AMPAR antagonist significantly reduced the synchronous delta activity (figure 5.5B) to 40 ± 7% of control (n=8, P<0.01) revealing the role of both KA and AMPA receptors in generation of delta oscillations.
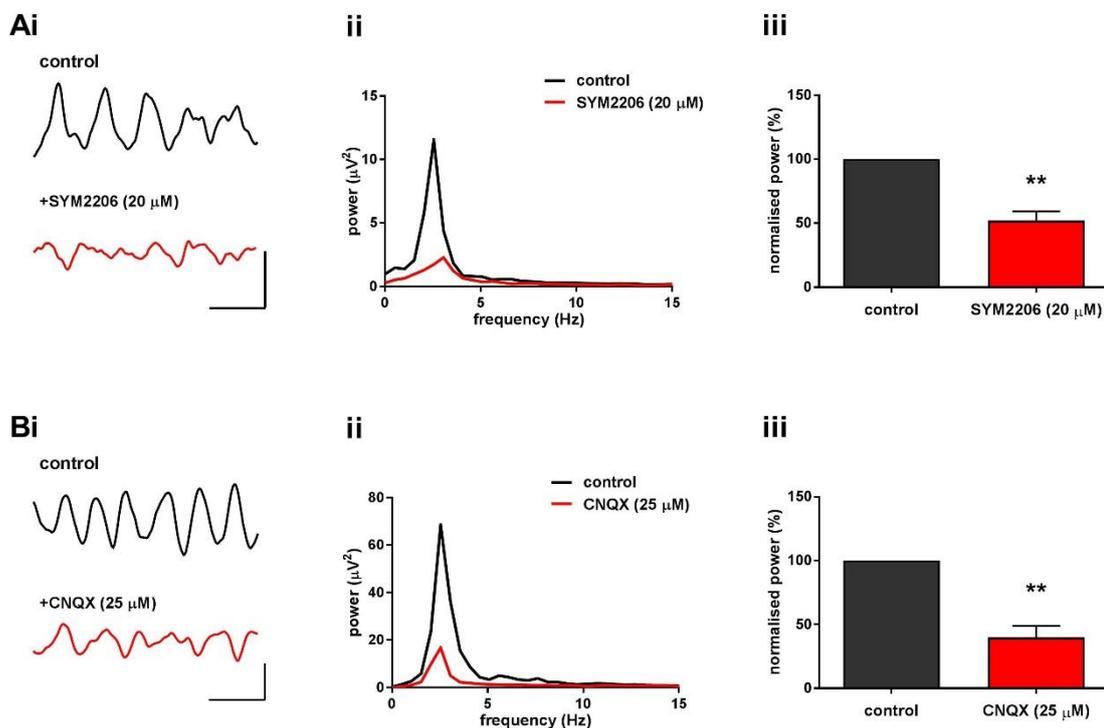
Figure 5.5 AMPA receptor block decreases delta oscillatory power

(A) Effect of SYM2206 (20 µM) on delta oscillations. **(i)** Raw data showing the changes in oscillatory activity before (black) and after (red) drug application (scale: 20 µV vs 500 ms). **(ii)** Representative power spectra of 60s of extracellular recording demonstrating peak responses before (black) and after (red) SYM2206 **(iii)** Bar graphs showing peak oscillatory power of oscillations before (grey) and after (red) drug application normalised to control. **p<0.01, n=8.

AMPA/kainate receptors block decreases delta oscillatory power

(B) Effect of CNQX (25 µM) on delta oscillations. **(i)** Raw data showing the changes in oscillatory activity before (black) and after (red) drug application (scale: 50 µV vs 500 ms). **(ii)** Representative power spectra of 60s of extracellular recording demonstrating peak responses before (black) and after (red) CNQX **(iii)** Bar graphs showing peak oscillatory power of oscillations before (grey) and after (red) drug application normalised to control. *** p<0.001, n=8.

5.2.4.2 NMDAR modulation of delta oscillations

The role of NMDA receptors was tested using 2-AP5, a competitive NMDAR antagonist. 50 µM 2-AP5 did not alter the delta peak (n=8, P>0.05) (figure 5.6) suggesting generation of delta oscillations does not require NMDA receptors, as obseerved in M1 (see chapter 4 for details).
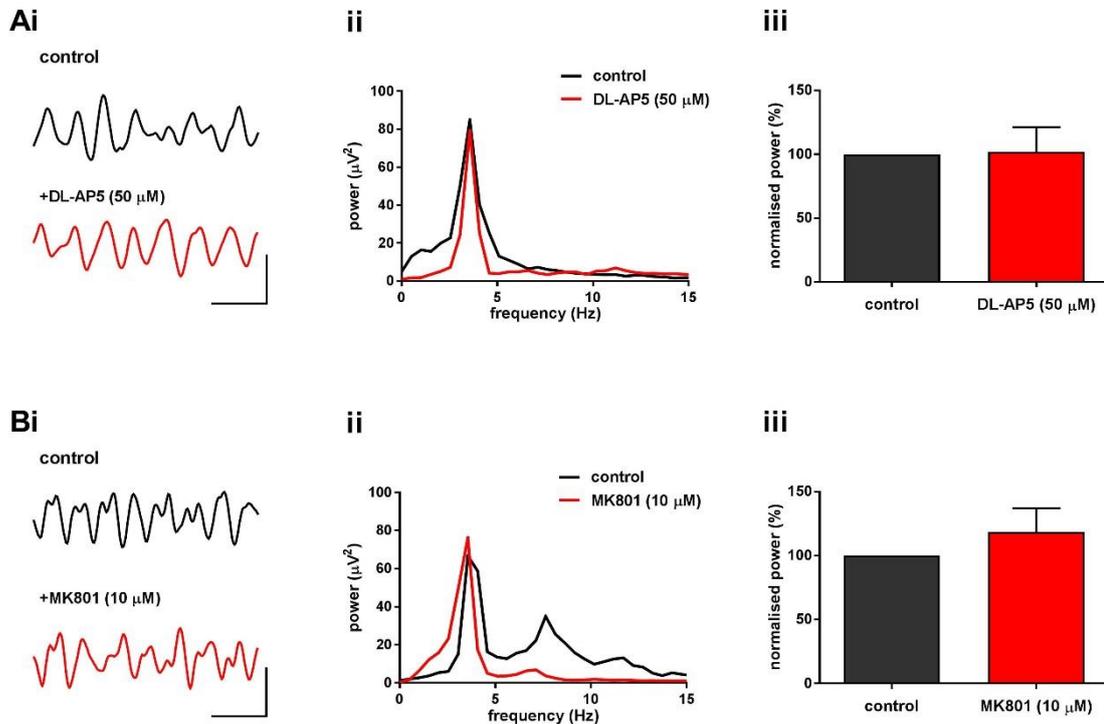
Figure 5.6 NMDA receptor block has no effect on delta oscillatory power

(A) Effect of 2-AP5 (50 µM) on delta oscillations. **(i)** Raw data showing the changes in oscillatory activity before (black) and after (red) drug application (scale: 50 µV vs 500 ms). **(ii)** Representative power spectra of 60s of extracellular recording demonstrating peak responses before (black) and after (red) DL-AP5 **(iii)** Bar graphs showing peak oscillatory power of oscillations before (grey) and after (red) drug application normalised to control. ns p>0.05, n=8.

(B) Effect of MK801 (10 µM) on delta oscillations. **(i)** Raw data showing the changes in oscillatory activity before (black) and after (red) drug application (scale: 50 µV vs 500 ms). **(ii)** Representative power spectra of 60s of extracellular recording demonstrating peak responses before (black) and after (red) MK801 **(iii)** Bar graphs showing peak oscillatory power of oscillations before (grey) and after (red) drug application normalised to control. ns p>0.05, n=8.

5.2.5 Summary of results

Pharmacology of delta oscillations in LV of S1 was summarised in table below

Drug (concentration)	% Change of Control	N	Significance
pirenzepine (10 µM) [mAch antagonist]	23 ± 0.5	8	***
gabazine (250 nM,2.5 µM) [GABAAR antagonist]	$36 \pm 3, 22 \pm 5$	8	**,***
picrotoxin (5 µM) [GABAAR antagonist]	38 ± 5	8	**
SYM2206 (20 µM) [AMPAR antagonist]	49 ± 4	8	**
CNQX (25 µM) [KA/AMPAR antagonist]	40 ± 7	8	**
AP-5 (50 µM) [NMDAR antagonist]	N/A	8	ns
MK 801 (10 µM) [NMDAR antagonist]	N/A	8	ns

Table 5.1 Pharmacology of delta oscillations in LV of S1

Peak power changes after application of various receptor modulators is represented as mean ± SEM when compared to control (normalised to 100%). N= number of recordings (obtained from 3 different animals), significance: ns $p > 0.05$, * $p < 0.05$, **$p < 0.01$, ***$p < 0.001$.

5.3   M1-S1 interactions at delta frequency

In order to study interactions between M1 and S1, I used a series of sagittal brain slice preparations designated as slice type A-F, detailed in Methods (section 2.2).

5.3.1 Correlation studies of delta oscillations in slice type A

It was observed in the experiments of pharmacological induction of delta oscillations in the presence of KA (150 nM), CCh (2 µM), SCH23390 (10 µM) and haloperidol (10 µM) in LV of M1 and S1 that delta oscillations in S1 were time delayed to that of M1. Mean peak power of delta oscillations were plotted against time both in M1 and S1. This revealed a significant time delay of 19 ± 3 min in incidence of delta oscillations in S1 (n=8, p<0.01). A linear regression graph suggested that intercepts were different when compared M1 with S1 delta mean peak suggesting a significant delay in elevation (n=8, p<0.001) (figure 5.7).
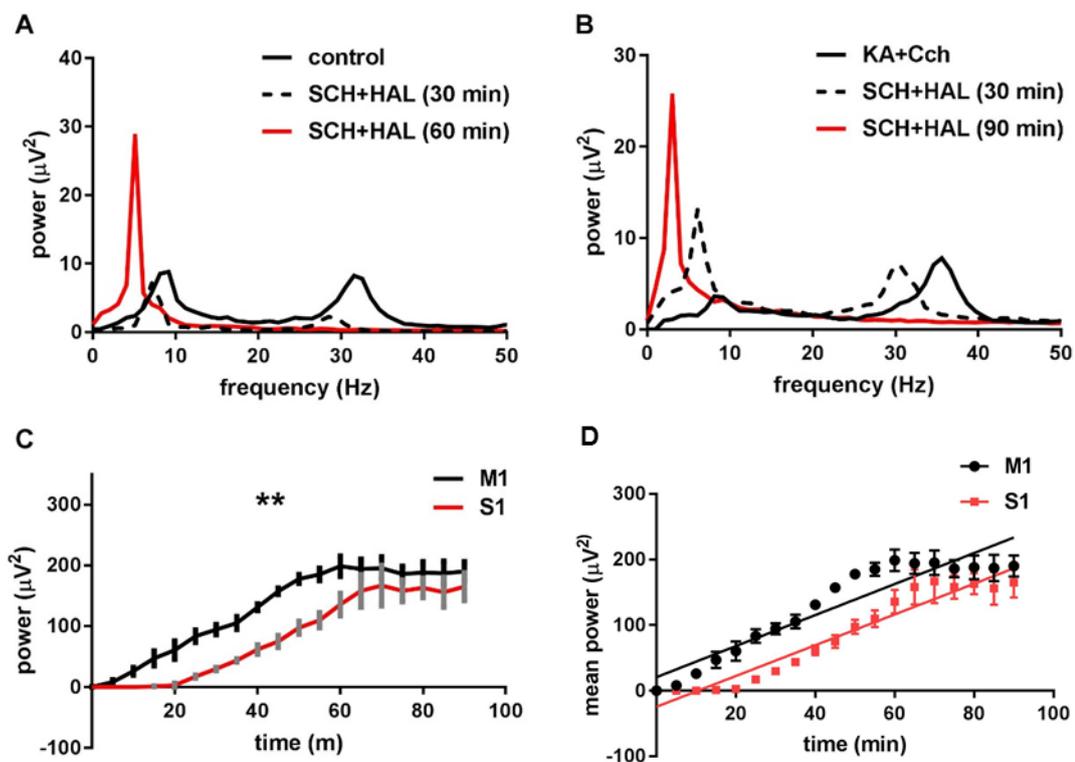
Figure 5.7 Development of delta oscillations in S1 is significantly time delayed with respect to delta in M1 in slice type A

(A) A representative power spectrum representing the transition of fast oscillations (black) to slow oscillations (dotted line) and to delta (red) oscillations in LV of M1 **(B)** in S1 **(C)** graph comparing the mean delay in incidence of delta oscillations in M1 (black) to that of S1 (red) **(D)** a linear regression graph showing significant difference in y-intercept (elevation) between M1 (black) and S1 (red) with slopes being almost equal (n=8, p<0.01, p<0.001).

To further investigate this, correlation analysis was conducted in various slice types (refer methods section). In slice type A, Auto-correlation enabled to identify the signal as delta (2-4 Hz) frequency in a given time (figures 5.8 A-B). Good correlation (correlation coefficient =0.5) of delta oscillations also existed between M1 and S1. However, delta oscillations in S1 were found to be phase lagged by 2.5 ± 0.6 ms with reference to M1 whilst delta in M1 was preceded by 2.4 + 0.4 ms with reference to S1 (figures 5.8 C-D) suggesting the origin of delta oscillations to be M1.
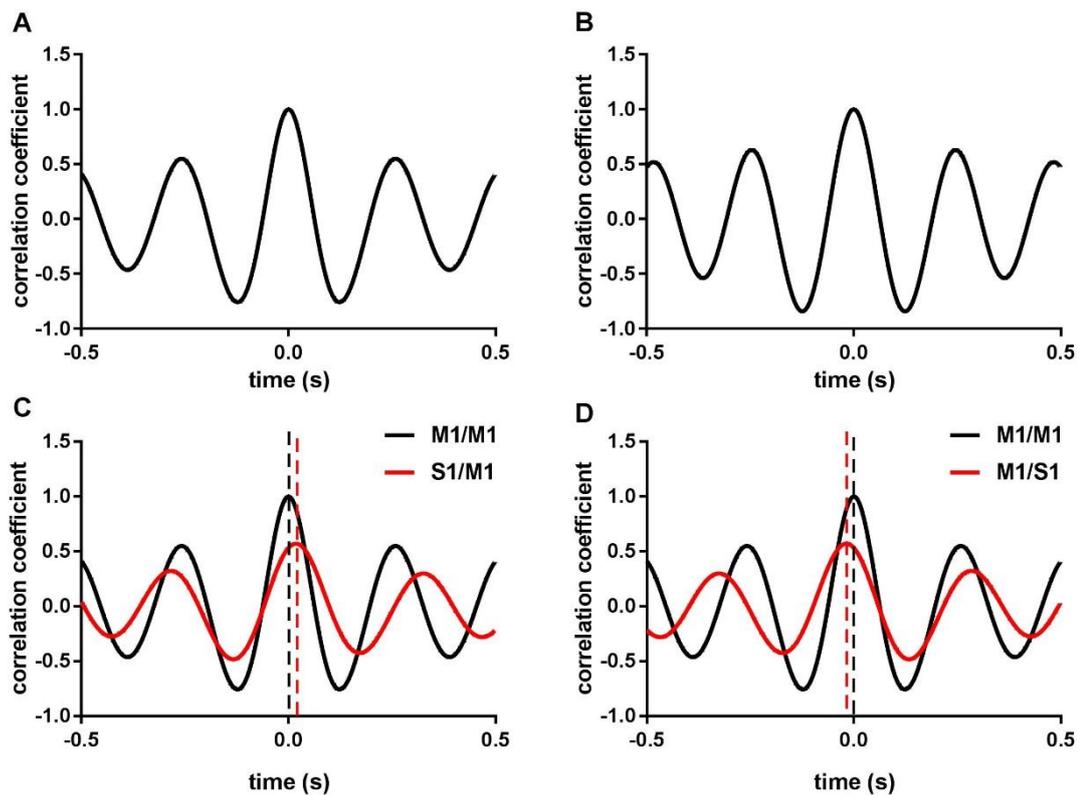
Figure 5.8 LV of M1 is the place of origin of the delta frequency activity in slice type A

(A) auto-correlation analysis of delta oscillations in M1 **(B)** in S1 **(C)** cross-correlation between M1/M1 (black) and S1/M1 (red) **(D)** cross-correlation between M1/M1(black) and M1/S1 (red). Red dashed line represents the deviation from zero (black dashed line).

5.3.2 Correlation studies of delta oscillations in slice type B

To further investigate if the time delay in incidence and phase delay in correlation studies of delta in S1 suggested that M1 to be the origin, a cut was made between two regions. In slice type B, it was noticed that delta oscillations emerged in M1 but not in S1 in the presence of KA (150 nM), CCh (2 µM), SCH23390 (10 µM) and Haloperidol (10 µM). Auto correlation revealed the oscillations to be in delta range (2-4 Hz) in M1 but theta range (6-11 Hz) in S1 suggesting there is no local delta rhythm generator in S1 (figure 5.9 A-D).
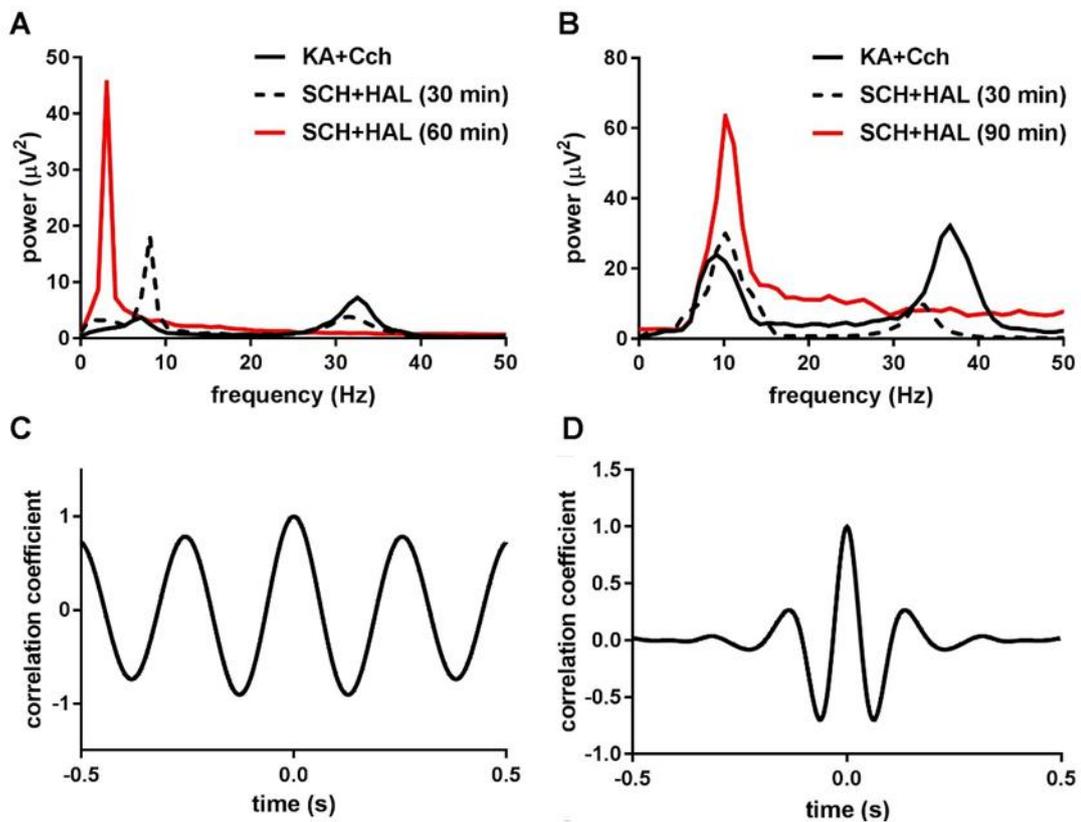
Figure 5.9 M1 drives the oscillatory activity at delta frequency in S1

(A) A representative power spectrum representing the transition of fast oscillations (black) to slow oscillations (dotted line) and to delta (red) oscillations in LV of M1 **(B)** An example power spectrum showing theta and gamma oscillations in the presence of KA and CCh (black) and in the presence of SCH+HAL (red) **(C)** correlation analysis of delta oscillations within M1 **(D)** correlation analysis revealed theta oscillations in S1. Note: there is no delta in S1 in this slice type.

5.3.3 Correlation studies of delta oscillations in slice type C

To examine if M1 solely can generate delta oscillations, slice type C was used. In this type of slice delta was induced with a high power in the presence of KA (150 nM), CCh (2 µM), SCH23390 (10 µM) and Haloperidol (10 µM) which were stable for 2-3hrs. Auto and cross correlation suggested that the frequency was in delta range and a good correlation exists within two electrodes placed slightly apart in the same slice (correlation coefficient=0.7).
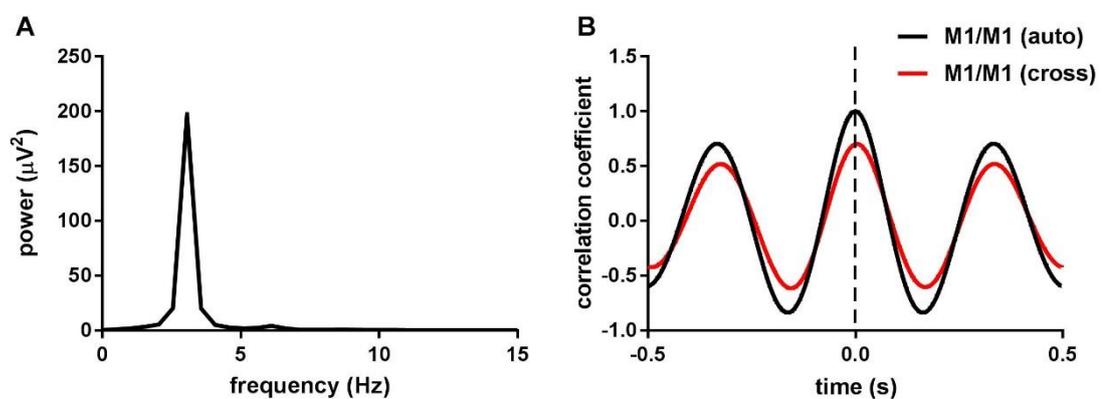
Figure 5.10 LV of M1 is the place origin of delta oscillations in slice type C

(A) A representative power spectrum of typical delta oscillation (4 Hz) in LV of M1 **(B)** auto and cross correlation analysis of delta oscillations in M1 within LV of single slice.

5.3.4 Correlation studies of delta oscillations in slice type D

Experiments were performed on slice type D, however, there was no delta transition in the S1 only slice type in the presence KA (150 nM), CCh (2 µM), SCH23390 (10 µM) and Haloperidol (10 µM). Correlation analysis revealed theta frequency range (6-11) suggesting delta oscillations were driven by M1 in intact slice as shown above (figure 5.11).
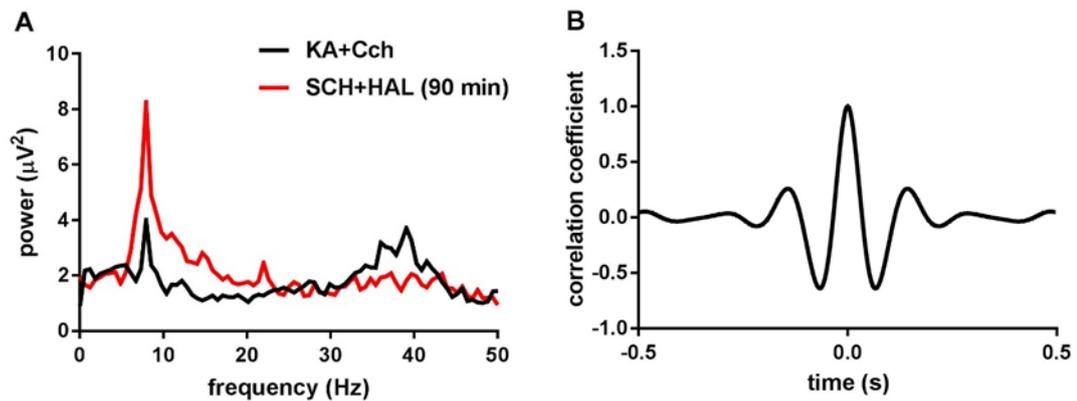
Figure 5.11 No transition to delta oscillations was found in S1 slice without M1 in slice type D.

(A) An example power spectrum showing theta and gamma oscillations in the presence of KA and CCh (black) and in the presence of SCH+HAL (red). **(B)** Correlation analysis of revealed theta oscillations within S1. Note: there is no delta oscillations.

5.3.5 Correlation studies of delta oscillations in slice type E

To investigate if adjacent regions (other than M1 and S1) contribution is necessary for pharmacological induction of delta oscillations in M1 and S1, experiments were performed in slice type E (micro slice) in which both M1 and S1 are collectively isolated from neighbouring regions (see Methods section for details). In the presence KA (150 nM), CCh (2 µM), SCH23390 (10 µM) and Haloperidol (10 µM) delta oscillations were reliably induced both in M1 and S1 with again a slight delay in S1. However, the power and stability (1 hr) was much less than that was noticed in intact slices. This is probably because of the many cuts that were made to obtain micro slice. Mean peak power was 40 ± 8 µV^2 and 25 ± 10 µV^2 in M1 and S1 respectively. A good correlation existed (correlation coefficient=0.3) between two regions with a phase lag of 2.3 ± 0.8 ms in S1 with reference to M1 (figure 5.12).
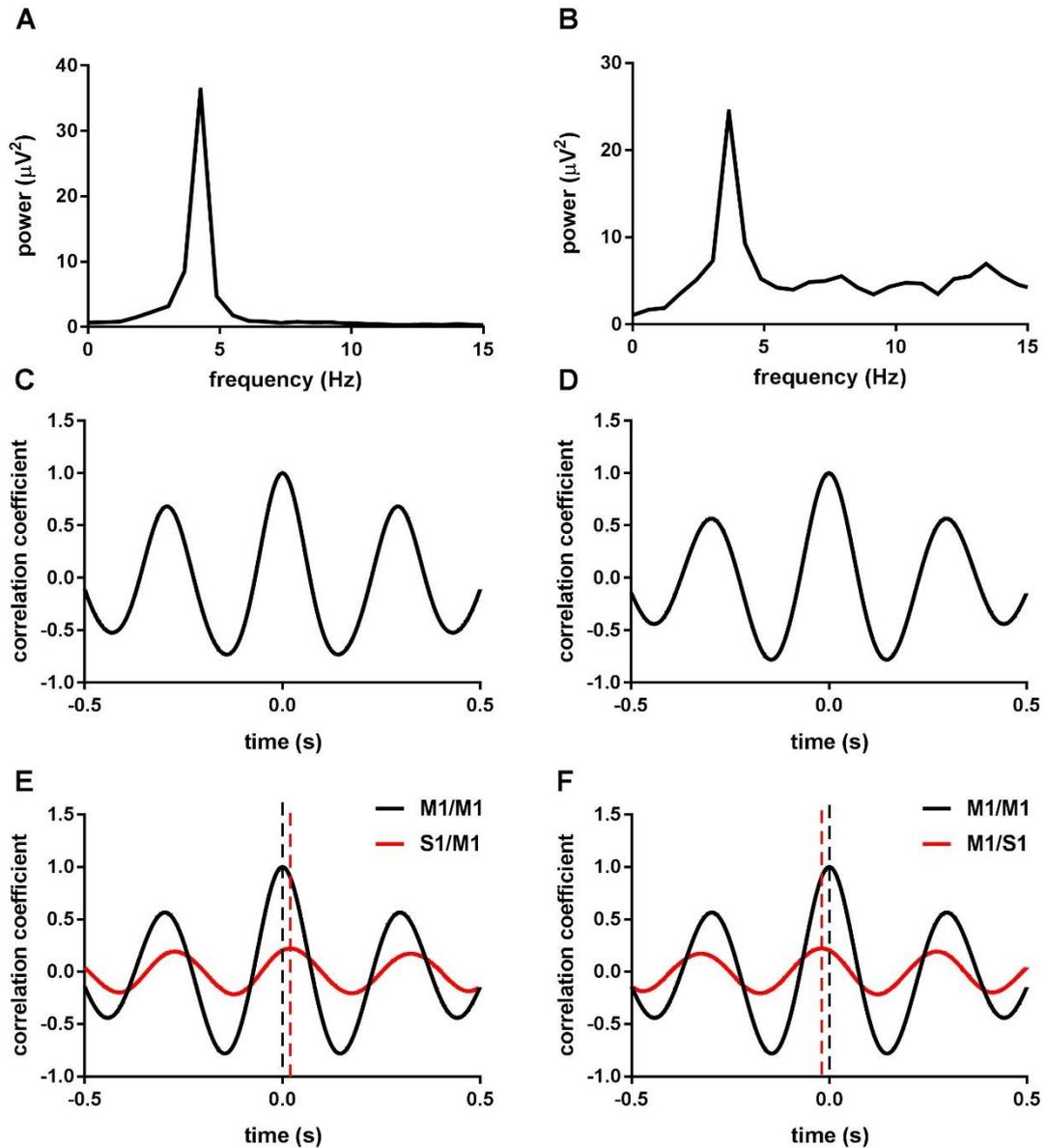
Figure 5.12 LV of M1 is the origin of delta oscillations and drives the activity in S1 in slice type E

(A) An example power spectrum of delta oscillations in LV of M1 **(B)** in S1 **(C)** auto-correlation analysis of delta oscillations in M1 and in **(D)** S1. **(E)** cross-correlation analysis between M1/M1 (black) and S1/M1 (red) **(F)** cross correlation analysis between M1/M1 (black) and M1/S1 (red). Red dashed line represents the deviation from zero (black dashed line).

169

5.4 Discussion

5.4.1 Mechanism of delta oscillations in S1

No spontaneous activity was observed when recorded in S1 similar to that of in M1 and gamma oscillations were induced upon the application of KA and CCh. Interactions between M1 and S1 at theta and gamma frequency were detailed in chapter 3. Persistent delta oscillations were induced in LV of S1 by maintaining a low cholinergic and low dopaminergic tone as this was the precondition to induce delta in M1 (section 4.1). Pharmacology performed revealed the dependence of delta oscillations in S1 are dependent on GABAR, AMPAR, mAChR and KAR. Similar pharmacological profile to that of M1 was identified in S1 probably because M1 drives S1 at this frequency. AMPAR contribute to overall excitation of the cells, CCh to activate the cells and GABAR to the set the frequency similar to that of gamma oscillations except that delta are found independent of NMDAR both in M1 and S1. Based on the suggestion that cortical delta oscillations are generated in a use-dependent manner, in that the cortical circuits that are active during awake states generate these oscillations in the succeeding sleep (Kattler *et al.,* 1994; Huber *et al.,* 2004) and in a region specific way, implying a self-organising property of local neuronal networks (Krueger and Oba´l, 1993; Vassalli and Dijk, 2009; Vyazovskiy *et al.,* 2011) reflecting previously prevalent gamma oscillations then become delta oscillations. However, delta oscillations in S1 showed a significant delay in occurrence which lead to further cut/isolated region studies (discussed below).

5.4.2 M1 and S1 interactions

Functional connectivity between M1 and S1 has been reported. Intra-cortical micro stimulation (ICMS) of S1 resulted in short latency and mono-synaptic EPSPs in cells that were present in M1 (Kosar *et al.,* 1985). Experiments described above showed that M1 and S1 interactions facilitated the expression of delta in both regions, with M1 providing the drive and activity in S1 following, as evidenced by the clear delay between delta induction in S1 when compared to M1 and the similarity of the S1 pharmacology to that in M1. Auto-correlation studies in slice type A, reflected a high correlation within the region in a time series and revealed the signal obtained to be in delta frequency range. However, cross-correlation studies revealed a phase lag in S1 when compared to M1 suggesting M1 to be a leading signal. This is in contrast to that of theta and gamma oscillations and beta oscillations in same regions. In an intact slice (slice type A), S1 seems to be the leading signal for both theta and gamma oscillations as there was a lag in M1 with reference to S1(section 3.3 for details). Although two signals were in near synchrony at beta frequency it was observed that desynchronisation first occurred in S1 and then followed by M1 upon the application of zolpidem (Prokic, 2011). It was reported that there were direct connections

between the two regions in rodents and cats (Asunama *et al.,* 1982, Donoghue and Parham, 1983; Porter and Sakamoto, 1988, Izraeli and Porter, 1995). To further explore this, a cut was made carefully between two regions and it was evident from the results obtained that M1 is be the source of origin of delta rhythm, since there is no occurrence of delta oscillations in S1 when separated from M1 by a cut. However, it was suspected that the origin of delta oscillations in M1 did involve neighbouring regions. It has been established that there are two pathways between S1 and M1 (intra-cortical) with one being direct and the other indirect via thalamus (Kaneko, 1994a, 1994b).To address this issue, a slice preparation (slice type C) with only M1, isolated from surrounding regions including S1 was recorded based on the fact that LTP in M1 of cats is induced by stimulation of M1 alone (Keller *et al.,* 1990) independent on S1. This type of slice has enabled delta induction proving M1 as the source of origin. Then recordings were made from slice type D in which only S1 was isolated, no activity was identified in contrast to that theta and gamma oscillations, as theta and gamma oscillations were induced in slice type C and D reflecting individual and independent rhythm generators at these frequencies (section 3.3 for details). Furthermore, a micro slice (slice type E) was prepared in which both M1 and S1 are collectively isolated from surrounding regions. Recordings from this type of slice has induced delta oscillations in both oscillations but the power was observed to be much lower compared to slice type A and also they were identified to be not persistent suggesting loss or damage of network connectivity due to several cuts made around the regions. It was possible to speculate that loss of M2 in this slice type could form the ground for this instability as there was evidence that optogenetic inhibition of inputs from M2 to M1/S1 had reduced the activity in behaving mice (Manita *et al.,* 2015). The role of M2 in delta oscillation generation was not explored in our study due to practical limitations.

The origin of delta oscillations from deep layers of M1 could mean that the retrograde and anterograde connections between two regions do not contribute to initiation of deep sleep states because M1 on its own had enabled the generation of delta oscillations. However, these connections may have a role in maintenance of delta oscillations since S1 followed M1 with a significant delay in intact slices (types A and E). The neuronal populations that were recruited for delta rhythm generation might be just resident in M1 and not in S1. For instance, betz cells were observed in layer V of M1 (Betz, 1894). These cells are unique in their morphology and may appear as both pyramidal and interneurons (Braak, 1976). Also, this fits with the idea of increasing power towards frontal parts of the brain (Werth *et al.,* 1997; Finelli *et al.,* 2001). Based on this it is reasonable to say that M1 is the source of origin for delta oscillations. However, S1 seems to be a potential source of theta and gamma frequency, although both M1 and S1 have individual rhythm generators. Given that delta oscillations are assumed to be sub served by previously active gamma oscillations (Kattler

et al., 1994; Huber *et al.,* 2004) in M1 however, this is not the case for S1 as it does not enable delta generation on an isolated slice preparation.

Nevertheless, further histological and immuno-labelling studies to determine the types of cells and receptors that were involved in the generation of delta oscillations and functional connectivity between two regions would be beneficial to further address this issue. Preparing slices in different plane other than sagittal would preserve thalamus and /or M2, S2 besides M1 and S1 and would provide an opportunity to investigate the influence of thalamus (if any) in delta rhythm generation since cells present across all layers in M1 have been implicated in long-range projections (Peter and Jones, 1984).

5.5 Final conclusions

Delta oscillations in S1 are dependent on both inhibitory and excitatory networks similar to that of in M1 and in line with pharmacology of gamma oscillations suggesting previously prevalent gamma oscillations then become delta oscillation due to changes in concentrations of neuromodulators. A significant time delay in occurrence and phase lag that was observed in correlation studies performed in various slice preparations revealed M1 as the rhythm generator. Inability of S1 to generate delta oscillations on its own suggests that S1 follows M1 at delta frequency in intact slice.

6. Dopamine augments an inward current in fast spiking interneurons in layer V of primary motor cortex

6.1 Introduction

6.1.1 Dopamine (DA)

In the current study, network activity in primary motor cortex (M1) has been shown to be powerfully modulated by DAR (see chapter 3) (Alexander *et al.,* 1986; Ozkan *et al.,* 2017; Johnson *et al.,* 2017). These actions of dopamine almost certainly depend on DAR present within M1 itself. M1 and PFC (pre-frontal cortex) show similar laminar organisation of receptors (although M1 has fewer DAR than PFC (Lidow *et al.,* 1989)) and D1-like DR are more abundant than D2-like DR in rat cortex (Boyson *et al.,* 1986). The laminar distribution of both D1-like and D2-like receptors is found to correspond to the dopaminergic terminals in M1 which are predominantly in deep layers (LV and LVI) (Martes *et al.,* 1985; Dawson *et al.,* 1986; Descarries et al 1987; Raghanti *et al.,* 2008; Vitrac *et al.,* 2014). Many studies have studied the differential effects of DA on firing rate in various regions such as ventrobasal thalamus (Munsch *et al.,* 2005; Yague *et al.,* 2013) and was shown that DA did not affect action potential firing evoked by somatic current injection (Zhou and Hablitz, 1999; Gonzalez-Islas and Hablitz, 2001). Some studies previously have indicated that in STN, firing rate of neurons was augmented upon DA administration (Mintz *et al.,* 1986; Kreiss *et al.,* 1996; Tofighy *et al.,* 2003; Cragg *et al.,* 2004; Loucif *et al.,* 2008). While some studies suggest that DA mediated depolarisation in STN was via D2-like DR (Zhu *et al.,* 2002; Tofighy *et al.,* 2003), others suggest via D1-like DAR (Baufreton *et al.,* 2003). DA regulation of various voltage-gated channels may reflect these diverse effects but firing rate has not been measured in our study.

6.1.2 Interneurons (IN)

Different types of interneurons with distinctive features have been identified in neocortex (Deuchars and Thomson, 1996; Thomson *et al.,* 1996; Tamas *et al.,* 1997; Kawaguchi and Kubota, 1997; Cauli *et al.,* 1997) and hippocampus (Halasy *et al.,* 1996; Miles *et al.,* 1996; Klausberger *et al.,* 2003, 2005). Although IN make up only a subset (10-20%) of the whole cell population (Benardo and Wong, 1995), they play a critical role in oscillatory neuronal activity in cortex (McBain and Fisahn. 2001). Post-synaptic pyramidal neurons that are present in peri-somatic region are the target sites for most FS cells in sensory and primary motor cortices (Kawaguchi and Kubota, 1997; Cauli *et al.,* 1997; Yamawaki *et al.,* 2008; Prokic *et al.,* 2015). The peri-somatic region is defined as "that part of the plasma membrane including the proximal dendrites, the cell body and the axon initial segment" (Szabo *et al.,* 2010). These FS cells are thought to regulate overall pyramidal activity (Freund and Katona, 2007) due to their ability to induce IPSCs with faster kinetics in conditions where excitatory synaptic inputs are abolished (Miles, 1990; Freund and Katona, 2007). FS cells that are characterised by rapid IPSC kinetics are suggested to be crucial for maintaining network

activity by regulating coherence and frequency in M1 (Bartos *et al.,* 2001, 2002; Yamawaki *et al.,* 2008; Prokic *et al.,* 2015).

6.1.3 DA and interneurons

DA effects on FS interneurons have been shown to be mediated by PKA-dependent suppression of leak, inward rectifying, and depolarisation-activated K^+ channels (Gorelova *et al.,* 2002) and amplification of depolarising currents mediated by HCN channels (Gorelova *et al.,* 2002; Trantham-Davidson *et al.,* 2008; Wu and Hablitz, 2005). Additionally, many reports have indicated that DA modulates $GABA_AR$. Pyramidal neurons localised in PFC have shown reduction in IPSCs via downregulation of D4 surface receptors (Seamans *et al.,* 2001; Wang *et al.,* 2002; Graziane *et al.,* 2009). Additionally, recent studies have indicated that DA modulates tonic currents in various regions of brain (Aman *et al.,* 2007; Yague *et al.,* 2013; Liang *et al.,* 2014) and may directly inhibit $GABA_AR$ (Hoerbelt *et al.,* 2015). These novel activities of DA may impel new definitions of dopaminergic signalling in the brain. Distinct types of cells express DAR with different combinations across the cortical layers (Wang *et al.,* 2006). DA was reported to modulate the intrinsic excitability of both pyramidal cells and interneurons (reviews Seamans and Yang, 2004; Tritsch and Sabatini, 2012). However, the modulatory effects on isolated cells and individual currents mediated by DA are often unclear due to complexity of network in which these cells are embedded, as well as the various types of receptors and signalling mechanisms.

Here, we have determined to investigate the effect of DA on pyramidal cells and FS interneurons in LV of M1 slices using whole-cell voltage clamp recordings. FS cells were identified based on the morphological features as described by Prokic *et al.,* (2015), based upon deep layer Betz cell-FS cell pairing.

175

6.2 Results

All the experiments in this chapter are whole cell, voltage clamp recordings with a holding current of -70 mV performed in layer V of M1 unless otherwise indicated. FS interneurons and pyramidal neurons were patched and were identified by their shape and size. Slice type F (refer methods section) was used in these experiments. With the internal solution used in the experiments (see methods section for full composition), the reversal potential of Cl (E_{Cl}) was 0 mV; therefore, $GABA_A$ receptor-mediated currents (IPSCs) appeared inward as shown in results below. Tonic/inward current is measured by the change in the baseline after the drug application in relation to control. Whereas, phasic current was measured by changes in the amplitude and time difference of IPSCs (IEI) before and after drug application.

6.2.1 GABAergic modulation of tonic and phasic currents in FS cells

To investigate the role of GABAR in tonic and phasic inhibition in FS cells of LV of M1, bicuculline (Bic, 20 μM) a competitive $GABA_A$R antagonist was bath applied. After drug application, both tonic and phasic components of inhibitory activity in FS cells were abolished suggesting constitutively active GABAergic inhibition in interneurons of LV of M1. Bic significantly decreased the holding current by 36.3 ± 6 pA (n=5, p<0.01). Mean amplitude change was found to be 61.5 ± 2 pA and 1.71 ± 0.1 pA in control and after application of Bic respectively, (n=5, p<0.01) whilst the mean inter event interval (IEI) increased from 187.3 ± 19 ms to 2511.2 ± 403 ms (n=5, p<0.05) (figures 6.1, 6.2) suggesting the reduction in both I_{tonic} and I_{phasic}.
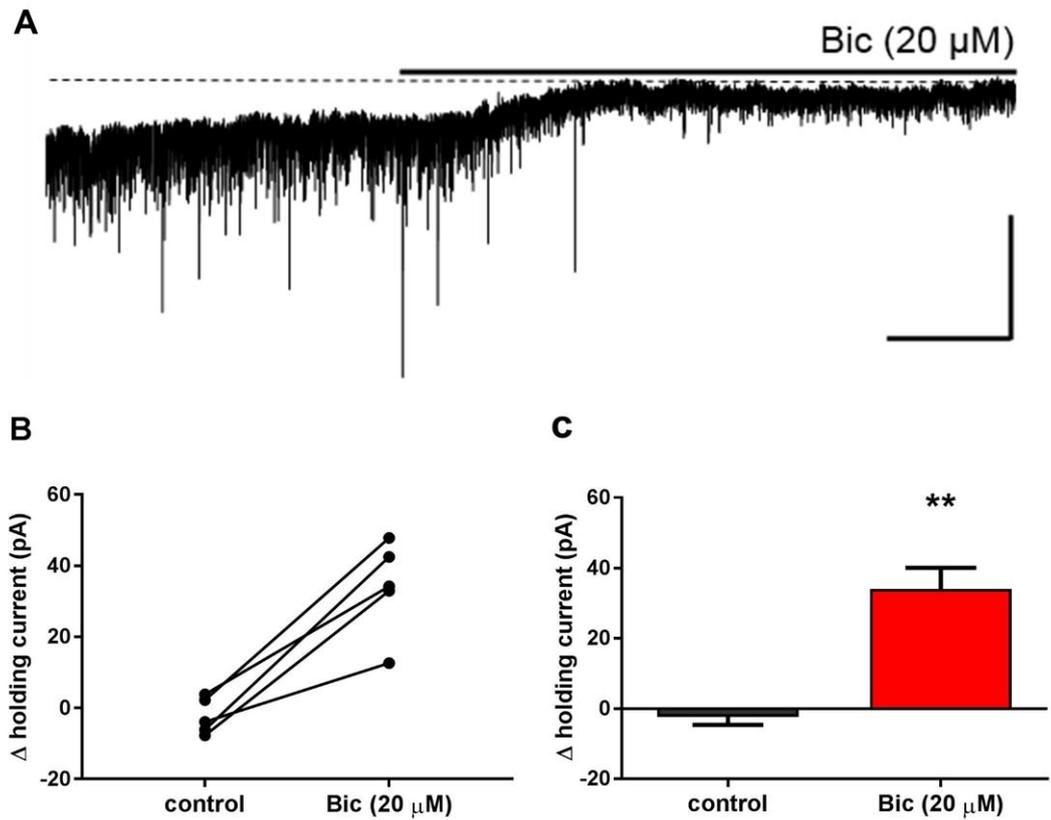
Figure 6.1 Bicuculline (Bic 20 μM) decreases tonic inhibitory current in FS interneurons in LV of M1

(A) Representative voltage clamp recording demonstrating the effect of Bic (scale: 50 pA, 1 min). Black horizontal line indicates the presence of drug in bath and dotted line indicates the relative current shift from baseline (control). **(B)** I_{tonic} before and after Bic application of individual FS cells. **(C)** Pooled data of I_{tonic} before (grey) and after (red) drug application (n=5, p<0.01).
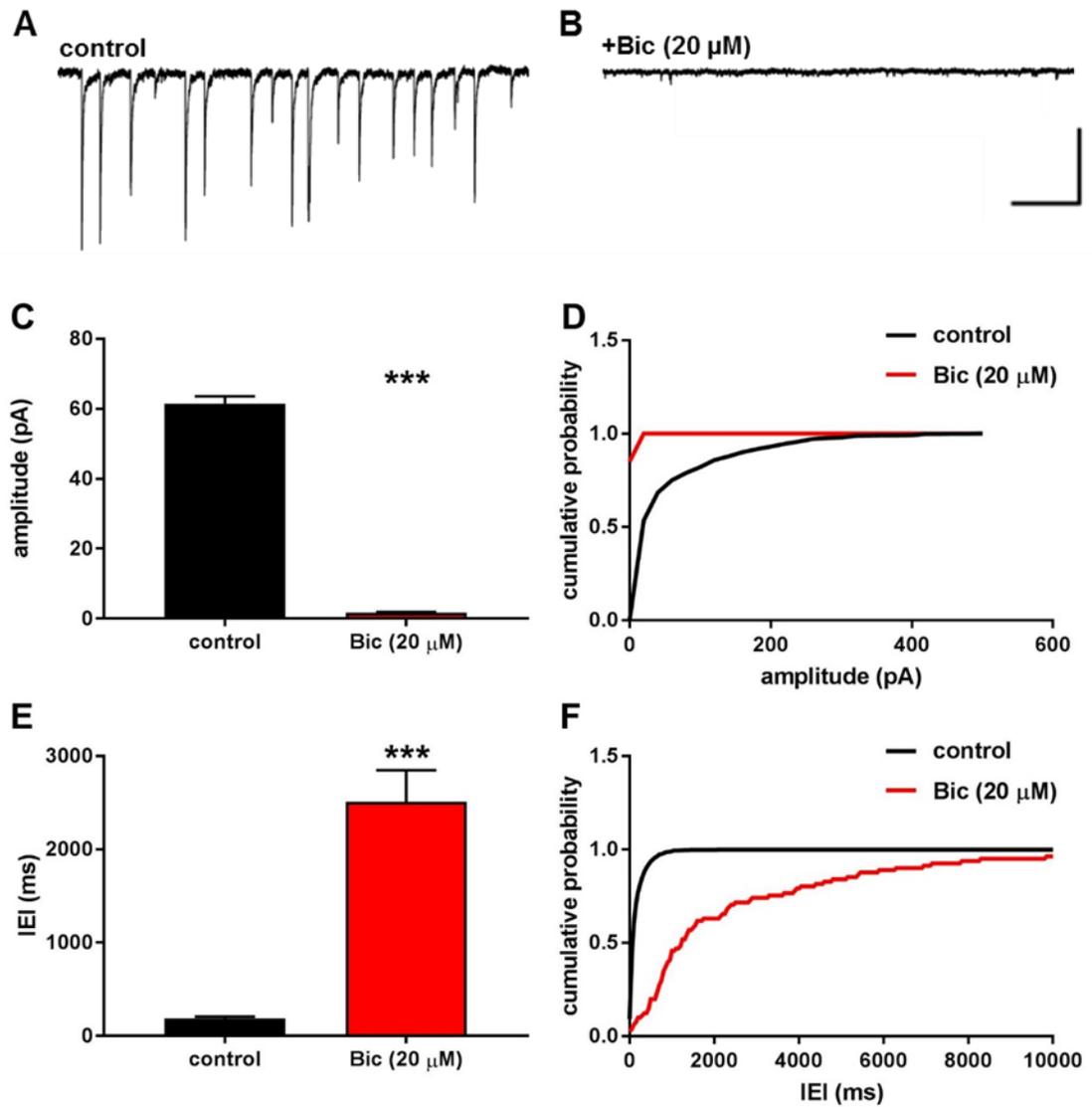
Figure 6.2 Bicuculline (Bic 20 µM) decreases phasic inhibitory current in FS interneurons in LV of M1

(A) (B) Representative voltage clamp recording from a FS cell demonstrating IPSCs before (left) and after (right) drug application (scale: 100 pA, 200 ms) **(C)** bar graph **(D)** cumulative probability plot showing the effect of drug on amplitude (n=5, P<0.001) **(E)** bar graph **(F)** cumulative probability plot showing the effect of drug on inter event interval (IEI) (n=5, p>0.001).

In order to confirm the actions of Bic were mediated solely by the $GABA_AR$, we next examined the effects of picrotoxin (PTX), a non-competitive channel blocker $GABA_AR$ which acts by preventing the entry of Cl⁻ ions into the neuron. PTX abolished both I_{tonic} and I_{phasic} confirming GABA receptors significant role in this constitutively active tonic and phasic currents in FS cells in LV of M1. Mean decrease in holding current by PTX was 20 ± 6 pA (n=5, p<0.01). Decrease in the mean amplitude was found to be 46.5 ± 5 pA and 1.81 ± 0.2 pA (n=5, p<0.01) and mean increase in IEI 137 ± 4 to 1790 ±214 (n=5, p>0.05, p<0.001 in control and in the presence of PTX respectively (figures 6.3, 6.4).
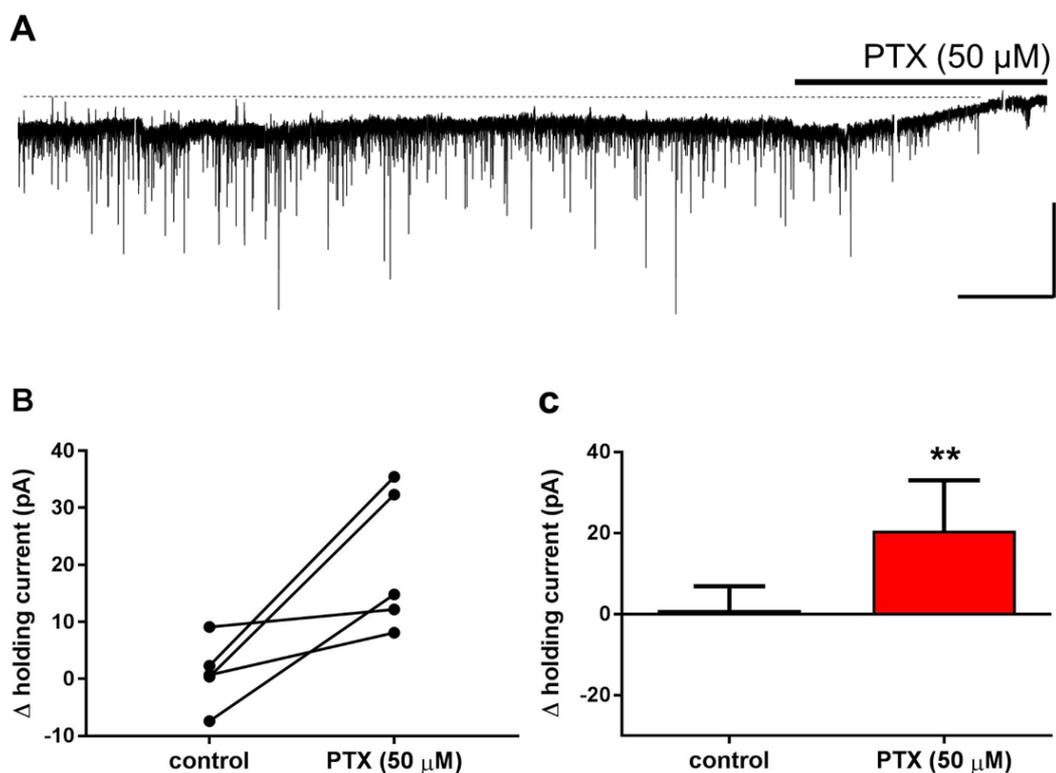
Figure 6.3 Picrotoxin (PTX 50 µM) decreases tonic inhibitory current in FS interneurons in LV of M1

(A) Representative voltage clamp recording demonstrating the effect of PTX (scale: 100 pA, 1 min). Black horizontal line indicates the presence of drug in bath and dotted line indicates the relative current shift from baseline (control). **(B)** I_{tonic} before and after PTX application of individual FS cells. **(C)** Pooled data of I_{tonic} before (grey) and after (red) drug application (n=5, p<0.01).
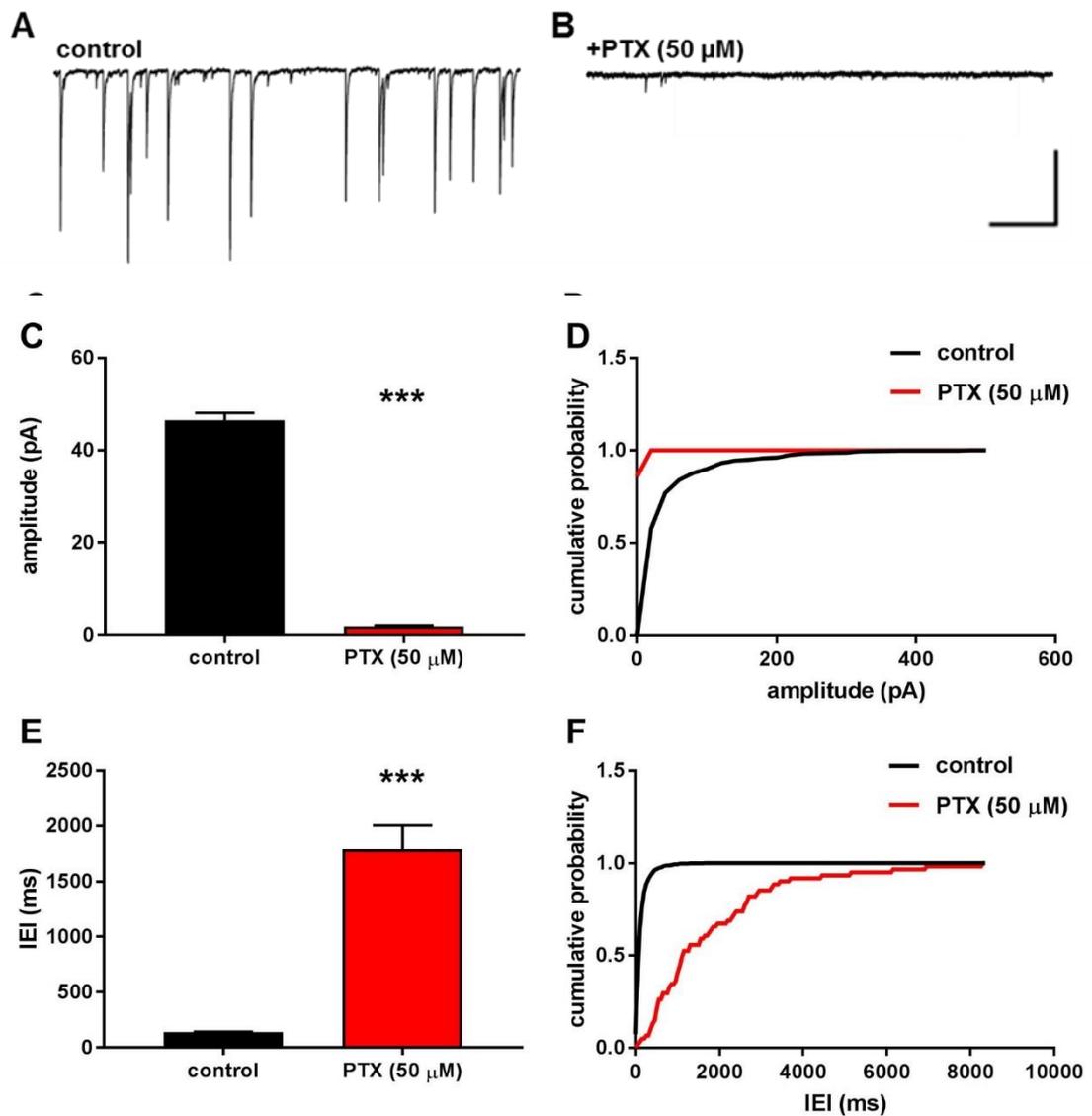
Figure 6.4 Picrotoxin (PTX 50 μM) decreases phasic inhibitory current in FS interneurons in LV of M1

(A) (B) Representative voltage clamp recording from a FS cell demonstrating IPSCs before (left) and after (right) drug application (scale: 100 pA, 200 ms) (C) bar graph (D) cumulative probability plot showing the effect of drug on amplitude (n=5, P<0.001) (E) bar graph (F) cumulative probability plot showing the effect of drug on inter event interval (IEI) (n=5, p>0.001).

6.2.2 Dopaminergic modulation of currents in FS cells

To determine the role of dopamine receptors on holding current (-70 mV), dopamine (DA) 30 µM was bath applied. DA induced a slow inward current (I_{DA}) which was reversed less than half upon wash. Mean increase in the holding current was -32 ± 11 pA from the baseline (n=5, $p<0.05$, $p<0.01$) in the presence of DA and was reduced to -11.5 ± 5 pA in wash (n=5, $p<0.05$). DA has shown no effect on both amplitude (41.7 ± 2 vs 39.4 ± 2) and IEI (174.4 ±4 vs 200 ± 5) of IPSCS (figure 6.5, 6.6).
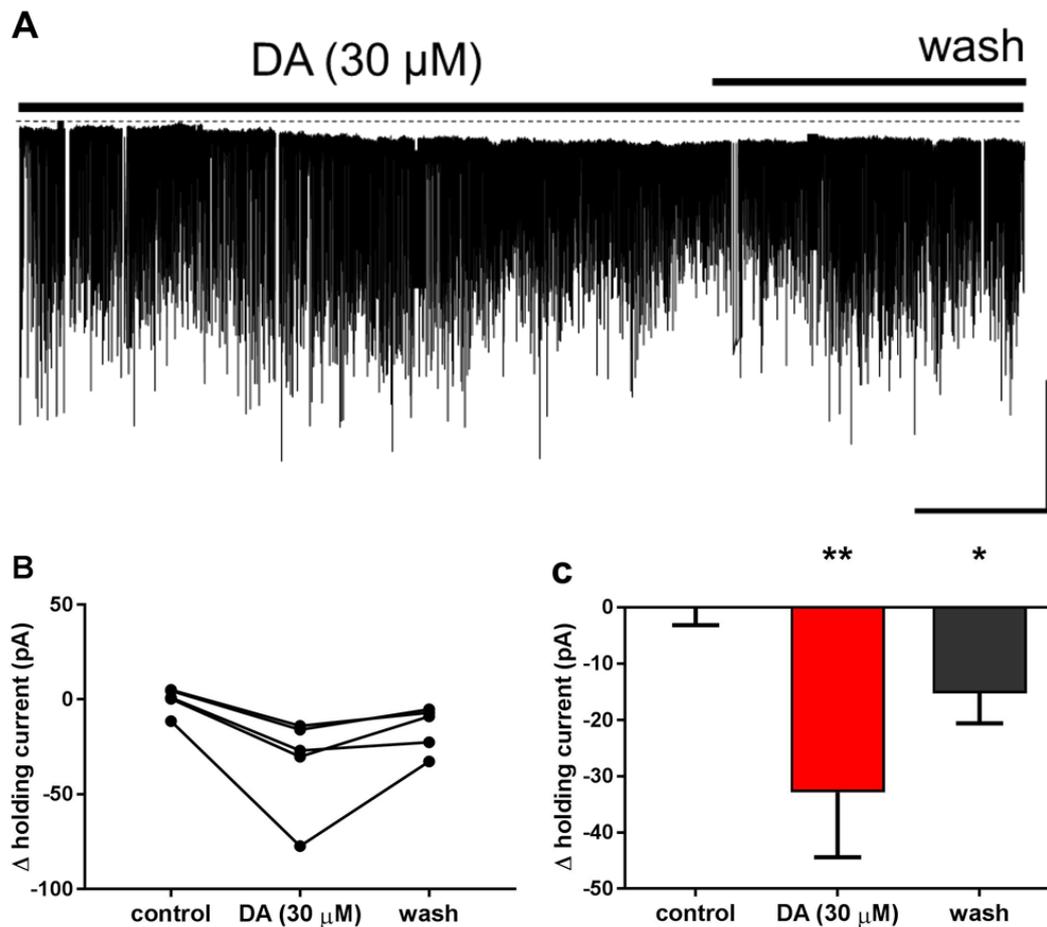
Figure 6.5 Dopamine (DA 30 µM) induces an inward current (I_{DA}) in FS interneurons

(A) Representative voltage clamp recording demonstrating the effect of DA (scale: 100 pA, 10 min) black horizontal lines indicates the presence of drug in bath and dotted line indicates the relative current shift from baseline (control). **(B)** I_{DA} before and after wash of individual FS cells. **(C)** Pooled data of I_{DA} before (grey) and after (red) wash (n=5, $p<0.01$, $p<0.05$).

Figure 6.6 Dopamine (DA 30 µM) has no effect on phasic inhibition in FS interneurons in LV of M1

(A) (B) Representative voltage clamp recording from a FS interneuron demonstrating IPSCs before (left) and after (right) drug application (scale: 100 pA, 200 ms) **(C)** bar graph **(D)** cumulative probability plot showing the effect of drug on amplitude (n=5, P>0.05). **(E)** Bar graph **(F)** cumulative probability plot showing the effect of drug on inter event interval (IEI) (n=5, p>0.05).

To investigate whether I_{DA} was mediated by GABA$_A$R, Bic (20 µM) and PTX (50 µM) were bath applied. The holding current was reduced upon application of either Bic or PTX. Mean I_{DA} of -34 ± 7 pA was reduced to -21 ± 3 pA and -18 ± 2 pA (when Bic (n=5, p<0.01) and PTX (n=5, p<0.05) were bath applied respectively) from baseline (control) (figures 6.7, 6.8).
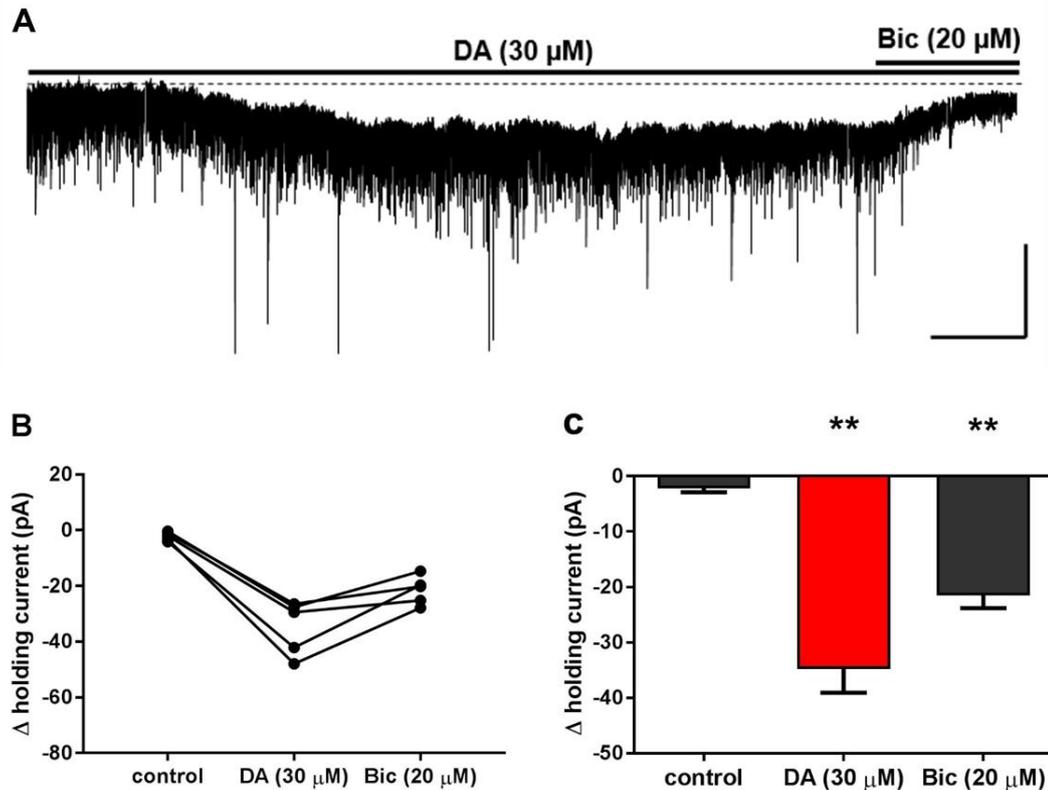
Figure 6.7 Bic decreased the holding current of I_{DA} in FS cells

(A) Representative voltage clamp recording demonstrating the effect of Bic (scale: 100 pA, 10 min) on I_{DA}. Black horizontal lines indicate the presence of drug in bath and dotted line indicates the relative current shift from baseline (control). **(B)** I_{DA} before and after Bic of individual FS cells. **(C)** Pooled data of I_{DA} before (grey) and after (red) application of Bic (n=5, p<0.01, p<0.01).
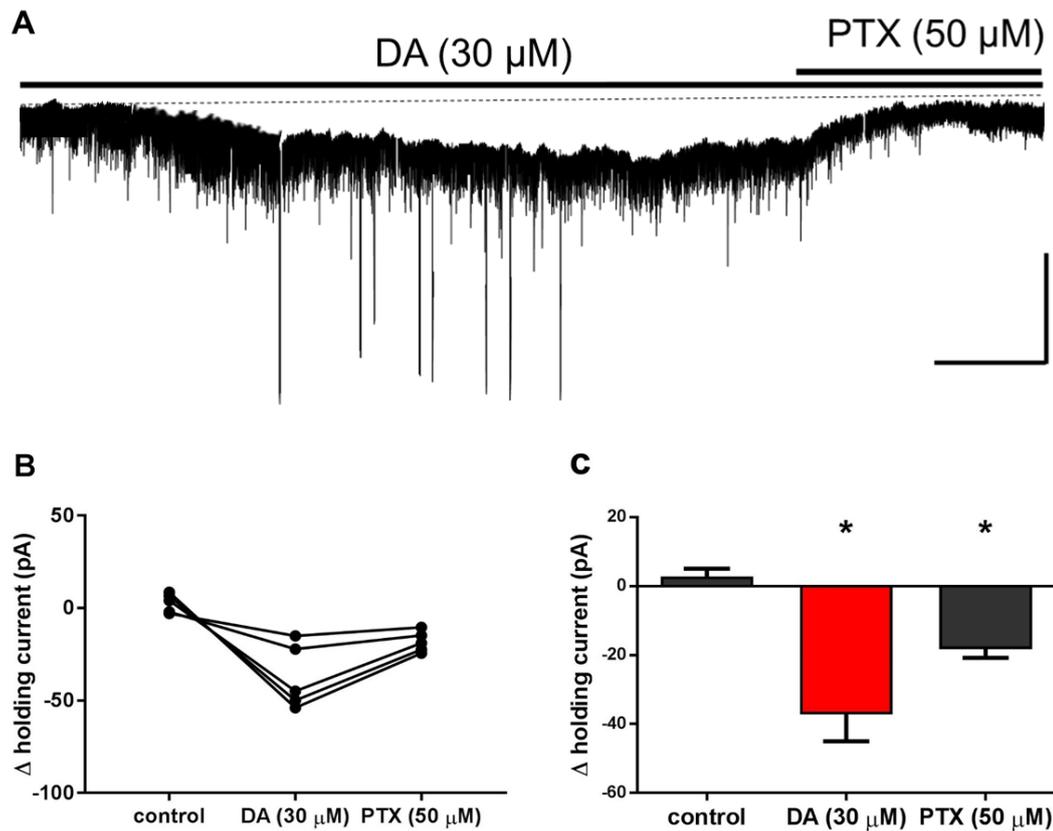
Figure 6.8 PTX reduced the holding current of I_{DA} in FS cells

(A) Representative voltage clamp recording demonstrating the effect of PTX (scale: 100 pA, 10 min) on I_{DA}. Black horizontal lines indicate the presence of drug in bath and dotted line indicates the relative current shift from baseline (control). **(B)** I_{DA} before and after PTX of individual FS cells. **(C)** Pooled data of I_{DA} before (grey) and after (red) application of PTX (n=5, p<0.05, p<0.05).

The experiments with Bic and PTX suggested a significant component ($\cong$ 20 pA) of I_{DA} was not mediated by $GABA_AR$. To confirm this, Bic, was applied prior to DA to examine if DA still induced inward current or increased the holding current in the presence of the $GABA_AR$ blockade. It was observed that DA still induced an inward current. Under these conditions, Bic reduced the holding current by 26.2 ± 1 pA. From this new baseline, DA induce a current (I_{DA}) of 13 ± 1 pA (n=5, p<0.01, p<0.05) confirming there is a non-GABAergic component in I_{DA} (figures 6.9).
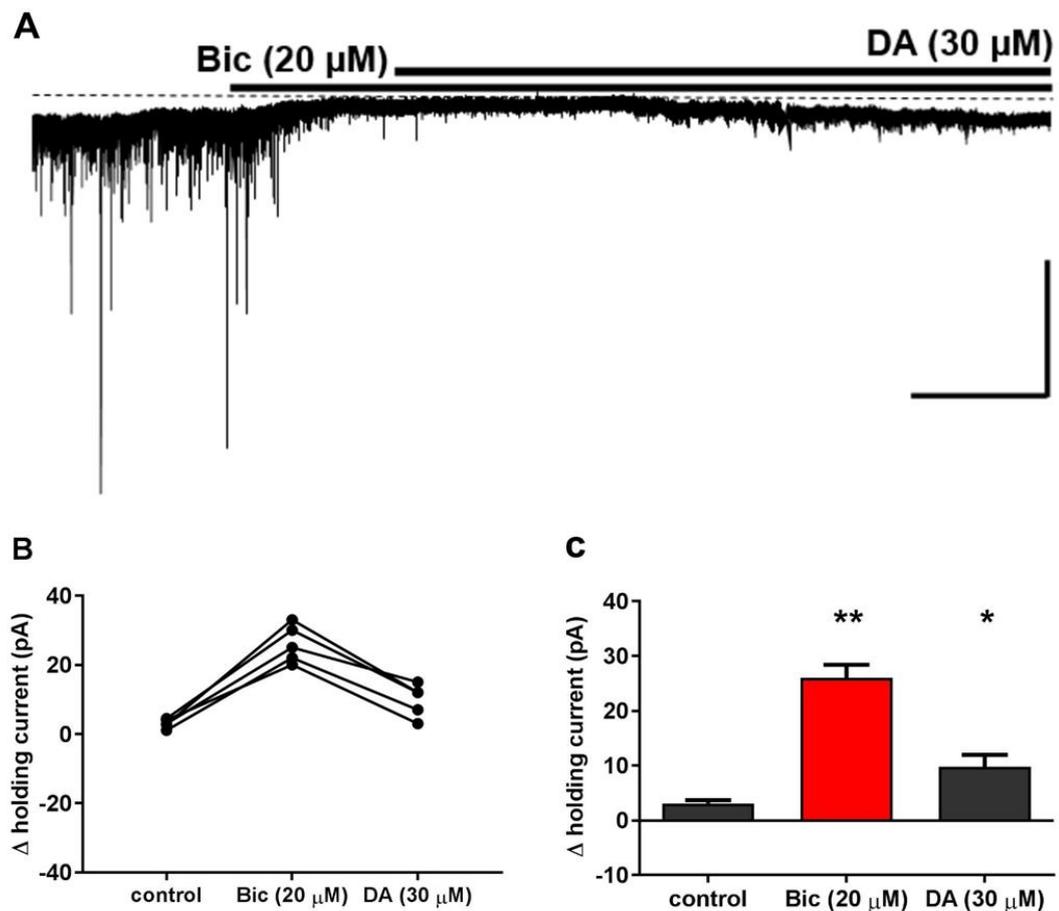
Figure 6.9 I_{DA} was induced in FS interneurons in the presence of Bic

(A) Representative voltage clamp recording demonstrating the effect of I_{DA} in the presence of Bic (scale: 100 pA, 10 min) on I_{DA}. Black horizontal lines indicate the presence of drug in bath and dotted line indicates the relative current shift from baseline (control). **(B)** I_{DA} before and after DA in the presence of Bic in individual FS cells. **(C)** Pooled data of I_{DA} before (grey) and after (red) application DA in the presence of Bic (n=5, p<0.05, p<0.01).

Further investigations were made to uncover the role of D1 receptors I_{DA}. D1 agonist, SKF38393 (10 µM) and antagonist, SCH23390, (2 µM) were bath applied. Both SKF38393 and SCH23390 have no effect on I_{phasic}, as the amplitude (34 ± 1 vs 36 ± 1; 33.2 ± 0.9 vs 30.3 ± 1.3) and IEI (227.6 ± 14 vs 231 ± 20; 237± 6.8 vs 250 ± 24) respectively, did not show any significant difference (figure 6.10, 6.11, 6.12). Please note that the raw data trace below implies a small change in holding current as well as IPSC amplitude but this was not found significant when data were pooled (n=5, p>0.05).
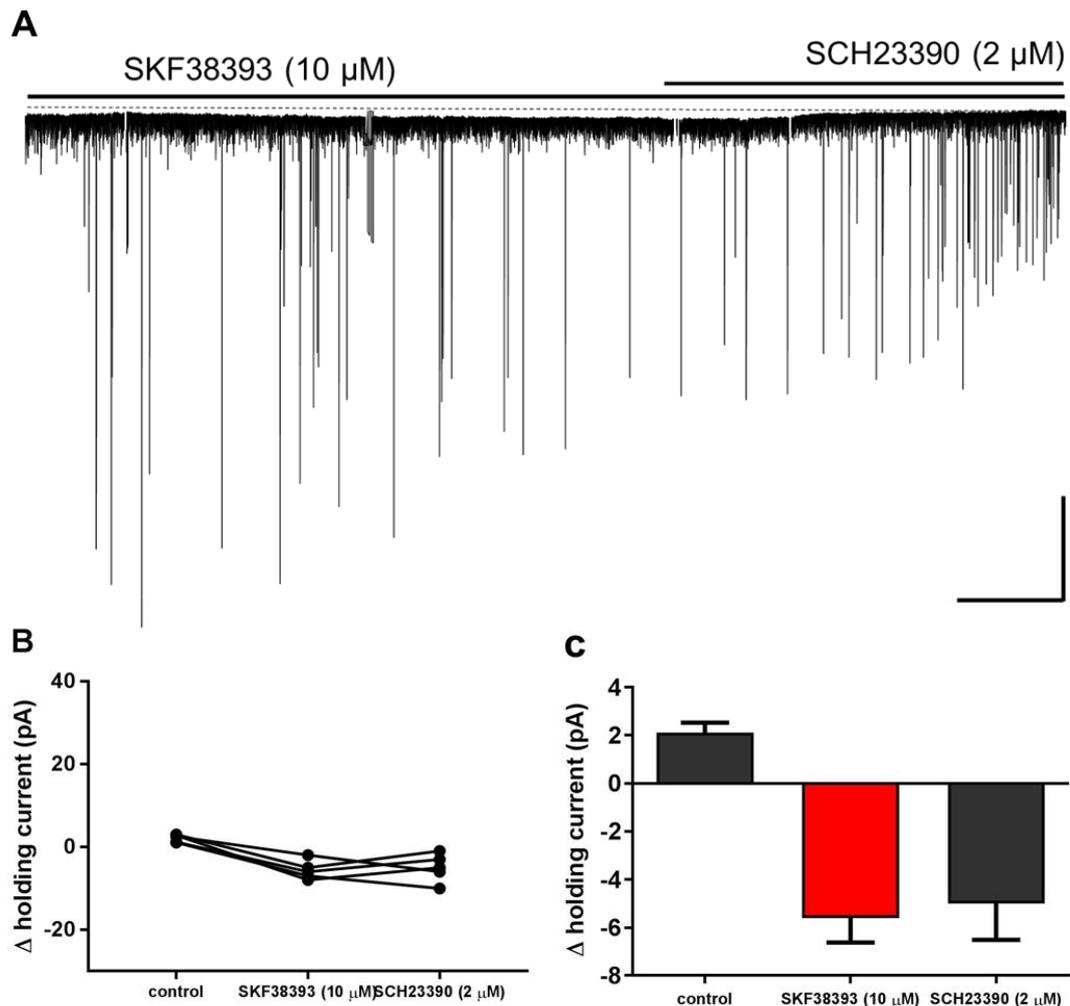
Figure 6.10 D1 agonist and antagonist does not affect holding current in FS interneurons

(A) Representative voltage clamp recording demonstrating the effect of D1R modulators (scale: 100 pA, 10 min) black horizontal lines indicates the presence of drug in bath and dotted line indicates the relative current shift from baseline (control). **(B)** Effect of D1R modulators on holding current of individual FS cells. **(C)** Pooled data of inward current in the presence of SKF38393 (grey) and SCH23390 (red) (n=5, p<0.01, p<0.05).
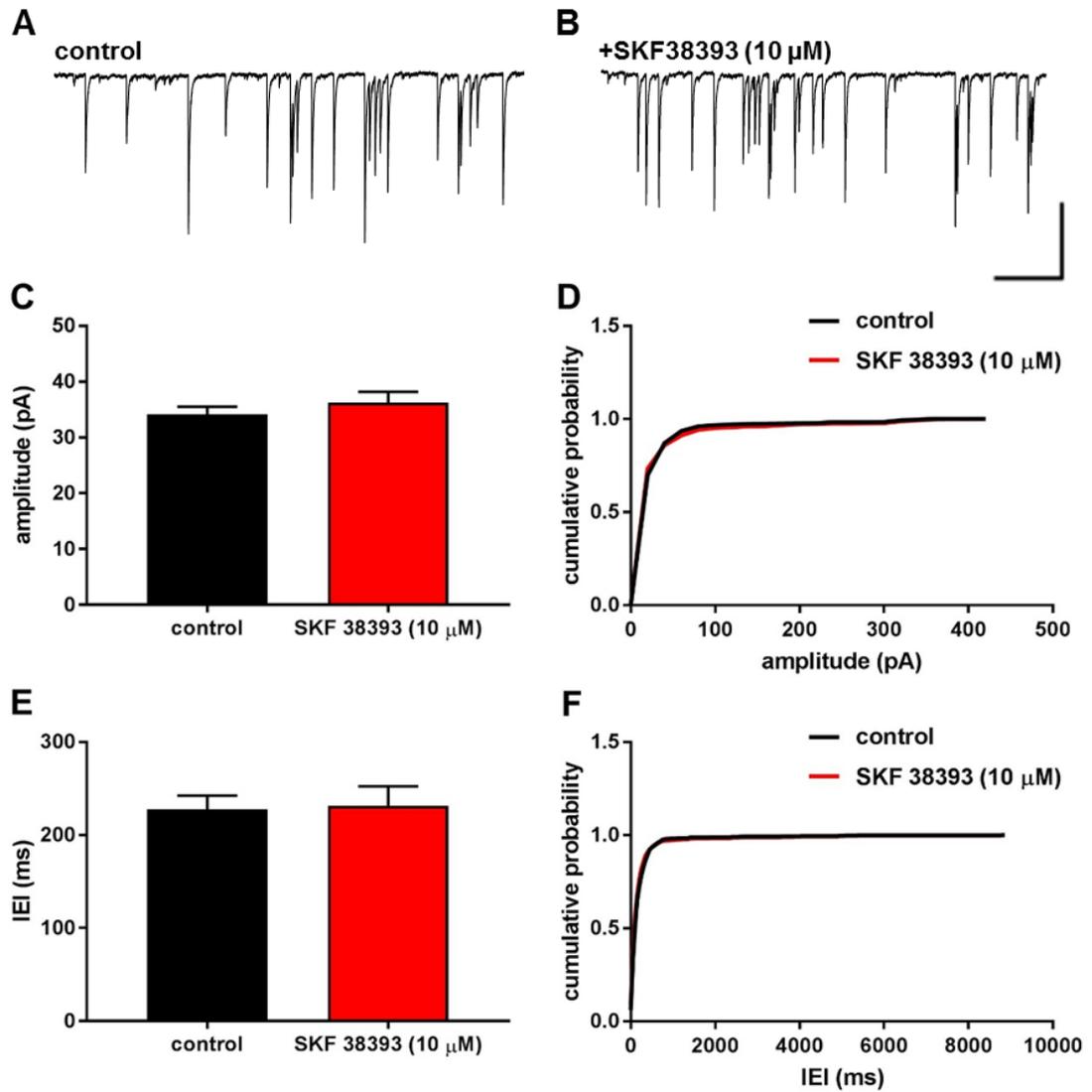
Figure 6.11 D1R agonist, SKF38390 has no effect on phasic inhibition in FS interneurons in LV of M1

(A) (B) Representative voltage clamp recording from a FS interneuron demonstrating IPSCs before (left) and after (right) drug application (scale: 100 pA, 200 ms) **(C)** bar graph **(D)** cumulative probability plot showing the effect of drug on amplitude (n=5, P>0.05). E) Bar graph **(F)** cumulative probability plot showing the effect of drug on inter event interval (IEI) (n=5, p>0.05).
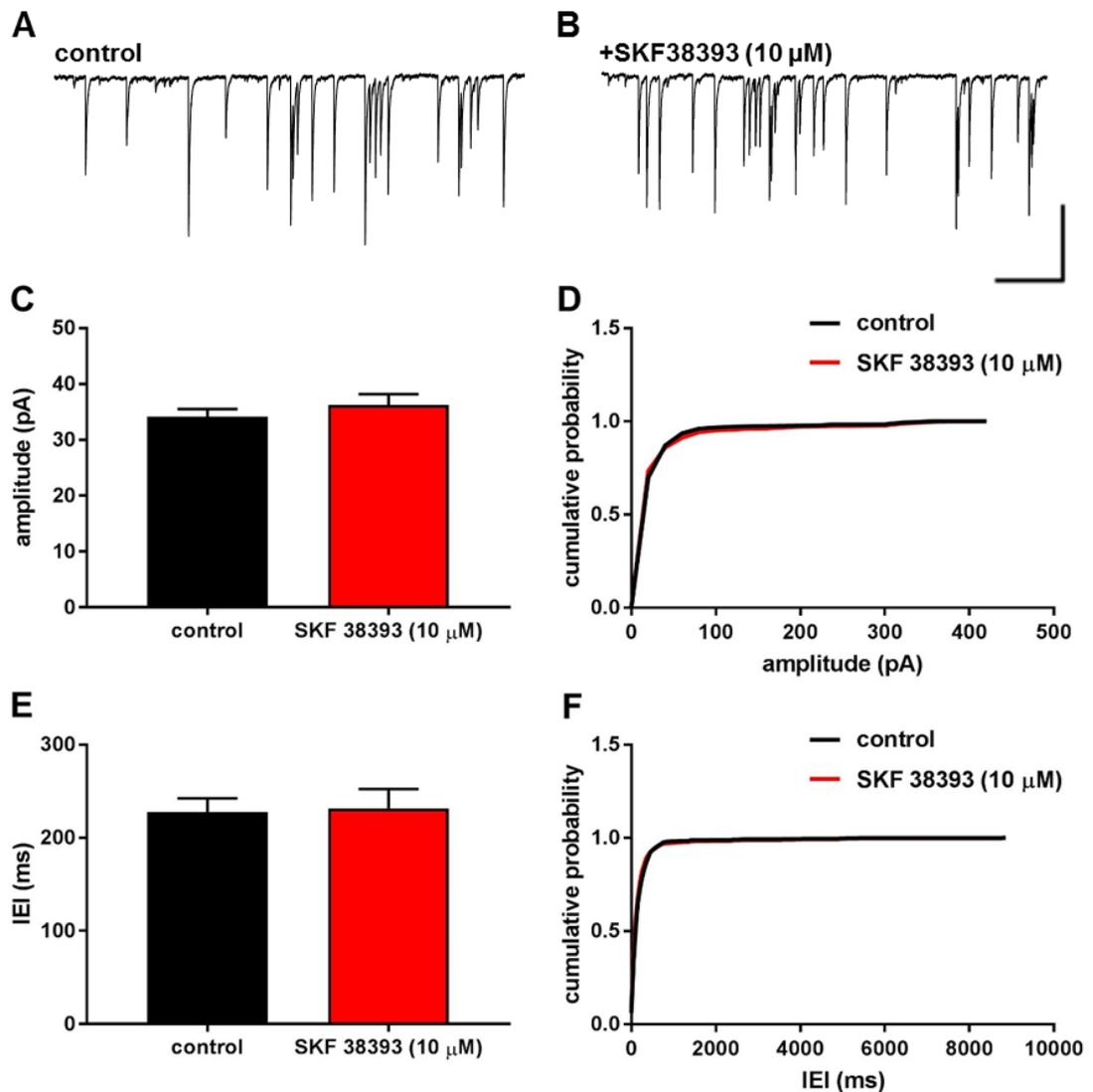
Figure 6.12 D1R antagonist, SCH23390 has no effect on phasic inhibition in FS interneurons in LV of M1

(A) (B) Representative voltage clamp recording from a FS interneuron demonstrating IPSCs before (left) and after (right) drug application (scale: 100 pA, 200 ms) **(C)** bar graph **(D)** cumulative probability plot showing the effect of drug on amplitude (n=5, P>0.05). **(E)** Bar graph **(F)** cumulative probability plot showing the effect of drug on inter event interval (IEI) (n=5, p>0.05).

Since the role of D1 agonist and antagonist was found to be insignificant, the role of D2 receptors were investigated. D2 agonist, quinpirole (10 μM) when bath applied induced an inward current by increasing holding current by -38 ± 6 pA (n=5, p<0.0.1) whilst D2 antagonist significantly decreased the holding current by -13 ± 8 of control (n=5, p<0.01). Both quinpirole and sulpiride have shown no contributions to I_{phasic} as the amplitude (38 ± 0.9 vs 30 ± 1.3; 38 ± 1.8 vs 34.5 ± 5) and IEI (142 ± 4.7 vs 161 ± 5.7; 150 ± 5.4 vs 160 ± 5.9) respectively, did not show any significant differences (figures 6.13, 6.14, and 6.15).
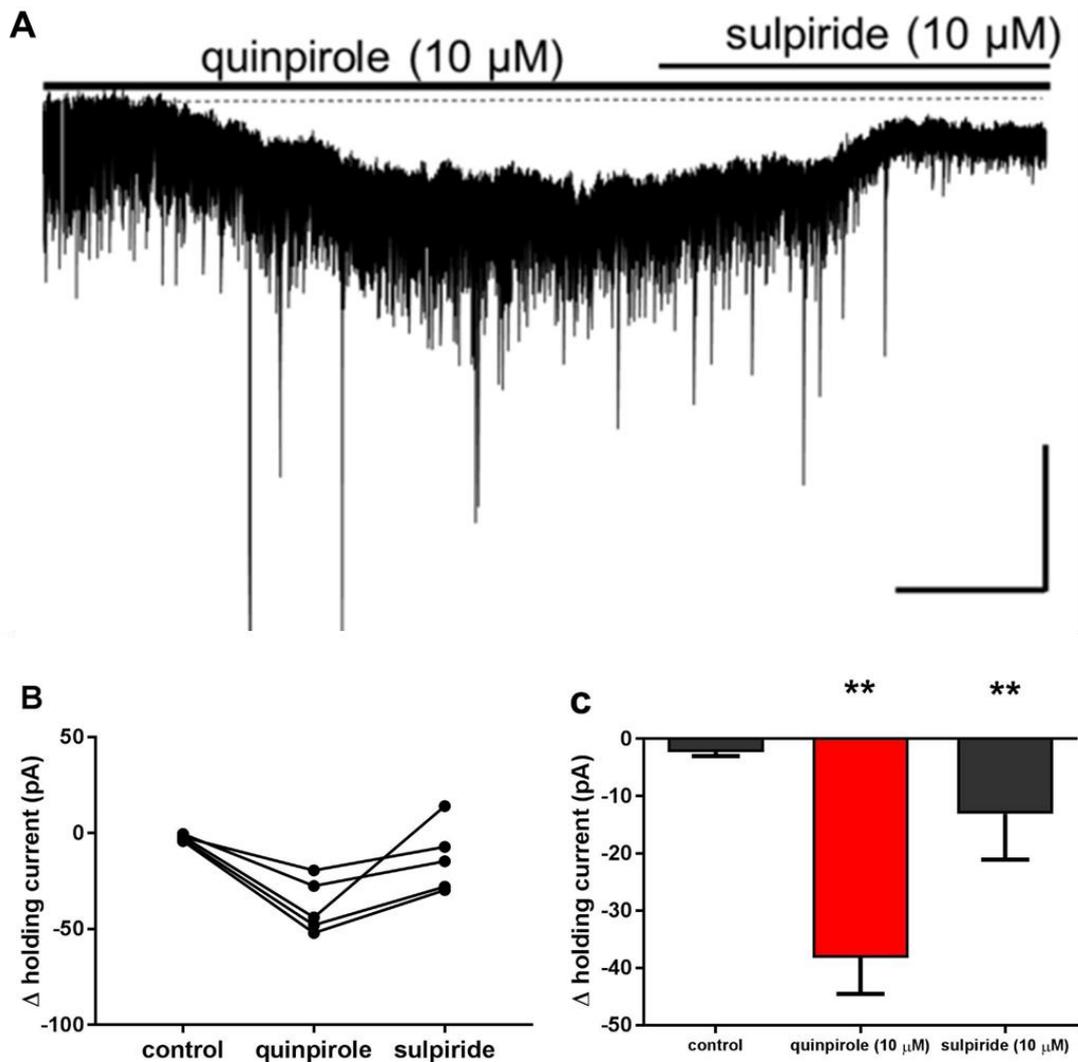
Figure 6.13 Quinpirole increased the holding current whilst sulpiride decreased it in FS interneurons

(A) Representative voltage clamp recording demonstrating the effect of D2R modulators (scale: 100 pA, 10 min) black horizontal lines indicates the presence of drug in bath and dotted line indicates the relative current shift from baseline (control). **(B)** Effect of D2R modulators on holding current of individual FS cells. **(C)** Pooled data of inward current in the presence of quinpirole (grey) and sulpiride (red) (n=5, p<0.01, p<0.05).
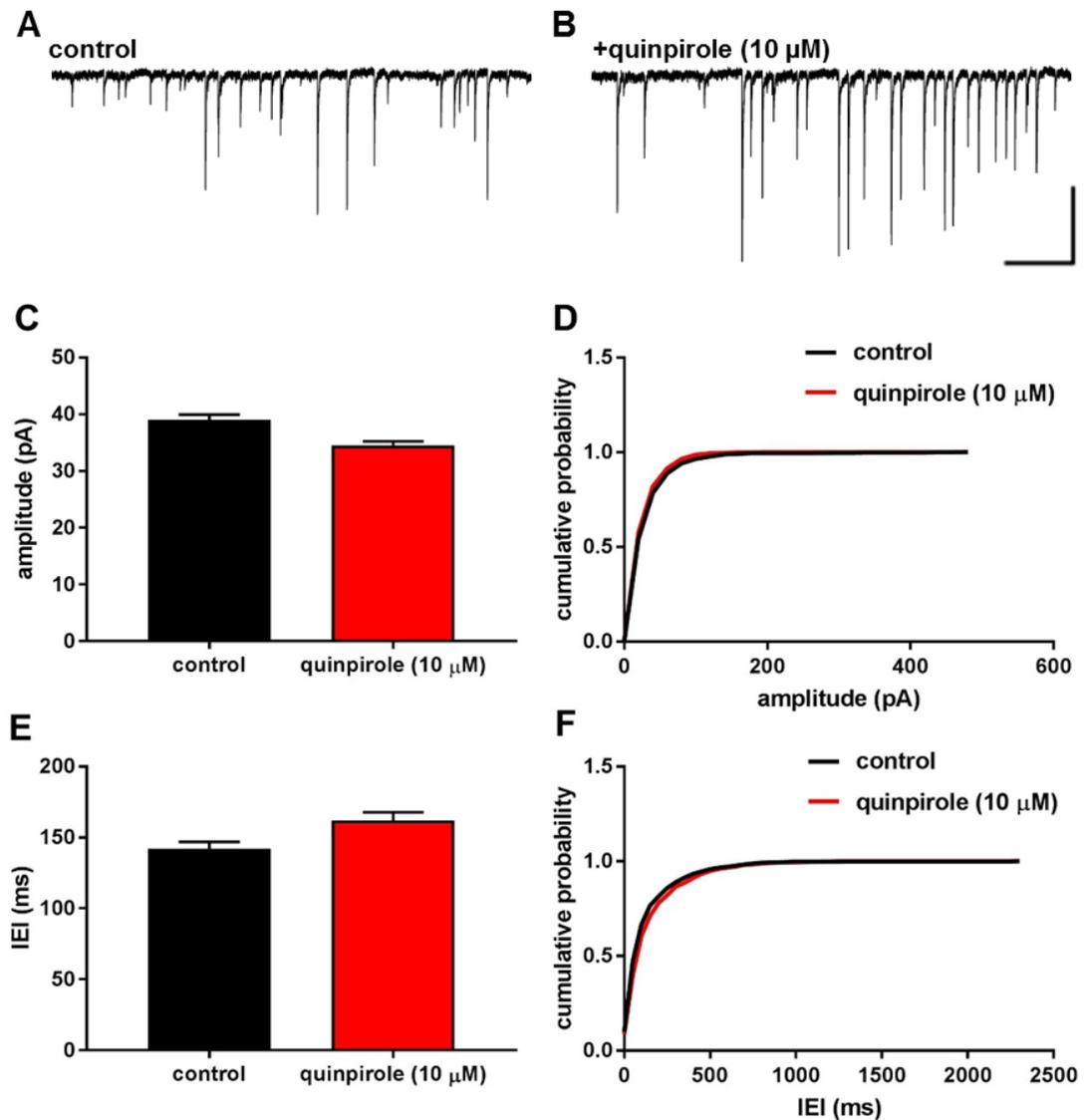
Figure 6.14 D2R agonist, quinpirole has shown no effect on phasic inhibition in FS interneurons in LV of M1

(A) (B) Representative voltage clamp recording from a FS interneuron demonstrating IPSCs before (left) and after (right) drug application (scale: 100 pA, 200 ms) **(C)** bar graph **(D)** cumulative probability plot showing the effect of drug on amplitude (n=5, P>0.05). **(E)** Bar graph **(F)** cumulative probability plot showing the effect of drug on inter event interval (IEI) (n=5, p>0.05).
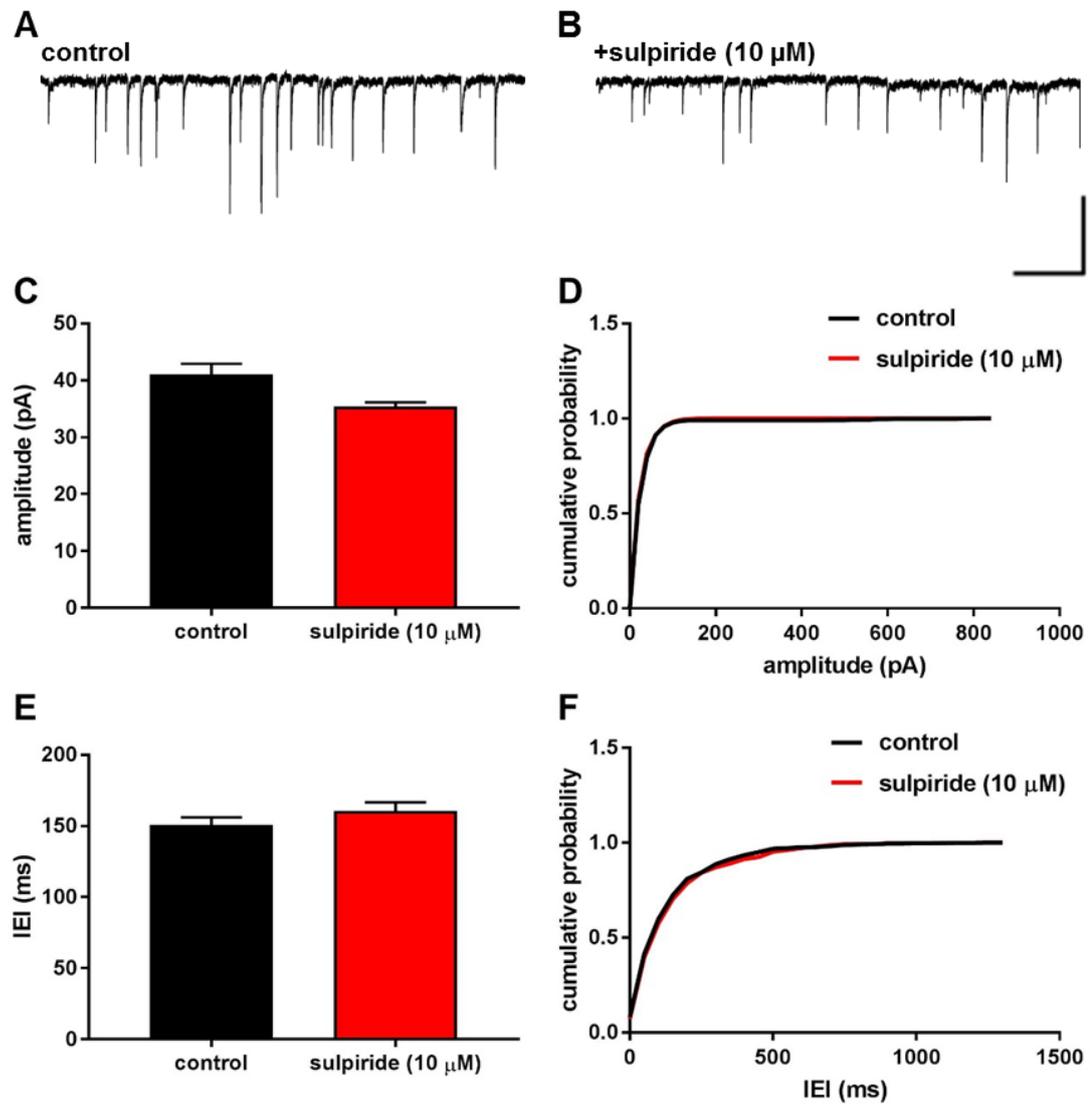
Figure 6.15 D2R antagonist, sulpiride has no effect on phasic inhibition in FS interneurons in LV of M1

(A) (B) Representative voltage clamp recording from a FS interneuron demonstrating IPSCs before (left) and after (right) drug application (scale: 100 pA, 200 ms) **(C)** bar graph **(D)** cumulative probability plot showing the effect of drug on amplitude (n=5, P>0.05). **(E)** Bar graph **(F)** cumulative probability plot showing the effect of drug on inter event interval (IEI) (n=5, p>0.05).

6.2.3 I_h current modulation of I_{DA} in FS cells in LV of M1

I_{DA} might be due to the activation of several types of ion channel, including TRP channels, I_h or tonic NMDAR currents besides D2-like DR. In order to investigate this, we first focused on I_h. To investigate if I_{DA} was mediated via hyperpolarising current (I_h) of HCN channels, ZD7288 (30 μM), an I_h blocker was bath applied as soon as the slice was placed on the recording chamber. In the presence of ZD7288, DA induced inward current by increasing the holding current by -48 ± 20 pA. Subsequent addition of Bic decreased the holding current (n=5, p<0.05, p<0.01) suggesting I_{DA} was I_h independent (figure 6.16).
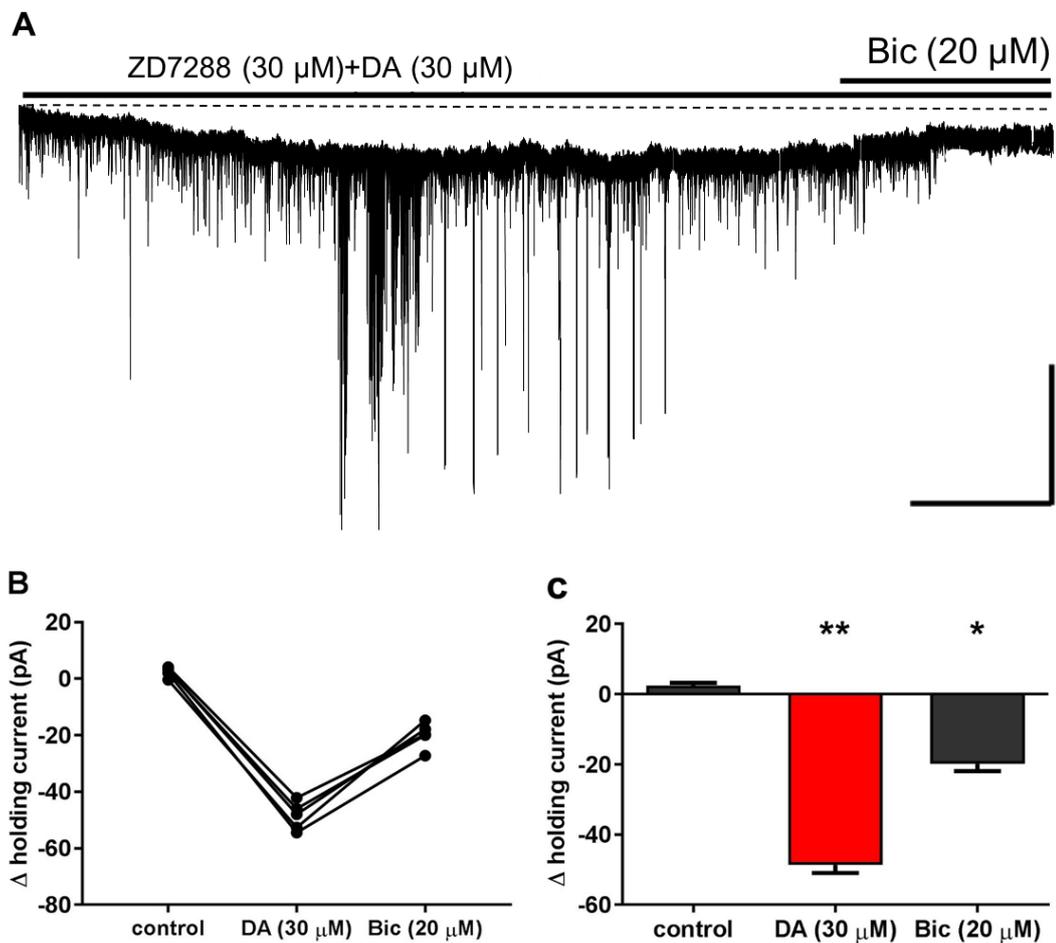
Figure 6.16 I_{DA} in FS interneurons was independent of I_h channels

(A) Representative voltage clamp recording demonstrating the effect of ZD7288 on I_{DA} (scale: 100 pA, 10 min). Black horizontal lines indicate the presence of drug in bath and dotted line indicates the relative current shift from baseline (control). **(B)** I_{DA} before and after Bic of individual FS cells. **(C)** Pooled data of I_{DA} before (grey) and after (red) application of Bic (n=5, p<0.01, p<0.01) in the presence of I_h channel blocker.

6.2.4 TRPC modulation of tonic and phasic currents in FS cells

Next, to uncover if TRP channels were involved in I_{DA}, TRP channel antagonists 2-APB and SKF96365 were bath applied. Both drugs significantly decreased the holding current that was increased by DA. Mean amplitude of -26.4 ± 2 pA and -27.2 ± 7 pA were reduced to - 0.65 ± 1.8 pA and 1 ± 0.3 pA in the presence of 2-ABP and SKF96365 respectively, n= 5, p<0.01(figures 6.17, 6.19). However, none of them showed significant effect on I_{phasic} (n=5, p>0.05) (figures 6.18, 6.20). Please note that in the presence of TRPC antagonist holding current was reduced slightly beyond baseline (control).
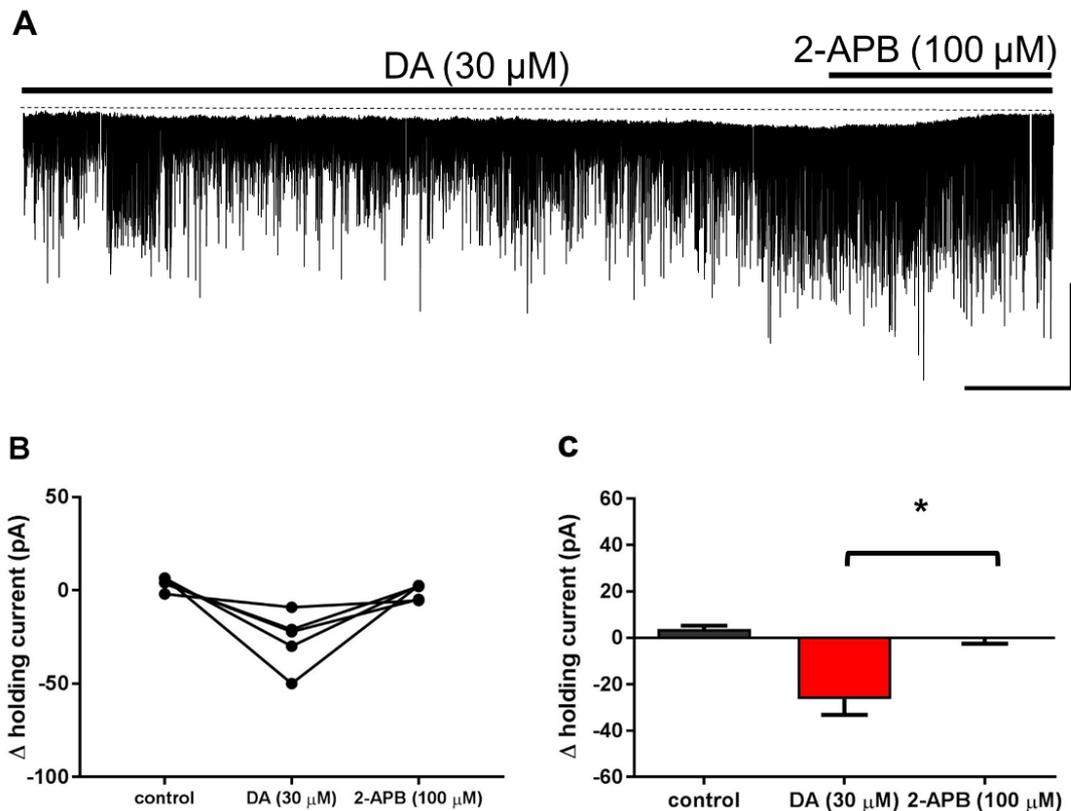
Figure 6.17 Blockade of TRP channels by 2-ABP (100 μM) decrease holding current slightly beyond control.

(A) Raw data of representative voltage clamp demonstrating the effect of SKF96365 on I_{DA} (scale: 100 pA, 10 min) black horizontal lines indicate the presence of drug in bath and dotted line indicates the relative shift from baseline (control). **(B)** Line graph showing the effect of DA and SKF96365 on holding current of individual FS cells. **(C)** Bar graph representing pooled data of I_{DA} in control (black), DA (red), SKF96365 (grey) (n=5, p<0.01).

Figure 6.18 2-ABP has no effect on phasic inhibition in FS interneurons in LV of M1

(A) (B) Representative voltage clamp recording from a FS interneuron demonstrating IPSCs before (left) and after (right) drug application (scale: 100 pA, 200 ms) **(C)** bar graph **(D)** cumulative probability plot showing the effect of drug on amplitude (n=5, P>0.05). **(E)** Bar graph **(F)** cumulative probability plot showing the effect of drug on inter event interval (IEI) (n=5, p>0.05).

Figure 6.19 Blockade of TRP channels by SKF96365 (100 µM) decreases holding current slightly beyond baseline.

(A) Raw data of representative voltage clamp demonstrating the effect of SKF96365 on I_{DA} (scale: 100 pA, 10 min) black horizontal lines indicate the presence of drug in bath and dotted line indicates the relative shift from baseline (control). **(B)** Line graph showing the effect of DA and SKF96365 on holding current of individual FS cells. **(C)** Bar graph representing pooled data of I_{DA} in control (black), DA (red), SKF96365 (grey) (n=5, p<0.01).

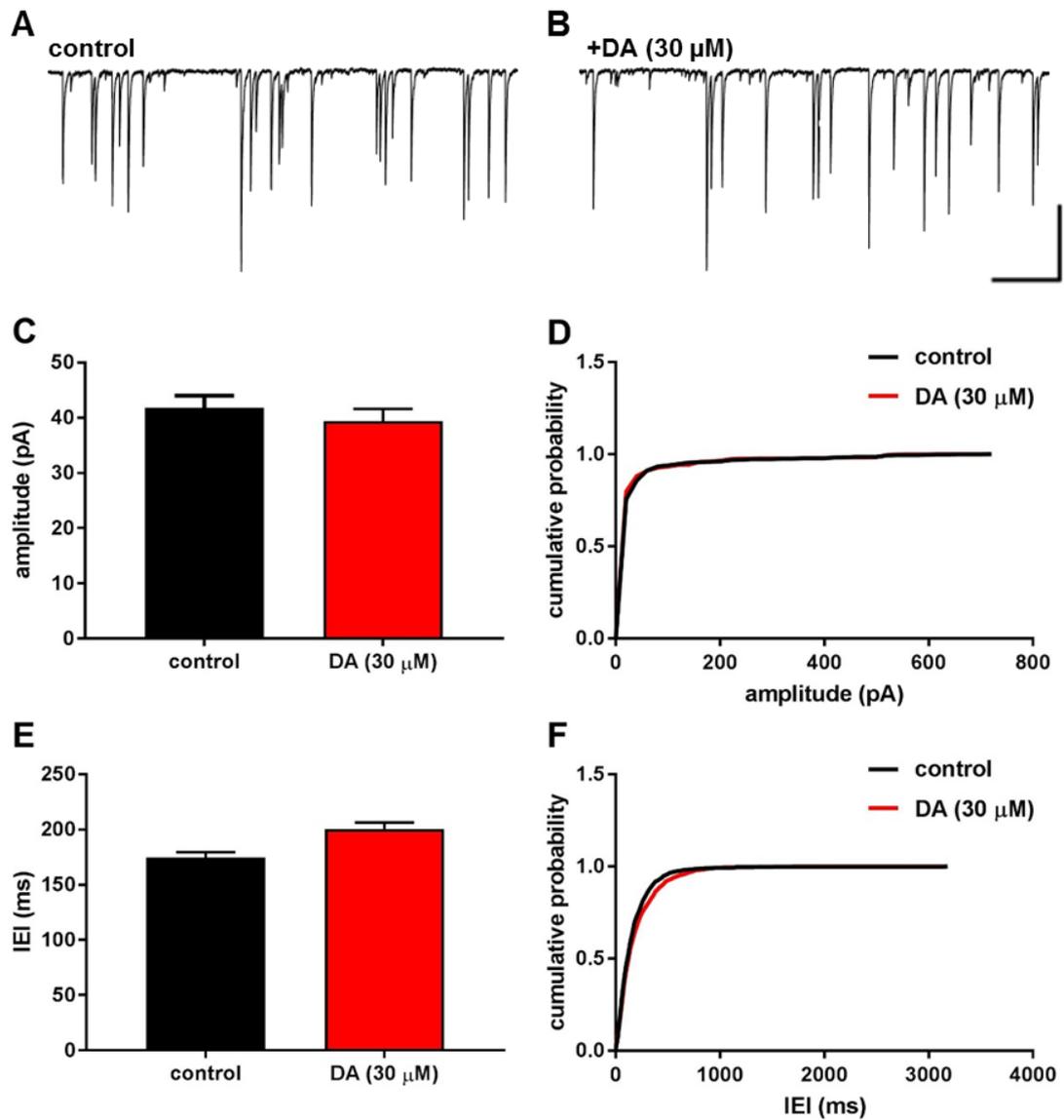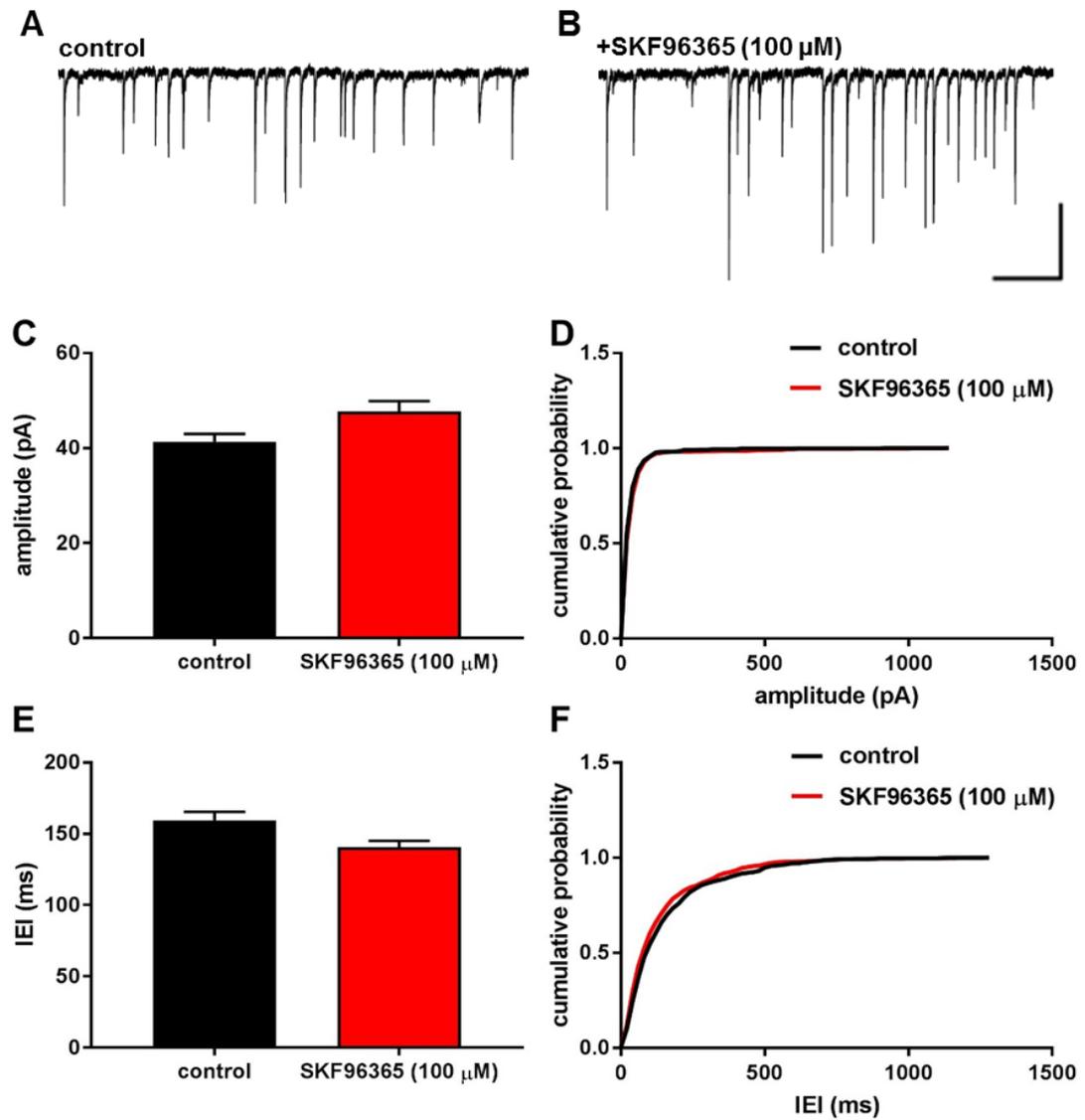**Figure 6.20 TRPC channel antagonist, SKF96365 has no effect on phasic inhibition in FS interneurons in LV of M1**

(A) (B) Representative voltage clamp recording from a FS interneuron demonstrating IPSCs before (left) and after (right) drug application (scale: 100 pA, 200 ms) **(C)** bar graph **(D)** cumulative probability plot showing the effect of drug on amplitude (n=5, P>0.05). **(E)** Bar graph **(F)** cumulative probability plot showing the effect of drug on inter event interval (IEI) (n=5, p>0.05).

As of now, the results above showed that DA induced an inward current in FS cells. I_{DA} was induced even in the presence of Bic but much smaller than with DA on its own. On the other hand, TRPC channel antagonist have shown a decrease in I_{DA} almost to the level of baseline suggesting a significant role in I_{DA}. Further investigation was made to determine if by blocking both GABAR and TRPC channels would decrease the holding current beyond baseline. When slices were treated with both SKF96365 (100 μM) and Bic (20 μM), I_{DA} was reversed more than 100% (control: -32 ± 9 pA to 33 ± 6 pA) which was significantly beyond control (n = 5, p<0.01 figure 6.21). This may suggest that all the tonic currents in FS cells are attributed to GABAR and DAR.
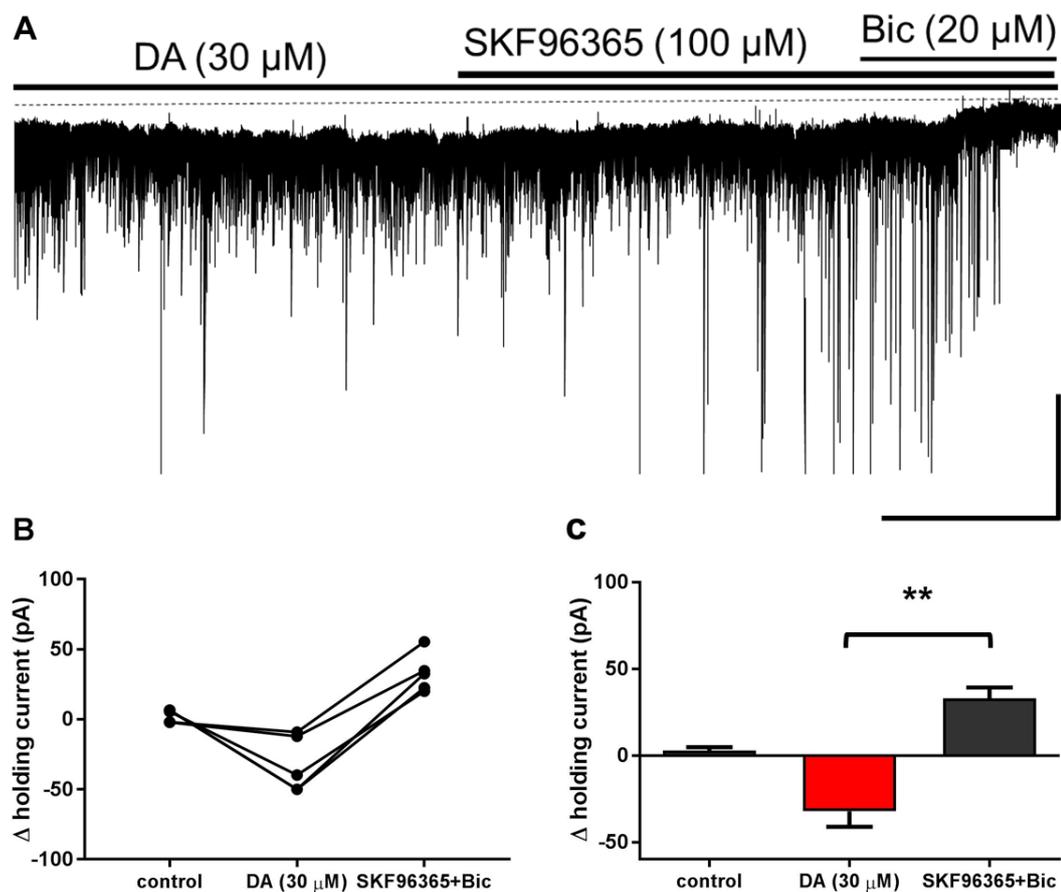
Figure 6.21 SKF96365 and Bic decreases holding current much beyond the baseline in FS cells.

(A) Representative voltage clamp recording demonstrating the effect SKF96365+Bic on I_{DA}. Black horizontal lines indicate the presence of drug in bath and dotted line indicates the relative current shift from baseline (control). **(B)** Line graph indicating I_{DA} in presence of SKF96365+Bic of individual FS cells. **(C)** Bar graph representing pooled data of I_{DA} in control (black), DA (red), SKF96365+Bic (grey) (n=5, p<0.01)

6.2.5 Effect of DA on holding current of pyramidal cells in LV of M1.

When treated slices with Bic (20 µM), pyramidal cells showed reduction in I_{tonic} and $I_{phasic.}$ Mean I_{tonic} was 15 ± 0.8 pA (n=5, $p<0.01$). DA, however, did not show any influence on holding current in pyramidal cells (n=5, $p>0.05$) (figure 6.22).
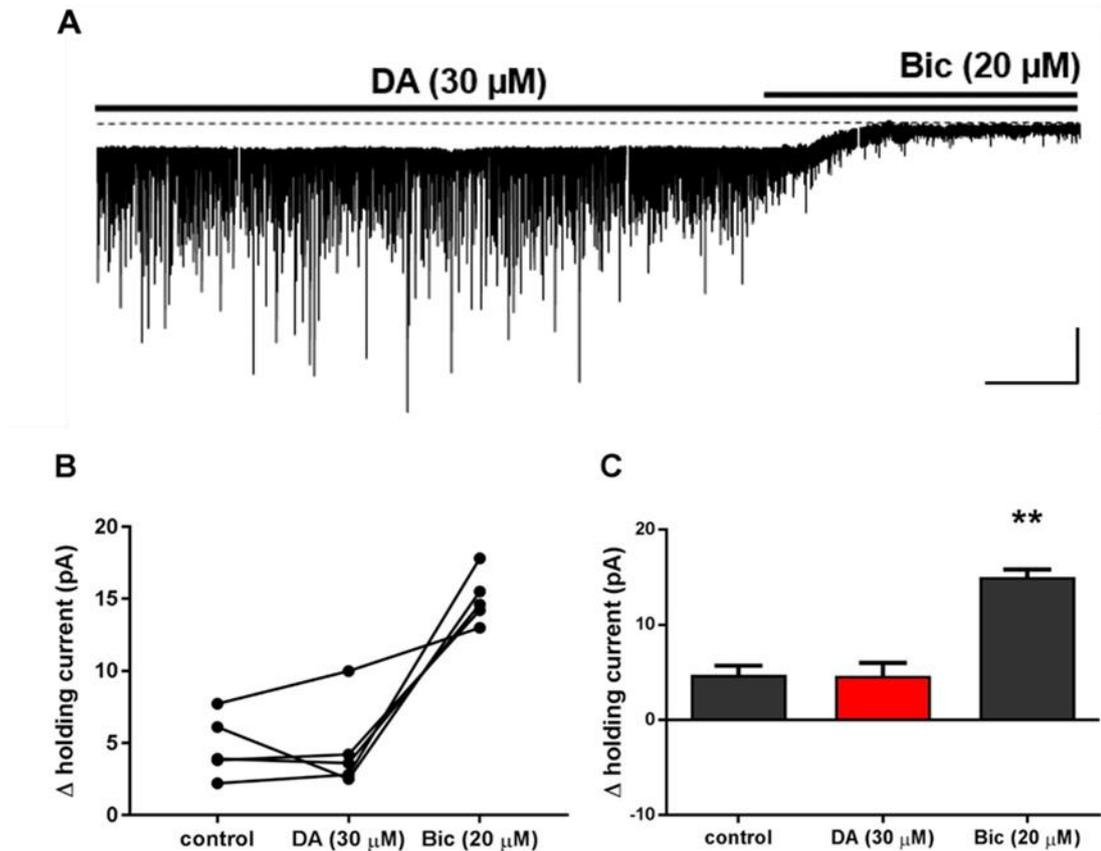
Figure 6.22 DA has no effect on holding current in pyramidal neurons in LV of M1

(A) Representative voltage clamp recording from a pyramidal cell demonstrating the effect of DA and Bic (scale: 20 pA, 2 min) black horizontal line indicates the presence of drug in bath and dotted line indicates the relative current shift from baseline (control). **(B)** Effect of DA and Bic on holding current of individual pyramidal cells **(C)** pooled data of change sin holding current before (grey) and after (red, black) drugs application (n=5, $p>0.05$ $p<0.01$).

6.3 Discussion

6.3.1 I_{tonic} and I_{phasic} in FS cells and pyramidal cells in LV of M1

The tonic activation of $GABA_AR$ was first reported in the voltage clamp recordings performed in cerebellar granule cells of rat (Kaneda *et al.,* 1995). In their study, $GABA_AR$ antagonists, Bic and GBZ, abolished spontaneous IPSCs as well as decreased the holding current, which was used to clamp the cell at a given membrane potential. This holding current reduction could reflect the reduction of number of open receptors (Kaneda *et al.,* 1995; Brickley *et al.,* 1996; Tia *et al.,* 1996; Wall and Usowicz, 1997). Several studies have shown I_{tonic} in several regions of brain such as: granule cells of dentate gyrus (Nusser and Mody, 2002), pyramidal neurons in LV of somatosensory cortex (Yamada *et al.,* 2004), thalamocortical relay neurons of the ventral basal complex (Porcello *et al.,* 2003), pyramidal neurons in CA1 (Bai *et al.,* 2001) and certain interneurons in CA1 (Semyanov *et al.,* 2003).

Phasic receptor activation is the transient mode of GABA exposure to postsynaptic receptors which could indicate fast diffusion away from release site (Overstreet *et al.,* 2003). Effective functioning of $GABA_AR$ requires binding of two GABA molecules (Baumann *et al.,* 2003) and the short dwell time may imply that not all the postsynaptic receptors are being occupied however, postsynaptic GABAR saturation may be observed in certain synapses. The occupancy extent varies with different synapses on different neurons and may even vary at synapses on a single neuron (Frerking *et al.,* 1996; Nusser *et al.,* 1997; Perrais *et al.,* 1999; Hajos *et al.,* 2000; Mozrzyymas et al. 2003). Phasic activation depends on various factors such as vesicle size and the amount of GABA in them, vesicle fusion type, synaptic cleft geometry, number and arrangement of GABA transporters. Governing time course and peak GABA concentration has enabled to study the occupancy as well as the channel opening, based on which kinetic properties of phasic receptor activation were established (Weiss *et al.,* 1989; Twyman *et al.,* 1990; Jones *et al.,* 1995; Jayaraman *et al.,* 1999; Haas *et al.,* 1995; Burkat *et al.,* 2001).

FS cells in LV of M1 at holding current -70 mV exhibited a constitutively active I_{tonic} and I_{phasic} when $GABA_AR$ antagonist, Bic, was bath applied. Since Bic is a competitive antagonist (Andrews and Johnston, 1979), PTX, a non-competitive antagonist (Krishek *et al.,* 1996) which was known to block the pore of these ligand gated channels (Krishek *et al.,* 1996; Thompson *et al.,* 2010) was bath applied and revealed active I_{tonic} and I_{phasic} similar to that of Bic. We found that I_{tonic} in FS cells was found much higher than that was observed in pyramidal cells without any externally applied GABA (Scimemi *et al.,* 2005) due to the differential regulation of GABA uptake as demonstrated in other studies (Semyanov *et al.,* 2003; Prokic *et al.,* 2015).

6.3.2 DA induces an inward current (I_{DA}) possibly mediated by D2-like receptors

Bath application of DA has induced an inward current in FS cells. The holding current of I_{DA} was reduced to a little extent on wash. 30 µM of DA was used throughout the experiments as this concentration has shown a maximum response in previous studies (Tofighy *et al.,* 2003; Loucif *et al.,* 2008). Initially DA was co-applied with ascorbic acid (AA) to prevent DA oxidation. 100 µM of AA was used given that this concentration does not affect IPSC kinetics (Yague *et al.,* 2013). However, AA often damaged the cell in our study and hence, was not applied in subsequent experiments. Oxidation of DA was identified by discolouration of the perfusing aCSF after 50 min of DA application. Since the time periods used in our study were less than the time required for DA oxidation, it was assumed that the inward current was mediated by DA prior to conversion into quinones and free radicals that causes neuro-toxicity (Sulzer and Zecca, 2000). This effect of DA on holding current contrasted with the work in ventrobasal thalamus (VB) of Wistar rats in which the D2R agonist quinpirole and the selective D4 agonist PD-168,077 strongly decreased $GABA_AR$ mediated inward current while D1R activation remained ineffective (Yague *et al.,* 2013) which could mean the DA action is mediated by distinct mechanisms in various regions of brain.

Application of Bic showed partial reduction in $I_{DA.}$ It is noteworthy that I_{tonic} revealed by Bic in the experiments where DA was pre-applied was significantly smaller than in control suggesting the possible involvement of GABAergic as well as non-GABAergic component in I_{DA}. Indeed, I_{DA} was induced in the presence of $GABA_AR$ antagonist, Bic but I_{DA} was much smaller in this case suggesting the involvement of GABAergic component in I_{DA}. Blocking GABAergic transmission by $GABA_AR$ antagonist and blocking glutamatergic transmission by blocking KAR, AMPAR and NMDAR using CNQX and 2-AP5 (data not shown) had no effect on I_{DA} reflecting the independency of synaptic transmission but a direct postsynaptic effect. IEM 1460 is known to block voltage dependent AMPAR, selective of GluA2 subunit lacking which are calcium permeable (Buldakova *et al.,* 1999). This compound has shown a selective block on synaptic excitation of FS interneurons but not medium spiny pyramidal neuron in mouse striatum (Gittis *et al.,* 2011) suggesting improvement in inhibitory functions. Therefore, all experiments were carried out with IEM 1460 in the internal solution (see methods for full composition).

To determine the involvement of receptor subtype mechanisms in $I_{DA,}$ D1- and D2- like DR specific agonists and antagonists were bath applied. Interestingly, SKF38393 and subsequent application of SCH23390 did not show any significant effect on holding current. In contrast, quinpirole, a non-selective D2 like DAR agonist that binds to both D2 and D3 receptors (Seeman and Van Tol, 1994) mimicked the effect of DA suggesting the actions of DA via D2 like receptors. To further confirm this, a non-selective D2 like receptor antagonist, sulpiride, which binds equally to both D2 and D3 receptors was administered (Seeman and

Van Tol, 1994). Sulpiride showed a significant reversal of I$_{quinpirole}$ suggesting a major role of D2-like DAR in I$_{DA}$ in accordance with previous studies that reported that DA induced a slow membrane depolarisation or an inward current mediated via D2-like DAR in several other brain regions (Uchimura *et al.,* 1986; Yang *et al.,* 1991; Munsch *et al.,* 2005).

Several *in vitro* studies reported that DA enhances the intrinsic excitability of pyramidal neurons in PFC by decreasing the resting membrane potential or by elevating a long lasting increase in number of action potentials via depolarisation in conditions where synaptic contributions were eliminated by pharmacological manipulations (Penit-Soria *et al.,* 1987; Yang and Seamans, 1996; Shi *et al.,* 1997; Ceci *et al.,* 1999; Lavin and Grace, 2001; Gulledge and Jaffe, 2001; Gao and Goldman-Rakic, 2003; Gulledge and Stuart, 2003; Wang and Goldman-Rakic, 2004; Kroener *et al.,* 2009; Moore *et al.,* 2011). One of the prominent effects of DA on pyramidal neurons is to increase in the frequency of spontaneous IPSCs and IPSPs indicating a net increase in GABAergic interneuron spiking activity mainly from PV-expressing FS basket and chandelier cells (Gulledge and Jaffe, 2001; Kröner *et al.,* 2007; Penit-Soria *et al.,* 1987; Seamans *et al.,* 2001b; Zhou and Hablitz, 1999). *In vitro* studies have suggested that D1-like DR induce depolarisation and increased excitability of FS interneurons in PFC slices (Gao and Goldman-Rakic, 2003; Gao *et al.,* 2003; Gorelova *et al.,* 2002; Kröner *et al.,* 2007; Towers and Hestrin, 2008; Trantham-Davidson *et al.,* 2008; Zhou and Hablitz, 1999). On the other hand, D2-like DR have also been shown to promote excitability in FS interneurons (Tseng and O'Donnell, 2004; Wu and Hablitz, 2005). DA did not show any effect on IPSC amplitude and IEI in FS cells of LV in M1. None of the DR modulators or TRPC antagonists have influenced phasic currents. Please note that the traces presented in the results above belong to a single recording and the effect of a drug shown in an individual trace might not reflect in pooled data using statistical analysis. For example, TRPC antagonist, SKF96365, has shown no effect on amplitude and IEI of IPSCs in figure 6.19 but the IEI has seen to be decreased implying increases in IPSC events in figure 6.20. This could probably reflect various cell types surrounding FS cell that was recorded from and also various receptor subtypes expressed on the cell. Further cell type characterisation and interactions with neighbouring cells would be beneficial as well as increasing `n` numbers. Exploring IPSC shape and decay time of individual recordings would uncover interesting mechanisms.

Additionally, DA has shown influence neither on holding current nor on IPSC amplitude and IEI in pyramidal cells holding at -70 mV in our study. *In vivo* studies in rats and cats revealed that pyramidal neuron activity was decreased upon administration of DA mediated via both D1 and D2-like DR (Awenowicz and Porter, 2002; Huda *et al.,* 2001). Pyramidal neurons in PFC have displayed a low event frequency (Hajos *et al.,* 2003). Vitrac *et al.,* (2014) have reported that DA enhances event rate of pyramidal neurons via D2 –like DRs which is in

line with excitation effect pyramidal neuron in LV of adult mice PFC mediated by D2-like DR (Gee *et al.,* 2012). However, DA has been reported to exhibit bi-directional modulation on PFC pyramidal neurons (Seamans *et al.,* 2001). In their study, DA decreased the IPSC amplitude via D2-like DR in 2- 20 min time period with a subsequent increase in IPSC amplitude which was mediated via D1-like DR with 20-40 min after DA application. In our current study the drug effect was analysed after 20 min of DA application which means insufficient time was given to investigate bi-directional effect of DA on FS cells in LV of M1. Also, it is presently not known whether DA mediated effects on pyramidal cells are mediated by direct actions onto pyramidal cells or via modulations of interneurons. Hence, further exploration is required to study the DA effect on pyramidal-interneuron possibly via dual patching technique.

6.3.3 DA mediated inward current (I_{DA}) is independent on I_h in FS cells

The inwardly rectifying hyperpolariaation-activated current (I_h) is mediated by the flow of Na^+ and K^+ ions via hyperpolarisation activated and cyclic nucleotide-gated channels (HCN), which open at potentials more negative than -50 mV and are classified as a non-specific cation conducting channels (Pape, 1996; Robinson & Siegelbaum, 2003; Biel et al. 2009; Shah *et al.,* 2010). These channels (HCN1-4 subunits) are expressed in thalamic relay neurons (McCormick and Pape, 1990a; McCormick and Pape, 1990b), hippocampus, neocortex, brain stem (Moosmang *et al.,* 1999; Notomi & Shigemoto, 2004). DA was implicated in modulating I_h in rat ventral tegmental neurons (Jiang *et al.,* 1993), in interneurons in Ll of neocortex (Wu and Hablitz, 2005), in relay neurons in the dorsal geniculate nucleus (dLGN) Govindaiah and Cox, 2005). This is based on the fact that HCN channels are regulated by intracellular cyclic nucleotide levels (Chen *et al.,* 2001) and dopamine receptor activation is known to alter intracellular cAMP levels (Missale *et al.,* 1998). To test the possibility of I_h in mediating effect on DA induced inward current, we have used a selective hyperpolarisation-activated cyclic nucleotide-gated channel antagonist, ZD7288. In the presence of ZD7288, application of DA still induced I_{DA} suggesting I_{DA} independent of I_h. This finding is in line with study in neurons of subthalamic nucleus (STN) (Loucif *et al.,* 2008).

6.3.4 I_{DA} was fully reversed by TRPC antagonists in FS cells

The transient receptor potential canonical (TRPC) channels are widely distributed in the brain (Strubing *et al.,* 2001; Riccio *et al.,* 2002). TRPC is a family of 7 proteins (TRPC1-TRPC7) that mediates a diverse group of non-selective cation currents (Harteneck *et al.,* 2000; Clapham *et al.,* 2001). A study performed in dorsal raphe serotonin neurons has revealed the involvement of DA mediated depolarisation or inward current (Aman *et al.,* 2007). To test the possibility of activation of cation channels via DAR in FS interneurons in

LV of M1, we have investigated the effect of TRPC antagonists, 2APB and SKF96365 (Li *et al.,* 1999; Clapham *et al.,* 2001) on I_{DA}. Both these drugs strongly reduced the amplitude of I_{DA} even beyond the baseline when bath applied. Subsequent bath application of Bic has revealed further I_{tonic} leading to further questions for future work.

Evidence exists that activation of D2-like DAR in accumbens has induced an inward current by supressing a potassium conductance (Uchimura *et al.,* 1986; Higashi *et al.,* 1989). This may not be true in our case as the IPSC solution contained CsCl which blocks potassium channels but could be ruled out by investigating the ability of DA to induce inward current by using cesium gluconate based internal solution and in the presence of extracellular cesium which block most potassium channels. The current-voltage plots using current clamp technique would provide more clues about the relationship before and after DA application. The other possible way to confirm that I_{DA} is mediated by cations is by replacing sodium chloride extracellular solution with choline chloride as shown in a study by Aman *et al.,* 2006. In their study, reducing sodium levels have shown a reduction in amplitude of I_{DA} as well as a negative shift of the reversal potential of I_{DA}. Moreover, the mechanism of I_{DA} induction can be investigated by using several second messenger modulators (Gi inhibitors).

There is growing evidence that DA modulates I_{tonic} in various regions of brain like striatal medium spiny neurons (Janssen *et al.,* 2009), ventrobasal thalamus (Yague *et al.,* 2013) and medium spiny neurons (MSNs) of the nucleus accumbens (Maguire *et al.,* 2014). In striatum, D1-like DR expressing MSNs display tonic current mediated by δ subunit containing $GABA_AR$ (Ade *et al.,* 2008; Kirmse *et al.,* 2008). Recent study has reported that DA directly modulates $GABA_AR$ that are present both synaptic and extra-synaptic sites (Hoerbelt *et al.,* 2015). This could possibly be the case with FS interneurons in M1 in our study but further experiments are necessary to prove DA modulation of I_{tonic}. This could be examined by observing if DA induces any inward currents in the presence of both GABAR antagonist and TRPC antagonist. Also, there exists a definite need for specific drugs targeting subunit specific GABA-DA interactions. Besides examining an constitutively active DA currents, another interesting aspect to investigate in order to uncover the mechanisms of I_{DA} is to investigate the effect of AMPH on holding current of whole cell recording as well as on I_{DA} based on the evidence that DA release is augmented by AMPH (Daberkow *et al.,* 2013, see review Calipiri and Ferris, 2013).

6.3.5 Final conclusions

Dopamine augmented an inward current in fast spiking interneurons in layer V of primary motor cortex via non-selective cation currents mediated by TRPC channels independent of I_h current via D2-like DAR. This suggests an absent role of D1-like DAR in I_{DA} and this could be further investigated by bath application of DR antagonists to test if there are any constitutively active currents.

7 General discussions, conclusions and future work

Initial investigations in the lab (Yamawaki, 2008) using coronal sensorimotor slices that are obtained from decapitated animals using standard storage glucose-based aCSF and the cutting aCSF was sucrose-based which contained neuro-protectants such as indomethacin, a cyclooxygenase inhibitor. There was no spontaneous activity in these slices, however, bath application of KA (400 nM) and CCh (50 μM) (as used by Buhl *et al.,* 1998) induced beta oscillations consistent with previous in-vivo studies (Murthy and Fetz, 1992; Baker *et al.,* 1997; Jensen *et al.,* 2005). Therefore, we have recently developed a novel slice preparation method (details in section 3.3) (Prokic *et al.,* 2011) by adding ascorbate, taurine and NAC. Also, indomethacin, uric acid and ascorbic acid and aminoguanidine were added to modified aCSF as neuro-protectants which aided preservation of inhibitory neurons critical for maintenance of rhythmic network activity. We determined to use the same slice preparation to induce oscillatory activity and to explore rhythms generated in both M1 and S1 at varied frequency ranges, with a view to exploring potential interactions between M1 and S1 in the functionally connected sagittal cortical slice. However, the mechanisms involved the usage of neuro-protectants have not been explored yet.

Co-application of KA and CCh reliably induced theta and gamma oscillations in both M1 and S1 which were stable for 3-4 hrs in line with other *in vitro* studies (Dickinson *et al.,* 2003). Basic pharmacology performed using various receptor modulators has revealed the contributions of $GABA_AR$, NMDAR, AMPAR and DAR. Gamma oscillations were decreased by $GABA_AR$ antagonists (gabazine and picrotoxin) and also by AMAPAR antagonist (SYM2206), whilst increasing theta power in these cases. $GABA_BR$ antagonist (CGP55845), GABA positive modulators such as diazepam, zolpidem, NMDAR antagonist (MK 801) and mGluR antagonists have shown an increase in both theta and gamma oscillations (Johnson *et al.,* 2017). Theta and gamma oscillations were found reliant on gap junctions as the activity was abolished when carbenoxolone, a gap junction blocker was bath applied (Johnson *et al.,* 2017) consistent with beta oscillations in M1 (Yamawaki *et al.,* 2008) and delta oscillations (chapter 4). Dependence of oscillatory activity on mAchR in M1 is reflected by the fact that the induction of oscillatory activity requires CCh. (Johnson *et al.,* 2017) along with KA and was further demonstarted by bath application of mAchR antagonist. Atropine abolished both theta and gamma oscillations (Johnson *et al.,* 2017) in consistent with various studies (Konopacki *et al.,* 1987; Lukatch and MacIver, 1997; Buhl *et al.,* 1998; Fisahn *et al.,* 1998).

Interactions between two different types of oscillations is defined as cross-frequency coupling (CFC). In the current study, PAC was performed between theta and gamma oscillations, with theta frequency (3 –10 Hz) as phase and gamma frequency (25-50 Hz) as amplitude that was driven by low frequency using a MATLAB script developed by Tort *et al.,* 2010. PAC was performed on 60 s epochs of data in various slice types (refer methods

section) and was represented as Modulation Index (MI) which indicates the degree of coupling between the two oscillations. It is interesting to note that isolated M1 slice type shows high MI. The presence of PV+ interneurons in deep layers of M1 could form the basis for high coupling in M1 based on the evidence that PV+ interneurons contribute to the generation and coupling of theta and gamma oscillations since selective removal of fast synaptic inhibition from PV+ cells using transgenic mouse protocols did not induce theta and gamma oscillations (Wulff *et al.,* 2009). However, the extent of coupling varied with each slice. This is probably caused by biological differences such as viability of each slice, receptor expression, interneurons and pyramidal cell expression in each slice obtained daily. As each subtype fire at distinct patters (phase) each subtype of interneurons probably has a unique role in entraining nested rhythms in various regions. Hence, the need for further investigations is high in order to uncover possible mechanisms behind the coupling.

The interlaminar (deep and superficial layers) synchrony within human cortex is linked to the degree of coupling between the theta and gamma oscillations (PAC) (MacGinn and Valiante, 2014) which needs further investigation in our slices. Also, pharmacological agents such as ketamine have been shown to influence PAC (Caixeta *et al.,* 2013). Therefore, it is essential to perform PAC before and after various receptor modulators to identify how they are contributing PAC giving plenty of room for future work. Interestingly, human hippocampus and cortex exhibited different properties in that PAC in hippocampus was the strongest at the phase of slow theta band (2.5-5 Hz) and both low (35-70 Hz) and high gamma (70-130 Hz) whilst, the phase of high theta band (4-9 Hz) was preferred with low gamma exhibiting greater coupling in cortex (Lega *et al.,* 2016). This observation may prove the difference of hippocampal theta oscillations between humans (< 5Hz) and rats (6-12Hz) (Lega *et al.,* 2012; Watrous *et al.,* 2013; Jacobs *et al.,* 2014) and may reflect the big brain size in humans. It would be beneficial to apply these frequency specific studies in the PAC data that was obtained in M1 and S1 of rat slices.

Although much literature is documented the origin of delta oscillations (1-4 Hz) in thalamus (Amzica *et al.,* 1992), relatively less is known about cortical based delta oscillations. A delta rhythm of purely cortical origin has been implicated in *in vivo* studies (Amzica and steriade, 1998; Fell *et al.,* 2002) but the mechanisms underlying were not as clear as those of thalamic origin (Pirchio *et al.,* 1997; Hughes *et al.,* 1999; 2002). A study has revealed that transition of NREM2 to NREM3&4 stages has required the neuromodulatory action of cortex itself but not thalamus (Krishnan *et al.,* 2016). We have assumed that the origin of delta oscillations could possibly be primary motor and sensory cortices with these regions being primary projection sites for thalamus, hence the term 'primary'. A recent *in vitro* study has indicated delta oscillations in secondary somatosensory cortex/parietal area, S2/Par2 slices prepared from male Wistar rats (Carracedo *et al.,* 2013). None of these studies have

indicated the mechanisms and origin of cortical delta rhythm probably because it is challenging to induce delta oscillations unlike gamma oscillations, which can be identified spontaneously or with minimal pharmacological manipulations. Anatomical studies have shown that M1 receives input from S1 and thalamus (Zin-Ka-Leu, 1998; Miyachi *et al.,* 2005) and the highly reciprocal nature of functional connections between M1 and S1 have been demonstrated in an optimum plane sensorimotor slice preparation developed by Rocco *et al.,* (2007). Sensorimotor integration has been studied *in vivo* (Smith *et al.,* 1983; Wannier *et al.,* 1991) but this does not enable a full understanding of the pathways.

Delta oscillations are pharmacologically induced in layer V of M1 and S1 by maintaining low cholinergic and low dopaminergic tone which is the characteristic in deep sleep stages and we have illustrated the transition from fast (gamma and theta) oscillations to slow (mu and beta) oscillations before a high amplitude delta rhythm emerged. Delta rhythm was characterised using various receptor modulators to determine the role of various receptors in rhythm generation. The current study suggests that these delta oscillations in both regions are dependent on GABAR, AMPAR, KAR, mAChR and gap junctions but are independent of NMDAR. mGluR do not seem to show much contribution in generation of delta rhythm however mGluR agonists showed a general reduction in the activity whilst the antagonists showed an increase in the activity which is significant only in case of group I mGluR antagonists (MPEP & MTEP). These suggestions were based on pharmacology performed using various receptor modulators.

Our current study (chapter 4 and 5) performed in LV of M1 and S1 demonstrates the generation of delta oscillations by pharmacological manipulations and investigates the contribution of various receptors involved in the rhythm generation and the pharmacological equivalent awake state. Characterisation of delta rhythm in control slice preparations may facilitate understanding of the mechanisms underlying various pathological conditions like Alzheimer's disease. Further research may be extended to comparing to a disease model and also examine delta in other regions such as V1. However, further work on characterisation of cell types recruited in generation of delta oscillations using calcium imaging and optogenetic techniques, would enable a better understanding of the mechanistic origin of the rhythm. Expression of receptors, receptor subtypes and receptor subunit could be of a great benefit using immunochemical studies and two-photon microscopy studies so that live cells can be imaged for extended time periods in deep tissue. The advantages of using two photon microscopy imaging technique are ther eis little damage to the surrounding tissue. Also, the contribution of various receptors could be confirmed using KO animal models. Additionally, it was believed LV to be the origin but this was not completely ruled out and it was evident that LVI has several cell types that could

contribute to rhythm generation. To address this tissue we should find a way to delineate LV and LVI and Grainger causality analysis might help address this issue.

Topographic maps of both M1 and S1 are well established (Brooks *et al.,* 1961, Woolsey 1952, Li and Waters 1991) and interactions between these two regions are known to play critical roles in motor learning and control skills (Asanuma and Arissian, 1984; Asanuma and Pavlides, 1997). The origin of delta oscillations from deep layers of M1 could mean that the retrograde and anterograde connections between the two regions do not contribute to initiation of deep sleep states. However, these connections may have a role in maintenance of delta oscillations since S1 followed M1 with a significant delay in intact slice (type A and E). The neuronal populations that were recruited for delta rhythm generation might be just resident in M1 and not in S1. For instance, betz cells were implicated in layer V of M1 (Betz, 1894). These cells are unique in their morphology and may appear as both pyramidal and interneurons (Braak, 1976). Based on this it is logical to say that M1 is the source of origin for delta oscillations. However, S1 has been identified to lead M1 at higher frequencies but both regions have individual rhythm generators. Nevertheless, further histological and immuno-labelling studies to determine the types of cells and receptor types that were involved in generation of delta oscillations and functional connectivity studies between two regions would be beneficial to further address this issue. Preparing slices in different plane other than sagittal would preserve thalamus and /or M2, S2 besides M1 and S1 and would provide an opportunity to investigate the influence of thalamus (if any) in delta, theta and gamma rhythm generation. Also, characterising cell types involved in each oscillation using optogenetic studies would give a better insight. Also, region specific stimulation studies may reveal the individual region contribution. Another way to look at is multi electrode recording which enables to examine the navigation pattern of oscillations between layers as well as between regions (for instance M1 and S1). Our current study is limited in terms of making cuts between regions during the experiments but if there is a secure way to perform cut, that would demonstrate the interaction between regions.

In the current study, DA modulated network activity at delta, theta and gamma frequencies. D1-like DR are more abundant than D2-like DR in rat cortex. DA effects on FS interneurons have been identified to be mediated by PKA-dependent suppression of leak, inward rectifying, and depolarisation-activated two pore domain K^+ channels (Gorelova *et al.,* 2002) and amplification of depolarising currents mediated by HCN channels (via G_s)Gorelova *et al.,* 2002; Trantham-Davidson *et al.,* 2008; Wu and Hablitz, 2005). Additionally, many reports have indicated that DA modulates $GABA_A R$. Here (chapter 6), we determined the effect of DA on pyramidal cells and FS interneurons in LV of M1 slices using voltage clamp, whole cell recordings. FS cells were identified as based on the morphological features as described by Prokic *et al.,* (2015) and are known to be highly encountered in deep layers

forming Betz cell-FS cell pairing. Our investigations revealed that DA induced a slow inward current via non-specific cation TRPC channels. Morphological, functional and electrical properties of cell types in M1 needs further examination using whole cell voltage clamp as well as current clamp techniques. Since, Betz-FS cell pairing was observed in LV of M1, dual patch recordings would uncover the mechanistic insights on how one cell interacts with the other. Also, stimulation techniques may be incorporated to observe how one cell type impacts on another cell type. Additionally, there is growing evidence that DA modulates I_{tonic} in various regions of brain. Given the link between I_{tonic} and delta subunit within extra synaptic GABA receptor complexes (Nusser *et al.,* 1998), this can be addressed by using the delta subunit-selective agonist, THIP in the experiments. On an interesting note, D2 mediated I_{DA} could account for vhanges in thet and gamma oscillations when DA and amphetamine were bath applied. It will be interesting to see if the oscillations were modulated by TRPC antagonists.

In conclusion, trans-cardial perfusion, sagittal slice preparation, modified aCSF solution as well as addition of neuro-protectants has greatly enhanced the slice viability. Co-application of KA and CCh induced persistent theta and gamma oscillations. These dual oscillations seem to have distinct mechanisms and were identified to be coupled from PAC analysis. However, the percentage of coupling varied in various types of slice preparations with high modulation index (MI) in M1 only slice followed by S1 only slice when compared to intact slice preparations. To our knowledge, this is the first demonstration of motor cortical delta oscillation *in vitro* which was identified to have a distinct mechanism in comparison with that of delta in secondary somatosensory/parietal area (S2/Par2) (also *in vitro)* (Carracedo *et al.,* 2013) These extracellular studies could prove significant in investigating neuronal network oscillations in pathological states such as PD, AD by using animal models that can enable the comparison of mechanisms. Delta oscillations were induced by KA, CCh, D1 and D2 antagonists and are reliant on both inhibitory and excitatory network activity. Pharmacologically induced delta oscillations were identified to be irreversible since the frequency of the oscillations had not changed when pharmacologically equivalent awake state was maintained possibly due to experimental limitations. This may imply the need other inhibitory input to reverse delta such as from thalamus. Therefore, a slice preparation with both cortex and thalamus preserved would probably enable delta reversal. Delta oscillations in S1 are dependent on both inhibitory and excitatory networks similar to that of in M1. A significant time delay in occurrence and phase lag that was observed in correlation studies performed in various slice preparations revealed M1 as the rhythm generator. Inability of S1 to generate delta oscillations on its own suggests that S1 follows M1 at delta frequency However, both M1 and S1 have local generators at nested theta and gamma band. Dopamine augmented an inward current in fast spiking interneurons in layer V of

primary motor cortex via non-selective cation currents mediated by TRPC channels independent on I_h current via D2-like DAR without affecting IPSC amplitude and IEI.

8 References

Ade KK, Janssen MJ, Ortinski PI, Vicini S. 2008. Differential tonic GABA conductances in striatal medium spiny neurons. *J Neurosci* 28: 1185-97

Adhikari A, Topiwala MA, Gordon JA. 2010. Synchronized activity between the ventral hippocampus and the medial prefrontal cortex during anxiety. *Neuron* 65: 257-69

Adrian ED. 1942. Olfactory reactions in the brain of the hedgehog. *The Journal of Physiology* 100: 459-73

Aeschbach D. 2009. Slow Waves and Learning: Beyond Correlations. *Sleep* 32: 1253-54

Aeschbach D, Borbely AA. 1993. All-night dynamics of the human sleep EEG. *Journal of sleep research* 2: 70-81

Aghajanian GK, Rasmussen K. 1989. Intracellular studies in the facial nucleus illustrating a simple new method for obtaining viable motoneurons in adult rat brain slices. *Synapse (New York, N.Y.)* 3: 331-8

Akbarian S, Sucher NJ, Bradley D, Tafazzoli A, Trinh D, et al. 1996. Selective alterations in gene expression for NMDA receptor subunits in prefrontal cortex of schizophrenics. *J Neurosci* 16: 19-30

Akgul G, McBain CJ. 2016. Diverse roles for ionotropic glutamate receptors on inhibitory interneurons in developing and adult brain. *The Journal of physiology* 594: 5471-90

Alexander GE, DeLong MR, Strick PL. 1986. Parallel organization of functionally segregated circuits linking basal ganglia and cortex. *Annual review of neuroscience* 9: 357-81

Allen PJ, Fish DR, Smith SJM. 1992. Very high-frequency rhythmic activity during SEEG suppression in frontal lobe epilepsy. *Electroencephalography and Clinical Neurophysiology* 82: 155-59

Alloway KD. 2008. Information processing streams in rodent barrel cortex: the differential functions of barrel and septal circuits. *Cerebral cortex (New York, N.Y. : 1991)* 18: 979-89

Aman TK, Shen RY, Haj-Dahmane S. 2007. D2-like dopamine receptors depolarize dorsal raphe serotonin neurons through the activation of nonselective cationic conductance. *The Journal of pharmacology and experimental therapeutics* 320: 376-85

Amzica F, Nuñez A, Steriade M. 1992. Delta frequency (1–4 Hz) oscillations of perigeniculate thalamic neurons and their modulation by light. *Neuroscience* 51: 285-94

Amzica F, Steriade M. 1998. Electrophysiological correlates of sleep delta waves1. *Electroencephalography and Clinical Neurophysiology* 107: 69-83

Andersen P, Bland B, Skrede K, Sveen O, R W. 1972. Single unit discharge in brain slices

maintained in vitro. *Acta Physiol Scand* 84: 1-2a

Andersen RA. 1995. Encoding of intention and spatial location in the posterior parietal cortex. *Cerebral cortex (New York, N.Y. : 1991)* 5: 457-69

Anderson CT, Sheets PL, Kiritani T, Shepherd GMG. 2010. Sublayer-specific microcircuits of corticospinal and corticostriatal neurons in motor cortex. *Nat Neurosci* 13: 739-44

Andrews PR, Johnston GA. 1979. GABA agonists and antagonists. *Biochemical pharmacology* 28: 2697-702

Armstrong-James M, Fox K. 1987. Spatiotemporal convergence and divergence in the rat S1 "barrel" cortex. *The Journal of comparative neurology* 263: 265-81

Asanuma H. 1981. Functional role of sensory inputs to the motor cortex. *Progress in neurobiology* 16: 241-62

Asanuma H, Arissian K. 1984. Experiments on functional role of peripheral input to motor cortex during voluntary movements in the monkey. *Journal of neurophysiology* 52: 212-27

Asanuma H, Pavlides C. 1997. Neurobiological basis of motor learning in mammals. *Neuroreport* 8: i-vi

Asanuma H, Ward JE. 1971. Patterns of contraction of distal forelimb muscles produced by intracortical stimulation in cats. *Brain Research* 27: 97-109

Aston-Jones G, Bloom FE. 1981. Activity of norepinephrine-containing locus coeruleus neurons in behaving rats anticipates fluctuations in the sleep-waking cycle. *J Neurosci* 1: 876-86

Awapara J, Landua AJ, Fuerst R, Seale B. 1950. Free gamma-aminobutyric acid in brain. *The Journal of biological chemistry* 187: 35-9

Awenowicz PW, andPorter,L.L. 2002. Local application of dopamineinhibits pyramidal tract neuron activity in the rodent motorcortex. *J. Neurophysiol* 88: 3439–51

Axmacher N, Draguhn A. 2004. Inhibition of GABA release by presynaptic ionotropic GABA receptors in hippocampal CA3. *Neuroreport* 15: 329-34

Axmacher N, Henseler MM, Jensen O, Weinreich I, Elger CE, Fell J. 2010. Cross-frequency coupling supports multi-item working memory in the human hippocampus. *Proceedings of the National Academy of Sciences* 107: 3228-33

Baghdoyan HAL, R. . 2012. The neurochemistry of sleep and wakefulness In *Basic neurochemistry : principles of molecular, cellular, and medical neurobiology*, ed. ST Brady, GJ Siegel, RW Albers, DL Price. New York: Academic Press

Bai D, Zhu G, Pennefather P, Jackson MF, MacDonald JF, Orser BA. 2001. Distinct functional and pharmacological properties of tonic and quantal inhibitory postsynaptic currents mediated by gamma-aminobutyric acid(A) receptors in hippocampal neurons. *Molecular pharmacology* 59: 814-24

Baker SN, Kilner JM, Pinches EM, Lemon RN. 1999. The role of synchrony and oscillations in the motor output. *Experimental brain research* 128: 109-17

Baker SN, Olivier E, Lemon RN. 1997. Coherent oscillations in monkey motor cortex and hand muscle EMG show task-dependent modulation. *The Journal of physiology* 501 (Pt 1): 225-41

Ball GJ, Gloor P, Schaul N. 1977. The cortical electromicrophysiology of pathological delta waves in the electroencephalogram of cats. *Electroencephalography and clinical neurophysiology* 43: 346-61

Barbas H. 2015. General cortical and special prefrontal connections: principles from structure to function. *Annual review of neuroscience* 38: 269-89

Bartos M, Vida, I., Frotscher, M., Geiger, J. R. P., & Jonas, P. 2001. Rapid signalling at inhibitory synapses in a dentate gyrus interneuron network", . *Journal of Neuroscience* 21: 2687-98

Bartos M, Vida I, Frotscher M, Meyer A, Monyer H, et al. 2002. Fast synaptic inhibition promotes synchronized gamma oscillations in hippocampal interneuron networks. *Proceedings of the National Academy of Sciences* 99: 13222-27

Bartos M, Vida I, Jonas P. 2007. Synaptic mechanisms of synchronized gamma oscillations in inhibitory interneuron networks. *Nat Rev Neurosci* 8: 45-56

Başar E, Başar-Eroglu C, Karakaş S, Schürmann M. 2001. Gamma, alpha, delta, and theta oscillations govern cognitive processes. *International Journal of Psychophysiology*

39: 241-48

Bastos AM, Usrey WM, Adams RA, Mangun GR, Fries P, Friston KJ. 2012. Canonical microcircuits for predictive coding. *Neuron* 76: 695-711

Baude A, Nusser Z, Roberts JD, Mulvihill E, McIlhinney RA, Somogyi P. 1993. The metabotropic glutamate receptor (mGluR1 alpha) is concentrated at perisynaptic membrane of neuronal subpopulations as detected by immunogold reaction. *Neuron* 11: 771-87

Baufreton J, Garret M, Rivera A, de la Calle A, Gonon F, et al. 2003. D5 (not D1) dopamine receptors potentiate burst-firing in neurons of the subthalamic nucleus by modulating an L-type calcium conductance. *J Neurosci* 23: 816-25

Baumann SW, Baur R, Sigel E. 2003. Individual Properties of the Two Functional Agonist Sites in GABA$_A$ Receptors. *The Journal of Neuroscience* 23: 11158-66

Bazelot M, Dinocourt C, Cohen I, Miles R. 2010. Unitary inhibitory field potentials in the CA3 region of rat hippocampus. *The Journal of physiology* 588: 2077-90

Bazhenov M, Timofeev I. 2006. Thalamocortical oscillations. *Scholarpedia* 1: 1319

Bazhenov M, Timofeev I, Steriade M, Sejnowski TJ. 1998. Computational Models of Thalamocortical Augmenting Responses. *The Journal of Neuroscience* 18: 6444-65

Bazhenov M, Timofeev I, Steriade M, Sejnowski TJ. 1999. Self-sustained rhythmic activity in the thalamic reticular nucleus mediated by depolarizing GABAA receptor potentials. *Nat Neurosci* 2: 168-74

Beaulieu C. 1993. Numerical data on neocortical neurons in adult rat, with special reference to the GABA population. *Brain research* 609: 284-92

Beaulieu C, Kisvarday Z, Somogyi P, Cynader M, Cowey A. 1992. Quantitative distribution of GABA-immunopositive and -immunonegative neurons and synapses in the monkey striate cortex (area 17). *Cerebral cortex (New York, N.Y. : 1991)* 2: 295-309

Bekkers JM, Stevens CF. 1989. NMDA and non-NMDA receptors are co-localized at individual excitatory synapses in cultured rat hippocampus. *Nature* 341: 230-33

Belforte JE, Zsiros V, Sklar ER, Jiang Z, Yu G, et al. 2010. Postnatal NMDA receptor ablation in corticolimbic interneurons confers schizophrenia-like phenotypes. *Nat Neurosci* 13: 76-83

Belluscio MA, Mizuseki K, Schmidt R, Kempter R, Buzsaki G. 2012. Cross-frequency phase-phase coupling between theta and gamma oscillations in the hippocampus. *J Neurosci* 32: 423-35

Beltramo R, D'Urso G, Dal Maschio M, Farisello P, Bovetti S, et al. 2013. Layer-specific excitatory circuits differentially control recurrent network dynamics in the neocortex. *Nat Neurosci* 16: 227-34

Benardo LS, Wong RKS. 1995. Inhibition in the Cortical Network In *The Cortical Neuron*, ed. MJ Gutnick, I Mody, pp. 141-55. Oxford, UK: Oxford University Press

Ben-Ari Y. 1985. Limbic seizure and brain damage produced by kainic acid: mechanisms and relevance to human temporal lobe epilepsy. *Neuroscience* 14: 375-403

Ben-Ari Y, Cossart R. 2000. Kainate, a double agent that generates seizures: two decades of progress. *Trends in neurosciences* 23: 580-7

Benchenane K, Peyrache A, Khamassi M, Tierney PL, Gioanni Y, et al. 2010. Coherent theta oscillations and reorganization of spike timing in the hippocampal- prefrontal network upon learning. *Neuron* 66: 921-36

Berger B, Doucet G, Descarries L. 1988. Density of the dopamine innervation in rat cerebral cortex after neonatal 6-hydroxydopamine or adult stage DSP-4 noradrenaline denervations: a quantitative radioautographic study. *Brain research* 441: 260-8

Berger H. 1929. Über das Elektrenkephalogramm des Menschen. *Archiv für Psychiatrie und Nervenkrankheiten* 87: 527-70

Berke JD, Okatan M, Skurski J, Eichenbaum HB. 2004. Oscillatory entrainment of striatal neurons in freely moving rats. *Neuron* 43: 883-96

Bettler B, Boulter J, Hermans-Borgmeyer I, O'Shea-Greenfield A, Deneris ES, et al. 1990. Cloning of a novel glutamate receptor subunit, GluR5: expression in the nervous system during development. *Neuron* 5: 583-95

Bettler B, Egebjerg J, Sharma G, Pecht G, Hermans-Borgmeyer I, et al. 1992. Cloning of a

putative glutamate receptor: a low affinity kainate-binding subunit. *Neuron* 8: 257-65

Bevan MD, Magill PJ, Terman D, Bolam JP, Wilson CJ. 2002. Move to the rhythm: oscillations in the subthalamic nucleus-external globus pallidus network. *Trends in neurosciences* 25: 525-31

Biel M, Wahl-Schott C, Michalakis S, Zong X. 2009. Hyperpolarization-activated cation channels: from genes to function. *Physiological reviews* 89: 847-85

Bland BH. 1986. The physiology and pharmacology of hippocampal formation theta rhythms. *Progress in neurobiology* 26: 1-54

Bland BH, Konopacki J, Dyck RH. 2002. Relationship between membrane potential oscillations and rhythmic discharges in identified hippocampal theta-related cells. *Journal of neurophysiology* 88: 3046-66

Boldyrev AA, Johnson P, Wei Y, Tan Y, Carpenter DO. 1999. Carnosine and taurine protect rat cerebellar granular cells from free radical damage. *Neuroscience Letters* 263: 169-72

Bonjean M, Baker T, Lemieux M, Timofeev I, Sejnowski T, Bazhenov M. 2011. Corticothalamic Feedback Controls Sleep Spindle Duration In Vivo. *The Journal of Neuroscience* 31: 9124-34

Borgers C, Kopell N. 2003. Synchronization in networks of excitatory and inhibitory neurons with sparse, random connectivity. *Neural computation* 15: 509-38

Bormann J. 2000. The 'ABC' of GABA receptors. *Trends in pharmacological sciences* 21: 16-9

Bormann J, Hamill OP, Sakmann B. 1987. Mechanism of anion permeation through channels gated by glycine and gamma-aminobutyric acid in mouse cultured spinal neurones. *The Journal of Physiology* 385: 243-86

Bornschlegl M, Asanuma H. 1987. Importance of the projection from the sensory to the motor cortex for recovery of motor function following partial thalamic lesion in the monkey. *Brain research* 437: 121-30

Boutrel B, Koob GF. 2004. What keeps us awake: the neuropharmacology of stimulants and wakefulness-promoting medications. *Sleep* 27: 1181-94

Bouyer JJ, Montaron MF, Rougeul A. 1981. Fast fronto-parietal rhythms during combined focused attentive behaviour and immobility in cat: cortical and thalamic localizations. *Electroencephalography and clinical neurophysiology* 51: 244-52

Bowery NG, Bettler B, Froestl W, Gallagher JP, Marshall F, et al. 2002. International Union of Pharmacology. XXXIII. Mammalian gamma-aminobutyric acid(B) receptors: structure and function. *Pharmacological reviews* 54: 247-64

Bowery NG, Hill DR, Hudson AL. 1983. Characteristics of GABAB receptor binding sites on rat whole brain synaptic membranes. *British journal of pharmacology* 78: 191-206

Bowery NG, Hudson AL, Price GW. 1987. GABAA and GABAB receptor site distribution in the rat central nervous system. *Neuroscience* 20: 365-83

Boyson SJ, McGonigle P, Molinoff PB. 1986. Quantitative autoradiographic localization of the D1 and D2 subtypes of dopamine receptors in rat brain. *J Neurosci* 6: 3177-88

Braak H, Braak E. 1976. The pyramidal cells of Betz within the cingulate and precentral gigantopyramidal field in the human brain. A Golgi and pigmentarchitectonic study. *Cell and tissue research* 172: 103-19

Bragin A, Jando G, Nadasdy Z, Hetke J, Wise K, Buzsaki G. 1995. Gamma (40-100 Hz) oscillation in the hippocampus of the behaving rat. *J Neurosci* 15: 47-60

Brecht M, Roth A, Sakmann B. 2003. Dynamic receptive fields of reconstructed pyramidal cells in layers 3 and 2 of rat somatosensory barrel cortex. *The Journal of Physiology* 553: 243-65

Brecht M, Sakmann B. 2002. Dynamic representation of whisker deflection by synaptic potentials in spiny stellate and pyramidal cells in the barrels and septa of layer 4 rat somatosensory cortex. *The Journal of physiology* 543: 49-70

Bressler SL, Freeman WJ. 1980. Frequency analysis of olfactory system EEG in cat, rabbit, and rat. *Electroencephalography and clinical neurophysiology* 50: 19-24

Brickley SG, Cull-Candy SG, Farrant M. 1996. Development of a tonic form of synaptic inhibition in rat cerebellar granule cells resulting from persistent activation of GABAA

receptors. *The Journal of physiology* 497 (Pt 3): 753-9

Brickley SG, Cull-Candy SG, Farrant M. 1999. Single-channel properties of synaptic and extrasynaptic GABAA receptors suggest differential targeting of receptor subtypes. *J Neurosci* 19: 2960-73

Brochier T, Boudreau MJ, Pare M, Smith AM. 1999. The effects of muscimol inactivation of small regions of motor and somatosensory cortex on independent finger movements and force control in the precision grip. *Experimental brain research* 128: 31-40

Brock J, Brown CC, Boucher J, Rippon G. 2002. The temporal binding deficit hypothesis of autism. *Development and psychopathology* 14: 209-24

Brodmann K. 1909. *Localization in the Cerebral Cortex.* Springer.

Brooks VB, Rudomin P, Slayman CL. 1961. Peripheral receptive fields of neurons in the cat's cerebral cortex. *Journal of Neurophysiology* 24: 302-25

Brown JH, Makman MH. 1972. Stimulation by dopamine of adenylate cyclase in retinal homogenates and of adenosine-3':5'-cyclic monophosphate formation in intact retina. *Proceedings of the National Academy of Sciences of the United States of America* 69: 539-43

Brown RE, Stevens DR, Haas HL. 2001. The physiology of brain histamine. *Progress in neurobiology* 63: 637-72

Brudzynski SM, Cruickshank JW, McLachlan RS. 1995. Cholinergic mechanisms in generalized seizures: importance of the zona incerta. *The Canadian journal of neurological sciences. Le journal canadien des sciences neurologiques* 22: 116-20

Brunel N, Wang XJ. 2003. What determines the frequency of fast network oscillations with irregular neural discharges? I. Synaptic dynamics and excitation-inhibition balance. *Journal of neurophysiology* 90: 415-30

Bruns A, Eckhorn R. 2004. Task-related coupling from high- to low-frequency signals among visual cortical areas in human subdural recordings. *International Journal of Psychophysiology* 51: 97-116

Buhl DL, Harris KD, Hormuzdi SG, Monyer H, Buzsaki G. 2003. Selective impairment of hippocampal gamma oscillations in connexin-36 knock-out mouse in vivo. *J Neurosci* 23: 1013-8

Buhl EH, Tamas G, Fisahn A. 1998. Cholinergic activation and tonic excitation induce persistent gamma oscillations in mouse somatosensory cortex in vitro. *The Journal of physiology* 513 (Pt 1): 117-26

Buldakova SL, Vorobjev VS, Sharonova IN, Samoilova MV, Magazanik LG. 1999. Characterization of AMPA receptor populations in rat brain cells by the use of subunit-specific open channel blocking drug, IEM-1460. *Brain research* 846: 52-8

Bureau I, von Saint Paul F, Svoboda K. 2006. Interdigitated Paralemniscal and Lemniscal Pathways in the Mouse Barrel Cortex. *PLoS Biology* 4: e382

Burkat PM, Yang J, Gingrich KJ. 2001. Dominant gating governing transient GABA(A) receptor activity: a first latency and Po/o analysis. *J Neurosci* 21: 7026-36

Burwell RD, Witter MP, Amaral DG. 1995. Perirhinal and postrhinal cortices of the rat: a review of the neuroanatomical literature and comparison with findings from the monkey brain. *Hippocampus* 5: 390-408

Buzsaki G. 1989. Two-stage model of memory trace formation: a role for "noisy" brain states. *Neuroscience* 31: 551-70

Buzsáki G. 2002. Theta Oscillations in the Hippocampus. *Neuron* 33: 325-40

Buzsáki G. 2006. *Rhythms of the brain.* Oxford: Oxford University Press.

Buzsáki G, Anastassiou CA, Koch C. 2012. The origin of extracellular fields and currents — EEG, ECoG, LFP and spikes. *Nat Rev Neurosci* 13: 407-20

Buzsaki G, Buhl DL, Harris KD, Csicsvari J, Czeh B, Morozov A. 2003. Hippocampal network patterns of activity in the mouse. *Neuroscience* 116: 201-11

Buzsaki G, Chrobak JJ. 1995. Temporal structure in spatially organized neuronal ensembles: a role for interneuronal networks. *Current opinion in neurobiology* 5: 504-10

Buzsaki G, Leung LW, Vanderwolf CH. 1983. Cellular bases of hippocampal EEG in the behaving rat. *Brain research* 287: 139-71

Buzsaki G, Wang XJ. 2012. Mechanisms of gamma oscillations. *Annual review of neuroscience* 35: 203-25

Buzsáki G, Watson BO. 2012. Brain rhythms and neural syntax: implications for efficient coding of cognitive content and neuropsychiatric disease. *Dialogues in Clinical Neuroscience* 14: 345-67

Caixeta FV, Cornelio AM, Scheffer-Teixeira R, Ribeiro S, Tort AB. 2013. Ketamine alters oscillatory coupling in the hippocampus. *Scientific reports* 3: 2348

Calipari ES, Ferris MJ. 2013. Amphetamine mechanisms and actions at the dopamine terminal revisited. *J Neurosci* 33: 8923-5

Campbell SL, Mathew SS, Hablitz JJ. 2007. Pre- and postsynaptic effects of kainate on layer II/III pyramidal cells in rat neocortex. *Neuropharmacology* 53: 37-47

Canolty RT, Edwards E, Dalal SS, Soltani M, Nagarajan SS, et al. 2006. High gamma power is phase-locked to theta oscillations in human neocortex. *Science* 313: 1626-8

Canolty RT, Knight RT. 2010. The functional role of cross-frequency coupling. *Trends in cognitive sciences* 14: 506-15

Cardin JA, Carlen M, Meletis K, Knoblich U, Zhang F, et al. 2009. Driving fast-spiking cells induces gamma rhythm and controls sensory responses. *Nature* 459: 663-67

Carlsson A. 2001. A paradigm shift in brain research. *Science* 294: 1021-4

Carlsson A, Waters N, Holm-Waters S, Tedroff J, Nilsson M, Carlsson ML. 2001. Interactions between monoamines, glutamate, and GABA in schizophrenia: new evidence. *Annual review of pharmacology and toxicology* 41: 237-60

Carracedo LM, Kjeldsen H, Cunnington L, Jenkins A, Schofield I, et al. 2013. A Neocortical Delta Rhythm Facilitates Reciprocal Interlaminar Interactions via Nested Theta Rhythms. *The Journal of Neuroscience* 33: 10750-61

Carskadon MA, Dement WC. 2011. Chapter 2 - Normal Human Sleep: An Overview.

Carta M, Fievre S, Gorlewicz A, Mulle C. 2014. Kainate receptors in the hippocampus. *The European journal of neuroscience* 39: 1835-44

Carvalho M, Carmo H, Costa VM, Capela JP, Pontes H, et al. 2012. Toxicity of amphetamines: an update. *Archives of toxicology* 86: 1167-231

Cauli B, Audinat E, Lambolez B, Angulo MC, Ropert N, et al. 1997. Molecular and physiological diversity of cortical nonpyramidal cells. *J Neurosci* 17: 3894-906

Caviness VS, Jr. 1975. Architectonic map of neocortex of the normal mouse. *The Journal of comparative neurology* 164: 247-63

Ceci A, Brambilla A, Duranti P, Grauert M, Grippa N, Borsini F. 1999. Effect of antipsychotic drugs and selective dopaminergic antagonists on dopamine-induced facilitatory activity in prelimbic cortical pyramidal neurons. An in vitro study. *Neuroscience* 93: 107-15

Celio MR. 1990. Calbindin D-28k and parvalbumin in the rat nervous system. *Neuroscience* 35: 375-475

Chavas J, Marty A. 2003. Coexistence of excitatory and inhibitory GABA synapses in the cerebellar interneuron network. *J Neurosci* 23: 2019-31

Chehelcheraghi M, van Leeuwen C, Steur E, Nakatani C. 2017. A neural mass model of cross frequency coupling. *PloS one* 12: e0173776

Chen JY, Chauvette S, Skorheim S, Timofeev I, Bazhenov M. 2012. Interneuron-mediated inhibition synchronizes neuronal activity during slow oscillation. *The Journal of physiology* 590: 3987-4010

Chen S, Wang J, Siegelbaum SA. 2001. Properties of hyperpolarization-activated pacemaker current defined by coassembly of HCN1 and HCN2 subunits and basal modulation by cyclic nucleotide. *The Journal of general physiology* 117: 491-504

Chen W, Zhang JJ, Hu GY, Wu CP. 1996. Electrophysiological and morphological properties of pyramidal and nonpyramidal neurons in the cat motor cortex in vitro. *Neuroscience* 73: 39-55

Cherubini E, Conti F. 2001. Generating diversity at GABAergic synapses. *Trends in neurosciences* 24: 155-62

Chu Z, Galarreta M, Hestrin S. 2003. Synaptic interactions of late-spiking neocortical neurons in layer 1. *J Neurosci* 23: 96-102

Clancy B, Cauller LJ. 1999. Widespread projections from subgriseal neurons (layer VII) to

layer I in adult rat cortex. *The Journal of comparative neurology* 407: 275-86

Clapham DE, Runnels LW, Strubing C. 2001. The TRP ion channel family. *Nat Rev Neurosci* 2: 387-96

Clemens Z, Borbély C, Weiss B, Erőss L, Szűcs A, et al. 2013. Increased mesiotemporal delta activity characterizes virtual navigation in humans. *Neuroscience Research* 76: 67-75

Clemens Z, Molle M, Eross L, Barsi P, Halasz P, Born J. 2007. Temporal coupling of parahippocampal ripples, sleep spindles and slow oscillations in humans. *Brain : a journal of neurology* 130: 2868-78

Cohen MX. 2008. Assessing transient cross-frequency coupling in EEG data. *Journal of neuroscience methods* 168: 494-9

Cohen MX, Axmacher N, Lenartz D, Elger CE, Sturm V, Schlaepfer TE. 2009. Good vibrations: cross-frequency coupling in the human nucleus accumbens during reward processing. *Journal of cognitive neuroscience* 21: 875-89

Cohen MX, Axmacher N, Lenartz D, Elger CE, Sturm V, Schlaepfer TE. 2009. Nuclei accumbens phase synchrony predicts decision-making reversals following negative feedback. *J Neurosci* 29: 7591-8

Cohen MX, Elger CE, Fell J. 2009. Oscillatory activity and phase-amplitude coupling in the human medial frontal cortex during decision making. *Journal of cognitive neuroscience* 21: 390-402

Colebatch JG, Deiber MP, Passingham RE, Friston KJ, Frackowiak RS. 1991. Regional cerebral blood flow during voluntary arm and hand movements in human subjects. *Journal of neurophysiology* 65: 1392-401

Colgin LL, Denninger T, Fyhn M, Hafting T, Bonnevie T, et al. 2009. Frequency of gamma oscillations routes flow of information in the hippocampus. *Nature* 462: 353-57

Compte A, Sanchez-Vives MV, McCormick DA, Wang XJ. 2003. Cellular and network mechanisms of slow oscillatory activity (<1 Hz) and wave propagations in a cortical network model. *Journal of neurophysiology* 89: 2707-25

Condorelli DF, Belluardo N, Trovato-Salinaro A, Mudo G. 2000. Expression of Cx36 in mammalian neurons. *Brain research. Brain research reviews* 32: 72-85

Conn PJ, Pin JP. 1997. Pharmacology and functions of metabotropic glutamate receptors. *Annual review of pharmacology and toxicology* 37: 205-37

Connolly CN, Wafford KA. 2004. The Cys-loop superfamily of ligand-gated ion channels: the impact of receptor structure on function. *Biochemical Society transactions* 32: 529-34

Connors BW. 2012. Tales of a Dirty Drug: Carbenoxolone, Gap Junctions, and Seizures. *Epilepsy Currents* 12: 66-68

Connors BW, Gutnick MJ, Prince DA. 1982. Electrophysiological properties of neocortical neurons in vitro. *Journal of neurophysiology* 48: 1302-20

Contractor A, Mulle C, Swanson GT. 2011. Kainate receptors coming of age: milestones of two decades of research. *Trends in neurosciences* 34: 154-63

Contreras D, Steriade M. 1995. Cellular basis of EEG slow rhythms: a study of dynamic corticothalamic relationships. *J Neurosci* 15: 604-22

Cossart R, Epsztein J, Tyzio R, Becq H, Hirsch J, et al. 2002. Quantal release of glutamate generates pure kainate and mixed AMPA/kainate EPSCs in hippocampal neurons. *Neuron* 35: 147-59

Cossart R, Esclapez M, Hirsch JC, Bernard C, Ben-Ari Y. 1998. GluR5 kainate receptor activation in interneurons increases tonic inhibition of pyramidal cells. *Nat Neurosci* 1: 470-8

Cossart R, Tyzio R, Dinocourt C, Esclapez M, Hirsch JC, et al. 2001. Presynaptic Kainate Receptors that Enhance the Release of GABA on CA1 Hippocampal Interneurons. *Neuron* 29: 497-508

Cragg SJ, Baufreton J, Xue Y, Bolam JP, Bevan MD. 2004. Synaptic release of dopamine in the subthalamic nucleus. *The European journal of neuroscience* 20: 1788-802

Creutzfeldt OD, Watanabe S, Lux HD. 1966. Relations between EEG phenomena and potentials of single cortical cells. I. Evoked responses after thalamic and erpicortical stimulation. *Electroencephalography and clinical neurophysiology* 20: 1-18

Crunelli V, Hughes SW. 2010. The slow (<1 Hz) rhythm of non-REM sleep: a dialogue between three cardinal oscillators. *Nat Neurosci* 13: 9-17

Csercsa R, Dombovari B, Fabo D, Wittner L, Eross L, et al. 2010. Laminar analysis of slow wave activity in humans. *Brain : a journal of neurology* 133: 2814-29

Csicsvari J, Jamieson B, Wise KD, Buzsaki G. 2003. Mechanisms of gamma oscillations in the hippocampus of the behaving rat. *Neuron* 37: 311-22

Cunningham MO, Davies CH, Buhl EH, Kopell N, Whittington MA. 2003. Gamma oscillations induced by kainate receptor activation in the entorhinal cortex in vitro. *J Neurosci* 23: 9761-9

Cunningham MO, Halliday DM, Davies CH, Traub RD, Buhl EH, Whittington MA. 2004. Coexistence of gamma and high-frequency oscillations in rat medial entorhinal cortex in vitro. *The Journal of physiology* 559: 347-53

Curro Dossi R, Pare D, Steriade M. 1992. Various types of inhibitory postsynaptic potentials in anterior thalamic cells are differentially altered by stimulation of laterodorsal tegmental cholinergic nucleus. *Neuroscience* 47: 279-89

Daberkow DP, Brown HD, Bunner KD, Kraniotis SA, Doellman MA, et al. 2013. Amphetamine paradoxically augments exocytotic dopamine release and phasic dopamine signals. *J Neurosci* 33: 452-63

Dale LB, Bhattacharya M, Anborgh PH, Murdoch B, Bhatia M, et al. 2000. G protein-coupled receptor kinase-mediated desensitization of metabotropic glutamate receptor 1A protects against cell death. *The Journal of biological chemistry* 275: 38213-20

Das NN, Gastaut H. 1957. Variation de l'activité électrique du cerveau, du coeur et des muscles squelettiques au cours de la méditation et de l'extase yogique. *Electroenceph. clin. Neurophysiol.*: 211-19

Dawson TM, Gehlert DR, McCabe RT, Barnett A, Wamsley JK. 1986. D-1 dopamine receptors in the rat brain: a quantitative autoradiographic analysis. *J Neurosci* 6: 2352-65

de Kock CP, Sakmann B. 2008. High frequency action potential bursts (>or= 100 Hz) in L2/3 and L5B thick tufted neurons in anaesthetized and awake rat primary somatosensory cortex. *The Journal of physiology* 586: 3353-64

Dearry A, Gingrich JA, Falardeau P, Fremeau RT, Jr., Bates MD, Caron MG. 1990. Molecular cloning and expression of the gene for a human D1 dopamine receptor. *Nature* 347: 72-6

DeCoteau WE, Thorn C, Gibson DJ, Courtemanche R, Mitra P, et al. 2007. Learning-related coordination of striatal and hippocampal theta rhythms during acquisition of a procedural maze task. *Proceedings of the National Academy of Sciences* 104: 5644-49

Deken SL, Wang D, Quick MW. 2003. Plasma Membrane GABA Transporters Reside on Distinct Vesicles and Undergo Rapid Regulated Recycling. *The Journal of Neuroscience* 23: 1563-68

Demarque M, Represa A, Becq H, Khalilov I, Ben-Ari Y, Aniksztejn L. 2002. Paracrine intercellular communication by a Ca2+- and SNARE-independent release of GABA and glutamate prior to synapse formation. *Neuron* 36: 1051-61

Dement W, Kleitman N. 1957. The relation of eye movements during sleep to dream activity: an objective method for the study of dreaming. *J Exp Psychol* 53: 339-46

Demiralp T, Bayraktaroglu Z, Lenz D, Junge S, Busch NA, et al. 2007. Gamma amplitudes are coupled to theta phase in human EEG during visual perception. *International Journal of Psychophysiology* 64: 24-30

Descarries L, Lemay B, Doucet G, Berger B. 1987. Regional and laminar density of the dopamine innervation in adult rat cerebral cortex. *Neuroscience* 21: 807-24

Deschenes M, Labelle A, Landry P. 1979. Morphological characterization of slow and fast pyramidal tract cells in the cat. *Brain research* 178: 251-74

Destexhe A, Babloyantz A, Sejnowski TJ. 1993. Ionic mechanisms for intrinsic slow oscillations in thalamic relay neurons. *Biophysical Journal* 65: 1538-52

Deuchars J, Thomson AM. 1996. CA1 pyramid-pyramid connections in rat hippocampus in vitro: dual intracellular recordings with biocytin filling. *Neuroscience* 74: 1009-18

Di Chiara G, Bassareo V. 2007. Reward system and addiction: what dopamine does and

doesn't do. *Current opinion in pharmacology* 7: 69-76

Dickinson R, Awaiz S, Whittington MA, Lieb WR, Franks NP. 2003. The effects of general anaesthetics on carbachol-evoked gamma oscillations in the rat hippocampus in vitro. *Neuropharmacology* 44: 864-72

Dingledine R, Borges K, Bowie D, Traynelis SF. 1999. The glutamate receptor ion channels. *Pharmacological reviews* 51: 7-61

Donoghue JP, Leibovic S, Sanes JN. 1992. Organization of the forelimb area in squirrel monkey motor cortex: representation of digit, wrist, and elbow muscles. *Experimental brain research* 89: 1-19

Donoghue JP, Parham C. 1983. Afferent connections of the lateral agranular field of the rat motor cortex. *The Journal of comparative neurology* 217: 390-404

Donoghue JP, Sanes JN, Hatsopoulos NG, Gaal G. 1998. Neural discharge and local field potential oscillations in primate motor cortex during voluntary movements. *Journal of neurophysiology* 79: 159-73

Donoghue JP, Wise SP. 1982. The motor cortex of the rat: cytoarchitecture and microstimulation mapping. *The Journal of comparative neurology* 212: 76-88

Dossi RC, Nunez A, Steriade M. 1992. Electrophysiology of a slow (0.5-4 Hz) intrinsic oscillation of cat thalamocortical neurones in vivo. *The Journal of physiology* 447: 215-34

Douglas RJ, Martin KA. 2004. Neuronal circuits of the neocortex. *Annual review of neuroscience* 27: 419-51

Draguhn A, Traub RD, Schmitz D, Jefferys JG. 1998. Electrical coupling underlies high-frequency oscillations in the hippocampus in vitro. *Nature* 394: 189-92

Dugladze T, Maziashvili N, Borgers C, Gurgenidze S, Haussler U, et al. 2013. GABA(B) autoreceptor-mediated cell type-specific reduction of inhibition in epileptic mice. *Proceedings of the National Academy of Sciences of the United States of America* 110: 15073-8

Dunlap K, Fischbach GD. 1981. Neurotransmitters decrease the calcium conductance activated by depolarization of embryonic chick sensory neurones. *The Journal of Physiology* 317: 519-35

Edin BB, Johansson N. 1995. Skin strain patterns provide kinaesthetic information to the human central nervous system. *The Journal of physiology* 487: 243-51

Edwards FA, Konnerth A, Sakmann B. 1990. Quantal analysis of inhibitory synaptic transmission in the dentate gyrus of rat hippocampal slices: a patch-clamp study. *The Journal of physiology* 430: 213-49

Egebjerg J, Bettler B, Hermans-Borgmeyer I, Heinemann S. 1991. Cloning of a cDNA for a glutamate receptor subunit activated by kainate but not AMPA. *Nature* 351: 745-8

Egger V, Nevian T, Bruno RM. 2008. Subcolumnar dendritic and axonal organization of spiny stellate and star pyramid neurons within a barrel in rat somatosensory cortex. *Cerebral cortex (New York, N.Y. : 1991)* 18: 876-89

Ehringer H, Hornykiewicz O. 1960. Distribution of noradrenaline and dopamine (3-hydroxytyramine) in the human brain and their behavior in diseases of the extrapyramidal system. *Parkinsonism & related disorders* 4: 53-7

Ekstrom AD, Caplan JB, Ho E, Shattuck K, Fried I, Kahana MJ. 2005. Human hippocampal theta activity during virtual navigation. *Hippocampus* 15: 881-9

Elul R. 1971. The genesis of the EEG. *International review of neurobiology* 15: 227-72

Ermentrout GB, Kopell N. 1998. Fine structure of neural spiking and synchronization in the presence of conduction delays. *Proceedings of the National Academy of Sciences of the United States of America* 95: 1259-64

Espana RA, Scammell TE. 2004. Sleep neurobiology for the clinician. *Sleep* 27: 811-20

Fabri M, Burton H. 1991. Topography of connections between primary somatosensory cortex and posterior complex in rat: a multiple fluorescent tracer study. *Brain research* 538: 351-7

Farkas T, Kis Z, Toldi J, Wolff JR. 1999. Activation of the primary motor cortex by somatosensory stimulation in adult rats is mediated mainly by associational connections from the somatosensory cortex. *Neuroscience* 90: 353-61

Farrant M, Nusser Z. 2005. Variations on an inhibitory theme: phasic and tonic activation of

GABA(A) receptors. *Nat Rev Neurosci* 6: 215-29

Feinberg I, Campbell IG. 1998. Haloperidol potentiates the EEG slowing of MK-801 despite blocking its motor effects: implications for the PCP model of schizophrenia. *Neuroreport* 9: 2189-93

Feinberg I, Floyd TC. 1979. Systematic trends across the night in human sleep cycles. *Psychophysiology* 16: 283-91

Feldmeyer D, Egger V, Lubke J, Sakmann B. 1999. Reliable synaptic connections between pairs of excitatory layer 4 neurones within a single 'barrel' of developing rat somatosensory cortex. *The Journal of physiology* 521 Pt 1: 169-90

Fell J, Elfadil H, Roschke J, Burr W, Klaver P, et al. 2002. Human scalp recorded sigma activity is modulated by slow EEG oscillations during deep sleep. *The International journal of neuroscience* 112: 893-900

Fell J, Fernandez G, Klaver P, Elger CE, Fries P. 2003. Is synchronized neuronal gamma activity relevant for selective attention? *Brain research. Brain research reviews* 42: 265-72

Fell J, Klaver P, Lehnertz K, Grunwald T, Schaller C, et al. 2001. Human memory formation is accompanied by rhinal-hippocampal coupling and decoupling. *Nat Neurosci* 4: 1259-64

Fellous JM, Sejnowski TJ. 2000. Cholinergic induction of oscillations in the hippocampal slice in the slow (0.5-2 Hz), theta (5-12 Hz), and gamma (35-70 Hz) bands. *Hippocampus* 10: 187-97

Ferezou I, Haiss F, Gentet LJ, Aronoff R, Weber B, Petersen CC. 2007. Spatiotemporal dynamics of cortical sensorimotor integration in behaving mice. *Neuron* 56: 907-23

FerrisJ ESCaMJ. 2013. Amphetamine Mechanisms and Actions at the Dopamine Terminal Revisited. *Neurosci.* 33: 8923–25

Finelli LA, Borbely AA, Achermann P. 2001. Functional topography of the human nonREM sleep electroencephalogram. *The European journal of neuroscience* 13: 2282-90

Fisahn A, Contractor A, Traub RD, Buhl EH, Heinemann SF, McBain CJ. 2004. Distinct roles for the kainate receptor subunits GluR5 and GluR6 in kainate-induced hippocampal gamma oscillations. *J Neurosci* 24: 9658-68

Fisahn A, Pike FG, Buhl EH, Paulsen O. 1998. Cholinergic induction of network oscillations at 40 Hz in the hippocampus in vitro. *Nature* 394: 186-9

Fisahn A, Yamada M, Duttaroy A, Gan JW, Deng CX, et al. 2002. Muscarinic induction of hippocampal gamma oscillations requires coupling of the M1 receptor to two mixed cation currents. *Neuron* 33: 615-24

Fishell G, Rudy B. 2011. Mechanisms of inhibition within the telencephalon: "where the wild things are". *Annual review of neuroscience* 34: 535-67

Fisher RS, Alger BE. 1984. Electrophysiological mechanisms of kainic acid-induced epileptiform activity in the rat hippocampal slice. *J Neurosci* 4: 1312-23

Fisher RS, Webber WR, Lesser RP, Arroyo S, Uematsu S. 1992. High-frequency EEG activity at the start of seizures. *Journal of clinical neurophysiology : official publication of the American Electroencephalographic Society* 9: 441-8

Fleckenstein AE, Volz TJ, Riddle EL, Gibb JW, Hanson GR. 2007. New insights into the mechanism of action of amphetamines. *Annual review of pharmacology and toxicology* 47: 681-98

Florez CM, McGinn RJ, Lukankin V, Marwa I, Sugumar S, et al. 2015. In vitro recordings of human neocortical oscillations. *Cerebral cortex (New York, N.Y. : 1991)* 25: 578-97

Ford JM, Roach BJ, Hoffman RS, Mathalon DH. 2008. The dependence of P300 amplitude on gamma synchrony breaks down in schizophrenia. *Brain research* 1235: 133-42

Freeman WJ. 1975. CHAPTER 1 - Topological Properties In *Mass Action in the Nervous System*, pp. 1-50. San Diego: Academic Press

Freeman WJ. 1975. CHAPTER 3 - Amplitude-Dependent Properties In *Mass Action in the Nervous System*, pp. 121-71. San Diego: Academic Press

Freeman WJ. 2007. Definitions of state variables and state space for brain-computer interface: Part 1. Multiple hierarchical levels of brain function. *Cognitive Neurodynamics* 1: 3-14

Frerking M, Malenka RC, Nicoll RA. 1998. Synaptic activation of kainate receptors on

hippocampal interneurons. *Nat Neurosci* 1: 479-86

Frerking M, Nicoll RA. 2000. Synaptic kainate receptors. *Current opinion in neurobiology* 10: 342-51

Frerking M, Ohliger-Frerking P. 2002. AMPA Receptors and Kainate Receptors Encode Different Features of Afferent Activity. *The Journal of neuroscience : the official journal of the Society for Neuroscience* 22: 7434-43

Frerking M, Schmitz D, Zhou Q, Johansen J, Nicoll RA. 2001. Kainate receptors depress excitatory synaptic transmission at CA3-->CA1 synapses in the hippocampus via a direct presynaptic action. *J Neurosci* 21: 2958-66

Frerking M, Wilson M. 1996. Saturation of postsynaptic receptors at central synapses? *Current opinion in neurobiology* 6: 395-403

Freund TF, Katona I. 2007. Perisomatic Inhibition. *Neuron* 56: 33-42

Frost Jr JD, Kellaway P, Gol A. 1966. Single-unit discharges in isolated cerebral cortex. *Experimental Neurology* 14: 305-16

Fuchs EC, Doheny H, Faulkner H, Caputi A, Traub RD, et al. 2001. Genetically altered AMPA-type glutamate receptor kinetics in interneurons disrupt long-range synchrony of gamma oscillation. *Proceedings of the National Academy of Sciences* 98: 3571-76

Fuchs EC, Zivkovic AR, Cunningham MO, Middleton S, Lebeau FE, et al. 2007. Recruitment of parvalbumin-positive interneurons determines hippocampal function and associated behavior. *Neuron* 53: 591-604

Fuentealba P, Begum R, Capogna M, Jinno S, Marton LF, et al. 2008. Ivy cells: a population of nitric-oxide-producing, slow-spiking GABAergic neurons and their involvement in hippocampal network activity. *Neuron* 57: 917-29

Fukuda T, Kosaka T. 2003. Ultrastructural study of gap junctions between dendrites of parvalbumin-containing GABAergic neurons in various neocortical areas of the adult rat. *Neuroscience* 120: 5-20

Fukuda T, Kosaka T, Singer W, Galuske RA. 2006. Gap junctions among dendrites of cortical GABAergic neurons establish a dense and widespread intercolumnar network. *J Neurosci* 26: 3434-43

Gabbott PL, Somogyi P. 1986. Quantitative distribution of GABA-immunoreactive neurons in the visual cortex (area 17) of the cat. *Experimental brain research* 61: 323-31

Gage PW. 1992. Activation and modulation of neuronal K+ channels by GABA. *Trends in Neurosciences* 15: 46-51

Gais S, Plihal W, Wagner U, Born J. 2000. Early sleep triggers memory for early visual discrimination skills. *Nat Neurosci* 3: 1335-39

Galarreta M, Hestrin S. 1999. A network of fast-spiking cells in the neocortex connected by electrical synapses. *Nature* 402: 72-5

Galarreta M, Hestrin S. 2002. Electrical and chemical synapses among parvalbumin fast-spiking GABAergic interneurons in adult mouse neocortex. *Proceedings of the National Academy of Sciences* 99: 12438-43

Galazo MJ, Martinez-Cerdeño V, Porrero C, Clascá F. 2008. Embryonic and Postnatal Development of the Layer I–Directed ("Matrix") Thalamocortical System in the Rat. *Cerebral Cortex* 18: 344-63

Gao WJ, Goldman-Rakic PS. 2003. Selective modulation of excitatory and inhibitory microcircuits by dopamine. *Proceedings of the National Academy of Sciences of the United States of America* 100: 2836-41

Gao W-J, Zheng Z-H. 2004. Target-specific differences in somatodendritic morphology of layer V pyramidal neurons in rat motor cortex. *The Journal of Comparative Neurology* 476: 174-85

Garcia-Cabezas MA, Barbas H. 2014. Area 4 has layer IV in adult primates. *The European journal of neuroscience* 39: 1824-34

Gee S, Ellwood,I.,Patel,T.,Luongo,F.,Deisseroth,K.,andSohal,V.S. 2012. Synaptic activity unmasks dopamine D2 receptor modulation of a specificclass of layer V pyramidal neurons in prefrontal cortex. *J. Neurosci* 32: 4959–71.

Geiger JR, Melcher T, Koh DS, Sakmann B, Seeburg PH, et al. 1995. Relative abundance of subunit mRNAs determines gating and Ca2+ permeability of AMPA receptors in

principal neurons and interneurons in rat CNS. *Neuron* 15: 193-204

Geisler C, Brunel N, Wang XJ. 2005. Contributions of intrinsic membrane dynamics to fast network oscillations with irregular neuronal discharges. *Journal of neurophysiology* 94: 4344-61

George R, Haslett WL, Jenden DJ. 1964. A cholinergic mechanism in the brainstem reticular formation: Induction of paradoxical sleep. *International journal of neuropharmacology* 3: 541-52

German CL, Baladi MG, McFadden LM, Hanson GR, Fleckenstein AE. 2015. Regulation of the Dopamine and Vesicular Monoamine Transporters: Pharmacological Targets and Implications for Disease. *Pharmacological reviews* 67: 1005-24

Gibbs EL, Gibbs FA. 1951. Electroencephalographic evidence of thalamic and hypothalamic epilepsy. *Neurology* 1: 136-44

Gibson JR, Beierlein M, Connors BW. 1999. Two networks of electrically coupled inhibitory neurons in neocortex. *Nature* 402: 75-9

Gil Z, Connors BW, Amitai Y. 1997. Differential regulation of neocortical synapses by neuromodulators and activity. *Neuron* 19: 679-86

Gittis AH, Leventhal DK, Fensterheim BA, Pettibone JR, Berke JD, Kreitzer AC. 2011. Selective inhibition of striatal fast-spiking interneurons causes dyskinesias. *J Neurosci* 31: 15727-31

Glickfeld LL, Roberts JD, Somogyi P, Scanziani M. 2009. Interneurons hyperpolarize pyramidal cells along their entire somatodendritic axis. *Nat Neurosci* 12: 21-3

Gloveli T, Dugladze T, Rotstein HG, Traub RD, Monyer H, et al. 2005. Orthogonal arrangement of rhythm-generating microcircuits in the hippocampus. *Proceedings of the National Academy of Sciences of the United States of America* 102: 13295-300

Gloveli T, Dugladze T, Saha S, Monyer H, Heinemann U, et al. 2005. Differential involvement of oriens/pyramidale interneurones in hippocampal network oscillations in vitro. *The Journal of Physiology* 562: 131-47

Goldin M, Epsztein J, Jorquera I, Represa A, Ben-Ari Y, et al. 2007. Synaptic kainate receptors tune oriens-lacunosum moleculare interneurons to operate at theta frequency. *J Neurosci* 27: 9560-72

Golebiewski H, Eckersdorf B, Konopacki J. 1996. Cholinergic/GABAergic interaction in the production of EEG theta oscillations in rat hippocampal formation in vitro. *Acta neurobiologiae experimentalis* 56: 147-53

Gonchar Y, Wang Q, Burkhalter A. 2007. Multiple distinct subtypes of GABAergic neurons in mouse visual cortex identified by triple immunostaining. *Frontiers in neuroanatomy* 1: 3

Gonzalez-Islas C, Hablitz JJ. 2001. Dopamine inhibition of evoked IPSCs in rat prefrontal cortex. *Journal of neurophysiology* 86: 2911-8

Gordon JA. 2011. Oscillations and hippocampal-prefrontal synchrony. *Current opinion in neurobiology* 21: 486-91

Gorelova N, Seamans JK, Yang CR. 2002. Mechanisms of dopamine activation of fast-spiking interneurons that exert inhibition in rat prefrontal cortex. *Journal of neurophysiology* 88: 3150-66

Govindaiah G, Cox CL. 2005. Excitatory actions of dopamine via D1-like receptors in the rat lateral geniculate nucleus. *Journal of neurophysiology* 94: 3708-18

Graham DG, Tiffany SM, Bell WR, Jr., Gutknecht WF. 1978. Autoxidation versus covalent binding of quinones as the mechanism of toxicity of dopamine, 6-hydroxydopamine, and related compounds toward C1300 neuroblastoma cells in vitro. *Molecular pharmacology* 14: 644-53

Graham SH, Chen J, Lan JQ, Simon RP. 1996. A dose-response study of neuroprotection using the AMPA antagonist NBQX in rat focal cerebral ischemia. *The Journal of pharmacology and experimental therapeutics* 276: 1-4

Graziane NM, Yuen EY, Yan Z. 2009. Dopamine D4 Receptors Regulate GABAA Receptor Trafficking via an Actin/Cofilin/Myosin-dependent Mechanism. *The Journal of biological chemistry* 284: 8329-36

Grenier F, Timofeev I, Steriade M. 2001. Focal synchronization of ripples (80-200 Hz) in

neocortex and their neuronal correlates. *Journal of neurophysiology* 86: 1884-98

Griffiths MJ, Messent M, MacAllister RJ, Evans TW. 1993. Aminoguanidine selectively inhibits inducible nitric oxide synthase. *British journal of pharmacology* 110: 963-8

Gulledge AT, Jaffe DB. 2001. Multiple effects of dopamine on layer V pyramidal cell excitability in rat prefrontal cortex. *Journal of neurophysiology* 86: 586-95

Gulledge AT, Stuart GJ. 2003. Excitatory actions of GABA in the cortex. *Neuron* 37: 299-309

Guntekin B, Saatci E, Yener G. 2008. Decrease of evoked delta, theta and alpha coherences in Alzheimer patients during a visual oddball paradigm. *Brain research* 1235: 109-16

Gupta A, Wang Y, Markram H. 2000. Organizing Principles for a Diversity of GABAergic Interneurons and Synapses in the Neocortex. *Science* 287: 273-78

Gurden H, Takita M, Jay TM. 2000. Essential role of D1 but not D2 receptors in the NMDA receptor-dependent long-term potentiation at hippocampal-prefrontal cortex synapses in vivo. *J Neurosci* 20: Rc106

Haas KF, Macdonald RL. 1999. GABA(A) receptor subunit γ2 and δ subtypes confer unique kinetic properties on recombinant GABA(A) receptor currents in mouse fibroblasts. *The Journal of Physiology* 514: 27-45

Haider B, Duque A, Hasenstaub AR, McCormick DA. 2006. Neocortical network activity in vivo is generated through a dynamic balance of excitation and inhibition. *J Neurosci* 26: 4535-45

Hajos F, Garthwaite J, Garthwaite G, Csillag A. 1989. Morphology of supravital brain slices pre-incubated in a physiological solution prior to fixation. *Acta morphologica Hungarica* 37: 181-99

Hajos M, Gartside,S.E.,Varga,V.,andSharp,T. 2003. Invivo inhibition of neuronal activity in the rat ventro medial prefrontal cortex by midbrain - raphenuclei:role of 5-HT1A receptors. *Neuropharmacology* 45: 72-81

Hajos N, Mody I. 2009. Establishing a physiological environment for visualized in vitro brain slice recordings by increasing oxygen supply and modifying aCSF content. *Journal of neuroscience methods* 183: 107-13

Hajos N, Nusser Z, Rancz EA, Freund TF, Mody I. 2000. Cell type- and synapse-specific variability in synaptic GABAA receptor occupancy. *The European journal of neuroscience* 12: 810-8

Hajos N, Paulsen O. 2009. Network mechanisms of gamma oscillations in the CA3 region of the hippocampus. *Neural networks : the official journal of the International Neural Network Society* 22: 1113-9

Halabisky B, Shen F, Huguenard JR, Prince DA. 2006. Electrophysiological classification of somatostatin-positive interneurons in mouse sensorimotor cortex. *Journal of neurophysiology* 96: 834-45

Halasy K, Buhl EH, Lorinczi Z, Tamas G, Somogyi P. 1996. Synaptic target selectivity and input of GABAergic basket and bistratified interneurons in the CA1 area of the rat hippocampus. *Hippocampus* 6: 306-29

Hallett PJ, Spoelgen R, Hyman BT, Standaert DG, Dunah AW. 2006. Dopamine D1 activation potentiates striatal NMDA receptors by tyrosine phosphorylation-dependent subunit trafficking. *J Neurosci* 26: 4690-700

Hamdy S, Aziz Q, Rothwell JC, Hobson A, Thompson DG. 1998. Sensorimotor modulation of human cortical swallowing pathways. *The Journal of physiology* 506 (Pt 3): 857-66

Hamdy S, Rothwell JC, Aziz Q, Singh KD, Thompson DG. 1998. Long-term reorganization of human motor cortex driven by short-term sensory stimulation. *Nat Neurosci* 1: 64-8

Handel B, Haarmeier T. 2009. Cross-frequency coupling of brain oscillations indicates the success in visual motion discrimination. *NeuroImage* 45: 1040-6

Harmony T. 2013. The functional significance of delta oscillations in cognitive processing. *Frontiers in Integrative Neuroscience* 7: 83

Harteneck C, Plant TD, Schultz G. 2000. From worm to man: three subfamilies of TRP channels. *Trends in neurosciences* 23: 159-66

Hasenstaub A, Shu Y, Haider B, Kraushaar U, Duque A, McCormick DA. 2005. Inhibitory postsynaptic potentials carry synchronized frequency information in active cortical networks. *Neuron* 47: 423-35

Hastings TG, Lewis DA, Zigmond MJ. 1996. Role of oxidation in the neurotoxic effects of intrastriatal dopamine injections. *Proceedings of the National Academy of Sciences of the United States of America* 93: 1956-61

Hayashi T, Nagai K. *Abstr. Commun XXth Int. Physiol Congr 1956*: 410.

He BJ, Zempel JM, Snyder AZ, Raichle ME. 2010. The temporal structures and functional significance of scale-free brain activity. *Neuron* 66: 353-69

Helm J, Akgul G, Wollmuth LP. 2013. Subgroups of parvalbumin-expressing interneurons in layers 2/3 of the visual cortex. *Journal of neurophysiology* 109: 1600-13

Helmholtz Hv, Southall JPC. 2011. *Helmholtz's treatise on physiological optics* Vol. 1.

Hentschke H, Perkins MG, Pearce RA, Banks MI. 2007. Muscarinic blockade weakens interaction of gamma with theta rhythms in mouse hippocampus. *The European journal of neuroscience* 26: 1642-56

Herb A, Burnashev N, Werner P, Sakmann B, Wisden W, Seeburg PH. 1992. The KA-2 subunit of excitatory amino acid receptors shows widespread expression in brain and forms ion channels with distantly related subunits. *Neuron* 8: 775-85

Hernandez-Perez JJ, Gutierrez-Guzman BE, Lopez-Vazquez MA, Olvera-Cortes ME. 2015. Supramammillary serotonin reduction alters place learning and concomitant hippocampal, septal, and supramammillar theta activity in a Morris water maze. *Frontiers in pharmacology* 6: 250

Herrmann CS, Demiralp T. 2005. Human EEG gamma oscillations in neuropsychiatric disorders. *Clinical neurophysiology : official journal of the International Federation of Clinical Neurophysiology* 116: 2719-33

Herrmann CS, Munk MH, Engel AK. 2004. Cognitive functions of gamma-band activity: memory match and utilization. *Trends in cognitive sciences* 8: 347-55

Hestrin S. 1993. Different glutamate receptor channels mediate fast excitatory synaptic currents in inhibitory and excitatory cortical neurons. *Neuron* 11: 1083-91

Higashi H, Inanaga K, Nishi S, Uchimura N. 1989. Enhancement of dopamine actions on rat nucleus accumbens neurones in vitro after methamphetamine pre-treatment. *The Journal of physiology* 408: 587-603

Hikosaka O, Wurtz RH. 1985. Modification of saccadic eye movements by GABA-related substances. I. Effect of muscimol and bicuculline in monkey superior colliculus. *Journal of neurophysiology* 53: 266-91

Hill DR. 1985. GABAB receptor modulation of adenylate cyclase activity in rat brain slices. *British journal of pharmacology* 84: 249-57

Hill DR, Bowery NG. 1981. 3H-baclofen and 3H-GABA bind to bicuculline-insensitive GABAB sites in rat brain. *Nature* 290: 149-52

Hiraba H, Yamaguchi Y, Satoh H, Ishibashi Y, Iwamura Y. 2000. Deficits of masticatory movements caused by lesions in the orofacial somatosensory cortex of the awake cat. *Somatosensory & motor research* 17: 361-72

Hirsch JA, Alonso J-M, Reid RC. 1995. Visually evoked calcium action potentials in cat striate cortex. *Nature* 378: 612-16

Hobson JA, Pace-Schott EF. 2003. Fundamental neuroscience In *Fundamental Neuroscience*, ed. SK McConnell, L Squire, FE Bloom, pp. 1085-108. Amsterdam: Academic Press

Hockenbury DH, Hockenbury SE. 2010. *Discovering psychology*. New York; Basingstoke: Worth ; Palgrave [distributor].

Hoerbelt P, Lindsley TA, Fleck MW. 2015. Dopamine Directly Modulates GABA$_A$ Receptors. *The Journal of Neuroscience* 35: 3525-36

Hoffer ME, Goldstein B, Shulman A. 2013. New concepts in electrophysiology and tinnitus. *The international tinnitus journal* 18: 6-15

Hollmann M, Hartley M, Heinemann S. 1991. Ca2+ permeability of KA-AMPA--gated glutamate receptor channels depends on subunit composition. *Science* 252: 851-3

Hollmann M, Heinemann S. 1994. Cloned glutamate receptors. *Annual review of neuroscience* 17: 31-108

Hollmann M, Rogers SW, O'Shea-Greenfield A, Deneris ES, Hughes TE, et al. 1990. Glutamate receptor GluR-K1: structure, function, and expression in the brain. *Cold Spring Harbor symposia on quantitative biology* 55: 41-55

Holscher C, Gigg J, O'Mara SM. 1999. Metabotropic glutamate receptor activation and blockade: their role in long-term potentiation, learning and neurotoxicity. *Neuroscience and biobehavioral reviews* 23: 399-410

Hooks BM, Hires SA, Zhang Y-X, Huber D, Petreanu L, et al. 2011. Laminar Analysis of Excitatory Local Circuits in Vibrissal Motor and Sensory Cortical Areas. *PLOS Biology* 9: e1000572

Hopfield JJ. 1995. Pattern recognition computation using action potential timing for stimulus representation. *Nature* 376: 33-36

Hormuzdi SG, Pais I, LeBeau FE, Towers SK, Rozov A, et al. 2001. Impaired electrical signaling disrupts gamma frequency oscillations in connexin 36-deficient mice. *Neuron* 31: 487-95

Hosp JA, Molina-Luna K, Hertler B, Atiemo CO, Luft AR. 2009. Dopaminergic modulation of motor maps in rat motor cortex: an in vivo study. *Neuroscience* 159: 692-700

Hsieh CY, Cruikshank SJ, Metherate R. 2000. Differential modulation of auditory thalamocortical and intracortical synaptic transmission by cholinergic agonist. *Brain research* 880: 51-64

Hu B, Yang N, Qiao QC, Hu ZA, Zhang J. 2015. Roles of the orexin system in central motor control. *Neuroscience and biobehavioral reviews* 49: 43-54

Huda K, Salunga TL, Matsunami K. 2001. Dopaminergic inhibition of excitatory inputs onto pyramidal tract neurons in cat motor cortex. *Neuroscience letters* 307: 175-8

Huffman KJ, Krubitzer L. 2001. Area 3a: topographic organization and cortical connections in marmoset monkeys. *Cerebral cortex (New York, N.Y. : 1991)* 11: 849-67

Hughes SW, Cope DW, Blethyn KL, Crunelli V. 2002. Cellular mechanisms of the slow (<1 Hz) oscillation in thalamocortical neurons in vitro. *Neuron* 33: 947-58

Hughes SW, Cope DW, Tóth TI, Williams SR, Crunelli V. 1999. All thalamocortical neurones possess a T-type Ca(2+) 'window' current that enables the expression of bistability-mediated activities. *The Journal of Physiology* 517: 805-15

Hunt MJ, Kasicki S. 2013. A systematic review of the effects of NMDA receptor antagonists on oscillatory activity recorded in vivo. *Journal of psychopharmacology (Oxford, England)* 27: 972-86

Hyman SE, Malenka RC, Nestler EJ. 2006. Neural mechanisms of addiction: the role of reward-related learning and memory. *Annual review of neuroscience* 29: 565-98

Ioannides AA, Kostopoulos GK, Liu L, Fenwick PB. 2009. MEG identifies dorsal medial brain activations during sleep. *NeuroImage* 44: 455-68

Iriki A, Pavlides C, Keller A, Asanuma H. 1989. Long-term potentiation in the motor cortex. *Science* 245: 1385-7

Iversen LL. 2010. Dopamine handbook.

Iversen SD, Iversen LL. 2007. Dopamine: 50 years in perspective. *Trends in neurosciences* 30: 188-93

Izraeli R, Porter LL. 1995. Vibrissal motor cortex in the rat: connections with the barrel field. *Experimental brain research* 104: 41-54

Jacobs J. 2014. Hippocampal theta oscillations are slower in humans than in rodents: implications for models of spatial navigation and memory. *Philosophical transactions of the Royal Society of London. Series B, Biological sciences* 369: 20130304

Jacobs J, Kahana MJ. 2010. Direct brain recordings fuel advances in cognitive electrophysiology. *Trends in cognitive sciences* 14: 162-71

Janssen MJ, Ade KK, Fu Z, Vicini S. 2009. Dopamine modulation of GABA tonic conductance in striatal output neurons. *J Neurosci* 29: 5116-26

Jasper HH, Andrews HL. 1938. BRAIN POTENTIALS AND VOLUNTARY MUSCLE ACTIVITY IN MAN. *Journal of Neurophysiology* 1: 87-100

Jay TM. 2003. Dopamine: a potential substrate for synaptic plasticity and memory mechanisms. *Progress in neurobiology* 69: 375-90

Jayaraman V, Thiran S, Hess GP. 1999. How Fast Does the γ-Aminobutyric Acid Receptor Channel Open? Kinetic Investigations in the Microsecond Time Region Using a

Laser-Pulse Photolysis Technique. *Biochemistry* 38: 11372-78

Jensen JL, Marstrand PC, Nielsen JB. 2005. Motor skill training and strength training are associated with different plastic changes in the central nervous system. *Journal of applied physiology (Bethesda, Md. : 1985)* 99: 1558-68

Jensen O, Colgin LL. 2007. Cross-frequency coupling between neuronal oscillations. *Trends in Cognitive Sciences* 11: 267-69

Jiang ZG, Pessia M, North RA. 1993. Dopamine and baclofen inhibit the hyperpolarization-activated cation current in rat ventral tegmental neurones. *The Journal of physiology* 462: 753-64

Jin H, Wu H, Osterhaus G, Wei J, Davis K, et al. 2003. Demonstration of functional coupling between gamma -aminobutyric acid (GABA) synthesis and vesicular GABA transport into synaptic vesicles. *Proceedings of the National Academy of Sciences of the United States of America* 100: 4293-8

Johansson K, Lindgren I, Widner H, Wiklund I, Johansson BB. 1993. Can sensory stimulation improve the functional outcome in stroke patients? *Neurology* 43: 2189-92

Johansson RS, Westling G. 1984. Roles of glabrous skin receptors and sensorimotor memory in automatic control of precision grip when lifting rougher or more slippery objects. *Experimental Brain Research* 56: 550-64

Johnson NW. 2017. *Mechanistic insights into neuronal oscillatory activity in the dopamine-intact and dopamine-depleted primary motor cortex.* Aston University

Johnson NW, Ozkan M, Burgess AP, Prokic EJ, Wafford KA, et al. 2017. Phase-amplitude coupled persistent theta and gamma oscillations in rat primary motor cortex in vitro. *Neuropharmacology* 119: 141-56

Jones BE. 2005. From waking to sleeping: neuronal and chemical substrates. *Trends in pharmacological sciences* 26: 578-86

Jones EG. 1986. Neurotransmitters in the cerebral cortex. *Journal of neurosurgery* 65: 135-53

Jones EG, Wise SP. 1977. Size, laminar and columnar distribution of efferent cells in the sensory-motor cortex of monkeys. *The Journal of comparative neurology* 175: 391-438

Jones MV, Westbrook GL. 1995. Desensitized states prolong GABAA channel responses to brief agonist pulses. *Neuron* 15: 181-91

Jones RS, Buhl EH. 1993. Basket-like interneurones in layer II of the entorhinal cortex exhibit a powerful NMDA-mediated synaptic excitation. *Neuroscience letters* 149: 35-9

Joseph GR. 2000. http://brainmind.com/BrainLecture5.html.

Jouvet M. 1969. Biogenic amines and the states of sleep. *Science* 163: 32-41

Nicol K et al. 2009. Learning-related alterations in theta-nested gamma oscillations in sheep inferotemporal cortex. *Society for Neuroscience*: 192.19

Kaelin-Lang A, Luft AR, Sawaki L, Burstein AH, Sohn YH, Cohen LG. 2002. Modulation of human corticomotor excitability by somatosensory input. *The Journal of physiology* 540: 623-33

Kaila K. 1994. Ionic basis of GABAA receptor channel function in the nervous system. *Progress in neurobiology* 42: 489-537

Kaiser J, Ripper B, Birbaumer N, Lutzenberger W. 2003. Dynamics of gamma-band activity in human magnetoencephalogram during auditory pattern working memory. *NeuroImage* 20: 816-27

Kales A, Rechtschaffen A, University of California LA, Brain Information S, National Institute of Neurological D, Blindness. 1968. *A manual of standardized terminology, techniques and scoring system for sleep stages of human subjects.* Washington, DC: United States Government Printing Office.

Kamarajan C, Porjesz B, Jones KA, Choi K, Chorlian DB, et al. 2004. The role of brain oscillations as functional correlates of cognitive systems: A study of frontal inhibitory control in alcoholism. *International journal of psychophysiology : official journal of the International Organization of Psychophysiology* 51: 155-80

Kaneda M, Farrant M, Cull-Candy SG. 1995. Whole-cell and single-channel currents

activated by GABA and glycine in granule cells of the rat cerebellum. *The Journal of physiology* 485 (Pt 2): 419-35

Kaneda M, Hashimoto M, Kaneko A. 1995. Neuronal nicotinic acetylcholine receptors of ganglion cells in the cat retina. *The Japanese journal of physiology* 45: 491-508

Kaneko T. 2013. Local connections of excitatory neurons in motor-associated cortical areas of the rat. *Front Neural Circuits* 7: 75

Kaneko T, Caria MA, Asanuma H. 1994. Information processing within the motor cortex. II. Intracortical connections between neurons receiving somatosensory cortical input and motor output neurons of the cortex. *The Journal of comparative neurology* 345: 172-84

Kaneko T, Cho R, Li Y, Nomura S, Mizuno N. 2000. Predominant information transfer from layer III pyramidal neurons to corticospinal neurons. *The Journal of comparative neurology* 423: 52-65

Karayannis T, Huerta-Ocampo I, Capogna M. 2007. GABAergic and pyramidal neurons of deep cortical layers directly receive and differently integrate callosal input. *Cerebral cortex (New York, N.Y. : 1991)* 17: 1213-26

Kattler H, Dijk DJ, Borbely AA. 1994. Effect of unilateral somatosensory stimulation prior to sleep on the sleep EEG in humans. *Journal of sleep research* 3: 159-64

Kawaguchi Y. 1993. Groupings of nonpyramidal and pyramidal cells with specific physiological and morphological characteristics in rat frontal cortex. *Journal of neurophysiology* 69: 416-31

Kawaguchi Y. 1993. Physiological, morphological, and histochemical characterization of three classes of interneurons in rat neostriatum. *J Neurosci* 13: 4908-23

Kawaguchi Y. 1995. Physiological subgroups of non-pyramidal cells with specific morphological characteristics in LII/III of rat frontal cortex. *J Neurosci* 15: 2638-55

Kawaguchi Y, Kubota Y. 1996. Physiological and morphological identification of somatostatin- or vasoactive intestinal polypeptide-containing cells among GABAergic cell subtypes in rat frontal cortex. *J Neurosci* 16: 2701-15

Kawaguchi Y, Kubota Y. 1997. GABAergic cell subtypes and their synaptic connections in rat frontal cortex. *Cerebral cortex (New York, N.Y. : 1991)* 7: 476-86

Kawaguchi Y, Kubota Y. 1998. Neurochemical features and synaptic connections of large physiologically-identified GABAergic cells in the rat frontal cortex. *Neuroscience* 85: 677-701

Kawaguchi YK, Y. 1997. "GABAergic cell subtypes and their synaptic connections in rat frontal cortex",. *Cerebral Cortex* 7: 476-86

Kebabian JW, Calne DB. 1979. Multiple receptors for dopamine. *Nature* 277: 93-96

Kebabian JW, Petzold GL, Greengard P. 1972. Dopamine-sensitive adenylate cyclase in caudate nucleus of rat brain, and its similarity to the "dopamine receptor". *Proceedings of the National Academy of Sciences* 69: 2145-49

Kehl SJ, McLennan H, Collingridge GL. 1984. Effects of folic and kainic acids on synaptic responses of hippocampal neurones. *Neuroscience* 11: 111-24

Keinanen K, Wisden W, Sommer B, Werner P, Herb A, et al. 1990. A family of AMPA-selective glutamate receptors. *Science* 249: 556-60

Keller A, Pavlides C, Asanuma H. 1990. Long-term potentiation in the cat somatosensory cortex. *Neuroreport* 1: 49-52

Kelly DC, Asghar AU, Marr CG, McQueen DS. 2001. Nitric oxide modulates articular sensory discharge and responsiveness to bradykinin in normal and arthritic rats in vivo. *Neuroreport* 12: 121-5

Kelsch W, Li Z, Eliava M, Goengrich C, Monyer H. 2012. GluN2B-Containing NMDA Receptors Promote Wiring of Adult-Born Neurons into Olfactory Bulb Circuits. *The Journal of Neuroscience* 32: 12603-11

Kelsch W, Li Z, Wieland S, Senkov O, Herb A, et al. 2014. GluN2B-containing NMDA receptors promote glutamate synapse development in hippocampal interneurons. *J Neurosci* 34: 16022-30

Kennedy RT, Thompson JE, Vickroy TW. 2002. In vivo monitoring of amino acids by direct sampling of brain extracellular fluid at ultralow flow rates and capillary

electrophoresis. *Journal of neuroscience methods* 114: 39-49

Keros S, Hablitz JJ. 2005. Subtype-specific GABA transporter antagonists synergistically modulate phasic and tonic GABAA conductances in rat neocortex. *Journal of neurophysiology* 94: 2073-85

Kimura F, Fukuda M, Tsumoto T. 1999. Acetylcholine suppresses the spread of excitation in the visual cortex revealed by optical recording: possible differential effect depending on the source of input. *The European journal of neuroscience* 11: 3597-609

Kirmse K DA, Kirischuk S, Grantyn R. 2008. GABA transporter 1 tunes GABAergic synaptic transmission at output neurons of the mouse neostriatum. *J Physiol (Paris)* 586: 5665–78.

Kirov SA, Sorra KE, Harris KM. 1999. Slices have more synapses than perfusion-fixed hippocampus from both young and mature rats. *J Neurosci* 19: 2876-86

Klausberger T, Magill PJ, Marton LF, Roberts JD, Cobden PM, et al. 2003. Brain-state- and cell-type-specific firing of hippocampal interneurons in vivo. *Nature* 421: 844-8

Klausberger T, Marton LF, O'Neill J, Huck JH, Dalezios Y, et al. 2005. Complementary roles of cholecystokinin- and parvalbumin-expressing GABAergic neurons in hippocampal network oscillations. *J Neurosci* 25: 9782-93

Knyazev GG. 2007. Motivation, emotion, and their inhibitory control mirrored in brain oscillations. *Neuroscience and biobehavioral reviews* 31: 377-95

Knyazev GG. 2012. EEG delta oscillations as a correlate of basic homeostatic and motivational processes. *Neuroscience and biobehavioral reviews* 36: 677-95

Koch C, Poggio T. 1999. Predicting the visual world: silence is golden. *Nat Neurosci* 2: 9-10

Konopacki J, Bland BH, MacIver MB, Roth SH. 1987. Cholinergic theta rhythm in transected hippocampal slices: independent CA1 and dentate generators. *Brain research* 436: 217-22

Konopacki J, Golebiewski H, Eckersdorf B, Blaszczyk M, Grabowski R. 1997. Theta-like activity in hippocampal formation slices: the effect of strong disinhibition of GABAA and GABAB receptors. *Brain research* 775: 91-8

Konopacki J, Kowalczyk T, Gołębiewski H. 2004. Electrical coupling underlies theta oscillations recorded in hippocampal formation slices. *Brain Research* 1019: 270-74

Koob GF, Volkow ND. 2010. Neurocircuitry of Addiction. *Neuropsychopharmacology* 35: 217-38

Kopell N, Ermentrout B. 2004. Chemical and electrical synapses perform complementary roles in the synchronization of interneuronal networks. *Proceedings of the National Academy of Sciences of the United States of America* 101: 15482-87

Kopra JJ, Panhelainen A, af Bjerkén S, Porokuokka LL, Varendi K, et al. 2017. Dampened Amphetamine-Stimulated Behavior and Altered Dopamine Transporter Function in the Absence of Brain GDNF. *The Journal of Neuroscience* 37: 1581

Koralek K-A, Olavarria J, Kellackey HP. 1990. Areal and laminar organization of corticocortical projections in the rat somatosensory cortex. *The Journal of Comparative Neurology* 299: 133-50

Korotkova T, Fuchs EC, Ponomarenko A, von Engelhardt J, Monyer H. 2010. NMDA receptor ablation on parvalbumin-positive interneurons impairs hippocampal synchrony, spatial representations, and working memory. *Neuron* 68: 557-69

Kosar E, Waters RS, Tsukahara N, Asanuma H. 1985. Anatomical and physiological properties of the projection from the sensory cortex to the motor cortex in normal cats: the difference between corticocortical and thalamocortical projections. *Brain research* 345: 68-78

Kowalczyk T, Bocian R, Konopacki J. 2013. The generation of theta rhythm in hippocampal formation maintained in vitro. *The European journal of neuroscience* 37: 679-99

Kramer MA, Tort AB, Kopell NJ. 2008. Sharp edge artifacts and spurious coupling in EEG frequency comodulation measures. *Journal of neuroscience methods* 170: 352-7

Kramis R, Vanderwolf CH, Bland BH. 1975. Two types of hippocampal rhythmical slow activity in both the rabbit and the rat: Relations to behavior and effects of atropine, diethyl ether, urethane, and pentobarbital. *Experimental Neurology* 49: 58-85

Kreiss DS, Anderson LA, Walters JR. 1996. Apomorphine and dopamine D(1) receptor agonists increase the firing rates of subthalamic nucleus neurons. *Neuroscience* 72: 863-76

Krieg WJ. 1946. Connections of the cerebral cortex; the albino rat; structure of the cortical areas. *The Journal of comparative neurology* 84: 277-323

Krishek BJ, Moss SJ, Smart TG. 1996. A functional comparison of the antagonists bicuculline and picrotoxin at recombinant GABAA receptors. *Neuropharmacology* 35: 1289-98

Krishnan B, Scott MT, Pollandt S, Schroeder B, Kurosky A, Shinnick-Gallagher P. 2016. Fear potentiated startle increases phospholipase D (PLD) expression/activity and PLD-linked metabotropic glutamate receptor mediated post-tetanic potentiation in rat amygdala. *Neurobiology of learning and memory* 128: 65-79

Kroener S, Chandler LJ, Phillips PE, Seamans JK. 2009. Dopamine modulates persistent synaptic activity and enhances the signal-to-noise ratio in the prefrontal cortex. *PloS one* 4: e6507

Kroner S, Krimer LS, Lewis DA, Barrionuevo G. 2007. Dopamine increases inhibition in the monkey dorsolateral prefrontal cortex through cell type-specific modulation of interneurons. *Cerebral cortex (New York, N.Y. : 1991)* 17: 1020-32

Krueger JM, Obal F. 1993. A neuronal group theory of sleep function. *Journal of sleep research* 2: 63-69

Kryzhanovskii GN, Shandra AA, Godlevskii LS, Mikhaleva, II. 1990. [Appearance of parkinsonian syndrome after administration of delta sleep-inducing peptide into the rat substantia nigra]. *Biulleten' eksperimental'noi biologii i meditsiny* 109: 119-21

Kulik A, Vida I, Fukazawa Y, Guetg N, Kasugai Y, et al. 2006. Compartment-dependent colocalization of Kir3.2-containing K+ channels and GABAB receptors in hippocampal pyramidal cells. *J Neurosci* 26: 4289-97

Kullmann Dimitri M, Moreau Alexandre W, Bakiri Y, Nicholson E. Plasticity of Inhibition. *Neuron* 75: 951-62

Kuramoto E, Furuta T, Nakamura KC, Unzai T, Hioki H, Kaneko T. 2009. Two types of thalamocortical projections from the motor thalamic nuclei of the rat: a single neuron-tracing study using viral vectors. *Cerebral cortex (New York, N.Y. : 1991)* 19: 2065-77

Kwan HC, Mackay WA, Murphy JT, Wong YC. 1978. An intracortical microstimulation study of output organization in precentral cortex of awake primates. *J Physiol (Paris)* 74: 231-3

Lakatos P, Karmos G, Mehta AD, Ulbert I, Schroeder CE. 2008. Entrainment of neuronal oscillations as a mechanism of attentional selection. *Science* 320: 110-3

Lakatos P, Shah AS, Knuth KH, Ulbert I, Karmos G, Schroeder CE. 2005. An oscillatory hierarchy controlling neuronal excitability and stimulus processing in the auditory cortex. *Journal of neurophysiology* 94: 1904-11

Larkum ME, Nevian T, Sandler M, Polsky A, Schiller J. 2009. Synaptic integration in tuft dendrites of layer 5 pyramidal neurons: a new unifying principle. *Science* 325: 756-60

Lavin A, Grace AA. 2001. Stimulation of D1-type dopamine receptors enhances excitability in prefrontal cortical pyramidal neurons in a state-dependent manner. *Neuroscience* 104: 335-46

Lawrence JJ, McBain CJ. 2003. Interneuron Diversity series: Containing the detonation – feedforward inhibition in the CA3 hippocampus. *Trends in Neurosciences* 26: 631-40

Le Moine C, Gaspar P. 1998. Subpopulations of cortical GABAergic interneurons differ by their expression of D1 and D2 dopamine receptor subtypes. *Brain research. Molecular brain research* 58: 231-6

Leary JB, Bondi CO, LaPorte MJ, Carlson LJ, Radabaugh HL, et al. 2017. The Therapeutic Efficacy of Environmental Enrichment and Methylphenidate Alone and in Combination after Controlled Cortical Impact Injury. *Journal of neurotrauma* 34: 444-50

LeBeau FE, Towers SK, Traub RD, Whittington MA, Buhl EH. 2002. Fast network

oscillations induced by potassium transients in the rat hippocampus in vitro. *The Journal of physiology* 542: 167-79

LeBeau FEN, Traub RD, Monyer H, Whittington MA, Buhl EH. 2003. The role of electrical signaling via gap junctions in the generation of fast network oscillations. *Brain Research Bulletin* 62: 3-13

Ledergerber D, Larkum ME. 2010. Properties of layer 6 pyramidal neuron apical dendrites. *J Neurosci* 30: 13031-44

Lee FJ, Xue S, Pei L, Vukusic B, Chery N, et al. 2002. Dual regulation of NMDA receptor functions by direct protein-protein interactions with the dopamine D1 receptor. *Cell* 111: 219-30

Lee S, Kruglikov I, Huang ZJ, Fishell G, Rudy B. 2013. A disinhibitory circuit mediates motor integration in the somatosensory cortex. *Nat Neurosci* 16: 1662-70

Lefort S, Tomm C, Floyd Sarria JC, Petersen CC. 2009. The excitatory neuronal network of the C2 barrel column in mouse primary somatosensory cortex. *Neuron* 61: 301-16

Lega B, Burke J, Jacobs J, Kahana MJ. 2016. Slow-Theta-to-Gamma Phase-Amplitude Coupling in Human Hippocampus Supports the Formation of New Episodic Memories. *Cerebral cortex (New York, N.Y. : 1991)* 26: 268-78

Lega BC, Jacobs J, Kahana M. 2012. Human hippocampal theta oscillations and the formation of episodic memories. *Hippocampus* 22: 748-61

Lei S, McBain CJ. 2002. Distinct NMDA Receptors Provide Differential Modes of Transmission at Mossy Fiber-Interneuron Synapses. *Neuron* 33: 921-33

Lei W, Jiao Y, Del Mar N, Reiner A. 2004. Evidence for differential cortical input to direct pathway versus indirect pathway striatal projection neurons in rats. *J Neurosci* 24: 8289-99

Lein ES, Hawrylycz MJ, Ao N, Ayres M, Bensinger A, et al. 2007. Genome-wide atlas of gene expression in the adult mouse brain. *Nature* 445: 168-76

Lena I, Parrot S, Deschaux O, Muffat-Joly S, Sauvinet V, et al. 2005. Variations in extracellular levels of dopamine, noradrenaline, glutamate, and aspartate across the sleep--wake cycle in the medial prefrontal cortex and nucleus accumbens of freely moving rats. *Journal of neuroscience research* 81: 891-9

Leresche N, Jassik-Gerschenfeld D, Haby M, Soltesz I, Crunelli V. 1990. Pacemaker-like and other types of spontaneous membrane potential oscillations of thalamocortical cells. *Neuroscience letters* 113: 72-7

Lerma J. 1997. Kainate reveals its targets. *Neuron* 19: 1155-8

Lerma J, Herranz AS, Herreras O, Abraira V, Martin del Rio R. 1986. In vivo determination of extracellular concentration of amino acids in the rat hippocampus. A method based on brain dialysis and computerized analysis. *Brain research* 384: 145-55

Lerma J, Marques JM. 2013. Kainate receptors in health and disease. *Neuron* 80: 292-311

Lerma J, Paternain AV, Rodriguez-Moreno A, Lopez-Garcia JC. 2001. Molecular physiology of kainate receptors. *Physiological reviews* 81: 971-98

Leung LS. 1982. Nonlinear feedback model of neuronal populations in hippocampal CAl region. *Journal of neurophysiology* 47: 845-68

Lewis DA, Hashimoto T, Volk DW. 2005. Cortical inhibitory neurons and schizophrenia. *Nat Rev Neurosci* 6: 312-24

Li CX, Waters RS. 1991. Organization of the mouse motor cortex studied by retrograde tracing and intracortical microstimulation (ICMS) mapping. *The Canadian journal of neurological sciences. Le journal canadien des sciences neurologiques* 18: 28-38

Li HS, Xu XZ, Montell C. 1999. Activation of a TRPC3-dependent cation current through the neurotrophin BDNF. *Neuron* 24: 261-73

Liang J, Marty VN, Mulpuri Y, Olsen RW, Spigelman I. 2014. Selective modulation of GABAergic tonic current by dopamine in the nucleus accumbens of alcohol-dependent rats. *Journal of neurophysiology* 112: 51-60

Lidow MS, Goldman-Rakic PS, Rakic P, Innis RB. 1989. Dopamine D2 receptors in the cerebral cortex: distribution and pharmacological characterization with [3H]raclopride. *Proceedings of the National Academy of Sciences of the United States of America* 86: 6412-6

Lin LD, Murray GM, Sessle BJ. 1993. The effect of bilateral cold block of the primate face

primary somatosensory cortex on the performance of trained tongue-protrusion task and biting tasks. *Journal of neurophysiology* 70: 985-96

Lisman J. 2005. The theta/gamma discrete phase code occuring during the hippocampal phase precession may be a more general brain coding scheme. *Hippocampus* 15: 913-22

Lisman JE. 1999. Relating hippocampal circuitry to function: recall of memory sequences by reciprocal dentate-CA3 interactions. *Neuron* 22: 233-42

Lisman JE, Idiart MA. 1995. Storage of 7 +/- 2 short-term memories in oscillatory subcycles. *Science* 267: 1512-5

Lisman John E, Jensen O. 2013. The Theta-Gamma Neural Code. *Neuron* 77: 1002-16

Llinás R, Mühlethaler M. 1988. Electrophysiology of guinea-pig cerebellar nuclear cells in the in vitro brain stem-cerebellar preparation. *The Journal of Physiology* 404: 241-58

Llinas RR. 1988. The intrinsic electrophysiological properties of mammalian neurons: insights into central nervous system function. *Science* 242: 1654-64

Logothetis NK, Wandell BA. 2004. Interpreting the BOLD signal. *Annual review of physiology* 66: 735-69

Lomeli H, Mosbacher J, Melcher T, Hoger T, Geiger JR, et al. 1994. Control of kinetic properties of AMPA receptor channels by nuclear RNA editing. *Science* 266: 1709-13

Loomis ALH, E. N.; Hobart, G. A. 1937. Cerebral states during sleep, as studied by human brain potentials. *J Exp Psychol* 21: 127-44

LoTurco JJ, Owens DF, Heath MJ, Davis MB, Kriegstein AR. 1995. GABA and glutamate depolarize cortical progenitor cells and inhibit DNA synthesis. *Neuron* 15: 1287-98

Loucif AJ, Woodhall GL, Sehirli US, Stanford IM. 2008. Depolarisation and suppression of burst firing activity in the mouse subthalamic nucleus by dopamine D1/D5 receptor activation of a cyclic-nucleotide gated non-specific cation conductance. *Neuropharmacology* 55: 94-105

Lu SM, Lin RC. 1993. Thalamic afferents of the rat barrel cortex: a light- and electron-microscopic study using Phaseolus vulgaris leucoagglutinin as an anterograde tracer. *Somatosensory & motor research* 10: 1-16

Lucas-Meunier E, Fossier P, Baux G, Amar M. 2003. Cholinergic modulation of the cortical neuronal network. *Pflugers Archiv : European journal of physiology* 446: 17-29

Luft AR, Kaelin-Lang A, Hauser TK, Buitrago MM, Thakor NV, et al. 2002. Modulation of rodent cortical motor excitability by somatosensory input. *Experimental brain research* 142: 562-9

Luft AR, Schwarz S. 2009. Dopaminergic signals in primary motor cortex. *International journal of developmental neuroscience : the official journal of the International Society for Developmental Neuroscience* 27: 415-21

Lukatch HS, MacIver MB. 1997. Physiology, pharmacology, and topography of cholinergic neocortical oscillations in vitro. *Journal of neurophysiology* 77: 2427-45

Magara F, Welker E, Wolfer DP, Drescher-Lindh I, Lipp HP. 1998. Increased asymmetries in 2-deoxyglucose uptake in the brain of freely moving congenitally acallosal mice. *Neuroscience* 87: 243-54

Maguire EP, Macpherson T, Swinny JD, Dixon CI, Herd MB, et al. 2014. Tonic inhibition of accumbal spiny neurons by extrasynaptic alpha4betadelta GABAA receptors modulates the actions of psychostimulants. *J Neurosci* 34: 823-38

Manita S, Suzuki T, Homma C, Matsumoto T, Odagawa M, et al. 2015. A Top-Down Cortical Circuit for Accurate Sensory Perception. *Neuron* 86: 1304-16

Mann EO, Mody I. 2010. Control of hippocampal gamma oscillation frequency by tonic inhibition and excitation of interneurons. *Nat Neurosci* 13: 205-12

Mann EO, Suckling JM, Hajos N, Greenfield SA, Paulsen O. 2005. Perisomatic feedback inhibition underlies cholinergically induced fast network oscillations in the rat hippocampus in vitro. *Neuron* 45: 105-17

Manns ID, Sakmann B, Brecht M. 2004. Sub- and suprathreshold receptive field properties of pyramidal neurones in layers 5A and 5B of rat somatosensory barrel cortex. *The Journal of physiology* 556: 601-22

Mao T, Kusefoglu D, Hooks BM, Huber D, Petreanu L, Svoboda K. 2011. Long-range neuronal circuits underlying the interaction between sensory and motor cortex. *Neuron* 72: 111-23

Maquet P. 2001. The role of sleep in learning and memory. *Science* 294: 1048-52

Markov NT, Vezoli J, Chameau P, Falchier A, Quilodran R, et al. 2014. Anatomy of hierarchy: feedforward and feedback pathways in macaque visual cortex. *The Journal of comparative neurology* 522: 225-59

Marquis KL, Paquette NC, Gussio RP, Moreton JE. 1989. Comparative electroencephalographic and behavioral effects of phencyclidine, (+)-SKF-10,047 and MK-801 in rats. *The Journal of pharmacology and experimental therapeutics* 251: 1104-12

Martres MP, Bouthenet ML, Sales N, Sokoloff P, Schwartz JC. 1985. Widespread distribution of brain dopamine receptors evidenced with [125I]iodosulpride, a highly selective ligand. *Science* 228: 752-5

Matta JA, Pelkey KA, Craig MT, Chittajallu R, Jeffries BW, McBain CJ. 2013. Developmental origin dictates interneuron AMPA and NMDA receptor subunit composition and plasticity. *Nat Neurosci* 16: 1032-41

Mattia A, Moreton JE. 1986. Electroencephalographic (EEG), EEG power spectra, and behavioral correlates in rats given phencyclidine. *Neuropharmacology* 25: 763-9

Mayer ML, Westbrook GL, Guthrie PB. 1984. Voltage-dependent block by Mg2+ of NMDA responses in spinal cord neurones. *Nature* 309: 261-3

McBain C, Dingledine R. 1992. Dual-component miniature excitatory synaptic currents in rat hippocampal CA3 pyramidal neurons. *Journal of neurophysiology* 68: 16-27

McBain CJ, Dingledine R. 1993. Heterogeneity of synaptic glutamate receptors on CA3 stratum radiatum interneurones of rat hippocampus. *The Journal of physiology* 462: 373-92

McBain CJ, Eaton JV, Brown T, Dingledine R. 1992. CNQX increases spontaneous inhibitory input to CA3 pyramidal neurones in neonatal rat hippocampal slices. *Brain research* 592: 255-60

McBain CJ, Fisahn A. 2001. Interneurons unbound. *Nat Rev Neurosci* 2: 11-23

McBain CJ, Mayer ML. 1994. N-methyl-D-aspartic acid receptor structure and function. *Physiological reviews* 74: 723-60

McCarley RW, Hobson JA. 1975. Neuronal excitability modulation over the sleep cycle: a structural and mathematical model. *Science* 189: 58-60

McCormick D, Williamson A. 1991. Modulation of neuronal firing mode in cat and guinea pig LGNd by histamine: possible cellular mechanisms of histaminergic control of arousal. *The Journal of Neuroscience* 11: 3188-99

McCormick DA. 1992. Neurotransmitter actions in the thalamus and cerebral cortex and their role in neuromodulation of thalamocortical activity. *Progress in neurobiology* 39: 337-88

McCormick DA, Connors BW, Lighthall JW, Prince DA. 1985. Comparative electrophysiology of pyramidal and sparsely spiny stellate neurons of the neocortex. *Journal of neurophysiology* 54: 782-806

McCormick DA, Pape HC. 1990. Noradrenergic and serotonergic modulation of a hyperpolarization-activated cation current in thalamic relay neurones. *The Journal of physiology* 431: 319-42

McCormick DA, Pape HC. 1990. Properties of a hyperpolarization-activated cation current and its role in rhythmic oscillation in thalamic relay neurones. *The Journal of physiology* 431: 291-318

McCormick DA, Prince DA. 1986. Mechanisms of action of acetylcholine in the guinea-pig cerebral cortex in vitro. *The Journal of physiology* 375: 169-94

McCormick F. 1996. Ras biology in atomic detail. *Nature structural biology* 3: 653-5

McGinn RJ, Valiante TA. 2014. Phase-amplitude coupling and interlaminar synchrony are correlated in human neocortex. *J Neurosci* 34: 15923-30

McGinty DJ, Harper RM. 1976. Dorsal raphe neurons: depression of firing during sleep in cats. *Brain research* 101: 569-75

Mercer A, Bannister AP, Thomson AM. 2006. Electrical coupling between pyramidal cells

in adult cortical regions. *Brain cell biology* 35: 13-27

Mercer A, West DC, Morris OT, Kirchhecker S, Kerkhoff JE, Thomson AM. 2005. Excitatory connections made by presynaptic cortico-cortical pyramidal cells in layer 6 of the neocortex. *Cerebral cortex (New York, N.Y. : 1991)* 15: 1485-96

Meyer G. 1987. Forms and spatial arrangement of neurons in the primary motor cortex of man. *The Journal of comparative neurology* 262: 402-28

Meyer HS, Wimmer VC, Oberlaender M, de Kock CP, Sakmann B, Helmstaedter M. 2010. Number and laminar distribution of neurons in a thalamocortical projection column of rat vibrissal cortex. *Cerebral cortex (New York, N.Y. : 1991)* 20: 2277-86

Middleton SJ, Racca C, Cunningham MO, Traub RD, Monyer H, et al. 2008. High-frequency network oscillations in cerebellar cortex. *Neuron* 58: 763-74

Miles R. 1990. Synaptic Excitation of Inhibitory Cells by Single Ca3 Hippocampal Pyramidal Cells of the Guinea-Pig Invitro. *J Physiol-London* 428: 61-77

Miles R, Toth K, Gulyas AI, Hajos N, Freund TF. 1996. Differences between somatic and dendritic inhibition in the hippocampus. *Neuron* 16: 815-23

Miller GM. 2011. The emerging role of trace amine-associated receptor 1 in the functional regulation of monoamine transporters and dopaminergic activity. *Journal of neurochemistry* 116: 164-76

Minlebaev M, Colonnese M, Tsintsadze T, Sirota A, Khazipov R. 2011. Early gamma oscillations synchronize developing thalamus and cortex. *Science* 334: 226-9

Mintz I, Hammond C, Feger J. 1986. Excitatory effect of iontophoretically applied dopamine on identified neurons of the rat subthalamic nucleus. *Brain research* 375: 172-5

Missale C, Nash SR, Robinson SW, Jaber M, Caron MG. 1998. Dopamine receptors: from structure to function. *Physiological reviews* 78: 189-225

Mitzdorf U. 1985. Current source-density method and application in cat cerebral cortex: investigation of evoked potentials and EEG phenomena. *Physiological reviews* 65: 37-100

Modebadze T. 2014. *Neuronal network dynamics during epileptogenesis in the medial temporal lobe.* Doctoral thesis. Aston University

Mody I, De Koninck Y, Otis TS, Soltesz I. 1994. Bridging the cleft at GABA synapses in the brain. *Trends in neurosciences* 17: 517-25

Moghaddam B. 2003. Bringing order to the glutamate chaos in schizophrenia. *Neuron* 40: 881-4

Möhler H. 1992. GABAergic synaptic transmission. Regulation by drugs. *Arzneimittelforschung* 42: 211-14

Mölle M, Marshall L, Gais S, Born J. 2002. Grouping of Spindle Activity during Slow Oscillations in Human Non-Rapid Eye Movement Sleep. *The Journal of Neuroscience* 22: 10941-47

Molnár Z, Cheung AFP. 2006. Towards the classification of subpopulations of layer V pyramidal projection neurons. *Neuroscience Research* 55: 105-15

Monaghan DT, Bridges RJ, Cotman CW. 1989. The excitatory amino acid receptors: their classes, pharmacology, and distinct properties in the function of the central nervous system. *Annual review of pharmacology and toxicology* 29: 365-402

Monsma FJ, Jr., Mahan LC, McVittie LD, Gerfen CR, Sibley DR. 1990. Molecular cloning and expression of a D1 dopamine receptor linked to adenylyl cyclase activation. *Proceedings of the National Academy of Sciences of the United States of America* 87: 6723-7

Montgomery SM, Betancur MI, Buzsáki G. 2009. Behavior-Dependent Coordination of Multiple Theta Dipoles in the Hippocampus. *The Journal of Neuroscience* 29: 1381-94

Monti JM, Monti D. 2007. The involvement of dopamine in the modulation of sleep and waking. *Sleep medicine reviews* 11: 113-33

Monto S, Palva S, Voipio J, Palva JM. 2008. Very Slow EEG Fluctuations Predict the Dynamics of Stimulus Detection and Oscillation Amplitudes in Humans. *The Journal of Neuroscience* 28: 8268-72

Monyer H, Burnashev N, Laurie DJ, Sakmann B, Seeburg PH. 1994. Developmental and regional expression in the rat brain and functional properties of four NMDA

receptors. *Neuron* 12: 529-40

Moore AR, Zhou WL, Potapenko ES, Kim EJ, Antic SD. 2011. Brief dopaminergic stimulations produce transient physiological changes in prefrontal pyramidal neurons. *Brain research* 1370: 1-15

Moosmang S, Biel M, Hofmann F, Ludwig A. 1999. Differential distribution of four hyperpolarization-activated cation channels in mouse brain. *Biological chemistry* 380: 975-80

Mormann F, Fell J, Axmacher N, Weber B, Lehnertz K, et al. 2005. Phase/amplitude reset and theta-gamma interaction in the human medial temporal lobe during a continuous word recognition memory task. *Hippocampus* 15: 890-900

Mormann F, Osterhage H, Andrzejak RG, Weber B, Fernández G, et al. 2008. Independent Delta/Theta Rhythms in the Human Hippocampus and Entorhinal Cortex. *Frontiers in Human Neuroscience* 2: 3

Mozrzymas JW. 2004. Dynamism of GABAA receptor activation shapes the "personality" of inhibitory synapses. *Neuropharmacology* 47: 945-60

Mozrzymas JW, Zarnowska ED, Pytel M, Mercik K. 2003. Modulation of GABA(A) receptors by hydrogen ions reveals synaptic GABA transient and a crucial role of the desensitization process. *J Neurosci* 23: 7981-92

Mucignat-Caretta C, Caretta A. 2002. Clustered distribution of cAMP-dependent protein kinase regulatory isoform RI alpha during the development of the rat brain. *The Journal of comparative neurology* 451: 324-33

Mucignat-Caretta C, Redaelli M, Caretta A. 2012. One nose, one brain: contribution of the main and accessory olfactory system to chemosensation. *Frontiers in neuroanatomy* 6: 46

Mulle C, Sailer A, Swanson GT, Brana C, O'Gorman S, et al. 2000. Subunit composition of kainate receptors in hippocampal interneurons. *Neuron* 28: 475-84

Müller W, Misgeld U. 1986. Slow cholinergic excitation of guinea pig hippocampal neurons is mediated by two muscarinic receptor subtypes. *Neuroscience Letters* 67: 107-12

Munsch T, Yanagawa Y, Obata K, Pape HC. 2005. Dopaminergic control of local interneuron activity in the thalamus. *The European journal of neuroscience* 21: 290-4

Murthy VN, Fetz EE. 1992. Coherent 25- to 35-Hz oscillations in the sensorimotor cortex of awake behaving monkeys. *Proceedings of the National Academy of Sciences of the United States of America* 89: 5670-74

Murthy VN, Fetz EE. 1996. Oscillatory activity in sensorimotor cortex of awake monkeys: synchronization of local field potentials and relation to behavior. *Journal of neurophysiology* 76: 3949-67

Murthy VN, Fetz EE. 1996. Synchronization of neurons during local field potential oscillations in sensorimotor cortex of awake monkeys. *Journal of neurophysiology* 76: 3968-82

Myme CI, Sugino K, Turrigiano GG, Nelson SB. 2003. The NMDA-to-AMPA ratio at synapses onto layer 2/3 pyramidal neurons is conserved across prefrontal and visual cortices. *Journal of neurophysiology* 90: 771-9

Nakahiro M, Arakawa O, Narahashi T. 1991. Modulation of gamma-aminobutyric acid receptor-channel complex by alcohols. *Journal of Pharmacology and Experimental Therapeutics* 259: 235-40

Nakanishi N, Shneider NA, Axel R. 1990. A family of glutamate receptor genes: evidence for the formation of heteromultimeric receptors with distinct channel properties. *Neuron* 5: 569-81

Nakanishi S. 1994. Metabotropic glutamate receptors: synaptic transmission, modulation, and plasticity. *Neuron* 13: 1031-7

Nelson RJ. 1987. Activity of monkey primary somatosensory cortical neurons changes prior to active movement. *Brain research* 406: 402-7

Neve KA, Seamans JK, Trantham-Davidson H. 2004. Dopamine receptor signaling. *Journal of receptor and signal transduction research* 24: 165-205

Newberry NR, Nicoll RA. 1985. Comparison of the action of baclofen with gamma-aminobutyric acid on rat hippocampal pyramidal cells in vitro. *The Journal of*

physiology 360: 161-85

Nguyen QT, Kleinfeld D. 2005. Positive feedback in a brainstem tactile sensorimotor loop. *Neuron* 45: 447-57

Nicoletti F, Bruno V, Copani A, Casabona G, Knopfel T. 1996. Metabotropic glutamate receptors: a new target for the therapy of neurodegenerative disorders? *Trends in neurosciences* 19: 267-71

Niedermeyer E, da Silva FL. 2005. *Electroencephalography : basic principles, clinical applications, and related fields*. Philadelphia: Lippincott williams and wilkins.

Niedermeyer E, Sherman DL, Geocadin RJ, Hansen HC, Hanley DF. 1999. The burst-suppression electroencephalogram. *Clinical EEG (electroencephalography)* 30: 99-105

Notomi T, Shigemoto R. 2004. Immunohistochemical localization of Ih channel subunits, HCN1-4, in the rat brain. *The Journal of comparative neurology* 471: 241-76

Nowak L, Bregestovski P, Ascher P, Herbet A, Prochiantz A. 1984. Magnesium gates glutamate-activated channels in mouse central neurones. *Nature* 307: 462-5

Nudo RJ, Jenkins WM, Merzenich MM, Prejean T, Grenda R. 1992. Neurophysiological correlates of hand preference in primary motor cortex of adult squirrel monkeys. *J Neurosci* 12: 2918-47

Nunez PS, R. 2006. *Electric fields of the brain : the neurophysics of EEG*. New York: Oxford University Press.

Nusser Z, Mody I. 2002. Selective modulation of tonic and phasic inhibitions in dentate gyrus granule cells. *Journal of neurophysiology* 87: 2624-8

Nusser Z, Sieghart W, Somogyi P. 1998. Segregation of different GABAA receptors to synaptic and extrasynaptic membranes of cerebellar granule cells. *J Neurosci* 18: 1693-703

Nutt DJ, Malizia AL. 2001. New insights into the role of the GABA(A)-benzodiazepine receptor in psychiatric disorder. *The British journal of psychiatry : the journal of mental science* 179: 390-6

O'Keefe J. 1976. Place units in the hippocampus of the freely moving rat. *Experimental neurology* 51: 78-109

O'Keefe J, Recce ML. 1993. Phase relationship between hippocampal place units and the EEG theta rhythm. *Hippocampus* 3: 317-30

O'Leary A, Koiv K, Raudkivi K, Harro J. 2016. Antidepressants differentially affect striatal amphetamine-stimulated dopamine and serotonin release in rats with high and low novelty-oriented behaviour. *Pharmacological research* 113: 739-46

Oren I, Paulsen O. 2010. Currents in space: understanding inhibitory field potentials. *The Journal of Physiology* 588: 2015-16

Osipova D, Hermes D, Jensen O. 2008. Gamma power is phase-locked to posterior alpha activity. *PloS one* 3: e3990

Overstreet LS, Westbrook GL, Jones MV. 2003. Measuring and Modeling the Spatiotemporal Profile of GABA at the Synapse In *Transmembrane Transporters*, pp. 259-75: John Wiley & Sons, Inc.

Owens DF, Boyce LH, Davis MB, Kriegstein AR. 1996. Excitatory GABA responses in embryonic and neonatal cortical slices demonstrated by gramicidin perforated-patch recordings and calcium imaging. *J Neurosci* 16: 6414-23

Owens DF, Liu X, Kriegstein AR. 1999. Changing properties of GABA(A) receptor-mediated signaling during early neocortical development. *Journal of neurophysiology* 82: 570-83

Pakhotin PI, Pakhotina ID, Andreev AA. 1997. Functional stability of hippocampal slices after treatment with cyclooxygenase inhibitors. *Neuroreport* 8: 1755-9

Palhalmi J, Paulsen O, Freund TF, Hajos N. 2004. Distinct properties of carbachol- and DHPG-induced network oscillations in hippocampal slices. *Neuropharmacology* 47: 381-9

Palmi M, Youmbi GT, Fusi F, Sgaragli GP, Dixon HB, et al. 1999. Potentiation of mitochondrial Ca2+ sequestration by taurine. *Biochemical pharmacology* 58: 1123-31

Palva JM, Palva S, Kaila K. 2005. Phase synchrony among neuronal oscillations in the human cortex. *J Neurosci* 25: 3962-72

Pape HC. 1996. Queer current and pacemaker: the hyperpolarization-activated cation current in neurons. *Annual review of physiology* 58: 299-327

Paperna T, Malach R. 1991. Patterns of sensory intermodality relationships in the cerebral cortex of the rat. *The Journal of comparative neurology* 308: 432-56

Pare D, Steriade M, Deschenes M, Oakson G. 1987. Physiological characteristics of anterior thalamic nuclei, a group devoid of inputs from reticular thalamic nucleus. *Journal of neurophysiology* 57: 1669-85

Paxinos G, Watson C. 2002. *The rat brain in stereotaxic coordinates*. San Diego [u.a.: Acad. Press.

Payne JA, Rivera C, Voipio J, Kaila K. 2003. Cation-chloride co-transporters in neuronal communication, development and trauma. *Trends in neurosciences* 26: 199-206

Pelkey KA, Barksdale E, Craig MT, Yuan X, Sukumaran M, et al. 2015. Pentraxins coordinate excitatory synapse maturation and circuit integration of parvalbumin interneurons. *Neuron* 85: 1257-72

Pelletier JC, Hesson DP, Jones KA, Costa A-M. 1996. Substituted 1,2-Dihydrophthalazines: Potent, Selective, and Noncompetitive Inhibitors of the AMPA Receptor. *Journal of Medicinal Chemistry* 39: 343-46

Penfield W, Boldrey E. 1937. Somatic motor and sensory representation in the cerebral cortex of man as studied by electrical stimulation. *Brain: A Journal of Neurology* 60: 389-443

Penit-Soria J, Audinat E, Crepel F. 1987. Excitation of rat prefrontal cortical neurons by dopamine: an in vitro electrophysiological study. *Brain research* 425: 263-74

Penny WD, Duzel E, Miller KJ, Ojemann JG. 2008. Testing for nested oscillation. *Journal of neuroscience methods* 174: 50-61

Penttonen M, Kamondi A, Acsady L, Buzsaki G. 1998. Gamma frequency oscillation in the hippocampus of the rat: intracellular analysis in vivo. *The European journal of neuroscience* 10: 718-28

Peters A, Jones EG. 1984. Classification of cortical neurons. In: Cellular components of the cerebral cortex, pp. 361–80. New York: Plenum

Petersen CC. 2007. The functional organization of the barrel cortex. *Neuron* 56: 339-55

Petersen CC, Sakmann B. 2000. The excitatory neuronal network of rat layer 4 barrel cortex. *J Neurosci* 20: 7579-86

Petreanu L, Mao T, Sternson SM, Svoboda K. 2009. The subcellular organization of neocortical excitatory connections. *Nature* 457: 1142-45

Pettersen KH, Hagen E, Einevoll GT. 2008. Estimation of population firing rates and current source densities from laminar electrode recordings. *Journal of computational neuroscience* 24: 291-313

Peyrache A, Dehghani N, Eskandar EN, Madsen JR, Anderson WS, et al. 2012. Spatiotemporal dynamics of neocortical excitation and inhibition during human sleep. *Proceedings of the National Academy of Sciences* 109: 1731-36

Pfurtscheller G, Neuper C. 1992. Simultaneous EEG 10 Hz desynchronization and 40 Hz synchronization during finger movements. *Neuroreport* 3: 1057-60

Pietersen AN, Patel N, Jefferys JG, Vreugdenhil M. 2009. Comparison between spontaneous and kainate-induced gamma oscillations in the mouse hippocampus in vitro. *The European journal of neuroscience* 29: 2145-56

Pin JP, Duvoisin R. 1995. The metabotropic glutamate receptors: structure and functions. *Neuropharmacology* 34: 1-26

Pinheiro PS, Lanore F, Veran J, Artinian J, Blanchet C, et al. 2013. Selective block of postsynaptic kainate receptors reveals their function at hippocampal mossy fiber synapses. *Cerebral cortex (New York, N.Y. : 1991)* 23: 323-31

Pirchio M, Turner JP, Williams SR, Asprodini E, Crunelli V. 1997. Postnatal development of membrane properties and delta oscillations in thalamocortical neurons of the cat dorsal lateral geniculate nucleus. *J Neurosci* 17: 5428-44

Polsky A, Mel BW, Schiller J. 2004. Computational subunits in thin dendrites of pyramidal cells. *Nat Neurosci* 7: 621-7

Porcello DM, Huntsman MM, Mihalek RM, Homanics GE, Huguenard JR. 2003. Intact synaptic GABAergic inhibition and altered neurosteroid modulation of thalamic relay neurons in mice lacking delta subunit. *Journal of neurophysiology* 89: 1378-86

Porter LL. 1991. Patterns of connectivity in the cat sensory-motor cortex: A light and electron microscope analysis of the projection arising from area 3a. *The Journal of Comparative Neurology* 312: 404-14

Porter LL. 1992. Patterns of projections from area 2 of the sensory cortex to area 3a and to the motor cortex in cats. *Experimental Brain Research* 91: 85-93

Porter LL. 1996. Somatosensory input onto pyramidal tract neurons in rodent motor cortex. *Neuroreport* 7: 2309-15

Porter LL, Izraeli R. 1993. The effects of localized inactivation of somatosensory cortex, area 3a, on area 2 in cats. *Somatosensory & motor research* 10: 399-413

Porter LL, Sakamoto K. 1988. Organization and synaptic relationships of the projection from the primary sensory to the primary motor cortex in the cat. *The Journal of comparative neurology* 271: 387-96

Porter LL, White EL. 1983. Afferent and efferent pathways of the vibrissal region of primary motor cortex in the mouse. *The Journal of comparative neurology* 214: 279-89

Prokic E. 2011. *Modulation of neuronal network activity in the primary motor cortex*. Doctoral thesis. Aston University

Prokic EJ, Weston C, Yamawaki N, Hall SD, Jones RSG, et al. 2015. Cortical oscillatory dynamics and benzodiazepine-site modulation of tonic inhibition in fast spiking interneurons. *Neuropharmacology* 95: 192-205

Purcell AE, Jeon OH, Zimmerman AW, Blue ME, Pevsner J. 2001. Postmortem brain abnormalities of the glutamate neurotransmitter system in autism. *Neurology* 57: 1618-28

Putman P. 2011. Resting state EEG delta-beta coherence in relation to anxiety, behavioral inhibition, and selective attentional processing of threatening stimuli. *International journal of psychophysiology : official journal of the International Organization of Psychophysiology* 80: 63-8

Raghanti MA, Stimpson CD, Marcinkiewicz JL, Erwin JM, Hof PR, Sherwood CC. 2008. Cortical dopaminergic innervation among humans, chimpanzees, and macaque monkeys: a comparative study. *Neuroscience* 155: 203-20

Rankin ML, Sibley DR. 2010. Constitutive phosphorylation by protein kinase C regulates D1 dopamine receptor signaling. *Journal of neurochemistry* 115: 1655-67

Rappelsberger P, Pockberger H, Petsche H. 1982. The contribution of the cortical layers to the generation of the EEG: field potential and current source density analyses in the rabbit's visual cortex. *Electroencephalography and clinical neurophysiology* 53: 254-69

Rasch B, Born J. 2013. About sleep's role in memory. *Physiological reviews* 93: 681-766

Rasch MJ, Gretton A, Murayama Y, Maass W, Logothetis NK. 2008. Inferring spike trains from local field potentials. *Journal of neurophysiology* 99: 1461-76

Rechtschaffen A, Kales A, University of California LA, Brain Information S, Network NNI. 1973. *A manual of standardized terminology, techniques and scoring system for sleep stages of human subjects*. Los Angeles, Calif.: Brain Information Service/Brain Research Institute, University of California.

Reep RL, Goodwin GS, Corwin JV. 1990. Topographic organization in the corticocortical connections of medial agranular cortex in rats. *The Journal of comparative neurology* 294: 262-80

Reimann Michael W, Anastassiou Costas A, Perin R, Hill SL, Markram H, Koch C. 2013. A Biophysically Detailed Model of Neocortical Local Field Potentials Predicts the Critical Role of Active Membrane Currents. *Neuron* 79: 375-90

Rekling JC, Shao XM, Feldman JL. 2000. Electrical Coupling and Excitatory Synaptic Transmission between Rhythmogenic Respiratory Neurons in the PreBötzinger Complex. *The Journal of neuroscience : the official journal of the Society for Neuroscience* 20: RC113-RC13

Ren K, Hylden JL, Williams GM, Ruda MA, Dubner R. 1992. The effects of a non-competitive NMDA receptor antagonist, MK-801, on behavioral hyperalgesia and

dorsal horn neuronal activity in rats with unilateral inflammation. *Pain* 50: 331-44

Resibois A, Rogers JH. 1992. Calretinin in rat brain: an immunohistochemical study. *Neuroscience* 46: 101-34

Riccio A, Medhurst AD, Mattei C, Kelsell RE, Calver AR, et al. 2002. mRNA distribution analysis of human TRPC family in CNS and peripheral tissues. *Brain research. Molecular brain research* 109: 95-104

Rice ME. 2000. Ascorbate regulation and its neuroprotective role in the brain. *Trends in neurosciences* 23: 209-16

Rice ME, Perez-Pinzon MA, Lee EJ. 1994. Ascorbic acid, but not glutathione, is taken up by brain slices and preserves cell morphology. *Journal of neurophysiology* 71: 1591-6

Richfield EK, Penney JB, Young AB. 1989. Anatomical and affinity state comparisons between dopamine D1 and D2 receptors in the rat central nervous system. *Neuroscience* 30: 767-77

Rioult-Pedotti MS, Friedman D, Hess G, Donoghue JP. 1998. Strengthening of horizontal cortical connections following skill learning. *Nat Neurosci* 1: 230-4

Rivara CB, Sherwood CC, Bouras C, Hof PR. 2003. Stereologic characterization and spatial distribution patterns of Betz cells in the human primary motor cortex. *The anatomical record. Part A, Discoveries in molecular, cellular, and evolutionary biology* 270: 137-51

Rivera C, Voipio J, Kaila K. 2005. Two developmental switches in GABAergic signalling: the K(+)–Cl(−) cotransporter KCC2 and carbonic anhydrase CAVII. *The Journal of Physiology* 562: 27-36

Rivera C, Voipio J, Payne JA, Ruusuvuori E, Lahtinen H, et al. 1999. The K+/Cl- co-transporter KCC2 renders GABA hyperpolarizing during neuronal maturation. *Nature* 397: 251-5

Roberts E, Frankel S. 1950. gamma-Aminobutyric acid in brain: its formation from glutamic acid. *The Journal of biological chemistry* 187: 55-63

Robinson RB, Siegelbaum SA. 2003. Hyperpolarization-activated cation currents: from molecules to physiological function. *Annual review of physiology* 65: 453-80

Rocco MM, Brumberg JC. 2007. The sensorimotor slice. *Journal of neuroscience methods* 162: 139-47

Rodriguez-Moreno A, Herreras O, Lerma J. 1997. Kainate receptors presynaptically downregulate GABAergic inhibition in the rat hippocampus. *Neuron* 19: 893-901

Rodriguez-Moreno A, Lerma J. 1998. Kainate receptor modulation of GABA release involves a metabotropic function. *Neuron* 20: 1211-8

Rondou P, Haegeman G, Van Craenenbroeck K. 2010. The dopamine D4 receptor: biochemical and signalling properties. *Cellular and molecular life sciences : CMLS* 67: 1971-86

Roopun AK, Middleton SJ, Cunningham MO, LeBeau FEN, Bibbig A, et al. 2006. A beta2-frequency (20–30 Hz) oscillation in nonsynaptic networks of somatosensory cortex. *Proceedings of the National Academy of Sciences* 103: 15646-50

Roopun AK, Traub RD, Baldeweg T, Cunningham MO, Whittaker RG, et al. 2009. Detecting seizure origin using basic, multiscale population dynamic measures: Preliminary findings. *Epilepsy & behavior : E&B* 14: 39-46

Rosenmund C, Stern-Bach Y, Stevens CF. 1998. The tetrameric structure of a glutamate receptor channel. *Science* 280: 1596-9

Rothwell JC, Traub MM, Day BL, Obeso JA, Thomas PK, Marsden CD. 1982. Manual motor performance in a deafferented man. *Brain : a journal of neurology* 105 (Pt 3): 515-42

Rouach N, Segal M, Koulakoff A, Giaume C, Avignone E. 2003. Carbenoxolone blockade of neuronal network activity in culture is not mediated by an action on gap junctions. *The Journal of physiology* 553: 729-45

Rouiller EM, Moret V, Liang F. 1993. Comparison of the connectional properties of the two forelimb areas of the rat sensorimotor cortex: support for the presence of a premotor or supplementary motor cortical area. *Somatosensory & motor research* 10: 269-89

Rowell JJ, Mallik AK, Dugas-Ford J, Ragsdale CW. 2010. Molecular analysis of neocortical

layer structure in the ferret. *The Journal of comparative neurology* 518: 3272-89

Rudolph M, Pospischil M, Timofeev I, Destexhe A. 2007. Inhibition Determines Membrane Potential Dynamics and Controls Action Potential Generation in Awake and Sleeping Cat Cortex. *The Journal of Neuroscience* 27: 5280-90

Sabolek HR, Penley SC, Hinman JR, Bunce JG, Markus EJ, et al. 2009. Theta and gamma coherence along the septotemporal axis of the hippocampus. *Journal of neurophysiology* 101: 1192-2000

Sadaghiani S, Scheeringa R, Lehongre K, Morillon B, Giraud AL, Kleinschmidt A. 2010. Intrinsic connectivity networks, alpha oscillations, and tonic alertness: a simultaneous electroencephalography/functional magnetic resonance imaging study. *J Neurosci* 30: 10243-50

Sakamoto T, Arissian K, Asanuma H. 1989. Functional role of the sensory cortex in learning motor skills in cats. *Brain research* 503: 258-64

Salzman CD, Britten KH, Newsome WT. 1990. Cortical microstimulation influences perceptual judgements of motion direction. *Nature* 346: 174-77

Sanchez-Vives MV, McCormick DA. 2000. Cellular and network mechanisms of rhythmic recurrent activity in neocortex. *Nat Neurosci* 3: 1027-34

Sanes JN, Donoghue JP. 2000. Plasticity and primary motor cortex. *Annual review of neuroscience* 23: 393-415

Sato TR, Svoboda K. 2010. The functional properties of barrel cortex neurons projecting to the primary motor cortex. *Journal of Neuroscience* 30: 4256-60

Saunders A, Granger AJ, Sabatini BL. 2015. Corelease of acetylcholine and GABA from cholinergic forebrain neurons. *eLife* 4: e06412

Sawaguchi T, Matsumura M, Kubota K. 1986. Catecholamine sensitivities of motor cortical neurons of the monkey. *Neuroscience letters* 66: 135-40

Schiller J, Major G, Koester HJ, Schiller Y. 2000. NMDA spikes in basal dendrites of cortical pyramidal neurons. *Nature* 404: 285-89

Schmitz D, Schuchmann S, Fisahn A, Draguhn A, Buhl EH, et al. 2001. Axo-axonal coupling. a novel mechanism for ultrafast neuronal communication. *Neuron* 31: 831-40

Schoepp DD, Johnson BG, Monn JA. 1992. Inhibition of cyclic AMP formation by a selective metabotropic glutamate receptor agonist. *Journal of neurochemistry* 58: 1184-6

Schroeder CE, Lakatos P. 2009. Low-frequency neuronal oscillations as instruments of sensory selection. *Trends in neurosciences* 32: 9-18

Schubert D, Kotter R, Zilles K, Luhmann HJ, Staiger JF. 2003. Cell type-specific circuits of cortical layer IV spiny neurons. *J Neurosci* 23: 2961-70

Schubert D, Staiger JF, Cho N, Kotter R, Zilles K, Luhmann HJ. 2001. Layer-specific intracolumnar and transcolumnar functional connectivity of layer V pyramidal cells in rat barrel cortex. *J Neurosci* 21: 3580-92

Schultz D, Miller JC. 2004. Fatigue and use of go/no-go pills in extraordinarily long combat sorties. *Aviation, space, and environmental medicine* 75: 370-1

Schutter DJ, Knyazev GG. 2012. Cross-frequency coupling of brain oscillations in studying motivation and emotion. *Motivation and emotion* 36: 46-54

Scimemi A, Semyanov A, Sperk G, Kullmann DM, Walker MC. 2005. Multiple and plastic receptors mediate tonic GABAA receptor currents in the hippocampus. *J Neurosci* 25: 10016-24

Scott L, Zelenin S, Malmersjö S, Kowalewski JM, Markus EZ, et al. 2006. Allosteric changes of the NMDA receptor trap diffusible dopamine 1 receptors in spines. *Proceedings of the National Academy of Sciences of the United States of America* 103: 762-67

Seamans JK, Durstewitz D, Christie BR, Stevens CF, Sejnowski TJ. 2001. Dopamine D1/D5 receptor modulation of excitatory synaptic inputs to layer V prefrontal cortex neurons. *Proceedings of the National Academy of Sciences of the United States of America* 98: 301-6

Seamans JK, Gorelova N, Durstewitz D, Yang CR. 2001. Bidirectional dopamine modulation of GABAergic inhibition in prefrontal cortical pyramidal neurons. *J Neurosci* 21: 3628-38

Seamans JK, Yang CR. 2004. The principal features and mechanisms of dopamine

modulation in the prefrontal cortex. *Progress in neurobiology* 74: 1-58

Seeman P, Lee T, Chau-Wong M, Wong K. 1976. Antipsychotic drug doses and neuroleptic/dopamine receptors. *Nature* 261: 717-19

Seeman P, Van Tol HH. 1994. Dopamine receptor pharmacology. *Trends in pharmacological sciences* 15: 264-70

Segal M, Barker JL. 1984. Rat hippocampal neurons in culture: voltage-clamp analysis of inhibitory synaptic connections. *Journal of Neurophysiology* 52: 469-87

Seidenbecher T, Laxmi TR, Stork O, Pape HC. 2003. Amygdalar and hippocampal theta rhythm synchronization during fear memory retrieval. *Science* 301: 846-50

Semyanov A, Walker MC, Kullmann DM. 2003. GABA uptake regulates cortical excitability via cell type-specific tonic inhibition. *Nat Neurosci* 6: 484-90

Shah D. 2017. Mechanisms of hyperexcitability and efficacy of antiepileptic drugs in hippocampal-entorhinal networks in the Reduced Intensity Status Epilepticus (RISE) model of chronic epilepsy. *Doctoral thesis.* Aston University

Shah MM, Hammond RS, Hoffman DA. 2010. Dendritic ion channel trafficking and plasticity. *Trends in neurosciences* 33: 307-16

Shaw PJ. 1993. Excitatory amino acid receptors, excitotoxicity, and the human nervous system. *Current opinion in neurology and neurosurgery* 6: 414-22

Sheer DE. 1989. Focused arousal and the cognitive 40-Hz event-related potentials: differential diagnosis of Alzheimer's disease. *Progress in clinical and biological research* 317: 79-94

Sheroziya MG, von Bohlen Und Halbach O, Unsicker K, Egorov AV. 2009. Spontaneous bursting activity in the developing entorhinal cortex. *J Neurosci* 29: 12131-44

Shi WX, Zheng P, Liang XF, Bunney BS. 1997. Characterization of dopamine-induced depolarization of prefrontal cortical neurons. *Synapse (New York, N.Y.)* 26: 415-22

Shigemoto R, Kinoshita A, Wada E, Nomura S, Ohishi H, et al. 1997. Differential Presynaptic Localization of Metabotropic Glutamate Receptor Subtypes in the Rat Hippocampus. *The Journal of Neuroscience* 17: 7503-22

Shigemoto R, Nomura S, Ohishi H, Sugihara H, Nakanishi S, Mizuno N. 1993. Immunohistochemical localization of a metabotropic glutamate receptor, mGluR5, in the rat brain. *Neuroscience letters* 163: 53-7

Shipp S. 2005. The importance of being agranular: a comparative account of visual and motor cortex. *Philosophical transactions of the Royal Society of London. Series B, Biological sciences* 360: 797-814

Shipp S, Adams RA, Friston KJ. 2013. Reflections on agranular architecture: predictive coding in the motor cortex. *Trends in neurosciences* 36: 706-16

Shu Y, Hasenstaub A, McCormick DA. 2003. Turning on and off recurrent balanced cortical activity. *Nature* 423: 288-93

Sibley DR. 1999. New insights into dopaminergic receptor function using antisense and genetically altered animals. *Annual review of pharmacology and toxicology* 39: 313-41

Sinfield JL, Collins DR. 2006. Induction of synchronous oscillatory activity in the rat lateral amygdala in vitro is dependent on gap junction activity. *The European journal of neuroscience* 24: 3091-5

Singer W. 1999. Neuronal Synchrony: A Versatile Code for the Definition of Relations? *Neuron* 24: 49-65

Sirota A, Montgomery S, Fujisawa S, Isomura Y, Zugaro M, Buzsaki G. 2008. Entrainment of neocortical neurons and gamma oscillations by the hippocampal theta rhythm. *Neuron* 60: 683-97

Skoglund TS, Pascher R, Berthold CH. 1997. The existence of a layer IV in the rat motor cortex. *Cerebral cortex (New York, N.Y. : 1991)* 7: 178-80

Sloper JJ, Hiorns RW, Powell TP. 1979. A qualitative and quantitative electron microscopic study of the neurons in the primate motor and somatic sensory cortices. *Philosophical transactions of the Royal Society of London. Series B, Biological sciences* 285: 141-71

Smith AM, Frysinger RC, Bourbonnais D. 1983. Interaction between motor commands and somatosensory afferents in the control of prehension. *Advances in neurology* 39:

373-85

Smolders I, Bortolotto ZA, Clarke VR, Warre R, Khan GM, et al. 2002. Antagonists of GLU(K5)-containing kainate receptors prevent pilocarpine-induced limbic seizures. *Nat Neurosci* 5: 796-804

Snyder GL, Allen PB, Fienberg AA, Valle CG, Huganir RL, et al. 2000. Regulation of phosphorylation of the GluR1 AMPA receptor in the neostriatum by dopamine and psychostimulants in vivo. *J Neurosci* 20: 4480-8

Snyder GL, Fienberg AA, Huganir RL, Greengard P. 1998. A dopamine/D1 receptor/protein kinase A/dopamine- and cAMP-regulated phosphoprotein (Mr 32 kDa)/protein phosphatase-1 pathway regulates dephosphorylation of the NMDA receptor. *J Neurosci* 18: 10297-303

Snyder SH, Taylor KM, Coyle JT, Meyerhoff JL. 1970. The role of brain dopamine in behavioral regulation and the actions of psychotropic drugs. *The American journal of psychiatry* 127: 199-207

Sohal VS, Zhang F, Yizhar O, Deisseroth K. 2009. Parvalbumin neurons and gamma rhythms enhance cortical circuit performance. *Nature* 459: 698-702

Sokoloff P, Diaz J, Le Foll B, Guillin O, Leriche L, et al. 2006. The dopamine D3 receptor: a therapeutic target for the treatment of neuropsychiatric disorders. *CNS & neurological disorders drug targets* 5: 25-43

Soltesz I, Deschenes M. 1993. Low- and high-frequency membrane potential oscillations during theta activity in CA1 and CA3 pyramidal neurons of the rat hippocampus under ketamine-xylazine anesthesia. *Journal of neurophysiology* 70: 97-116

Soltesz I, Lightowler S, Leresche N, Jassik-Gerschenfeld D, Pollard CE, Crunelli V. 1991. Two inward currents and the transformation of low-frequency oscillations of rat and cat thalamocortical cells. *The Journal of physiology* 441: 175-97

Somogyi P, Klausberger T. 2005. Defined types of cortical interneurone structure space and spike timing in the hippocampus. *The Journal of Physiology* 562: 9-26

Soso MJ, Fetz EE. 1980. Responses of identified cells in postcentral cortex of awake monkeys during comparable active and passive joint movements. *Journal of neurophysiology* 43: 1090-110

Sotero RC. 2016. Topology, Cross-Frequency, and Same-Frequency Band Interactions Shape the Generation of Phase-Amplitude Coupling in a Neural Mass Model of a Cortical Column. *PLOS Computational Biology* 12: e1005180

Spain WJ. 1994. Serotonin has different effects on two classes of Betz cells from the cat. *Journal of neurophysiology* 72: 1925-37

Spain WJ, Schwindt PC, Crill WE. 1991. Post-inhibitory excitation and inhibition in layer V pyramidal neurones from cat sensorimotor cortex. *The Journal of physiology* 434: 609-26

Spain WJ, Schwindt PC, Crill WE. 1991. Two transient potassium currents in layer V pyramidal neurones from cat sensorimotor cortex. *The Journal of physiology* 434: 591-607

Staiger JF, Zuschratter W, Luhmann HJ, Schubert D. 2009. Local circuits targeting parvalbumin-containing interneurons in layer IV of rat barrel cortex. *Brain structure & function* 214: 1-13

Staley K. 1992. Enhancement of the excitatory actions of GABA by barbiturates and benzodiazepines. *Neuroscience letters* 146: 105-7

Stam CJ, Jones BF, Nolte G, Breakspear M, Scheltens P. 2007. Small-world networks and functional connectivity in Alzheimer's disease. *Cerebral cortex (New York, N.Y. : 1991)* 17: 92-9

Stanger HL, Alford R, Jane DE, Cunningham MO. 2008. The role of GLU K5-containing kainate receptors in entorhinal cortex gamma frequency oscillations. *Neural plasticity* 2008: 401645

Stein V, Nicoll RA. 2003. GABA generates excitement. *Neuron* 37: 375-8

Stell BM, Mody I. 2002. Receptors with different affinities mediate phasic and tonic GABA(A) conductances in hippocampal neurons. *J Neurosci* 22: Rc223

Steriade M, Datta S, Pare D, Oakson G, Curro Dossi RC. 1990. Neuronal activities in brain-stem cholinergic nuclei related to tonic activation processes in thalamocortical

systems. *J Neurosci* 10: 2541-59

Steriade M, Deschenes M, Domich L, Mulle C. 1985. Abolition of spindle oscillations in thalamic neurons disconnected from nucleus reticularis thalami. *Journal of neurophysiology* 54: 1473-97

Steriade M, Dossi RC, Nunez A. 1991. Network modulation of a slow intrinsic oscillation of cat thalamocortical neurons implicated in sleep delta waves: cortically induced synchronization and brainstem cholinergic suppression. *J Neurosci* 11: 3200-17

Steriade M, McCormick DA, Sejnowski TJ. 1993. Thalamocortical oscillations in the sleeping and aroused brain. *Science* 262: 679-85

Steriade M, Nunez A, Amzica F. 1993. Intracellular analysis of relations between the slow (< 1 Hz) neocortical oscillation and other sleep rhythms of the electroencephalogram. *J Neurosci* 13: 3266-83

Steriade M, Timofeev I. 2003. Neuronal plasticity in thalamocortical networks during sleep and waking oscillations. *Neuron* 37: 563-76

Steriade M, Timofeev I, Grenier F. 2001. Natural waking and sleep states: a view from inside neocortical neurons. *Journal of neurophysiology* 85: 1969-85

Stickgold R, James L, Hobson JA. 2000. Visual discrimination learning requires sleep after training. *Nat Neurosci* 3: 1237-38

Stivers JA, Skirboll LR, Long R, Crawley JN. 1988. Anatomical analysis of frontal cortex sites at which carbachol induces motor seizures in the rat. *Pharmacology, biochemistry, and behavior* 30: 129-36

Stoney SD, Jr., Thompson WD, Asanuma H. 1968. Excitation of pyramidal tract cells by intracortical microstimulation: effective extent of stimulating current. *Journal of neurophysiology* 31: 659-69

Storozhuk VM, Khorevin VI, Rozumna NM, Villa AE, Tetko IV. 2004. Dopamine modulation of glutamate metabotropic receptors in conditioned reaction of sensory motor cortex neurons of the cat. *Neuroscience letters* 356: 127-30

Struber D, Basar-Eroglu C, Hoff E, Stadler M. 2000. Reversal-rate dependent differences in the EEG gamma-band during multistable visual perception. *International journal of psychophysiology : official journal of the International Organization of Psychophysiology* 38: 243-52

Strubing C, Krapivinsky G, Krapivinsky L, Clapham DE. 2001. TRPC1 and TRPC5 form a novel cation channel in mammalian brain. *Neuron* 29: 645-55

Stuart G, Spruston N, Häusser M. 2008. *Dendrites.* Oxford: Oxford University Press.

Sulzer D, Zecca L. 2000. Intraneuronal dopamine-quinone synthesis: a review. *Neurotoxicity research* 1: 181-95

Swanson GT, Kamboj SK, Cull-Candy SG. 1997. Single-channel properties of recombinant AMPA receptors depend on RNA editing, splice variation, and subunit composition. *J Neurosci* 17: 58-69

Szabo GG, Holderith N, Gulyas AI, Freund TF, Hajos N. 2010. Distinct synaptic properties of perisomatic inhibitory cell types and their different modulation by cholinergic receptor activation in the CA3 region of the mouse hippocampus. *The European journal of neuroscience* 31: 2234-46

Takahashi K, Lin JS, Sakai K. 2006. Neuronal activity of histaminergic tuberomammillary neurons during wake-sleep states in the mouse. *J Neurosci* 26: 10292-8

Tallon-Baudry C, Bertrand O. 1999. Oscillatory gamma activity in humans and its role in object representation. *Trends in cognitive sciences* 3: 151-62

Tamás G, Buhl EH, Lörincz A, Somogyi P. 2000. Proximally targeted GABAergic synapses and gap junctions synchronize cortical interneurons. *Nature neuroscience* 3: 366-71

Tamas G, Buhl EH, Somogyi P. 1997. Fast IPSPs elicited via multiple synaptic release sites by different types of GABAergic neurone in the cat visual cortex. *The Journal of physiology* 500 (Pt 3): 715-38

Tanaka YH, Tanaka YR, Fujiyama F, Furuta T, Yanagawa Y, Kaneko T. 2011. Local connections of layer 5 GABAergic interneurons to corticospinal neurons. *Front Neural Circuits* 5: 12

Tao JX, Chen XJ, Baldwin M, Yung I, Rose S, et al. 2011. Interictal regional delta slowing is an EEG marker of epileptic network in temporal lobe epilepsy. *Epilepsia* 52: 467-

Tass P, Rosenblum MG, Weule J, Kurths J, Pikovsky A, et al. 1998. Detection of n:m Phase Locking from Noisy Data : Application to Magnetoencephalography *Phys. Rev. Lett.* 81: 3291-94

Telenczuk B, Dehghani N, Le Van Quyen M, Cash SS, Halgren E, et al. 2017. Local field potentials primarily reflect inhibitory neuron activity in human and monkey cortex. *Scientific reports* 7: 40211

Terunuma M, Vargas KJ, Wilkins ME, Ramirez OA, Jaureguiberry-Bravo M, et al. 2010. Prolonged activation of NMDA receptors promotes dephosphorylation and alters postendocytic sorting of GABAB receptors. *Proceedings of the National Academy of Sciences of the United States of America* 107: 13918-23

Thompson AJ, Lester HA, Lummis SC. 2010. The structural basis of function in Cys-loop receptors. *Quarterly reviews of biophysics* 43: 449-99

Thompson AM. 2010 Neocortical layer 6, a review. *Frontiers in neuroanatomy*

Thomson AM, Deuchars J, West DC. 1996. Neocortical local synaptic circuitry revealed with dual intracellular recordings and biocytin-filling. *Journal of physiology, Paris* 90: 211-5

Thomson AM, Lamy C. 2007. Functional Maps of Neocortical Local Circuitry. *Frontiers in Neuroscience* 1: 19-42

Thomson AM, Morris OT. 2002. Selectivity in the inter-laminar connections made by neocortical neurones. *Journal of Neurocytology* 31: 239-46

Tia S, Wang JF, Kotchabhakdi N, Vicini S. 1996. Developmental Changes of Inhibitory Synaptic Currents in Cerebellar Granule Neurons: Role of GABA$_A$ Receptor $\alpha6$ Subunit. *The Journal of Neuroscience* 16: 3630-40

Tiesinga P, Sejnowski TJ. 2009. Cortical enlightenment: are attentional gamma oscillations driven by ING or PING? *Neuron* 63: 727-32

Tiesinga PH, Fellous JM, Jose JV, Sejnowski TJ. 2001. Computational model of carbachol-induced delta, theta, and gamma oscillations in the hippocampus. *Hippocampus* 11: 251-74

Tiesinga PH, Jose JV. 2000. Robust gamma oscillations in networks of inhibitory hippocampal interneurons. *Network (Bristol, England)* 11: 1-23

Tiitinen H, Sinkkonen J, Reinikainen K, Alho K, Lavikainen J, Naatanen R. 1993. Selective attention enhances the auditory 40-Hz transient response in humans. *Nature* 364: 59-60

Timofeev I, Grenier F, Bazhenov M, Sejnowski TJ, Steriade M. 2000. Origin of slow cortical oscillations in deafferented cortical slabs. *Cerebral cortex (New York, N.Y. : 1991)* 10: 1185-99

Timofeev I, Grenier F, Steriade M. 2000. Impact of intrinsic properties and synaptic factors on the activity of neocortical networks in vivo. *Journal of Physiology-Paris* 94: 343-55

Timofeev I, Grenier F, Steriade M. 2001. Disfacilitation and active inhibition in the neocortex during the natural sleep-wake cycle: An intracellular study. *Proceedings of the National Academy of Sciences of the United States of America* 98: 1924-29

Timofeev I, Steriade M. 1996. Low-frequency rhythms in the thalamus of intact-cortex and decorticated cats. *Journal of neurophysiology* 76: 4152-68

Tofighy A, Abbott A, Centonze D, Cooper AJ, Noor E, et al. 2003. Excitation by dopamine of rat subthalamic nucleus neurones in vitro-a direct action with unconventional pharmacology. *Neuroscience* 116: 157-66

Tort AB, Komorowski R, Eichenbaum H, Kopell N. 2010. Measuring phase-amplitude coupling between neuronal oscillations of different frequencies. *Journal of neurophysiology* 104: 1195-210

Tort AB, Komorowski RW, Manns JR, Kopell NJ, Eichenbaum H. 2009. Theta-gamma coupling increases during the learning of item-context associations. *Proceedings of the National Academy of Sciences of the United States of America* 106: 20942-7

Tort AB, Rotstein HG, Dugladze T, Gloveli T, Kopell NJ. 2007. On the formation of gamma-coherent cell assemblies by oriens lacunosum-moleculare interneurons in the hippocampus. *Proceedings of the National Academy of Sciences of the United*

States of America 104: 13490-5

Tort ABL, Kramer MA, Thorn C, Gibson DJ, Kubota Y, et al. 2008. Dynamic cross-frequency couplings of local field potential oscillations in rat striatum and hippocampus during performance of a T-maze task. *Proceedings of the National Academy of Sciences* 105: 20517-22

Tossman U, Jonsson G, Ungerstedt U. 1986. Regional distribution and extracellular levels of amino acids in rat central nervous system. *Acta Physiol Scand* 127: 533-45

Toth T, Crunelli V. 1992. Computer simulation of the pacemaker oscillations of thalamocortical cells. *Neuroreport* 3: 65-8

Tovar KR, Maher BJ, Westbrook GL. 2009. Direct actions of carbenoxolone on synaptic transmission and neuronal membrane properties. *Journal of neurophysiology* 102: 974-8

Towers SK, Hestrin S. 2008. D1-like dopamine receptor activation modulates GABAergic inhibition but not electrical coupling between neocortical fast-spiking interneurons. *J Neurosci* 28: 2633-41

Trampus M, Ferri N, Adami M, Ongini E. 1993. The dopamine D1 receptor agonists, A68930 and SKF 38393, induce arousal and suppress REM sleep in the rat. *European Journal of Pharmacology* 235: 83-87

Trantham-Davidson H, Kroner S, Seamans JK. 2008. Dopamine modulation of prefrontal cortex interneurons occurs independently of DARPP-32. *Cerebral cortex (New York, N.Y. : 1991)* 18: 951-8

Traub RD, Bibbig A, Fisahn A, LeBeau FE, Whittington MA, Buhl EH. 2000. A model of gamma-frequency network oscillations induced in the rat CA3 region by carbachol in vitro. *The European journal of neuroscience* 12: 4093-106

Traub RD, Kopell N, Bibbig A, Buhl EH, LeBeau FEN, Whittington MA. 2001. Gap Junctions between Interneuron Dendrites Can Enhance Synchrony of Gamma Oscillations in Distributed Networks. *The Journal of Neuroscience* 21: 9478-86

Traub RD, Pais I, Bibbig A, LeBeau FEN, Buhl EH, et al. 2003. Contrasting roles of axonal (pyramidal cell) and dendritic (interneuron) electrical coupling in the generation of neuronal network oscillations. *Proceedings of the National Academy of Sciences* 100: 1370-74

Traub RD, Whittington MA. 2010. *Cortical oscillations in health and disease.* Oxford University Press, USA.

Traub RD, Whittington MA, Colling SB, Buzsaki G, Jefferys JG. 1996. Analysis of gamma rhythms in the rat hippocampus in vitro and in vivo. *The Journal of physiology* 493 (Pt 2): 471-84

Traub RD, Whittington MA, Stanford IM, Jefferys JGR. 1996. A mechanism for generation of long-range synchronous fast oscillations in the cortex. *Nature* 383: 621-24

Traynelis SF, Wollmuth LP, McBain CJ, Menniti FS, Vance KM, et al. 2010. Glutamate receptor ion channels: structure, regulation, and function. *Pharmacological reviews* 62: 405-96

Trevelyan AJ. 2009. The direct relationship between inhibitory currents and local field potentials. *J Neurosci* 29: 15299-307

Tritsch NX, Sabatini BL. 2012. Dopaminergic modulation of synaptic transmission in cortex and striatum. *Neuron* 76: 33-50

Trulson ME, Jacobs BL. 1979. Raphe unit activity in freely moving cats: correlation with level of behavioral arousal. *Brain research* 163: 135-50

Trulson ME, Preussler DW, Howell GA. 1981. Activity of substantia nigra units across the sleep-waking cycle in freely moving cats. *Neuroscience letters* 26: 183-8

Tseng KY, O'Donnell P. 2004. Dopamine-glutamate interactions controlling prefrontal cortical pyramidal cell excitability involve multiple signaling mechanisms. *J Neurosci* 24: 5131-9

Twyman RE, Rogers CJ, Macdonald RL. 1990. Intraburst kinetic properties of the GABAA receptor main conductance state of mouse spinal cord neurones in culture. *The Journal of physiology* 423: 193-220

Uchimura N, Higashi H, Nishi S. 1986. Hyperpolarizing and depolarizing actions of dopamine via D-1 and D-2 receptors on nucleus accumbens neurons. *Brain*

research 375: 368-72

Ueki Y, Mima T, Kotb MA, Sawada H, Saiki H, et al. 2006. Altered plasticity of the human motor cortex in Parkinson's disease. *Annals of neurology* 59: 60-71

Ursin R. 1968. The two stages of slow wave sleep in the cat and their relation to REM sleep. *Brain research* 11: 347-56

Valeyev AY, Cruciani RA, Lange GD, Smallwood VS, Barker JL. 1993. Cl− channels are randomly activated by continuous GABA secretion in cultured embryonic rat hippocampal neurons. *Neuroscience Letters* 155: 199-203

van Brederode JF, Helliesen MK, Hendrickson AE. 1991. Distribution of the calcium-binding proteins parvalbumin and calbindin-D28k in the sensorimotor cortex of the rat. *Neuroscience* 44: 157-71

van Brederode JF, Snyder GL. 1992. A comparison of the electrophysiological properties of morphologically identified cells in layers 5B and 6 of the rat neocortex. *Neuroscience* 50: 315-37

Van Der Werf YD, Altena E, Schoonheim MM, Sanz-Arigita EJ, Vis JC, et al. 2009. Sleep benefits subsequent hippocampal functioning. *Nat Neurosci* 12: 122-23

Van Vreeswijk C, Abbott LF, Bard Ermentrout G. 1994. When inhibition not excitation synchronizes neural firing. *Journal of Computational Neuroscience* 1: 313-21

Vanderwolf CH. 1969. Hippocampal electrical activity and voluntary movement in the rat. *Electroencephalography and Clinical Neurophysiology* 26: 407-18

Vanhatalo S, Palva JM, Holmes MD, Miller JW, Voipio J, Kaila K. 2004. Infraslow oscillations modulate excitability and interictal epileptic activity in the human cortex during sleep. *Proceedings of the National Academy of Sciences of the United States of America* 101: 5053-7

Vanini G, Wathen BL, Lydic R, Baghdoyan HA. 2011. Endogenous GABA levels in the pontine reticular formation are greater during wakefulness than during rapid eye movement sleep. *J Neurosci* 31: 2649-56

Vassalli A, Dijk DJ. 2009. Sleep function: current questions and new approaches. *The European journal of neuroscience* 29: 1830-41

Vazquez J, Baghdoyan HA. 2001. Basal forebrain acetylcholine release during REM sleep is significantly greater than during waking. *American journal of physiology. Regulatory, integrative and comparative physiology* 280: R598-601

Verdoorn TA, Burnashev N, Monyer H, Seeburg PH, Sakmann B. 1991. Structural determinants of ion flow through recombinant glutamate receptor channels. *Science* 252: 1715-8

Vertes RP, Kocsis B. 1997. Brainstem-diencephalo-septohippocampal systems controlling the theta rhythm of the hippocampus. *Neuroscience* 81: 893-926

Vessey JP, Lalonde MR, Mizan HA, Welch NC, Kelly ME, Barnes S. 2004. Carbenoxolone inhibition of voltage-gated Ca channels and synaptic transmission in the retina. *Journal of neurophysiology* 92: 1252-6

Vicini S, Wang JF, Li JH, Zhu WJ, Wang YH, et al. 1998. Functional and pharmacological differences between recombinant N-methyl-D-aspartate receptors. *Journal of neurophysiology* 79: 555-66

Vigneswaran G, Kraskov A, Lemon RN. 2011. Large identified pyramidal cells in macaque motor and premotor cortex exhibit "thin spikes": implications for cell type classification. *J Neurosci* 31: 14235-42

Villablanca J. 1974. *The role of the thalamus on sleep control: Sleep-wakefulness studies in chronic "diencephalic" and "athalamic" cats.* pp. 51-81. London: Academic Press.

Villablanca J, Salinas-Zeballos ME. 1972. Sleep-wakefulness, EEG and behavioral studies of chronic cats without the thalamus: the 'athalamic' cat. *Archives italiennes de biologie* 110: 383-411

Vitrac C, Péron, S., Frappé, I., Fernagut, P.-O., Jaber, M., Gaillard, A., & Benoit-Marand, M. (2014). . 2014. Dopamine control of pyramidal neuron activity in the primary motor cortex via D2 receptors. *Front Neural Circuits* 8

Vogel W, Broverman DM, Klaiber EL. 1968. EEG and mental abilities. *Electroencephalography and clinical neurophysiology* 24: 166-75

Vogt C, Vogt O. 1919. *Journal für Psychologie und Neurologie*.

Von Bonin G, Green JR. 1949. Connections between orbital cortex and diencephalon in the macaque. *The Journal of comparative neurology* 90: 243-54

Von Economo C. 1929. The cytoarchitectonics of the human cerebral cortex. *Journal of the American Medical Association* 93: 794-94

von Engelhardt J, Bocklisch C, Tonges L, Herb A, Mishina M, Monyer H. 2015. GluN2D-containing NMDA receptors-mediate synaptic currents in hippocampal interneurons and pyramidal cells in juvenile mice. *Frontiers in cellular neuroscience* 9: 95

von Nicolai C, Engler G, Sharott A, Engel AK, Moll CK, Siegel M. 2014. Corticostriatal Coordination through Coherent Phase-Amplitude Coupling. *The Journal of Neuroscience* 34: 5938-48

Voytek B, Canolty RT, Shestyuk A, Crone NE, Parvizi J, Knight RT. 2010. Shifts in Gamma Phase–Amplitude Coupling Frequency from Theta to Alpha Over Posterior Cortex During Visual Tasks. *Frontiers in Human Neuroscience* 4: 191

Vyazovskiy VV, Olcese U, Hanlon EC, Nir Y, Cirelli C, Tononi G. 2011. Local sleep in awake rats. *Nature* 472: 443-47

Wafford KA. 2005. GABAA receptor subtypes: any clues to the mechanism of benzodiazepine dependence? *Current opinion in pharmacology* 5: 47-52

Wafford KA, Bain CJ, Whiting PJ, Kemp JA. 1993. Functional comparison of the role of gamma subunits in recombinant human gamma-aminobutyric acidA/benzodiazepine receptors. *Molecular pharmacology* 44: 437-42

Wafford KA, Thompson SA, Thomas D, Sikela J, Wilcox AS, Whiting PJ. 1996. Functional characterization of human gamma-aminobutyric acidA receptors containing the alpha 4 subunit. *Molecular pharmacology* 50: 670-8

Walker MP, Stickgold R. 2006. Sleep, memory, and plasticity. *Annual review of psychology* 57: 139-66

Wall MJ, Usowicz MM. 1997. Development of action potential-dependent and independent spontaneous GABAA receptor-mediated currents in granule cells of postnatal rat cerebellum. *The European journal of neuroscience* 9: 533-48

Wang J, O'Donnell P. 2001. D(1) dopamine receptors potentiate nmda-mediated excitability increase in layer V prefrontal cortical pyramidal neurons. *Cerebral cortex (New York, N.Y. : 1991)* 11: 452-62

Wang X, Zhong P, Yan Z. 2002. Dopamine D4 receptors modulate GABAergic signaling in pyramidal neurons of prefrontal cortex. *J Neurosci* 22: 9185-93

Wang XJ. 1993. Ionic basis for intrinsic 40 Hz neuronal oscillations. *Neuroreport* 5: 221-4

Wang XJ. 1994. Multiple dynamical modes of thalamic relay neurons: rhythmic bursting and intermittent phase-locking. *Neuroscience* 59: 21-31

Wang XJ. 1999. Fast burst firing and short-term synaptic plasticity: a model of neocortical chattering neurons. *Neuroscience* 89: 347-62

Wang XJ, Rinzel J. 1992. Alternating and Synchronous Rhythms in Reciprocally Inhibitory Model Neurons. *Neural Computation* 4: 84-97

Wang X-J, Buzsáki G. 1996. Gamma Oscillation by Synaptic Inhibition in a Hippocampal Interneuronal Network Model. *The Journal of Neuroscience* 16: 6402-13

Wang Y, Goldman-Rakic PS. 2004. D2 receptor regulation of synaptic burst firing in prefrontal cortical pyramidal neurons. *Proceedings of the National Academy of Sciences of the United States of America* 101: 5093-8

Wang Y, Markram H, Goodman PH, Berger TK, Ma J, Goldman-Rakic PS. 2006. Heterogeneity in the pyramidal network of the medial prefrontal cortex. *Nat Neurosci* 9: 534-42

Wannier TM, Maier MA, Hepp-Reymond MC. 1991. Contrasting properties of monkey somatosensory and motor cortex neurons activated during the control of force in precision grip. *Journal of neurophysiology* 65: 572-89

Watanabe M, Inoue Y, Sakimura K, Mishina M. 1992. Developmental changes in distribution of NMDA receptor channel subunit mRNAs. *Neuroreport* 3: 1138-40

Watkins JC, Evans RH. 1981. Excitatory amino acid transmitters. *Annual review of pharmacology and toxicology* 21: 165-204

Watrous AJ, Lee DJ, Izadi A, Gurkoff GG, Shahlaie K, Ekstrom AD. 2013. A comparative study of human and rat hippocampal low-frequency oscillations during spatial

navigation. *Hippocampus* 23: 656-61

Watson C, Paxinos G, Puelles L. 2012. *The mouse nervous system*. London, UK; Waltham, MA, USA: Elsevier/Academic Press.

Watt AJ, van Rossum MC, MacLeod KM, Nelson SB, Turrigiano GG. 2000. Activity coregulates quantal AMPA and NMDA currents at neocortical synapses. *Neuron* 26: 659-70

Wei Y, Krishnan GP, Bazhenov M. 2016. Synaptic Mechanisms of Memory Consolidation during Sleep Slow Oscillations. *The Journal of Neuroscience* 36: 4231-47

Weiler N, Wood L, Yu J, Solla SA, Shepherd GMG. 2008. Top-down laminar organization of the excitatory network in motor cortex. *Nat Neurosci* 11: 360-66

Weiss D, Magleby K. 1989. Gating scheme for single GABA-activated Cl- channels determined from stability plots, dwell-time distributions, and adjacent-interval durations. *The Journal of Neuroscience* 9: 1314-24

Welker E, Hoogland PV, Van der Loos H. 1988. Organization of feedback and feedforward projections of the barrel cortex: a PHA-L study in the mouse. *Experimental brain research* 73: 411-35

Werner P, Voigt M, Keinanen K, Wisden W, Seeburg PH. 1991. Cloning of a putative high-affinity kainate receptor expressed predominantly in hippocampal CA3 cells. *Nature* 351: 742-4

Werth E, Achermann P, Borbely AA. 1996. Brain topography of the human sleep EEG: antero-posterior shifts of spectral power. *Neuroreport* 8: 123-7

Werth E, Achermann P, Borbely AA. 1997. Fronto-occipital EEG power gradients in human sleep. *Journal of sleep research* 6: 102-12

White EL, DeAmicis RA. 1977. Afferent and efferent projections of the region in mouse sml cortex which contains the posteromedial barrel subfield. *The Journal of Comparative Neurology* 175: 455-81

Whiting PJ, McAllister G, Vassilatis D, Bonnert TP, Heavens RP, et al. 1997. Neuronally restricted RNA splicing regulates the expression of a novel GABAA receptor subunit conferring atypical functional properties [corrected; erratum to be published]. *J Neurosci* 17: 5027-37

Whittington MA, Traub RD, Jefferys JG. 1995. Synchronized oscillations in interneuron networks driven by metabotropic glutamate receptor activation. *Nature* 373: 612-5

Whittington MA, Traub RD, Kopell N, Ermentrout B, Buhl EH. 2000. Inhibition-based rhythms: experimental and mathematical observations on network dynamics. *International journal of psychophysiology : official journal of the International Organization of Psychophysiology* 38: 315-36

Wichmann T, DeLong MR. 1999. Oscillations in the basal ganglia. *Nature* 400: 621-2

Williams JH, Kauer JA. 1997. Properties of carbachol-induced oscillatory activity in rat hippocampus. *Journal of neurophysiology* 78: 2631-40

Willoughby JO, Fitzgibbon SP, Pope KJ, Mackenzie L, Davey M, et al. 2003. Mental Tasks Induce Gamma EEG with Reduced Responsiveness in Primary Generalized Epilepsies. *Epilepsia* 44: 1406-12

Wilson HR, Cowan JD. 1972. Excitatory and inhibitory interactions in localized populations of model neurons. *Biophysical journal* 12: 1-24

Wisden W, Seeburg PH. 1993. A complex mosaic of high-affinity kainate receptors in rat brain. *J Neurosci* 13: 3582-98

Wisor JP, Nishino S, Sora I, Uhl GH, Mignot E, Edgar DM. 2001. Dopaminergic role in stimulant-induced wakefulness. *J Neurosci* 21: 1787-94

Wolpert DM, Ghahramani Z, Jordan MI. 1995. An internal model for sensorimotor integration. *Science* 269: 1880-2

Womelsdorf T, Schoffelen J-M, Oostenveld R, Singer W, Desimone R, et al. 2007. Modulation of Neuronal Interactions Through Neuronal Synchronization. *Science* 316: 1609-12

Wong RK, Prince DA, Basbaum AI. 1979. Intradendritic recordings from hippocampal neurons. *Proceedings of the National Academy of Sciences of the United States of America* 76: 986-90

Woolsey CN. 1946. Contralateral, ipsilateral and bilateral representation of cutaneous

receptors in somatic areas I and II of the cerebral cortex of pig, sheep and other mammals. *surgery* 19: 684--702

Woolsey CN. 1958. *Organization of somatic sensory and motor areas of the cerebral cortex. In: Biological and biochemical bases of behavior.* WI: University of Wisconsin Press. 63--81 pp.

Woolsey CN, Fairman D. 1952. Contralateral, ipsilateral, and bilateral representation of cutaneous receptors in somatic areas I and II of the cerebral cortex of pig, sheep, and other mammals. *Surgery* 19: 684-702

Woolsey CN, Settlage PH, Meyer DR, Sencer W, Pinto Hamuy T, Travis AM. 1952. Patterns of localization in precentral and "supplementary" motor areas and their relation to the concept of a premotor area. *Research publications - Association for Research in Nervous and Mental Disease* 30: 238-64

Woolsey TA, Van der Loos H. 1970. The structural organization of layer IV in the somatosensory region (SI) of mouse cerebral cortex. The description of a cortical field composed of discrete cytoarchitectonic units. *Brain research* 17: 205-42

Wu J, Hablitz JJ. 2005. Cooperative activation of D1 and D2 dopamine receptors enhances a hyperpolarization-activated inward current in layer I interneurons. *J Neurosci* 25: 6322-8

Wu JY, Prentice H. 2010. Role of taurine in the central nervous system. *Journal of biomedical science* 17 Suppl 1: S1

Wulff P, Ponomarenko AA, Bartos M, Korotkova TM, Fuchs EC, et al. 2009. Hippocampal theta rhythm and its coupling with gamma oscillations require fast inhibition onto parvalbumin-positive interneurons. *Proceedings of the National Academy of Sciences of the United States of America* 106: 3561-6

Wyart V, de Gardelle V, Scholl J, Summerfield C. 2012. Rhythmic fluctuations in evidence accumulation during decision making in the human brain. *Neuron* 76: 847-58

Xi ZX, Ramamoorthy S, Shen H, Lake R, Samuvel DJ, Kalivas PW. 2003. GABA transmission in the nucleus accumbens is altered after withdrawal from repeated cocaine. *J Neurosci* 23: 3498-505

Xiong Y, Peterson PL, Lee CP. 1999. Effect of N-acetylcysteine on mitochondrial function following traumatic brain injury in rats. *Journal of neurotrauma* 16: 1067-82

Xu TX, Yao WD. 2010. D1 and D2 dopamine receptors in separate circuits cooperate to drive associative long-term potentiation in the prefrontal cortex. *Proceedings of the National Academy of Sciences of the United States of America* 107: 16366-71

Xu X, Callaway EM. 2009. Laminar Specificity of Functional Input to Distinct Types of Inhibitory Cortical Neurons. *The Journal of neuroscience : the official journal of the Society for Neuroscience* 29: 70-85

Yague JG, Cavaccini A, Errington AC, Crunelli V, Di Giovanni G. 2013. Dopaminergic modulation of tonic but not phasic GABAA-receptor-mediated current in the ventrobasal thalamus of Wistar and GAERS rats. *Experimental neurology* 247: 1-7

Yamada J, Furukawa T, Ueno S, Yamamoto S, Fukuda A. 2007. Molecular basis for the GABAA receptor-mediated tonic inhibition in rat somatosensory cortex. *Cerebral cortex (New York, N.Y. : 1991)* 17: 1782-7

Yamada J YS, Ueno S, Furukawa T, Fukuda, A. *FENS Forum2004,* 2: A083.27

Yamamoto C, McIlwain H. 1966. Electrical activities in thin sections from the mammalian brain maintained in chemically-defined media in vitro. *Journal of neurochemistry* 13: 1333-43

Yamawaki N, Borges K, Suter BA, Harris KD, Shepherd GMG. 2014. A genuine layer 4 in motor cortex with prototypical synaptic circuit connectivity. *eLife* 3: e05422

Yamawaki N, Stanford IM, Hall SD, Woodhall GL. 2008. Pharmacologically induced and stimulus evoked rhythmic neuronal oscillatory activity in the primary motor cortex in vitro. *Neuroscience* 151: 386-95

Yang CR, Bourque CW, Renaud LP. 1991. Dopamine D2 receptor activation depolarizes rat supraoptic neurones in hypothalamic explants. *The Journal of physiology* 443: 405-19

Yang CR, Seamans JK. 1996. Dopamine D1 receptor actions in layers V-VI rat prefrontal

cortex neurons in vitro: modulation of dendritic-somatic signal integration. *J Neurosci* 16: 1922-35

Yang N, Zhang KY, Wang FF, Hu ZA, Zhang J. 2014. Dopamine inhibits neurons from the rat dorsal subcoeruleus nucleus through the activation of alpha2-adrenergic receptors. *Neuroscience letters* 559: 61-6

Yener GG, Başar E. 2010. Sensory evoked and event related oscillations in Alzheimer's disease: a short review. *Cognitive Neurodynamics* 4: 263-74

Yordanova J, Banaschewski T, Kolev V, Woerner W, Rothenberger A. 2001. Abnormal early stages of task stimulus processing in children with attention-deficit hyperactivity disorder--evidence from event-related gamma oscillations. *Clinical neurophysiology : official journal of the International Federation of Clinical Neurophysiology* 112: 1096-108

Young CK, Eggermont JJ. 2009. Coupling of mesoscopic brain oscillations: recent advances in analytical and theoretical perspectives. *Progress in neurobiology* 89: 61-78

Young NA, Vuong J, Teskey GC. 2012. Development of motor maps in rats and their modulation by experience. *Journal of neurophysiology* 108: 1309-17

Yu J, Anderson CT, Kiritani T, Sheets PL, Wokosin DL, et al. 2008. Local-Circuit Phenotypes of Layer 5 Neurons in Motor-Frontal Cortex of YFP-H Mice. *Frontiers in Neural Circuits* 2: 6

Yu X, Ye Z, Houston CM, Zecharia AY, Ma Y, et al. 2015. Wakefulness Is Governed by GABA and Histamine Cotransmission. *Neuron* 87: 164-78

Zhou FM, Hablitz JJ. 1999. Dopamine modulation of membrane and synaptic properties of interneurons in rat cerebral cortex. *Journal of neurophysiology* 81: 967-76

Zhou QY, Grandy DK, Thambi L, Kushner JA, Van Tol HH, et al. 1990. Cloning and expression of human and rat D1 dopamine receptors. *Nature* 347: 76-80

Zhu Y, Zhu JJ. 2004. Rapid arrival and integration of ascending sensory information in layer 1 nonpyramidal neurons and tuft dendrites of layer 5 pyramidal neurons of the neocortex. *J Neurosci* 24: 1272-9

Zhu ZT, Shen KZ, Johnson SW. 2002. Pharmacological identification of inward current evoked by dopamine in rat subthalamic neurons in vitro. *Neuropharmacology* 42: 772-81

Zilles K, Schlaug G, Matelli M, Luppino G, Schleicher A, et al. 1995. Mapping of human and macaque sensorimotor areas by integrating architectonic, transmitter receptor, MRI and PET data. *Journal of anatomy* 187 (Pt 3): 515-37

Zin-Ka-Ieu S, Roger M, Arnault P. 1998. Direct contacts between fibers from the ventrolateral thalamic nucleus and frontal cortical neurons projecting to the striatum: a light-microscopy study in the rat. *Anatomy and Embryology* 197: 77-87